LEABHARLANN CHOLÁISTE NA TRÍONÓIDE, BAILE ÁTHA CLIATH | TRINITY COLLEGE LIBRARY DUBLIN
Ollscoil Átha Cliath | The University of Dublin

Terms and Conditions of Use of Digitised Theses from Trinity College Library Dublin

Copyright statement

All material supplied by Trinity College Library is protected by copyright (under the Copyright and Related Rights Act, 2000 as amended) and other relevant Intellectual Property Rights. By accessing and using a Digitised Thesis from Trinity College Library you acknowledge that all Intellectual Property Rights in any Works supplied are the sole and exclusive property of the copyright and/or other IPR holder. Specific copyright holders may not be explicitly identified. Use of materials from other sources within a thesis should not be construed as a claim over them.

A non-exclusive, non-transferable licence is hereby granted to those using or reproducing, in whole or in part, the material for valid purposes, providing the copyright owners are acknowledged using the normal conventions. Where specific permission to use material is required, this is identified and such permission must be sought from the copyright holder or agency cited.

Liability statement

By using a Digitised Thesis, I accept that Trinity College Dublin bears no legal responsibility for the accuracy, legality or comprehensiveness of materials contained within the thesis, and that Trinity College Dublin accepts no liability for indirect, consequential, or incidental, damages or losses arising from use of the thesis for whatever reason. Information located in a thesis may be subject to specific use constraints, details of which may not be explicitly described. It is the responsibility of potential and actual users to be aware of such constraints and to abide by them. By making use of material from a digitised thesis, you accept these copyright and disclaimer provisions. Where it is brought to the attention of Trinity College Library that there may be a breach of copyright or other restraint, it is the policy to withdraw or take down access to a thesis while the issue is being resolved.

Access Agreement

By using a Digitised Thesis from Trinity College Library you are bound by the following Terms & Conditions. Please read them carefully.

I have read and I understand the following statement: All material supplied via a Digitised Thesis from Trinity College Library is protected by copyright and other intellectual property rights, and duplication or sale of all or part of any of a thesis is not permitted, except that material may be duplicated by you for your research use or for educational purposes in electronic or print form providing the copyright owners are acknowledged using the normal conventions. You must obtain permission for any other use. Electronic or print copies may not be offered, whether for sale or otherwise to anyone. This copy has been supplied on the understanding that it is copyright material and that no quotation from the thesis may be published without proper acknowledgement.

Mechanoregulation of Bone Formation

From Embryogenesis to Evolution

Niamh C. Nowlan, B.A., B.A.I.

A thesis submitted to the University of Dublin in partial fulfilment of the requirements for the degree of

Doctor in Philosophy

October 2007

Supervisors

Prof. Patrick J. Prendergast

Dr. Paula Murphy

Prof. K. Ito, M.D., Sc.D.	**Prof. T.C. Lee, M.D., Ph.D.**
TU/e Eindhoven	
External examiner	Internal examiner

TRINITY COLLEGE
2 7 MAY 2008
LIBRARY DUBLIN
THO81S
8423

Declaration

I declare that I am the sole author of this thesis and that the work presented in it, unless otherwise referenced, is entirely my own. I also declare that the work has not been submitted, in whole or in part, to any other University as an exercise for a degree or other qualification.

I agree that the library of Trinity College Dublin may lend or copy this thesis upon request.



Niamh Nowlan

October 2007

Acknowledgements

I have been so lucky to have two exceptional individuals, Prof. Patrick Prendergast and Dr. Paula Murphy, as supervisors for my PhD. Their enthusiasm and passion for research and discovery have been a constant source of motivation for me, and their co-operation and open mindedness in collaborating on such an inter-disciplinary project led to an extraordinarily exciting and rewarding research experience for which I am truly grateful.

Thank-you to the technical and administrative staff in engineering, and in particular to Sheena, whose help with meetings, conferences orders, flights and lots more was invaluable. I would like to express my sincere gratitude to Kristen Summerhurst in Zoology, who, with endless patience, taught a wealth of molecular techniques to a biology novice. Thank-you also to Suzanne Miller and Dr. Kevin Mitchell in the Genetics Department for the use of, and assistance with, their sectioning equipment. Over the years, many people have advised me on aspects of my project, in particular John Britton, Damien Byrne, Danny Kelly and Alex Lennon, and I am very grateful for their assistance.

They say that your school days are the best days of your life, but I know that my days as a postgrad beat school hands down. This is due in no small part to the wonderful, genuine people that have worked in Mechanical Engineering and Zoology. Great memories of conferences at home and away, of viva nights, Christmas parties, nights in O'Neill's or Kennedy's and the laughter-filled tea breaks will always stay with me. So thank-you to all the past and present postgrads and staff for being so much fun. Thanks also to my great friends at home and abroad for their encouragement and support.

Thank-you to Sheila and Hugh for being there for me when I needed them, and finally, very special thanks are due to my parents. Throughout my academic career, they have never stopped supporting and encouraging me. They taught me that achievement is its own reward, and although they have never once pressured me to succeed, I hope that I have made them proud.

This research was funded by the Irish Research Council for Science, Engineering and Technology (IRCSET) under the National Development Plan (NDP).

Publications and presentations resulting from this study

Nowlan, N.C., Murphy P. and Prendergast, P.J., "A Dynamic Pattern of Mechanical Stimulation Promotes Ossification in Avian Embryonic Long Bones", in review, (*Journal of Biomechanics).*

Nowlan, N.C., Murphy P. and Prendergast, P.J. "Mechanical Stimuli Resulting From Embryonic Muscle Contractions Promote Avian Periosteal Bone Collar Formation", In *Proceedings of the 2007 Summer Bioengineering Conference of the American Society of Mechanical Engineering*, Keystone, Colorado, U.S.A., 2007 [Presented June 22nd 2007, Colorado, U.S.A.].

Nowlan, N.C., Murphy P. and Prendergast, P.J. "Mechanics in embryonic bone development", 2007 Engineers Ireland Biomedical Research Medal [Presented May 22nd 2007, Royal College of Surgeons in Ireland, Dublin].

Nowlan, N.C., Murphy P. and Prendergast, P.J. "Mechanobiology of Embryonic Limb Development", *Annals of the New York Academy of Science, Special Volume on Reproductive Biomechanics*, 2007, Vol. 1101, pp. 389-411.

Nowlan, N.C., Murphy P. and Prendergast, P.J. "Finite element analyses of avian embryonic long bones indicate that mechanical forces due to embryonic muscle contractions commit cartilage cells to the osteogenic pathway", In *Proceedings of the 13th Annual Conference of the Section of Bioengineering of the Royal Academy of Medicine in Ireland*, Fermanagh, Ireland, p. 8, 2007 [Presented January 26th 2007, Fermanagh, Ireland].

Nowlan, N.C., Murphy P. and Prendergast, P.J. "The characterisation of mechanical stresses in the growing avian embryonic limb", In *Proceedings of*

the 5th World Congress of Biomechanics, Munich, Germany, 2006 [Presented August 1st 2006, Munich, Germany].

Nowlan, N.C., Murphy P. and Prendergast, P.J. "The calculation of mechanical stresses in the growing avian embryonic limb using optical projection tomography", In *Proceedings of the 2006 Summer Bioengineering Conference of the American Society of Mechanical Engineering*, Amelia Island, Florida, U.S.A., 2006 [Presented June 22nd 2006, Florida, U.S.A.].

Nowlan, N.C., Murphy P. and Prendergast, P.J. "The influence of mechanical forces in the growing embryonic limb", In *Proceedings of the 52nd Annual Meeting of the Orthopaedic Research Society*, Chicago, Illinois, U.S.A, 2006 [Presented March 20th 2006, Chicago, U.S.A.].

Nowlan, N.C., Murphy P. and Prendergast, P.J. "The calculation of mechanical stresses in the growing embryonic chick limb using optical projection tomography images", In *Proceedings of the 12th Annual Conference of the Section of Bioengineering of the Royal Academy of Medicine in Ireland*, Galway, Ireland, p. 125, 2006 [Presented January 28th 2006, Galway, Ireland].

Nowlan, N.C., Murphy P. and Prendergast, P.J. "Computation of stresses in the growing embryonic chick limb", In *Proceedings of the 2nd International Conference on Computational Bioengineering*, Lisbon, Portugal, Vol. 2, pp. 861-872, 2005 [Presented September 16th 2005, Lisbon, Portugal].

Nowlan, N.C. and Prendergast, P.J. "Evolution of mechanoregulation of bone growth will lead to non-optimal bone phenotypes", *Journal of Theoretical Biology*, 2005, Vol 235 (3), pp. 408-418.

Nowlan, N.C. and Prendergast, P.J. "Has evolution led to the optimal skeleton", In *Proceedings of the 8th Annual Sir Bernard Crossland Symposium*, Belfast, Ireland, p. 195, 2005 [Presented April 6th 2005, Belfast, Ireland].

Nowlan, N.C. and Prendergast, P.J. "Optimality and evolution: a study using a computational model", In *Proceedings of the 11th Annual Conference of the*

Section of Bioengineering of the Royal Academy of Medicine in Ireland, Dublin, Ireland, p. 4, 2005 [Presented January 28th 2005, Dublin, Ireland].

Nowlan, N.C. and Prendergast, P.J. "A scheme for investigating the evolution of bone remodelling laws", In *Book of Abstracts of the International Workshop for Numerical Models of Bone Adaptation and Repair*, Ulm, Germany, p. 22, 2004 [Presented July 12th 2004, Ulm, Germany].

Nowlan, N.C. and Prendergast, P.J. "A scheme for investigating the evolution of bone remodelling laws", In *Proceedings of the 10th Annual Conference of the Section of Bioengineering of the Royal Academy of Medicine in Ireland*, Limerick, Ireland, p. 31, 2004 [Presented January 31st 2004, Limerick, Ireland].

Contents

Nomenclature i

List of Figures iii

List of Tables vii

Chapter 1 Introduction 1

Mechanical forces provide an essential influence on development of the skeletal tissues. It is proposed that mechanoregulation directs embryonic long bone ossification and the underlying molecular events

Chapter 2 Literature Review 13

Experimental and computational embryonic limb mechanobiology has demonstrated the importance of embryonic muscle contractions for normal skeletal development; previous studies are described and discussed.

Chapter 3 A Dynamic Pattern of Mechanical Stimulation Promotes Ossification in Avian Embryonic Long Bones 33

Finite Element analyses of avian embryonic long bones at three developmental time-points are performed, using realistic rudiment morphologies and muscle loads. Patterns of biophysical stimuli are correlated with differentiation events in the embryonic long bone.

Chapter 4 Correlation of *in vivo* Mechanosensitive Gene Expression with Mechanical Stimulation 51

Expression patterns of a set of genes involved in bone formation, also having mechanosensitive properties, are compared with stage-matched patterns of biophysical stimuli obtained from Chapter 3. Genes showing a correlation with biophysical stimuli are identified as having a potential mechanoregulatory role in embryonic bone formation. An altered mechanical environment is induced in the chick embryo using a neuromuscular blocking agent, and the gene expression patterns of candidate genes are compared between control and

immobilised limbs, thereby corroborating the mechanosensitivity of the candidate genes.

Chapter 5 Evolution of mechanoregulation of bone growth will lead to non-optimal bone phenotypes 89

A computational model is created to simulate the evolution of mechanoregulation in bone growth. A population of individuals is created where each individual is assigned a diploid gene set which controls the growth and remodelling of the bone. The simulation continues for many generations, and includes selection, mutations and a varying environment. The results indicate that a population may converge to one bone growth algorithm but, more usually, a range of mechanoregulation algorithms for different individuals will persist after many generations. Even if the population converges to one mechanoregulation law, convergence to the 'optimum' bone was never found.

Chapter 6 Discussion 111

Embryonic mechanobiology has been largely overlooked since the early 1900s and has only recently been re-discovered. The implications of this research are discussed in the context of modern biological and engineering research, and the limitations of the study are outlined.

Chapter 6 Conclusions 129

The main results of this study are listed and perspectives for future work are proposed

Bibliography 135

Appendices 153

Nomenclature

Gene Names

Bmp..... Bone morphogenetic protein

ColX..... Collagen X

FGF(r) ..... Fibroblast growth factor (receptor)

GDF..... Growth differentiation factor

Igf-1..... Insulin-like growth factor 1

Ihh ..... Indian hedgehog

Il-6..... Interleukin-6

Mmp..... Matrix metalloproteinase

Ptc1..... Patched

PTHrP..... Parathyroid hormone-related protein

Runx2..... Runt-related transcription factor 2 (also known as Cbfa1; core binding factor alpha1)

Tgfβ..... Transforming growth factor-beta

Vegf..... Vascular endothelial growth factor

Staging Systems

E ..... Embryonic days (mouse)

HH..... Hamburger and Hamilton staging system (chick)

Roman Letters

c..... Growth rate constant

E..... Young's modulus (Mpa)

k..... Permeability (m^4/N.s)

S..... Stimulus

ν..... Poisson's ratio

Greek Letters

γ_{oct}..... Octahedral shear strain

ε_1..... Maximum principal strain

σ_1 .....Maximum principal stress

τ ..... Shear stress

ψ ..... Stress stimulus

Chemicals/ Solutions

CHAPS..... 3-[(3-Cholamidopropyl)dimethylammonio]-1-propanesulfonate

EDTA..... Ethylenediamine tetraacetic acid

KOH..... Potassium hydroxide

PFA ..... Paraformaldehyde

SSC..... Saline-sodium citrate buffer

TBST..... Tris-Buffered Saline Tween-20

Other

ECM..... Extracellular matrix

EST..... Expressed sequence tag

MGI..... Mouse genome informatics

(m)RNA ..... (Messenger) Ribonucleic acid

OPT..... Optical Projection Tomography

List of Figures

1.1: Longitudinal sections of human embryonic femora (Gardner & Gray, 1970). 4
1.2: Endochondral ossification progression in long bone (Provot & Schipani, 2005) 5
1.3: Feedback loops and interactions at the fetal growth plate (Provot & Schipani, 2005) 8
2.1: Comparison of long bone development in mammals and birds.. 16
2.2: Comparison of mineralization between cultured and in vivo murine metatarsal rudiments (Tanck et al.) 19
2.3: Explanted knee joints of 7-day old chick embryos, cultivated for 6 days (Lelkes, 1958). 21
2.4: Predicted formation of a secondary ossification centre, growth plate and articular cartilage (Stevens et al., 1999) 27
2.5: Stress patterns for DDH loading histories (Shefelbine & Carter, 2004) 28
3.1: Skeletal patterning and axis definition in the chick wing (from Gilbert *et al.*, 2000). 36
3.2: Stills from 3D scans of limbs stained for cartilage, tendon and muscle. 38
3.3: Obtaining a mesh. 40
3.4: Illustration of boundary conditions and loading schemes 41
3.5: Comparison of biophysical stimuli between specimens A and B. 43
3.6: FE analysis results for HH32. 45
3.7: FE analysis results for HH30, HH32 and HH34 47
3.8: Biophysical stimuli plotted along logitudinal, ventral paths at HH30, HH32 and HH34. 48
4.1: Published expression patterns of candidate genes in the mouse (Maes et al., 2002, Minina et al., 2005, Long et al., 2001). 58
4.2: ColX expression at stages HH30, HH32 and HH34. 64
4.3: ColX expression in HH34 metatarsal rudiments 64
4.4: FGFr2 expression at stages HH30, HH32 and HH34. 65
4.5: Ihh expression at stages HH30, HH32 and HH34. 66
4.6: PTHrP expression at stages HH30, HH32 and HH34. 67

4.7: Control and immobilised embryos at stage HH36. 69
4.8: Length of tibiotarsus and length of bone for control and immobilised groups. 70
4.9: Calcified proportion of tibiotarsus for control and immobilised groups 70
4.10: ColX expression at Days 8, 9 and 11 in the tibiotarsus in control and immobilised specimens. 72
4.11: Ihh expression at Day 8 in the tibiotarsus in control and immobilised specimens.. 73
4.12: Ihh expression at Day 9 in the tibiotarsus in control and immobilised specimens 74
4.13: Ihh expression at Day 11 in representative tibiotarsi from the control and immobilised specimens 75
4.14: PTHrP expression at Day 8 in the tibiotarsus and in the metacarpals in control and immobilised specimens 76
4.15: Schematics of ColX, FGFr2, Ihh & PTHrP expression patterns..... 78
4.16: Comparison of gene expression patterns with fluid velocity 80
4.17: Comparison of gene expression patterns with strain..... 81
4.18: ColX expression correlates with predicted maximum principal strain 82
4.19: Proximal ulna of a young turtle with cartilage cone (Haines, 1969). 83
4.20: Two sections from same treated specimen showing alteration in both ColX and Ihh expression patterns 87
5.1: Diploid gene set 93
5.2: Recombination 94
5.3: Torsional moment applied to simulation over lifetime of bone with 10% variation 96
5.4: Schematic of Computational Implementation..... 97
5.5: Effect of varying c on the growth of a bone 98
5.6: Fitness values for bones grown with varying values of c 98
5.7: Fitness values for bones grown with varying c, when the mean moment, the mean-10% and the mean+10% are applied 98
5.8: Gene and c values for population after 1000 generations (basic simulation, Gene-pool 1, Run A) 101

5.9: Gene and c values for population after 1000 generations (basic simulation, Gene-pool 2, Run A) 101
5.10: Gene and c values for population after 1000 generations (varying selection strength + mutations, Gene-pool 2, Run A) 102
5.11: Gene and c values for population after 1000 generations (varying selection strength + mutations, Gene-pool 2, Run B) 103
5.12: Gene frequency data (varying selection strength + mutations, Gene-pool 2, Run A) 104
5.13: Gene frequency data (varying selection strength + mutations, Gene-pool 2, Run B) 104
5.14: Sample heritability graph for one recombination. 107
6.1: ColX expression in the hypertrophic chondrocytes of the mouse (Dacquin et al., 2004) 116
6.2: FGFr2 expression in the mouse forelimb (Minina et al., 2005) 118
6.3: Ihh expression in the mouse forelimb showing no change in the intensity of detection at older stages (Minina et al., 2005) 119
6.4: Lower intensity of Ihh expression at older stages 120
6.5: Mechanoregulation rule described by Lacroix et al. (2002) 120
6.6: Steps involved in cellular mechanotransduction 122
6.7: Biological, mechanical and integrated approaches to embryonic bone development. 126
C.1: Octahedral shear strain, μstrain, HH30_A. 160
C.2: Maximum principal stress, kPa, HH30_A 160
C.3: Maximum principal strain, μstrain, HH30_A 161
C.4: Fluid Velocity, μm/sec, HH30_A 161
C.5: Stimulus, HH30_A. 162
C.6: Pore fluid pressure, kPa, HH30_A. 162
C.7: Octahedral shear strain, μstrain, HH30_B 163
C.8: Maximum principal stress, kPa, HH30_B. 163
C.9: Maximum principal strain, μstrain, HH30_B 164
C.10: Fluid velocity, μm/sec, HH30_B 164
C.11: Stimulus, HH30_B. 165
C.12: Pore fluid pressure, kPa, HH30_B. 165
C.13: Octahedral shear strain, μstrain, HH32_A. 166
C.14: Maximum principal stress, kPa, HH32_A 166

C.15: Maximum principal strain, μstrain, HH32_A..... 167
C.16: Fluid velocity, μm/sec, HH32_A..... 167
C.17: Stimulus, HH32_A..... 168
C.18: Pore fluid pressure, kPa, HH32_A..... 168
C.19: Octahedral shear strain, μstrain, HH32_B..... 169
C.20: Maximum principal stress, kPa, HH32_B..... 169
C.21: Maximum principal strain, μstrain, HH32_B..... 170
C.22: Fluid velocity, μm/sec, HH32_B..... 170
C.23: Stimulus, HH32_B..... 171
C.24: Pore fluid pressure, kPa, HH32_B..... 171
C.25: Octahedral shear strain, μstrain, HH34_A..... 172
C.26: Maximum principal stress, kPa, HH34_A..... 172
C.27: Maximum principal strain, μstrain, HH34_A..... 173
C.28: Fluid velocity, μm/sec, HH34_A..... 173
C.29: Stimulus, HH34_A..... 174
C.30: Pore fluid pressure, kPa, HH34_A..... 174
C.31: Octahedral shear strain, μstrain, HH34_B..... 175
C.32: Maximum principal stress, kPa, HH34_B..... 175
C.33: Maximum principal strain, μstrain, HH34_B..... 176
C.34: Fluid velocity, μm/sec, HH34_B..... 176
C.35: Stimulus, HH34_B..... 177
C.36: Pore fluid pressure, kPa, HH34_B..... 177

List of Tables

1.1: Mechanosensitive Genes 9
2.1: Mechanical properties of embryonic tissues 24
3.1: Parameters used for joint reaction force 42
3.2: Cross-sectional areas and muscle forces values for ventral and dorsal muscles. 43
3.3: Maximum values of stimuli over flexion and extension contractions for HH30, HH32 and HH34 48
4.1: Roles of candidate mechanosensitive genes selected for analysis 58
4.2: Summary of numbers and treatment timing for Sets A and B 62
4.3: Percentage of control and experimental embryos moving per day of experiment. 69
4.4: Number of specimens analysed per day of harvesting for control and immobilised groups. 69
4.5: Number of specimens successfully stained for ColX, Ihh and PTHrP expression at Days 8, 9 and 11 71
5.1: Effect of varying strength of selection on probabilities of selection ... 97
5.2: Test results of Gene-pools 1-4. 100
6.1: Maximum values of octahedral shear strain and fluid velocity. 117
B.1: Muscle force calculations for stages HH30, HH32 & HH34 158
D.1: Detailed mechanosensitive gene data from literature 180
E.1: Summary data for immobilisation experiments; numbers of control and experimental specimens, survival rates and rates of movement 184
E.2: Data for experimental specimens from immobilisation experiments.. 185
E.3: Data for control specimens from immobilisation experiments..... 188

Introduction

1.1.	**Mechanoregulation of Bone Development**	**2**
1.1.1.	Embryonic Ossification	2
1.1.2.	Molecular Events in Skeletogenesis	3
1.1.3.	Mechanosensitive Genes	7
1.1.4.	Evolution of Mechanoregulation	10
1.2.	**Objectives of the thesis**	**10**

1.1. Mechanoregulation of Bone Development

Skeletal mechanobiology is the study of how mechanical forces "modulate morphological and structural fitness of the skeletal tissues– bone, cartilage, ligament and tendon" (van der Meulen and Huiskes, 2002). The adaptation of skeletal tissue to mechanical forces was first explored in 1891 by Wilhelm Roux (Lee and Taylor, 1999), the founder of experimental embryology. Since then, mechanical forces have been shown to be important for fracture healing (Augat *et al.*, 1998), bone remodelling (Huiskes *et al.*, 2000), adaptation to increased (Bass *et al.*, 2002) or decreased mechanical loading (Morey and Baylink, 1978), osteoporosis (Turner, 1999) and osteoarthritis (Scott and Athanasiou, 2006). Mechanical forces have also been shown to be important for embryonic bone formation, in particular those forces due to spontaneous muscle contractions *in utero*. Rodríguez *et al.* (1988a; 1988b) describe how fetal immobilization due to congenital myotonic dystrophy or spinal muscular atrophy can have a dramatic effect on the human skeleton, in particular on the long bones, which were found to be thin, hypomineralized and elongated, often with multiple diaphyseal or metaphyseal fractures. Aspects of embryonic skeletal development such as ossification (Crelin and Koch, 1967; Glucksman, 1941; Klein-Nulend *et al.*, 1986; Tanck *et al.*, 2000), joint formation (Fell and Canti, 1934; Lelkes, 1958), and patterning and shape development (Fell and Robinson, 1929) have all been shown to be affected by an alteration in the mechanical environment. Therefore, while there is evidence of mechanoregulation operating throughout the formation, homeostasis and repair of the skeleton, bone formation in the embryo must be examined in order to understand the mechanisms involved in establishing the complex integrated system of skeletal mechanoregulation.

1.1.1. Embryonic Ossification

Two types of ossification occur during embryonic skeletal development; intramembranous and endochondral. Intramembranous ossification occurs when bone develops directly from mesenchyme and is found in the flat bones of the skull and face (Rubin and Farber, 1988). In endochondral ossification, bone replaces a pre-existing cartilaginous template (Hall, 1987). In the long bone, a cartilaginous template of each rudiment is ossified by a precise series

of events. First there is hypertrophy of the chondrocytes in the mid-diaphysis of the rudiment, followed by the formation of the periosteum via intramembranous ossification around the circumference (Hall, 1987; Ham and Cormack, 1979). This is a two step process; firstly as a result of signaling from the pre-hypertrophic chondrocytes at the mid-diaphysis, the cells in the inner (cambial) layer of the perichondrium differentiate directly into osteoblasts (Hall, 1987). This is followed by the deposition of woven bone, the "bone collar" around the cartilaginous core of the future long bone (Calplan and Pechak, 1987). Then, in the mammal, following invasion by blood vessels, the cartilage core of the rudiment begins to be mineralized, and replaced by bone via endochondral ossification (Hall, 1987), while in the bird, the cartilage core is resorbed to form the marrow cavity without any endochondral ossification in the diaphysis (Fell, 1925).

In the mammal, the endochondral ossification at the centre of the cartilage and the periosteal bone collar at the circumference are known collectively as the primary ossification centre. As ossification progresses two zones of ossification, known as growth plates, progress distally and proximally along the diaphysis of the bone (Jee, 1988), leaving behind internal bone of ossified spicules, which is then remodelled into cancellous bone or resorbed to form the marrow cavity (Carter and Beaupré, 2001), as shown in Figure 1.1. At 11 weeks, the human embryonic femur is roughly 16.7 mm long, and endochondral ossification, trabeculae and forming marrow cavity are present at the mid-diaphysis (Figure 1.1A). At 35 weeks (length=70 mm), mineralization fronts have advanced to form epiphyses at the ends of the diaphyses, where the epiphyses are the regions of cartilage at the ends of the bone (Figure 1.1B),. In mammals, secondary ossification centres later develop in the upper and lower epiphyseal cartilages of most long bones. Eventually, the epiphyseal plates, or growth plates, are closed when the epiphyseal and metaphyseal trabeculae fuse (Jee, 1988).

1.1.2. Molecular Events in Skeletogenesis

Growth and differentiation in the embryonic long bone are determined by proliferation and differentiation of the chondrocytes contained within the cartilage.

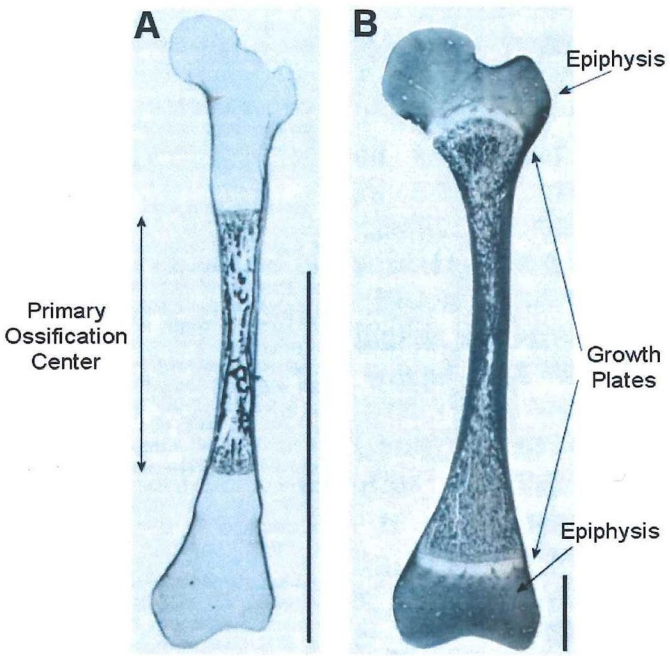


Figure 1.1: Longitudinal sections of human embryonic femora at (A) 11 and (B) 35 weeks of gestation, adapted from Gardner & Gray (1970). Scale bars 1cm.

Chondrocytes undergo tightly co-ordinated phases of cell, maturation and apoptosis (Kronenberg, 2003), and disruption of any part of this cycle can lead to abnormal development.

For example, a gain of function mutation in the fibroblast growth factor receptor 3 (FGFr3) gene, which negatively regulates proliferation, leads to reduced proliferation of chondrocytes and premature cessation of growth in the long bones, causing achondroplasia, or dwarfism (Shiang *et al.*, 1994). The stage of differentiation of chondrocytes is reflected in which collagen genes are expressed, with round proliferative chondrocytes predominantly producing type II collagen encoded by the Col II gene, and hypertrophic cells producing predominantly type X collagen encoded by the ColX gene. A longitudinal section through the developing bone will show zones of cartilage which are progressively more immature towards the epiphysis, as shown in the legend to the left of Figure 1.2. A number of signalling molecules and transcription factors have also been associated with the different stages of bone development, as illustrated for a selection of genes on the right hand side of Figure 1.2.

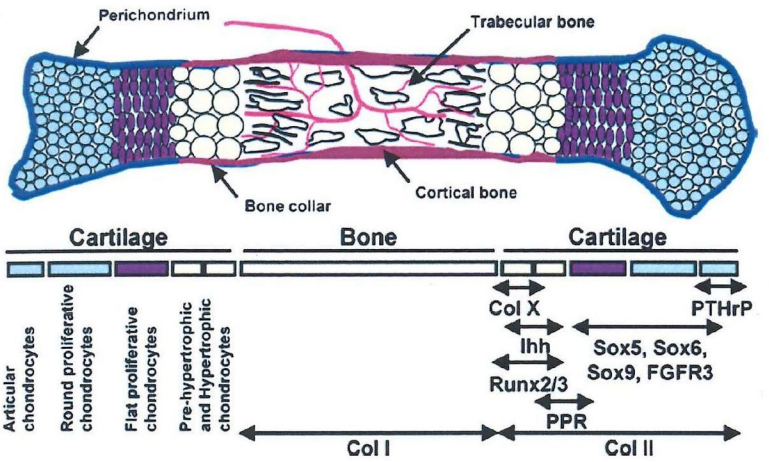


Figure 1.2: Schematic of endochondral ossification progression in long bone at late stage of mammalian fetal development. Characteristic markers such as ColX (hypertrophic chondrocytes), Sox5, Sox6, Solx9 and Fgfr3 (proliferative chondrocytes), Ihh and Runx2/3 (pre-hypertrophic and hypertrophic chondrocytes) and PTHrP (articular chondrocytes) are highlighted (from Provot and Schipani, 2005)

Secreted signalling molecules facilitate communication between neighbouring cells, communication which is necessary for inductive interactions and the co-ordinated step wise differentiation of component cells, while transcription factors act directly within component cells to alter the set of genes being transcribed and therefore the differentiation state of the cells. Two families of transcription factors; the Sox and Runx (runt-related protein) families, are particularly important. Three members of the Sox family (Sox5, Sox6 and Sox9) are expressed in proliferating chondrocytes, the earliest acting and best characterised being Sox9. Sox 9, which is expressed as soon as chondrocytes first condense at the core of the early limb bud (Ng *et al.*, 1997; Zhao *et al.*, 1997), maintains proliferation of chondrocytes (Akiyama *et al.*, 2002) and directly turns on expression of collagen genes including Col II, the major marker of proliferating cells. Runx2 and 3, which are expressed in chondrocytes entering hypertrophy (Yoshida *et al.*, 2004), regulate the expression of Collagen X. Runx2 (also known as Cbfa1) is necessary for osteoblast differentiation (Otto *et al.*, 2004).

A number of signalling pathways are involved in regulating the transition of cells from immature proliferative chondrocytes to mature hypertrophic chondrocytes to eventual apoptosis. The Ihh gene is expressed by pre-hypertrophic and hypertrophic chondrocytes (Vortkamp *et al.*, 1996) and encodes a signalling molecule that is essential for normal bone development. Multiple regulatory roles for Ihh during bone formation were demonstrated in an Ihh null knockout mouse created by St-Jacques *et al.* (1999), which exhibited reduced chondrocyte proliferation, abnormal chondrocyte maturation, and a complete absence of mature osteoblasts (St-Jacques *et al.*, 1999). In the Ihh null mutant, the absence of mature osteoblasts in the long bones meant that no bone collar formed, indicating that Ihh signalling from the proliferative region is necessary to induce the differentiation of the perichondrium into an osteogenic tissue from which the first osteoblasts will differentiate (St-Jacques *et al.*, 1999). Endochondral ossification is also affected in the Ihh null mutant mouse, where although calcification occurs at the core of the rudiment, the absence of mature osteoblasts leads to an absence of trabecular bone at birth. The presence of mature osteoblasts in regions of intramembranous ossification in the mouse mutant suggests two distinct pathways for osteoblast development, with Ihh dependant osteoblast differentiation in the periosteal bone collar and in endochondral ossification and Ihh independent osteoblast differentiation in intramembranous ossification (St-Jacques *et al.*, 1999).

Cross-regulation (cross talk) between the Ihh and Parathyroid hormone-related protein (PTHrP) pathways controls the timing and progression of chondrocyte differentiation. Ihh stimulates PTHrP expression while PTHrP and its receptor (PTHrPR, also known as PTHr1 and PPR), in turn, repress Ihh expression generating a negative feedback loop (Lanske *et al.*, 1996). PTHrP signalling negatively regulates the switch from a proliferative immature chondrocyte to a post-proliferative mature, hypertrophic chondrocyte (Provot and Schipani, 2005). When chondrocyte differentiation has begun (cells have become pre-hypertrophic), they express Ihh, upregulating PTHrP and thereby preventing differentiation of additional chondrocytes. Once cells have stopped expressing Ihh (when they have become hypertrophic), PTHrP will be downregulated due to attenuation of the feedback mechanism, therefore allowing the next phase of differentiation to commence (Vortkamp *et al.*, 1996). It has also been

suggested that Patched (Ptc1), a downstream target of Ihh, may also play a role in the Ihh-PTHrP feedback loop (Vortkamp *et al.*, 1996).

Two other signalling pathways have been implicated in the regulation of bone formation stimulated by Bone Morphogenetic Proteins (BMPs) and Fibroblast Growth factors (FGFs). BMPs are positive modulators of proliferation and negatively affect maturation (hypertrophy) (Minina *et al.*, 2002; Minina *et al.*, 2001), while FGF signalling, through FGFr3, negatively regulates proliferation (Ornitz and Marie, 2002) and therefore tips the balance toward hypertrophy and differentiation. Conversely, FGFr2, another FGF receptor, has been identified as a positive regulator of proliferation (Eswarakumar *et al.*, 2002).

It is clear therefore that a carefully controlled balance between proliferation and differentiation is mediated by a number of complex feedback loops at the fetal growth plate, as illustrated in Figure 1.3, and it is this balance which ultimately determines the size and shape of each bone. Ihh induces expression of BMPs which themselves induce Ihh expression in a positive feedback loop (arrows in Figure 1.3 indicate upregulation). Runx2 also upregulates Ihh expression, while, conversely, FGFs repress Ihh expression (horizontal lines indicate downregulation). PTHrP, Ihh and BMPs are positive modulators of proliferation and negatively affect maturation (hypertrophy). Some members of the FGF family are negative modulators of proliferation (e.g., FGFr3 (Ornitz and Marie, 2002)) and, with Runx2, are important positive modulators of chondrocyte hypertrophy.

1.1.3. Mechanosensitive Genes

Many of the genes instrumental to bone formation in the embryo have been shown to be responsive to mechanical stimulation under certain assay conditions, and have been called mechanosensitive genes. The expression of such genes is up- or down- regulated in response to a mechanical stimulus. Most experiments to reveal mechanosensitivity have placed cells or tissues under mechanical stimulation in culture and subsequently performed microarray analysis to compare the expression of many genes between stimulated and control cells (e.g., Cillo *et al.*, 2000; Jackson *et al.*, 2006; Lau *et al.*, 2006; Wong *et al.*, 2003).

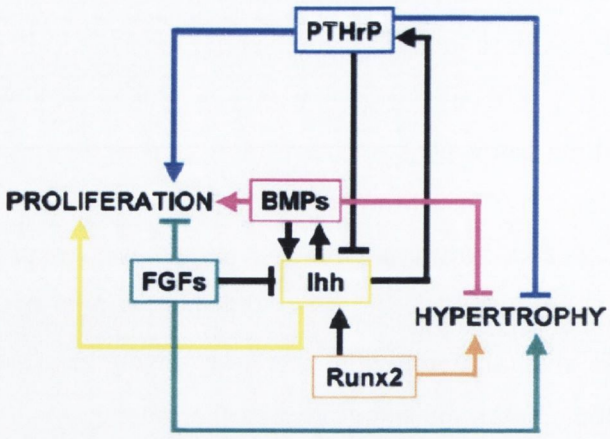


Figure 1.3: Schematic representation of feedback loops and interactions of PTHrP, Ihh, BMPs and FGFs in the fetal growth plate (from Provot and Schipani, 2005).

Using this method, hundreds of potential mechanosensitive genes can be identified simultaneously. However, in order to relate the mechanosensitivity of a gene to a specific *in vivo* event, it is necessary to examine the sensitivity of the gene to mechanical stimulation in a normal tissue context *in vivo*. A limited number of studies have examined gene expression in vivo using methods such as distraction osteogenesis (Sato *et al.*, 1999), increased mechanical loading of the mandibular joint (Ng *et al.*, 2006b), or hindlimb-suspension (Hardiman *et al.*, 2005). Only one study has attempted to examine gene mechanosensitivity *in vivo* during development, where the expression patterns of three genes encoding signalling molecules implicated in regulating joint formation were compared between the presumptive joint regions of control and immobilized chick embryonic hindlimbs (Kavanagh *et al.*, 2006). A number of genes influential to bone development that have been identified as being mechanosensitive, with details of the type of study that was performed in order to test mechanosensitivity, are listed in Table 1.1.

Table 1.1: Genes involved in bone formation that have been identified as mechanosensitive, with references and the experimental system used to alter the mechanical environment.

Gene/Protein	Reference	Method
IGF-1, BMP & Wnt pathways	(Lau et al., 2006)	*In vitro;* fluid shear stimulation of C3H and B6 murine osteoblasts
PTHrP, Ihh	(Ng *et al.*, 2006a; Ng *et al.*, 2006b)	*In vivo;* mechanical stimulation of mandibular condyle (rat)
PTHrP	(Tanaka et al., 2005)	*In vitro;* cyclic mechanical stimulation of rat growth plate chondrocytes
Runx2, MMP-13, ColX, VEGF	(Wong et al., 2003)	*In vitro;* bovine chondrocytes under cyclic tension and cyclic hydrostatic pressure
Ihh	(Wu et al., 2001)	*In vitro;* cyclic mechanical stimulation of embryonic chick chondrocytes
TGFβ, IGF-1, FGF-2, IL-6	(Cillo et al., 2000)	*In vitro;* tensile stretch stimulation of human osteoblast-like cells
BMP-2, BMP-4	(Sato et al., 1999)	*In vivo;* femoral distraction osteogenesis (rat)
FGFr2	(Sironen et al., 2002)	*In vitro;* chondrocyte cell line under continuous hydrostatic pressure
FGF-2, FGFr2	(Li and Hughes-Fulford, 2006)	*In vitro;* mechanical stimulation of bone marrow stromal cells from $Fgf2^{-/-}$ and $Fgf2^{+/+}$ mice
FGF-1-2, FGFr1-4	(Jackson et al., 2006)	*In vitro;* four point bending of MC3T3-E1 preosteoblasts
Runx2, Qsteopontin, ColX	(Sundaramurthy and Mao, 2006)	*Ex vivo;* mechanical stimulation of neonatal rabbit distal femoral condyle explants
Osteopontin, Osteocalcin, IGF-1, TGFβ	(Raab-Cullen *et al.*, 1994)	*In vivo;* four point bending of rat tibiae

IGF-1: insulin-like growth factor 1

BMP: Bone morphogenetic protein

PTHrP: Parathyroid hormone-related protein

Ihh: Indian Hedgehog

Runx2: runt-related transcription factor 2 (also known as Cbfa1: core binding factor alpha1)

MMP-13: matrix metalloproteinase 13 (also known as collagenase 3)

ColX: Collagen X

VEGF: Vascular endothelial growth factor

TGFβ: Transforming growth factor-beta

FGF(r): Fibroblast growth factor (receptor), (FGF-2 also known as bFGF: Basic fibroblast growth receptor)

IL-6: Interleukin-6

1.1.4. Evolution of Mechanoregulation

We can also learn about the mechanoregulation of bone development by considering the system from an evolutionary perspective. At a population level, the system of mechanoregulation, like other biological processes, is likely to exhibit variation between individuals. It has been indicated that bone remodelling rates were significantly lower in Pleistocene humans (200-300 thousand years ago) than in more recent populations (Abbott *et al.*, 1996)– this demonstrates the evolution of skeletal mechanoregulatory mechanisms. However, while several studies have investigated the evolution and/or variation of skeletal patterning or specific skeletal elements (such as variation in the postcranial skeletons of apes (Young, 2003), as reviewed in (Hall, 2005)), the evolution of, or the variation present in, the mechanoregulatory mechanisms has not been previously addressed in detail. Studying the evolution of skeletal mechanoregulation could also lead to a deeper understanding of the underlying processes. By exploring the mechanoregulation algorithms within a population over evolutionary time, it is hoped that a better understanding of the remodelling response of the individual and its relationship to their genes would be gained, so as to better predict the effects of mechanical stimulation on bone growth and development, for example, in clinical procedures such as joint replacements.

1.2. Objectives of the thesis

The implications of embryonic bone mechanobiology are important, not only in terms of a better understanding of a fundamental concept of how cells interpret mechanical stimulation, but also potentially from a clinical standpoint. An insight into the mechanoregulation of the embryonic skeleton could potentially assist treatment of conditions where foetal movement is reduced or eliminated in order to minimise their effect on the bones. Better knowledge of the stimuli required for the normal growth and development of embryonic cartilage or bone would also have implications for growing such tissues *in vitro* for eventual implantation.

The principal objective and challenge of the work is to characterise the biophysical stimuli at a range of stages of chick limb development, and to relate changes in the distribution or magnitudes of these stimuli to the activity of a candidate set of mechanosensitive genes. A secondary objective of the work is to investigate variations in the rules or laws governing mechanoregulation by simulating how mechanoregulation of bone growth is subject to selection pressures during evolution. The body of work involved the following steps:

- Characterisation of biophysical stimuli: by using novel scanning techniques designed for embryonic specimens, anatomically accurate rudiment and muscle morphologies of embryonic skeletal elements can be obtained, enabling characterisation of biophysical stimuli at a range of developmental timepoints (Chapter 3).
- Comparison of gene expression and biophysical stimuli patterns: anatomically accurate morphologies lead to more realistic patterns of stimuli, which could then be compared to gene expression patterns of molecular components of the system in order to identify candidate mechanosensitive genes influential over a specific time span during embryonic bone formation (Chapter 4).
- Corroboration of candidate mechanoregulatory genes: These candidate genes could then be corroborated by altering the mechanical environment and identifying any effects on the gene expression patterns (Chapter 4).
- Evolution of mechanoregulation: in an exploratory study, the evolution of representative mechanosensitive genes was investigated using a computational model which simulated how mechanoregulation of bone growth is subject to selection pressures during evolution (Chapter 5).

In summary, the author's thesis is that biophysical stimuli mechanoregulate ossification events through the action of mechanosensitive genes, where mechanoregulation is an ontogenetic process which has evolved. The author proposes to conduct the investigation using a systems approach, where

biological and computational methods are integrated to investigate and corroborate testable hypotheses.

Literature Review*

2.1.	**Introduction**	**14**
2.2.	**Experimental Embryonic Limb Mechanobiology**	**14**
2.2.1.	Avian vs. Mammalian Embryonic Bone Formation	15
2.2.2.	Shape	17
2.2.3.	Ossification	18
2.2.4.	Joint Formation	20
2.2.5.	Additional Effects of Immobilization	21
2.3.	**Computational Embryonic Mechanobiology**	**23**
2.3.1.	Mechanical Properties of Embryonic Tissues	23
2.3.2.	Single Time-Point Analyses	25
2.3.3.	Simulation Models	27
2.4.	**Evolution of Bone and Mechanoregulation of Bone**	**29**
2.5.	**Concluding Remarks**	**30**

* Published in part in: Nowlan, N.C., Murphy P. and Prendergast, P.J. "Mechanobiology of Embryonic Limb Development", Annals of the New York Academy of Science, 2007, Vol. 1101, pp. 389-411.

2.1. Introduction

Research into embryonic limb mechanobiology can be classified into two categories: experimental and computational studies. Experimental embryonic limb mechanobiology uses animal models, such as the chick for example, or explants of embryonic tissues or limbs in order to investigate the effect of an altered mechanical environment on aspects of limb development, such as the joint morphogenesis or sesamoid formation. In more recent years, computational mechanobiology has been used to characterise the biophysical stimuli present in the embryonic limb, and to predict the influence of mechanical forces on tissue differentiation and growth, enabling hypotheses to be posed and tested using computational models.

2.2. Experimental Embryonic Limb Mechanobiology

Experiments where the mechanical environment in the embryo is altered can be broadly grouped into two categories: (i) *in vivo* experiments, mainly immobilization procedures, but also other surgical procedures such as muscle ablation or partial neural tube excision. In *in vivo* immobilization studies, embryonic muscle contractions are prevented by the application of neuro-muscular blocking agents. (ii) *ex vivo*, comprising *in vitro* and grafting experiments. *In vitro* experiments involve removing the limb (or part thereof) from an embryo and growing it in culture. Numerous aspects of skeletal development have been examined by culturing embryonic rudiments *in vitro*, e.g. such as patterning and shape development (Fell and Robinson, 1929), ossification (both periosteal (Glucksman, 1941) and endochondral (Crelin and Koch, 1967; Klein-Nulend *et al.*, 1986; Tanck *et al.*, 2000) and joint formation (Fell and Canti, 1934; Lelkes, 1958). Grafting experiments also involve separation of the limb or skeletal rudiments from the embryo, and are among the most commonly performed scientific procedures in the chick. In a limb graft, the test limb can be attached to the coelemic cavity of a "host embryo", or, for a chorioallantoic membrane graft, the graft is implanted into the chorio-allantois of the host – a thin vascular membrane extending from the embryo. The grafted structure (e.g., femur) receives nourishment and oxygen from the bloodstream of the host, but probably no innervation, according to Murray and Selby (1930). Assuming all muscle tissue is removed prior to grafting, growth

in the absence of muscle contractions can then be examined. However, as with all of the above experimental procedures, forces due to growth related strains or pressures (Henderson and Carter, 2002; Skalak *et al.*, 1982; Taber and Humphrey, 2001; Thorogood, 1983) or forces due to the surrounding environment (Murray and Selby, 1930) are *not* eliminated.

2.2.1. Avian vs. Mammalian Embryonic Bone Formation

The embryonic chick has been used extensively to study the influence of muscle contractions on embryonic skeletal growth. The chick shares many features of embryonic development with mammals and has the huge advantage of development external to the mother, allowing procedures and alterations to be performed and the effects on the embryo examined. The chick embryo is also quite resilient, and can withstand procedures such as immobilization and muscle ablation. However, it is seldom acknowledged that long bone development in fowl is significantly different from mammals. Two major differences exist between avian and mammalian skeletal development, (Figure 2.1). Firstly, avian long bones have no primary (endochondral) ossification centre (Fell, 1925) and secondly, in the embryonic chick, vascularization of the primary cartilage is not present prior to mineralization (Hall, 1987). In the chick, by 6 to 6.5 days of incubation, chondrocytes in the mid-diaphysis undergo hypertrophy, and by 6.5 to 7 days of incubation, bone collar formation begins in the mid region of the diaphysis with the deposition of osteoid below the perichondrium (Hall, 1987). The first mineralization takes place 0.5 to 1 days later (Hall, 1987) in the form of laminae of bone which eventually fuse to form a thin, compact cylinder- the periosteal bone collar. This cylinder increases in thickness, and becomes richly vascularized, giving rise to trabeculae (Fell, 1925).

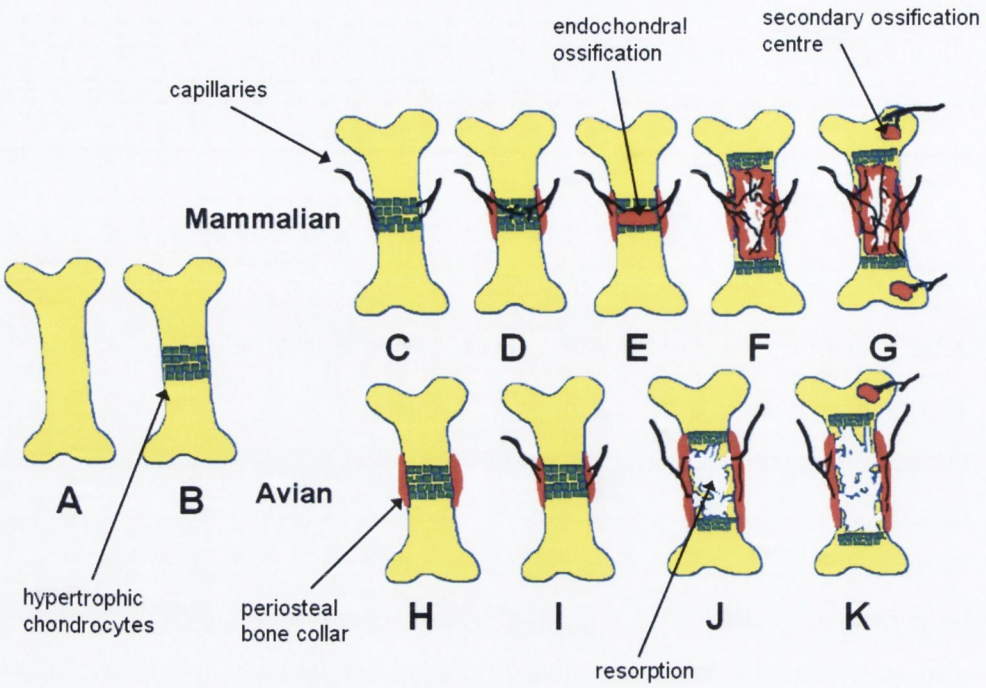


Figure 2.1: Comparison of long bone development in mammals and birds. Mammalian and avian long bone development begins with a cartilaginous template (A). Next, the chondrocytes in the mid-diaphysis undergo hypertrophy (B). In the mammal (C-G), the cartilage is first invaded by capillaries (C) before the periosteal bone collar forms (D). Blood vessels penetrate to the middle of the rudiment, which undergoes endochondral ossification (E). Growth fronts progress and some bone is resorbed to form the marrow cavity (F). Secondary ossification centers form in most mammalian long bones (G). In the bird (H-K), periosteal ossification (H) occurs before vascularization (I). As the collar grows, cartilage is resorbed to form the marrow cavity (J). Only in some long bones in the bird will a secondary ossification centre form after hatching (K) (see text for references).

At this point, erosion of the cartilage inside the bone collar begins, and progresses in long finger-like protuberances (Murray and Selby, 1930). As stated by Hall (1987), and in contrast to the mammal, the primary cartilage in the chick is never invaded by blood vessels during embryonic life. As ossification continues, the periosteal bone collar advances along the diaphysis to the proximal and distal epiphyses, increasing in thickness by addition of osseous trabeculae and the enlargement of those already formed (Fell, 1925). Haines' (1969) description of reptilian bone development is analogous to that

of the chick. According to Fell (1925), core endochondral ossification in the chick takes places only in the extremities of the diaphysis, in positions analogous to secondary ossification sites in the mammal; however, the presence or otherwise of secondary ossification centres in the chick (*Gallus gallus)* is still not a settled issue, with several researchers reporting only one secondary ossification centre in the proximal tibiotarsus (Doménech-Ratto *et al.*, 1999; Hogg, 1980), and others also identifying one in the distal femur, but not in every specimen examined (Blumer *et al.*, 2005).

Another disadvantage of the chick is that gene expression data for genes involved in bone formation are much more limited than in mammalian models, in particular the mouse, and the molecular events involved in endochondral ossification of the long bones have been more extensively characterised than in intramembranous ossification. However, many of the early events of the ossification process occur in both types of ossification, such as hypertrophy and proliferation of chondrocytes, and formation and progression of the growth plates (Hall, 1987).

2.2.2. Shape

In vitro (Fell, 1931; 1969) and chorioallantoic graft (Murray and Selby, 1930) studies have both indicated that shape and growth of the early cartilaginous skeletal long bone rudiments can proceed fairly normally in the absence of muscle contractions with the following exceptions. In the case of chorioallantoic grafts of the femur (Murray and Selby, 1930), smaller articular structures and reduced inter-condyloid fossae were found, and the groove across the head of the femur, which normally holds the acetabular ligament, was missing. Abnormal curvature of the rudiments grown *in vitro* was found by Murray and Selby (1930) and also by Thorogood (1983). Long and Lisenmayer (1998) examined the role of the perichondrium using an organ culture system of chicken embryonic tibiotarsi, where growth in the absence of a perichondrium was compared to that of controls. The perichondrium-free tibiotarsi exhibited a higher growth rate, and based on their findings, the authors suggest that the presence of the perichondrium negatively regulates hypertrophy and proliferation of chondrocytes.

2.2.3. Ossification

The literature describing experimental work on the mechanobiology of embryonic ossification is disjointed, with a range of (sometimes sparse) data on different species, types of ossification, bone locations and embryonic ages. It has been shown that periosteal ossification in chick long bones will occur in grafts (Murray and Selby, 1930) and in culture (Glucksman, 1941), and endochondral ossification will occur in murine long bone (Klein-Nulend *et al.*, 1986; Tanck *et al.*, 2000) and pubic bone (Crelin and Koch, 1967) rudiments in culture. Periosteal ossification does not proceed in a normal fashion in a chorio-allantoic graft of the embryonic avian femur (6 or 7 days of incubation)(Murray and Selby, 1930) with greater deposition of bone on the concave curve of the bone compared to a normal avian femur. Glucksman (1939; 1941) cultured embryonic chick bone rudiments (from 7 to 13 days incubation) in such a position that they exerted pressure on each other as they grew. The author found that increased tension increased the rate of bone formation while reduced tension diminished ossification, and concluded that mechanical stress stimulates osteogenesis *in vitro*. Klein-Nulend *et al.* (1986) cultured embryonic mouse long bone rudiments aged embryonic day 16 (E16) *in vitro* and examined the effect on calcification of intermittently or continuously compressing the gas phase above the culture medium. The authors found that the compressive force resulted in increased calcification of the growth plate cartilage, with intermittent forces having a greater effect than continuous forces, and concluded that mechanical loading seems to be an important regulator of biomineralization (Klein-Nulend *et al.*, 1986). Tanck *et al.* (2000) cultured embryonic mouse metatarsal rudiments at E15 and E17 *in vitro*, and compared the geometry of the primary ossification centres of the cultured rudiments to those of controls. The authors found that the mineralization front *in vivo* was almost straight, but was convex for *in vitro* grown rudiments, as shown in Figure 2.2.

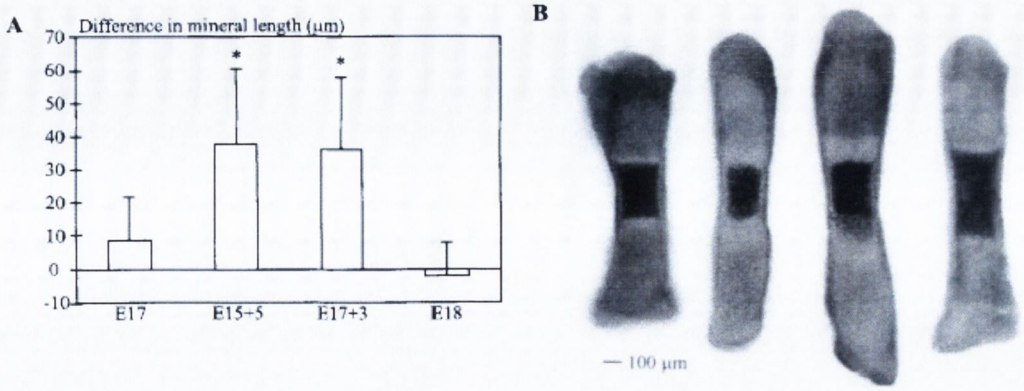


*Figure 2.2: Comparison of mineralization between cultured and in vivo murine metatarsal rudiments (from Tanck et al. (2000)). (A) Difference in length of the mineralized zone between the centre and periphery pf the metatarsal diaphysis (E17= mineralized metatarsal at 15 days of gestation, E15+5= metatarsal at 15 days of gestation with 5 days of culture, E17+3= metatarsal at 17 days of gestation with 3 days of culture, E18= metatarsal at 18 days of gestation). *p<0.05, compared with E17 and E18. Error bars represent the SD. (B) Representative pictures of the metatarsals from the four groups, from left to right: E17, E15+5, E17+3, E18.*

Trepczik *et al.* (2007) found that mechanical stimulation of *ex vivo* murine metatarsal rudiments affected both endochondral and periosteal ossification in the rudiments. Periosteal bone collar growth and the region of interest (ROI) comprising the two hypertrophic zones and the intermediate calcifying zone increased in the stimulated group. The portion of the ROI that had undergone mineralization was smaller in the stimulated group, while the absolute amount of mineralized area was the same for the control and stimulated groups. Endochondral ossification *in vitro* was observed in mouse pubic bone rami rudiments excised at E13, and in cultures of human embryonic mandibular condyles (Ben-Ami *et al.*, 1993). Felts (1959) in 1959 implanted mouse and rat post-natal (2 & 5 days) long bones subcutaneously into a litter mate or adult of the same species, and claims to have observed normal ossification patterns and largely normal shape development of the rudiments. He concluded that long bone size, shape and ossification events are independent of the mechanical environment, although the author never attempted to quantify the mechanical environment of the subcutaneous implant. It is also important to note that ossification occurring *ex vivo* could be due to prior commitment of the cells

towards a certain developmental fate (Thorogood, 1983); therefore the timing of the manipulation may be of crucial importance and just because ossification was observed in grafted or cultured limbs does not mean cartilage differentiation is entirely independent of mechanical environment. Although the study of Sundaramurthy and Mao (2006) was performed on neo-natal rather than embryonic skeletal elements, it is included in this review because it demonstrates modulation of secondary ossification centre formation by mechanical loading. The authors found that when distal femoral condyle explants from neonatal rabbits were submitted to cyclic loading, a structure reminiscent of the secondary ossification centre appeared whereas no secondary ossification centre was detected in any of the unloaded control specimens. The mechanically loaded specimens expressed Runx2, osteopontin and Type X collagen, which were absent in the unloaded controls, and loaded specimens also had a significantly higher number of hypertrophic chondrocytes than controls. The authors conclude that mechanical stresses accelerate the formation of the secondary ossification centre, and therefore modulate endochondral ossification.

2.2.4. Joint Formation

Joint formation is one aspect of skeletal embryogenesis commonly acknowledged to be strongly influenced by mechanical forces, specifically those forces due to muscle contractions *in ovo/ in utero*. Formation of a typical diarthrodial embryonic joint takes place in two stages; firstly, the joint region becomes recognizable as three layers; an interzone and the two future epiphyseal surfaces, and secondly, the joint cavity is formed (Thorogood, 1983). The first stage occurs *in vitro* (Kardon, 1998; Lelkes, 1958), in chorioallantoic grafts (Murray, 1926) and in embryos immobilized using neuro-muscular blocking agents (Mikic *et al.*, 2000; Osborne *et al.*, 2002), however, mechanical stimulation is needed for cavitation (Mikic *et al.*, 2000; Osborne *et al.*, 2002; Thorogood, 1983). Rudiments cultured *in vitro* result in cartilaginous fusion of the opposed joint elements, unless the limbs are artificially stimulated, in which case fusion does not occur (Lelkes, 1958), as shown in Figure 2.3.

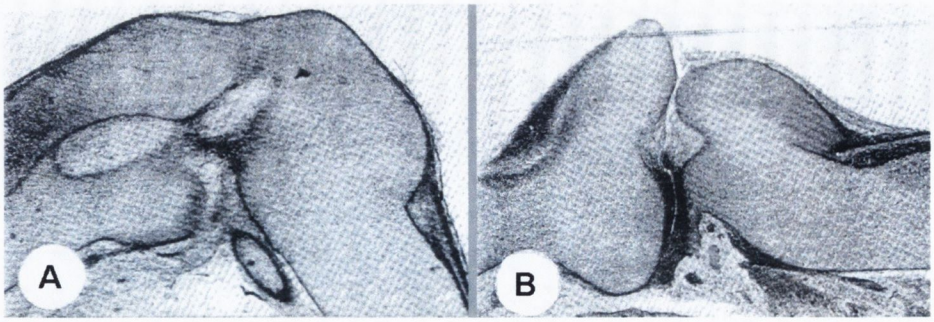


Figure 2.3: Explanted knee joints of 7-day old chick embryos, cultivated for 6 days (adapted from Lelkes (1958)). In (A) the explant was not moved and resulted in cartilaginous fusion of the femur and tibia; in (B) the joint was moved 5 times a day and articular surfaces are well developed.

Mikic *et al.* (2000) treated chick embryos *in ovo* with a neuromuscular blocking agent and found partial or absent cavitation, and post-cavitational joint fusion if the drug was applied after initial cavitation occurred. Osborne *et al.* (2002) examined joint formation in the chick with two different methods of immobilization; rigid paralysis (dynamic stimulation removed) and flaccid paralysis (static and dynamic stimulation removed). Immobilization using either method before and during the time of normal cavitation of joints resulted in loss of cavitation. If immobilization was induced after a cavity had arisen, loss of cavitation occurred for flaccid but not for rigid paralysis. Kavanagh *et al.* (2006) examined the expression patterns of signalling molecules implicated in regulating joint formation, growth differentiation factor (GDF)-5 and fibroblast growth factor (FGF)-2 and 4, in the presumptive joint regions of control and immobilized chick embryonic hindlimbs. The authors found that joint line FGF-2 expression was diminished in immobilized limbs, while FGF-4 and GDF-5 expression patterns were unaffected by immobilization, and conclude that FGF-2 has a direct mechano-dependant role in the cavitation process.

2.2.5. Additional Effects of Immobilization

Immobilization has been used, not just for examining joint formation as described above, but for many aspects of skeletal development. Immobilization is effected in the avian embryo by cutting a "window" in the eggshell, dropping a quantity of a neuromuscular blocking agent such as decamethonium bromide (Hosseini and Hogg, 1991a; 1991bb; Mikic *et al.*, 2000) daily onto the

chorioallantoic membrane, and sealing up the window with tape after each administration of the drug. Immobilization has also been effected by injecting botulinum toxin directly into the chorioallantoic vein (Murray and Drachman, 1969). Hosseini and Hogg (1991a; 1991bb) demonstrated that immobilization has a significant effect on skeletal growth and development. They found that the lengths of many bones were reduced by immobilization, and slender bones were prone to distortion. Hall *et al.*(1990) discovered that skeletal elements are differentially affected by the lack of muscle contractions, with only 27% of clavicular growth (by mass) but 77% of mandibular growth occurring in paralysed embryos. Mikic *et al.* (2000) found that the menisci and sesamoids of the joints were absent for late stage immobilized chick embryos. In another study, Mikic *et al.* (2004) found that the cartilage from immobilized embryos had a lower glycosaminoglycan (GAG) content, and was mechanically weaker than cartilage from control embryos. Germiller and Goldstein (1997) found that immobilization led to a reduction in chondrocyte proliferation in the avian embryonic growth plate. Two methods have been used to examine the effect of mechanical forces on bone development in the embryonic rat, namely immobilization (Rodriguez *et al.*, 1992) and induced oligohydramnios (Palacios *et al.*, 1992). Rodriguez et al. (1992) studied the effects of foetal immobilization administering D-Tubocurarine subcutaneously to rat foetuses *in utero* from day 17 of gestation to term. The authors found that the femora of experimental foetuses exhibited alterations in shape and transverse diaphyseal growth, with a decrease in the total cross-sectional area and in the thickness of the periosteum, and a rounder femoral cross-section in comparison to controls. Palacios *et al.* (1992) induced oligohydramnios (a condition where motion of the foetus is restricted due to reduced amniotic fluid) by daily extraction of amniotic fluid from rat foetuses from day 17 to term. While joint development was affected, with multiple articular contractures, no alterations in femoral shape or transverse growth of the metaphysis and diaphysis were noted in the experimental foetuses, leading the authors to conclude that the main mechanical factor affecting embryonic bone development is muscular elasticity, while motion is important for foetal joint development.

Other surgical techniques can also be used to induce immobilization. Wong *et al.* (1993) produced hindlimb muscle atrophy in the embryonic chick by

excising the lumbrosacral portion of the neural tube. Rudiments from immobilized embryos were significantly shorter than controls, with greater flaring at the ends, smaller chondroepiphyses, and irregular and flattened articular surfaces. The bones from denervated embryos also had decreased mechanical strength. Therefore, a large body of evidence suggests that mechanical forces generated by muscle contractions play a role in embryonic skeletal morphogenesis.

2.3. Computational Embryonic Mechanobiology

Computational mechanobiology problems may be classified into two types (Prendergast, 2004). The first kind is a single time-point analysis where biophysical stimuli are computed and used to predict tissue differentiation and remodelling when the forces are known. The second kind - we may call it simulation modelling - takes the initial condition and simulates a process of adaptation and differentiation over time. The most commonly used method for computing biophysical stimuli is Finite Element (FE) analysis, a numerical method where computers find approximate solutions to large sets of equations (Prendergast, 1997). Although a wide range of biophysical stimuli have been used either to measure or to predict the effect of mechanical stimulation on tissues, there are two possible effects of stimulation on a cell; a change in cell shape (for example, due to an applied strain) or a change in cell volume (due to a change in pressure).

2.3.1. Mechanical Properties of Embryonic Tissues

Finite element analysis requires accurate material properties, but embryonic tissues have not yet been extensively characterized with respect to their mechanical properties, mainly due to the difficulties associated with testing very small specimens. Tanck *et al.* (2004) examined the effect of mineralization on the mechanical properties of embryonic mouse rib rudiments using four-point bending tests in combination with FE analysis, and found an increase of two orders of magnitude during endochondral ossification. Mikic *et al.* (2004) performed stress-relaxation mechanical tests on cores from control and immobilized embryonic chick cartilage, and found reduced values for both the instantaneous and relaxed moduli in the cartilage from the immobilized embryos. Williamson *et al.* (2001) performed static and dynamic compression

tests on bovine articular cartilage, and found the confined compression modulus of embryonic cartilage increased 180% in the calf and adult. This group also tested the free swelling compressive moduli for the surface and middle layers of the articular cartilage and found a 2-2.5 fold increase in modulus between the fetal and newborn stages of development. Brown and Singerman (1986) performed mechanical tests of cylindrical specimens from the chondroepiphysis of human still born femoral heads in order to calculate the equilibrium modulus. These values are summarized in Table 2.1.

The behaviour of embryonic muscle becomes an important consideration for those working on computer models of embryonic limb morphogenesis. For such models, information on the timing and extent of the forces generated by embryonic muscle contractions is critical. Landmesser and Morris (1975) describe the development of functional innervation in the hind limb of the chick embryo between Hamburger Hamilton (HH) stages 25 and 43.

Table 2.1: Mechanical properties of mouse, chick, bovine and human embryonic cartilaginous tissue

Authors	**Animal**	**Embryonic Age**	**Embryonic Tissue Type**	**Parameter Measured**	**Value**
Tanck *et al.*(2004)	Mouse	16 and 17 embryonic days	Cartilage	Young's Modulus	1.11 ± 0.62 MPa
			Calcified Cartilage	Young's Modulus	117 ± 62 MPa
Mikic *et al.*(2004)	Chick (Control)	Day 14 of incubation	Cartilage	Instantaneous Modulus	0.25 MPa
				Equilibrium Modulus	0.08 MPa
	Chick (Immobilized)		Cartilage	Instantaneous Modulus	0.125 MPa
				Equilibrium Modulus	0.058 MPa
Williamson *et al.*(2001)	Bovine	Mid-third trimester (238.2 days)	Articular Cartilage	Confined Compressive Mod.	0.11 ± 0.03 MPa
			Articular Cartilage (surface layers)	Free swelling compressive Mod.	0.106 ± 0.007 MPa
			Articular Cartilage (middle layers)	Free swelling compressive Mod.	0.153 ± 0.003 MPa
Brown & Singerman (1986)	Human	Full term (9 months)	Chondroepiphysis of femoral head	Equilibrium Modulus	0.699 MPa
				Permeability	2.5×10^{-15} m^4Ns^{-1}

The authors found that most limb muscles or primitive muscle masses become functionally innervated at the same time at around HH27-28, just prior to regular movement of the limbs in the chick embryo. The authors also provide isometric twitch tension data for HH33 chick muscles from which force per unit area values can be deduced. Reiser and Stokes (1982) describe the development of contractile properties of avian embryonic skeletal muscle in terms of twitch and tetanic responses, including force per unit mass values. The authors found that in the last week *in ovo*, the normalized twitch and tetanic forces of the posterior latissmus dorsi muscle, normalised to the mass, increased 3- and 12- fold respectively; from 0.53 mN/mg to 2.10 mN/mg for the twitch response and from 0.76 mN/mg to 9.15 mN/mg for the tetanic response. A decrease in the time to peak twitch force and time to one-half relaxation of the twitch response also took place over this time period. Kardon (1998) provides a thorough account of muscle and tendon morphogenesis in the embryonic chick limb, and describes the close association of the development of these two tissues types.

2.3.2. Single Time-Point Analyses

Carter and co-workers have used computational mechanobiology to examine many aspects of skeletal development such as the influence of stresses on embryonic chondrogenesis and osteogenesis (Carter *et al.*, 1987), alteration of ossification in culture (Wong and Carter, 1990b), the evolution of long bone epiphyses (Carter *et al.*, 1998b) and sesamoid bone formation (Sarin and Carter, 2000). In 1987 Carter *et al.* (1987) hypothesized, following Pauwels (1960), that mechanical stresses influence chondroosseous biology through a combination of intermittently applied shear stresses (or strain energy) and hydrostatic (dilatational) pressure in an FE model. A plane-strain 2-D FE model of the human femur was created for 5 time-points, 3 embryonic stages and 2 post-natal stages. The same shape and loads were used throughout and the material properties assigned were changed to reflect the pattern of ossification. Although a much simplified model, it gives insightful results. High strain energy density values are predicted at the midshaft region in the all cartilage model but, once ossification has begun, strain energy density is highest immediately ahead of the front, peaking at the periosteal surface. In later stages, the region of high strain energy shifts to the centre of the

chondroepiphysis, where the secondary ossification centre appears. Biaxial compressive stresses are predicted near the joint surface and therefore the authors propose that this stimulus inhibits ossification, enabling maintenance of articular cartilage.

Wong and Carter (1990b), performed an analysis of the Klein-Nulend *et al.* embryonic mouse metatarsal organ culture experiment (Klein-Nulend *et al.*, 1986), where intermittent hydrostatic pressure was found to lead to increased calcification in long bone rudiments *in vitro*. An osteogenic index (Carter and Wong, 1988), a combination of the influence of the tissue shear and hydrostatic stresses, was used to predict ossification patterns. The index is given by

$$I = \sum_{i=1}^{c} n_i (S_i + kD_i)$$

where n_i = number of load cycles of load case i, S_i = cyclic octahedral stress, D_i = dilatational (hydrostatic) stress, k= empirical constant, and c = total number of load cases. The authors hypothesized that, once calcification had begun, externally applied hydrostatic pressure produced local shear stresses at the mineralization front, which may have led to increased calcification rates. When a model of the same experiment was created by Tanck *et al.* (1999), with poroelastic (fluid and solid phase) instead of single-phase elastic properties, the hypothesis of Wong and Carter (1990b) could not be confirmed. Results from this axi-symmetric poroelastic FE model indicated that hydrostatic pressure, rather than distortional strain were likely to have enhanced the mineralization process.

Tanck *et al.* (2000) also performed a 3-D poroelastic FE analysis in order to explore the results of another organ culture experiment where a curved mineralization front was found in explanted embryonic mouse metatarsal rudiments (as illustrated in Figure 2.4). The results of the model indicated that fluid pressure was approximately the same at the centre as at the periphery during flexion and extension contractions, and since the rate of mineralization was higher at the centre, pressure was unlikely to be involved in regulation of growth of the mineralization front. The authors concluded that the distributions of distortional strain were compatible with the difference in mineralization geometry.

Sarin and Carter (2000) used FE analysis to investigate endochondral ossification of sesamoid bones such as the patella. A 2-D linear elastic model of a sesamoid cartilage embedded within a fibrous tendon that wraps around a bone prominence was performed. The authors found that high contact pressures inhibit ossification and promote the maintenance of an articular cartilage layer, and high octahedral pressures predict regions favourable for the onset of endochondral ossification as found in sesamoids *in vivo*.

2.3.3. Simulation Models

Simulation type models have been created to model growth and endochondral ossification (Stevens *et al.*, 1999; Van Donkelaar *et al.*, 2006), joint development (Heegaard *et al.*, 1999) and growth front morphology in developmental dysplasia of the hip (Shefelbine and Carter, 2004). Stevens *et al.* (1999) created a model of long bone development incorporating biological and mechanobiological influences (van der Meulen *et al.*, 1993) on endochondral growth and ossification. A time-dependant linear elastic FE model was used to 'grow' the rudiment according to a bone-remodelling algorithm dependant on a calculated cartilage maturation rate. Despite some simplifications such as isometric scaling and constant joint pressures throughout, the results of the simulation predicted events such as a secondary ossification centre, and formation of the growth plate and articular cartilage, as shown in Figure 2.4.

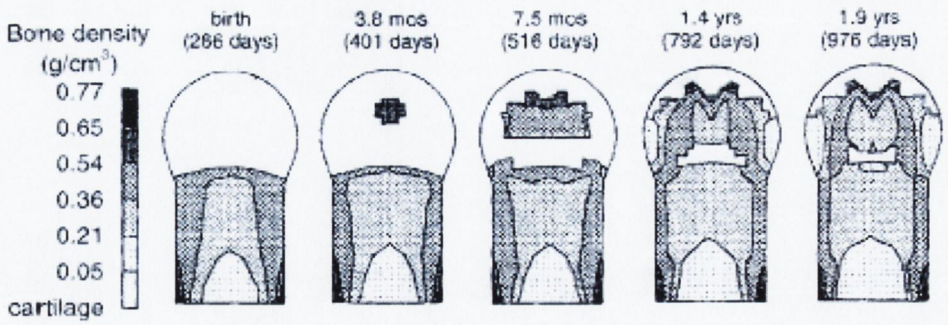


Figure 2.4: Simulation results predict the formation of a secondary ossification centre, growth plate and articular cartilage (from Stevens et al. (1999))

Heegaard *et al.* (1999) simulated morphogenesis of a human interphalangeal joint between days 55 and 70 of fetal life. When using a growth rate based on biological and mechanobiological influences, they found that more congruent articular joint surfaces were formed, whereas if only a baseline biological rate was used the epiphyses would increase in size but remain incongruent. The authors conclude that mechanics are critical to normal joint morphogenesis.

Shefelbine and Carter (2004) described a 3-D model of a third trimester human femur in order to investigate if alterations in hip joint reaction forces could explain abnormal growth front morphology and bony deformities in patients with developmental dysplasia of the hip (DDH). A growth rate based on biological and mechanobiological contributions was used to predict growth front morphology for normal and a range of DDH load histories (greater hip force angles). The octahedral and hydrostatic stress patterns found by the model, as shown in Figure 2.5, predicted that abnormal loads would lead to altered growth front morphology resulting in coxa valga (large neck-shaft) in DDH. The interaction between the perichondrium and the PTHrP-Ihh control loop is simulated by van Donkelaar et al. (2006), and the results indicate that the location of the perichondrium determines the pattern of early mineralization in a cartilaginous anlage.

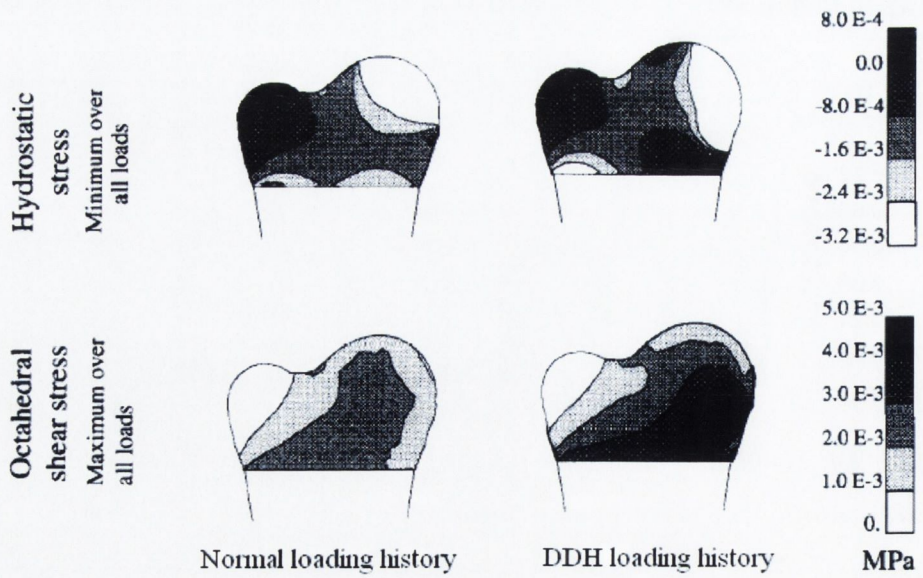


Figure 2.5: Minimum hydrostatic stress and maximum octahedral stress patterns for normal and developmental dysplasia of the hip (DDH) loading histories (adapted from Shefelbine and Carter (2004))

2.4. Evolution of Bone and Mechanoregulation of Bone

As previously described differences between avian and mammalian skeletal development demonstrate, some aspects of skeletal development have diverged between species over evolutionary time. In 1968 Gegenbaur, (cited by Haines, 1969), suggested that endochondral ossification was a much later phylogenetic development than periosteal bone, a suggestion that was questioned by Haines (1969) due to the discovery of endochondral ossification in ancient fishes of the Devonian period (cephalaspids, (Stensiö, 1932)). In some animals, such as the fish belonging to the Chondostei and Dipnoi lineages, the ancestral forms had well developed endochondral bone while in extant types this endochondral bone has been reduced or lost (Watson and Gill, 1925). Secondary ossification centres of ossification were first seen in the Jurassic period (206-144 mya) in the Sapheosaurus (Fuchs, 1908; cited by Haines, 1942), and can be found in many extant lizards and mammals. However, many secondary centres of ossification seem to have been lost in birds (see Section 2.2.1). Sesamoids, while common in mammals and birds, are rarely found in turtles and never in crocodiles (Haines, 1969).

In some animals, such as crocodiles, turtles and birds, periosteal ossification advances faster than erosion of the diaphysis, leaving cartilage in the form of cartilage cones which disappear as development progresses. In a study examining the evolution of epiphyses, Carter *et al.* (1998b) constructed two different FE models of the embryonic chondroepiphysis; the first involved a model with cartilage cones and little cancellous bone to represent crocodiles, turtles and birds, and a second model with well-ossified cancellous bone to represent the mammalian chondroepiphysis. In the FE model which included cartilage cones, the cancellous bone of the epiphysis was not as dense as the mammalian cancellous bone, which led to a lower osteogenic index in the chondroepiphysis. A lower osteogenic index, in the context of this model, leads to a reduced likelihood of bone formation, and Carter *et al.* (1998b) suggest that the reduced osteogenic index in the chondroepiphysis may be why secondary ossification centres do not always form in some animal groups such as birds (Blumer *et al.*, 2005; Doménech-Ratto *et al.*, 1999; Hogg, 1980).

Mechanoregulation of skeletogenesis has been shown to have evolved. Abbott *et al.* (1996) performed histomorphometric analysis of bone fragments in order to compare bone remodelling between Pleistocene humans (200–300 thousand years ago) and a Recent population (the Pecos Pueblo population, New Mexico, occupied from about 1300 to 1828 AD). By comparing osteon population density (the number of osteons in the tissue) and calculating the activation frequency (the mean annual number of new osteons being created) and bone formation rate, the authors found that bone turnover was significantly slower in the Pleistocene populations than in the Pecos Pueblo population. Ruff and Hayes (1983) compared the geometry of long bones of the Pecos Pueblos with modern samples, and found that modern tibiae and femora samples are generally more cylindrical in shape than the Pecos samples. The authors suggest that this difference has evolved due to different loading patterns, but as discussed by Brothwell (1975), it is important to consider the possibility of differential growth changes in conjunction with genetic and adaptive changes as causes for morphological changes over evolutionary time. Therefore, although evidence exists to demonstrate the evolution of the mechanisms governing mechanoregulation, there is limited information on any inherent population level variation in these mechanisms. In addition, while it has been shown that many animals develop bone shapes that are optimal, or close to optimal (Currey and Alexander, 1985), this does not necessarily mean that the mechanoregulation processes are also optimal, even though this has been assumed by some researchers (Bagge, 2000).

2.5. Concluding Remarks

In this chapter, a range of techniques and approaches to embryonic limb mechanobiology have been described. Experimental and computational studies have demonstrated the importance of mechanical forces for embryonic skeletogenesis, but the necessary timing, extent and mechanisms of these forces act remain, as yet, unknown. Several researchers have investigated the evolution of mechanoregulation using archaeological data and theoretical analyses. However, the variance and optimality of the rules governing mechanoregulation in extant populations remains to be explored.

In this thesis, the author advances upon previously developed FE models of embryonic long bone formation to include realistic morphologies and muscle loading at a range of timepoints. The stage-dependant patterns of biophysical stimuli can be correlated with ossification events such as cartilage differentiation and formation and progression of the bone collar. The complexity of these analyses will also enable comparison of predicted biophysical stimuli patterns with gene expression patterns, providing a novel means of identifying potential mechanosensitive genes, building on previous *in vitro* and *in vivo* mechanosensitive gene identification methods.

Following previous research on avian immobilisation, a neuromuscular blocking agent is used to alter the mechanical environment of the embryonic chick, and previously reported effects on skeletal development are verified. Candidate mechanosensitive genes identified by comparing their expression patterns with patterns of biophysical stimuli are characterised in control and immobilised embryos in order to corroborate the mechanosensitive action *in vivo* of these genes.

Finally, experimental evidence of the evolution of mechanoregulation is implemented in a theoretical framework in order to investigate the variation and optimality of the parameters governing mechanoregulation.

A Dynamic Pattern of Mechanical Stimulation Promotes Ossification in Avian Embryonic Long Bones*

3.1.	**Introduction**	**34**
3.2.	**Methods**	**36**
3.2.1.	Data Collection	37
3.2.2.	Finite Element Analysis	39
3.3.	**Results**	**42**
3.3.1.	Muscle Forces	42
3.3.2.	Comparison between specimens	42
3.3.3.	Comparison between aspects and contractions	43
3.3.4.	Comparison between stages	46
3.4.	**Discussion**	**48**

* Accepted: Nowlan, N.C., Murphy, P. and Prendergast, P.J. "A Dynamic Pattern of Mechanical Stimulation Promotes Ossification in Avian Embryonic Long Bones", Journal of Biomechanics.

3.1. Introduction

Mechanical forces due to muscle contractions are important for normal embryonic bone growth (Palacios *et al.*, 1992). The embryonic chick has been used to study the influence of muscle contractions on embryonic skeletal growth (Nowlan *et al.*, 2007). In the chick, by 6 to 6.5 days of incubation, chondrocytes in the mid-diaphysis undergo hypertrophy, and by 6.5 to 7 days of incubation, bone collar formation begins in the mid region of the diaphysis with the deposition of osteoid below the perichondrium. The first mineralization takes place 0.5 to 1 days later in the form of laminae of bone which eventually fuse to form a thin, compact cylinder – the periosteal bone collar (Hall, 1987). Genes have been identified that direct or influence early limb bud formation, for example, the expression of the signalling molecules FGF10 and Wnt8c mark the site of hindlimb bud formation 6 hours before the limb bud becomes visible (Kawakami *et al.*, 2001). In the later developing limb bud, the initiation and progression of ossification is regulated in part by Indian Hedgehog (Ihh) and PTHrP signalling pathways (Vortkamp *et al.*, 1996). However, no explicit link between the mechanical forces generated by muscle contractions and the progression of ossification in the developing limb has yet been elucidated.

Several researchers have attempted to model the effect of mechanical forces due to muscle contractions using Finite Element (FE) analysis but, although a correlation between mechanical stimulation and ossification has generally been predicted in previous models, conflicting conclusions have been proposed. The results from Carter *et al.* (1987), who used a series of 2-D plane-strain FE models of the embryonic and post-natal femur, supported the hypothesis that ossification is accelerated by intermittently applied shear stresses and inhibited or prevented by intermittently applied hydrostatic pressure. Wong and Carter (1990b) performed an FE analysis of the *in* vitro culture study of embryonic mouse skeletal rudiments by Klein-Nulend at al. (1986), and suggest that the increased mineralization rates observed *in vitro* were due to local shear stresses at the mineralization front induced by externally applied hydrostatic pressure. They modelled embryonic cartilage as having linear elastic (single phase) material properties, but when the analysis was repeated by Tanck *et al.* (1999)

using poroelastic (fluid and solid phase) material properties, the same conclusion of shear stress stimulated ossification was not corroborated. In their 3D FE model, Tanck *et al.* (1999) found that distortional strains occurred in the region where mineralization proceeded, but concluded that the distortional (shear) strain was probably too small to have stimulated this. They concluded instead that the diffusion of ions as a result of the applied hydrostatic pressure itself may have enhanced the mineralization process *in vitro*. However, Tanck *et al.* (2000) returned to the hypothesis of strain-mediated mineralization in their FE analysis of the effect of embryonic muscle contractions at the mineralization front of a metatarsal rudiment and concluded that distortional strain rather than hydrostatic fluid pressure is a likely initiator of mineralization for *in vivo* embryonic bone growth. A number of further studies by Carter and co-workers have used a combination of the maximum octahedral shear stress and the minimum hydrostatic pressure as mechanoregulators of endochondral ossification (Wong and Carter, 1990ab), in investigating the endochondral ossification of long bones (Stevens *et al.*, 1999), and sesamoids (Sarin and Carter, 2000) and the formation of *coxa valga* in developmental dysplasia of the hip (Shefelbine and Carter, 2004). Heegaard *et al.* (1999) used local peak hydrostatic stress as a mechanobiological stimulus in their model of embryonic joint morphogenesis.

It is possible that the difficulty in discriminating between the various hypotheses relating to how mechanical forces modulate embryonic bone development is due to simplifications of the morphology, material properties and muscle loading schemes used in previous finite element models. In this chapter, we use optical projection tomography to create a finite element model incorporating realistic 3-D tissue morphologies for bone and more realistic representations of muscle loading. We use the model to test the hypothesis that patterns of biophysical stimuli resulting from mechanical loading due to muscle contractions initiate and propagate ossification in avian embryonic long bones. The quantitative nature of the model combined with its increased morphological accuracy allows quantification of biophysical stimuli active during bone formation in limb development.

3.2. Methods

FE analyses of embryonic chick hindlimb rudiments for a range of developmental stages before and during ossification were performed. Accurate 3D morphologies for skeletal rudiments were obtained and muscle loading magnitudes, locations and attachment sites were calculated from 3D data of the muscle masses and tendons present at each stage examined (Nowlan *et al.*, 2006). The chick embryo staging system developed by Hamburger and Hamilton (HH) (1992) was used. We have observed by histological staining that ossification begins in the tibiotarsus rudiment of the chick between stages HH32 and HH33; therefore we focused on the tibiotarsus rudiment at stages HH30, HH32 and HH34, corresponding to between approximately 7, 8 and 9 days of incubation. Two rudiments for each stage, (i.e., six bones), were modelled in total.

Slightly different terminologies are used to describe the anatomies of animals and humans. In the avian forelimb, proximal is closest to the body and distal is towards the fingertips, the thumb is anterior and the little finger posterior, while the back of the hand is dorsal and the palm ventral, as shown in Figure 3.1 (Gilbert, 2000).

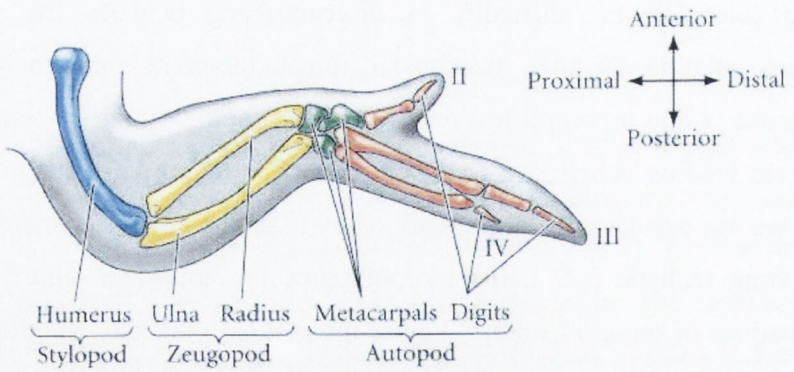


Figure 3.1: Skeletal patterning and axis definition in the chick wing (from Gilbert, 2000)

3.2.1. Data Collection

Optical Projection Tomography (OPT)

Optical Projection Tomography (OPT) (Sharpe *et al.*, 2002) constructs an image by measuring the amount of light transmitted or emitted by an object when light is shone upon it. A specimen is rotated through 360° and a series of snapshots taken at different angles are integrated, using a back-projection algorithm, to give a complete 3D image of the specimen. The resolution is 15μm (Sharpe *et al.*, 2002). OPT can be used to scan coloured specimens, such as those stained with histological stains or after an *in situ* hybridisation procedure. Specimens stained with fluorescent markers can also be scanned. OPT was used to obtain 3D data for cartilage, calcified tissue, muscle and tendon morphologies (Figure 3.2a-c). The specimens stained for cartilage and bone were scanned to obtain the morphology of the rudiments, and those stained for muscle and tendon used to estimate the magnitude, orientation and attachment sites of the muscle forces at each stage.

Obtaining Tissue Morphologies

Cartilage and calcified tissue elements were stained using a modification (0.1% concentration of Alcian Blue instead of 0.015%) of the protocol described by Hogan *et al.* (1994) (see Appendix A for detailed protocol), where Alcian Blue was used for staining cartilage, and Alizarin Red for calcified tissue (Figure 3.2a). At least ten specimens per stage were stained and scanned.

For the specimens stained for muscle and tendon, a minimum of two limbs for each of the three stages were analysed. Control (sense) probes were routinely included. Scleraxis, a bHLH (basic-Helix-Loop-Helix) transcription factor, has been identified as a highly specific marker for tendons and ligaments in the developing limb (Schweitzer *et al.*, 2001). The tendons in the developing limb were visualised by performing whole-mount *in situ* hybridisations (Wilkinson, 1992) using a probe for Scleraxis (chick EST database, clone ID ChEST654f15) (Figure 3.2b). The full *in situ* hybridisation protocol is described in Chapter 4 (Section 4.2.4).

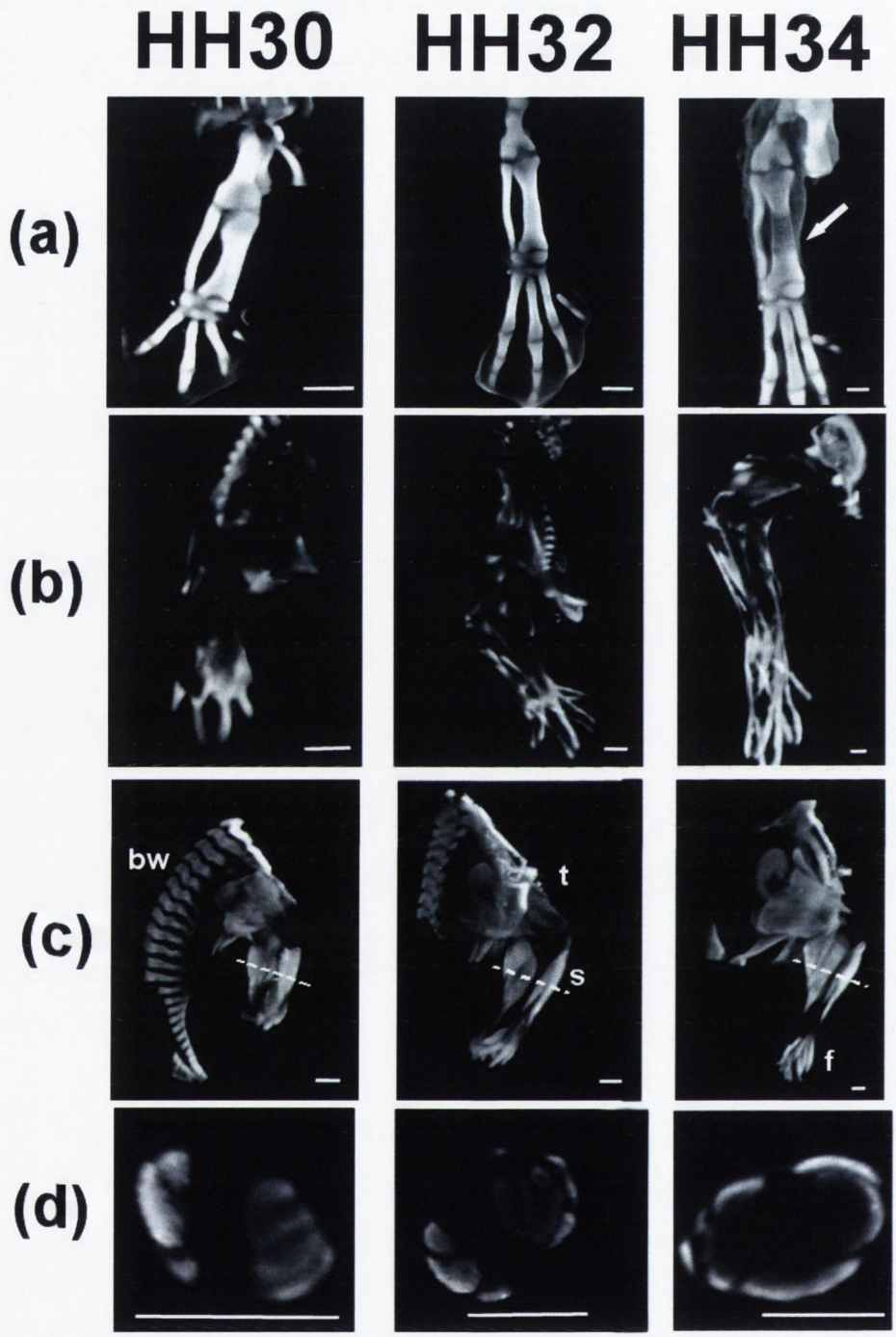


Figure 3.2: Stills from 3D scans of stained tissues at stages HH30, HH32 and HH34. Scale bars approximately 1mm. (a): cartilage (alcian blue), note the darker area (arrow) at the midpoint of the tibiotarsus indicating the first appearance of the bone collar (b): tendon (Scleraxis in situ), (c): muscle (anti-myosin antibody) with planes at which cross-sections were taken, 'bw' indicates body wall, 't' thigh, 's' shank and 'f' footplate muscles masses (d): cross-sections of muscle data from which muscle forces were calculated.

Differentiating muscle cells were stained by immunohistochemistry using a monoclonal antibody (MF20, Developmental Studies Hybridoma bank, 1/20 dilution) that specifically binds to a muscle specific protein, myosin (primary antibody) (Figure 3.2c). The presence of the anti-myosin antibody was subsequently detected by the binding of a fluorescently labelled secondary antibody (Alexa Fluor 488 goat anti-mouse IgG, Molecular Probes, 1/200 dilution, excitation and emission wavelengths 495 nm and 519 nm respectively) (see Appendix A for detailed protocol).

3.2.2. Finite Element Analysis

Morphology

A 3D image VTK (Visualization Toolkit[1]) format was obtained from the OPT data for cartilage and calcified tissue. The VTK representation was imported into Rhino[2], a modelling tool. Slices were taken of the VTK image, and the slices lofted to form a surface. This surface was then imported into CUBIT[3], where it was meshed and converted to a format suitable for Abaqus[4] finite element software. This process is illustrated in Figure 3.3.

The 3D tendon and muscle data were examined, and the number of relevant muscles acting on the rudiments at each stage identified. The transverse cross-sectional area of each muscle was taken at the longitudinal mid–point of the muscle masses (Figure 3.2c-d), and the resultant force calculated using a force per unit area value for embryonic chick muscle of 1.11 mN/mm^2, as derived from Landmesser and Morris (1975). Muscle cross-sectional areas were measured for two specimens at each stage, and the values averaged for calculating the force (see Appendix B). The attachment point for each muscle was located on the rudiment by visual comparison of the 3-D tendon data with a merged 3-D movie of the cartilage and muscle data at corresponding stages.

---

[1] http://public.kitware.com/VTK, last accessed 22-01-2007

[2] ©, http://www.rhino3d.com/, last accessed 22-11-2006

[3] ©, http://cubit.sandia.gov/, last accessed 22-11-2006

[4] ©, http://www.hks.com/, last accessed 22-11-2006

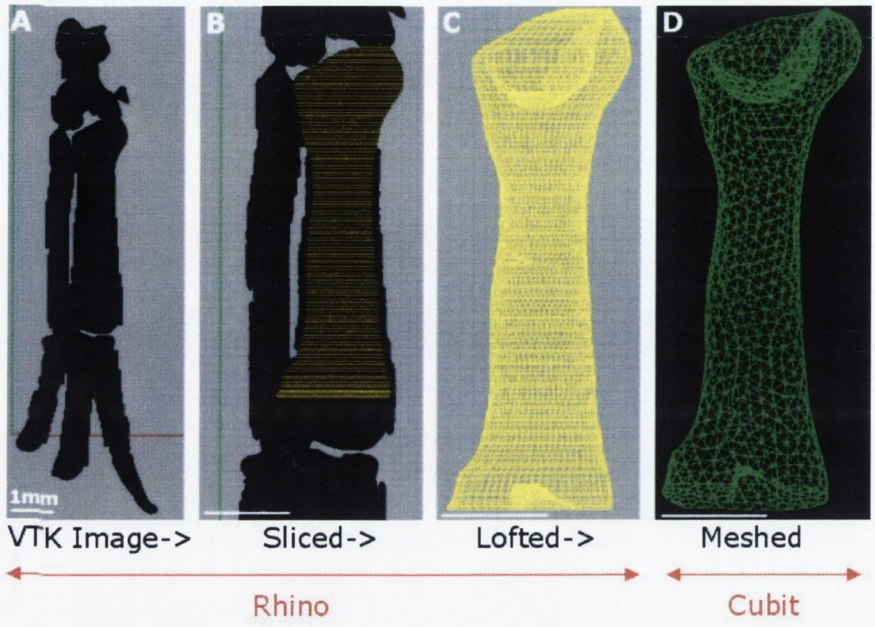


Figure 3.3: A 3D image from the OPT scan was sliced and lofted in Rhino, and the resulting shape meshed in Cubit.

Material Properties

At stages HH30 and HH32, the rudiment consists of cartilage only, while at Stage HH34 onwards, cartilage and calcified tissue are present (Fig 1a). As cartilage is a biphasic material, a poroelastic analysis was performed. Ten-node tetrahedral elements were used for the FE analysis, which was performed in Abaqus®. The mechanical properties calculated by Tanck *et al.* (2004) for the Young's modulus of unmineralized and mineralized embryonic mouse ribs were used, with the values from Tanck *et al.* (2000) for permeability and Poisson's ratio. The properties, for unmineralised and mineralized cartilage, are as follows: 1.1 MPa and 117 MPa for Young's modulus [E], 6.7×10^{-15} $m^4/N.s$ and 6.7×10^{-16} $m^4/N.s$ for permeability (k) and 0.25 and 0.30 for Poisson's ratio [v], respectively. A porosity of 0.8 (Kelly and Prendergast, 2005) was used. The calcified cartilage collar was modelled as a shell which extends into the rudiment to a thickness of 0.1 mm, a figure obtained by the depth of Alizarin Red staining in transverse cryostat sections of tibiotarsi (not shown).

Boundary Conditions

Following Tanck et al. (2000), one loading cycle consisted of two muscle twitches, a flexion contraction followed by an extension contraction where each twitch lasted for 1.4 seconds which includes ramp up, hold and ramp

down phases. As also described in that study, it was assumed that during the flexion contractions, each muscle on the ventral aspect of the rudiment was activated, while during the extension contraction the muscles on the dorsal aspect were activated. This has been shown to be the case in avian embryonic development, between seven and nine days of incubation (Bekoff, 1976). The force of each muscle transmitted by the adjoining tendons was estimated as being spread over an element face at the distal end of the rudiment in the form of a surface traction. Two of the nodes at the proximal end of the rudiment were restrained from movement, while the rest of the nodes at the proximal end were restrained in the vertical direction only. A spring was attached to a rigid plate connected to the distal end of the rudiment to simulate the restraint of the opposing joint, as illustrated in Figure 3.4. The stiffness of the spring was calculated as that of an opposing block of cartilage of varying height according to stage, as detailed in Table 3.1. A zero pore-pressure boundary condition was specified on all the external nodes of the rudiment, thereby allowing fluid flow out of the structure. For each analysis, the following parameters were computed; maximum principal stress, maximum principal strain, octahedral strain, relative fluid-solid velocity and hydrostatic pressure. A stimulus (S) was defined, following Prendergast *et al.* (1997a), as a combination of the shear strain and fluid velocity, as defined by

$$S = \frac{\gamma_{oct}}{a} + \frac{v}{b}$$

where a= 0.0375, and b=3μms^{-1}.

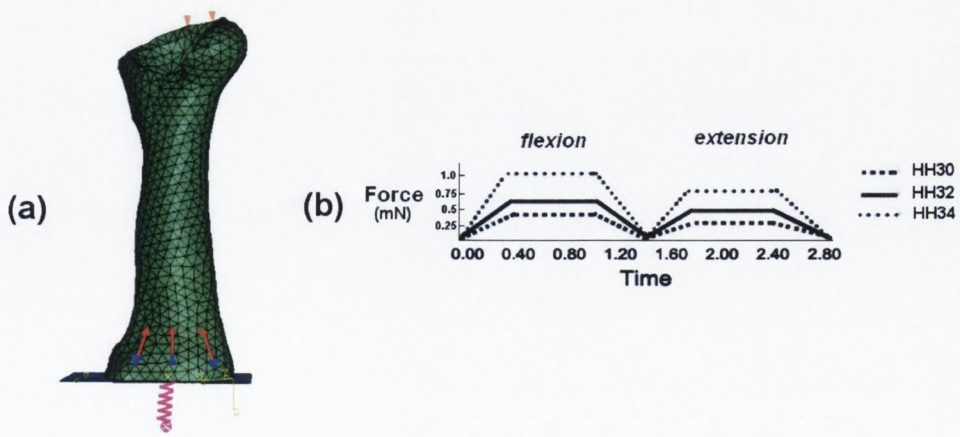


Figure 3.4: Illustration of (a) distal spring restraint, fixed nodes, loads for flexion contraction at HH32, and (b) loading regimes for HH30, HH32 and HH34.

Table 3.1: Length of spring, average area of rudiment base and average stiffness values for springs used to represent joint reaction force at stages HH30, HH32 and HH34

STAGE	Length of Spring (l)	Average area of base of rudiment (A)	Stiffness, $k = \frac{EA}{l}$
HH30	0.1 mm	0.15 mm²	1.5 N/mm
HH32	0.3 mm	0.9 mm²	3.3 N/mm
HH34	0.5 mm	0.875 mm²	2.4 N/mm

3.3. Results

3.3.1. Muscle Forces

The forces were calculated for ventral and dorsal muscles at stages HH30, HH32 and HH34 as shown in . By HH34, the force exerted by the ventral muscles was found to increase to 0.962 mN, and by the dorsal muscles to 0.607 mN.

3.3.2. Comparison between specimens

Morphological analyses were carried out, and two specimens that were typical for each stage were chosen for FE analysis. The length of these rudiments was, on average, 2.3mm at stage HH30, 4.2mm at HH32 and 5.7mm at HH34. The FE analysis for two specimens at each stage showed that, although peak values did not correlate exactly between specimens, these peak values were within 10% of each other at stages HH32 and HH34 (see Appendix C). However, the patterns of mechanical stimuli were very similar, as shown in a comparison of fluid velocity, and maximum principal stresses for specimens A and B at stage HH34 (Figure 3.5). Therefore, in order to avoid repetition, the results shown in the following sections are from one set of specimens (Set A), but the patterns have been corroborated in a second complete set. The results are presented as a series of dorsal and/or ventral views at the mid time-point of the flexion and extension contractions, i.e., 0.7 seconds into each contraction.

Table 3.2: Mean values for cross-sectional areas of ventral and dorsal muscles and the resultant force exerted by flexion and extension contractions. Muscle areas averaged from data from two specimens at each stage.

	Ventral Muscles (Flexion)		**Dorsal Muscles (Extension)**	
STAGE	Average Area (mm^2)	Average Force (mN)	Average Area (mm^2)	Average Force (mN)
HH30	0.326 (±0.1)	0.362	0.188 (±0.03)	0.209
HH32	0.489 (±0.36)	0.543	0.285 (±0.23)	0.317
HH34	0.837 (±0.3)	0.929	0.560 (±0.13)	0.621

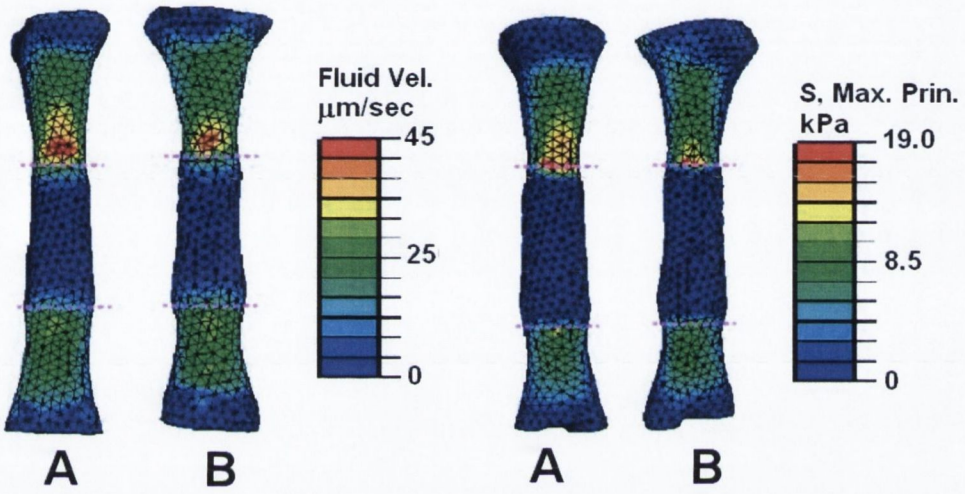


Figure 3.5: Comparison of fluid velocity (ventral aspect) and maximum principal stress (dorsal aspect) for specimens A and B at stage HH34. Dashed line indicates length of bone collar.

3.3.3. Comparison between aspects and contractions

The most dramatic changes in biophysical stimuli patterns took place at the surface of the rudiments, and therefore the results presented here focus primarily on the ventral and dorsal surfaces of the rudiments at each stage. The stress, strain, octahedral strain and fluid velocity differed in some respects as regards relative levels of concentration during different contractions, or between ventral and dorsal aspects, as shown for a single FE analysis of a HH32 rudiment in Figure 3.6. With stress and strain, the concentrations reached higher values on the opposite side to load application; i.e., higher on the dorsal aspect during the flexion contraction (in which the load is applied ventrally) and on the ventral aspect during the extension contraction (Figure 3.6a-c). Octahedral strain tended to be highest during the flexion contraction on

the ventral aspect than at any other time during the loading cycle (Figure 3.6b), and the fluid velocity also reached higher levels on the ventral aspect during both contractions (Figure 3.6d). The fluid velocity profiles did not follow the load application profiles exactly, with a low point occurring before the load goes to zero in between the two contractions (data not shown). Stress values tended to be very low on the aspect of load application (Figure 3.6c). During the flexion contraction, hydrostatic pressure was positive on the ventral aspect and negative on the dorsal aspect, while during the extension contraction the opposite was true. At HH32, the stimuli were concentrated at the proximal end of the rudiment during the extension contraction (Figure 3.6a-d). During the loading cycle, stress and strain values were at a maximum throughout the 'hold' phase, while fluid velocity, hydrostatic pressure and stimulus (S) peaked at the top of the first ramp phase of each contraction.

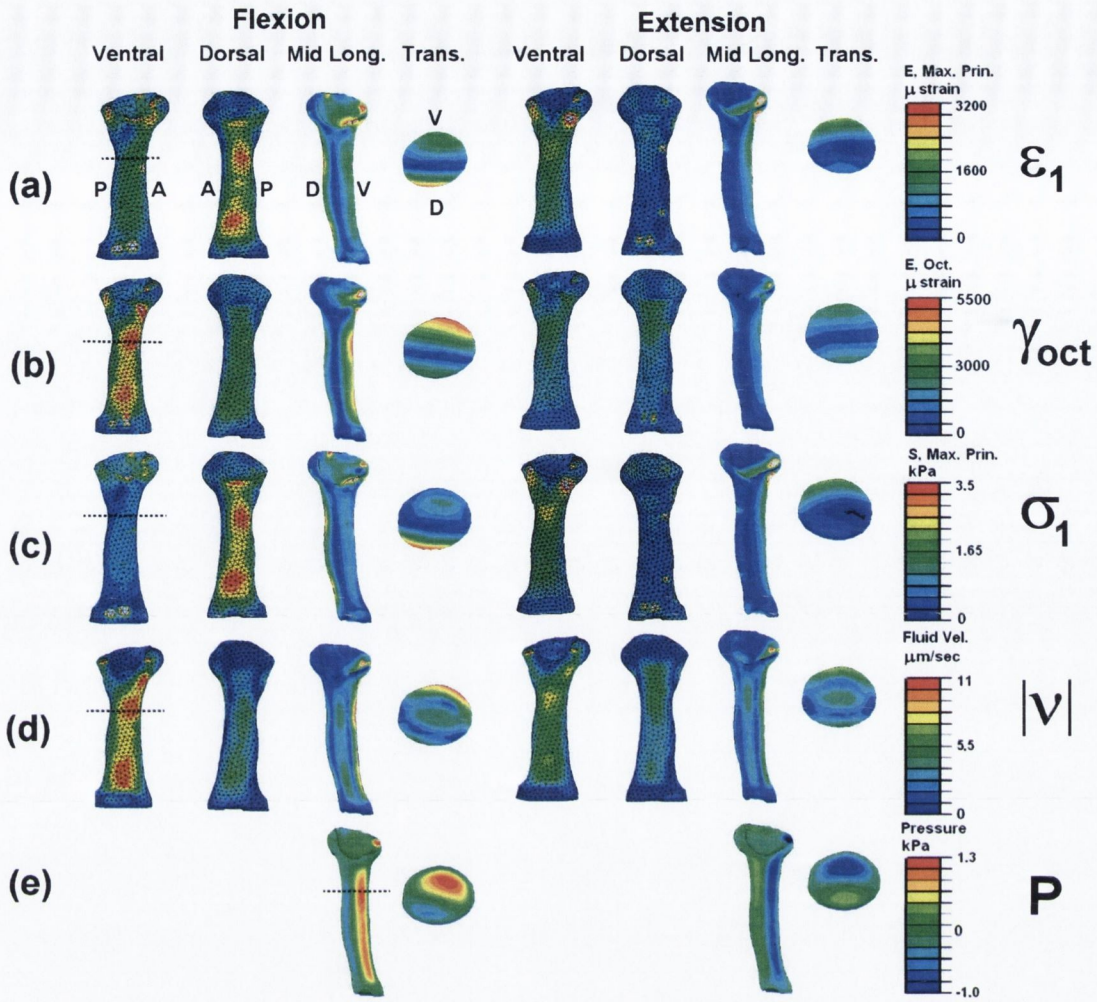


Figure 3.6: FE analysis results for HH32 mid-flexion and mid-extension contractions. Ventral, dorsal, mid-longitudinal (Mid. Long.) section and transverse (Trans.) section views (transverse sections taken at level illustrated by dashed line. Proximal is up, distal is down. During flexion, loads are applied on the ventral aspect, and during extension on the dorsal aspect. 'A' represents anterior, 'P' posterior, 'V' ventral and 'D' dorsal. Views for all representations as detailed in (a). (a): Maximum principal strain (μstrain), (b): Octahedral strain (μstrain), (c): Maximum principal stress (kPa), (d): Fluid velocity (μm/sec), (e): Hydrostatic pressure (kPa).

3.3.4. Comparison between stages

All stimuli changed in pattern and magnitude as the rudiment grows and develops. Within each stage, the patterns obtained for the maximum principal stress (σ_1), maximum principal strain (ε_1), octahedral shear strain (γ_{oct}) fluid velocity (v) and stimulus (S) were quite similar to each other (Figure 3.7). In the earliest stage examined, HH30, concentrations of each of these variables occurred at the mid-diaphysis. Later, at HH32, although the rudiment was still composed only of cartilage, a slight bulge was present at the mid-diaphysis (indicated by arrow on Figure 3.7a). This caused the concentration of biophysical stimuli to relocate distal and proximal to the mid-diaphysis, giving two distinct concentrations above and below the site where the periosteal bone collar would *later* form (HH32, Figure 3.7a-f). The pattern was extended at stage HH34, with concentrations located even more proximally and distally to where the bone collar had now formed.

When the fluid velocity and octahedral shear strain at the surface were plotted along the length of the rudiments (for a path along the ventral surface of the rudiments), both separately and combined as the stimulus S, dynamic changes in stimuli become more evident. At HH30, one peak at the mid-diaphysis is predicted. At HH32 two peaks distal and proximal to the mid-diaphysis are predicted, where the value of the stimulus at the mid-point however is similar to that at HH30. At HH34, much larger and more separated peaks are predicted, with very low stimulus values at the mid-diaphysis (Figure 3.8). At HH34, the peak values of stimuli were higher at the proximal end of the rudiment (Figure 3.7a-f). Peak values for each of the stimuli increased by an average of 5.5 fold over the three stages, as shown in Table 3.3.

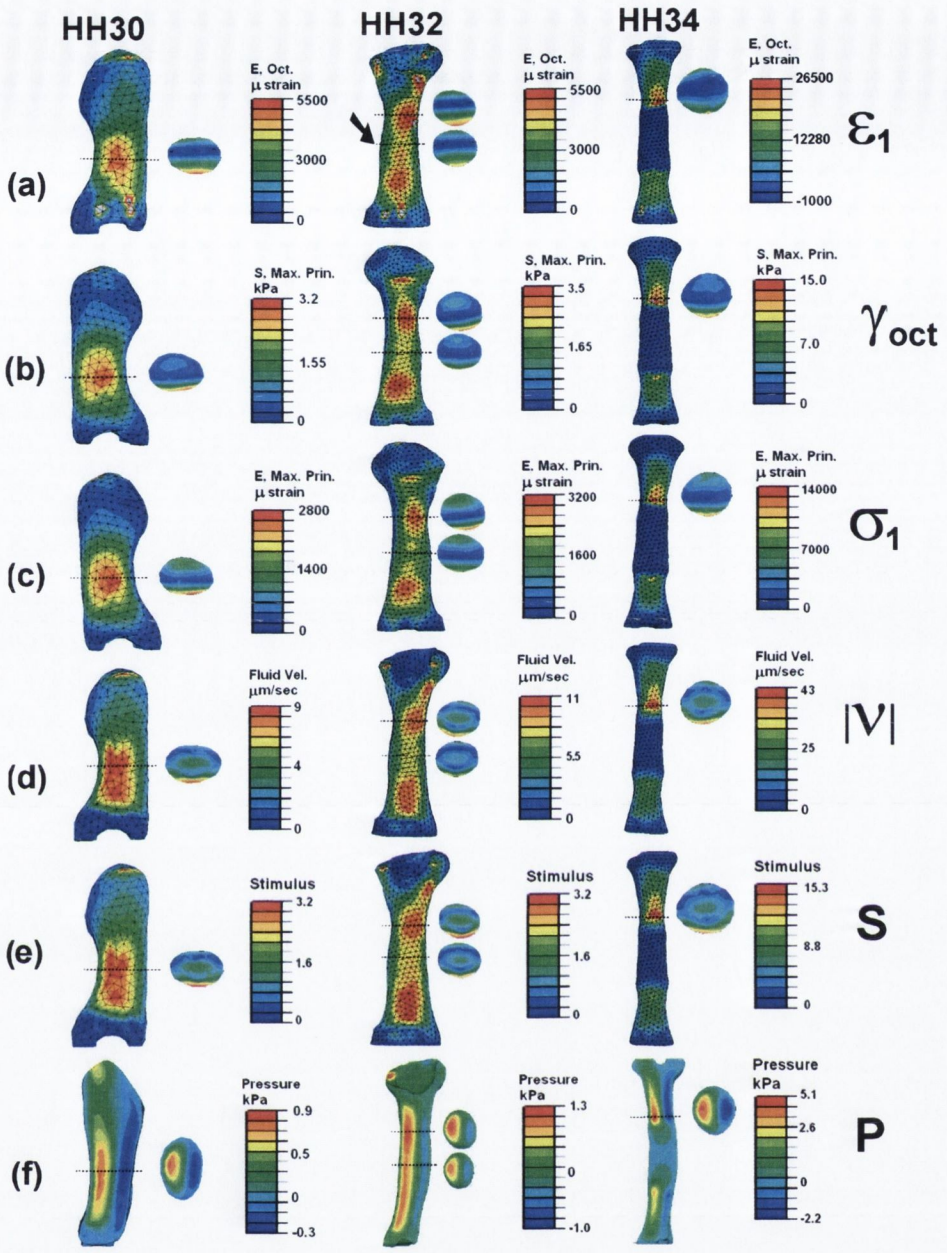


Figure 3.7: Mechanical stimuli patterns at HH30, HH32 and HH34, mid-flexion contraction. Transverse sections are at level indicated and in distal direction. Arrow in (a) indicates bulge at mid-diaphysis at HH32.

(a): Maximum principal strain (μstrain), dorsal aspect.

(b): Octahedral strain (μstrain), ventral aspect,

(c): Maximum principal stress (kPa), dorsal aspect,

(d): Fluid velocity (μm/sec), ventral aspect,

(e): Stimulus, ventral aspect,

(f): Hydrostatic pressure (kPa), midline longitudinal section.

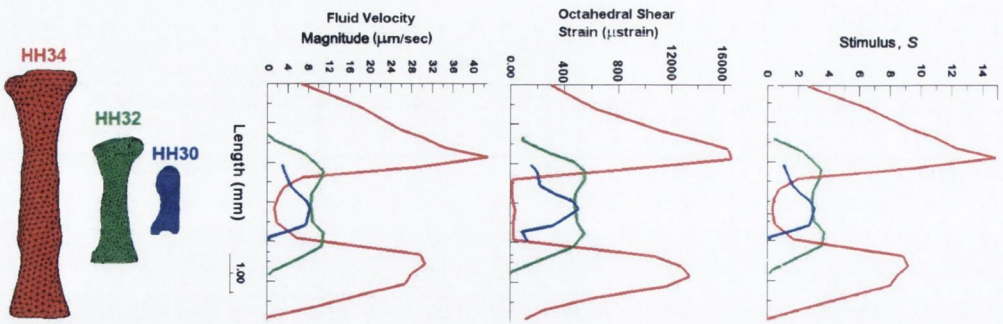


Figure 3.8: Comparison of fluid velocity, octahedral shear strain and stimulus values mid-flexion along the length of the ventral aspect of rudiments at HH30, HH32 and HH34.

Table 3.3: Maximum values of stimuli over flexion and extension contractions for HH30, HH32 and HH34.

STAGE	Maximum Principal Strain (μstrain)	Octahedral Shear Strain (μstrain)	Maximum Principal Stress (kPa)	Fluid Velocity (μm/sec)	Hydrostatic Pressure (kPa)
HH30	0–2800	0–5500	-0.1–3.2	0–9	-0.9 – 0.9
HH32	0–3200	0–5500	-0.1–3.5	0–11	-0.98 – 1.3
HH34	0–14000	0–30000	0–15.0	0–43	-2.2 – 5.1

3.4. Discussion

All of the mechanical stimuli examined showed dramatic changes in pattern as mineralization and bone formation proceed in the rudiment. At the earliest stage examined, (HH30), stress, strain (maximum principal and octahedral shear), hydrostatic pressure and fluid velocity were at a high level of concentration at the mid-diaphysis of the long bone rudiment at the location where the periosteal bone collar will begin to form 1-1.5 days later. At approximately HH32, the diameter of the rudiment at the mid-diaphysis expands, probably due to hypertrophy of the chondrocytes in this region. This leads to an instability whereby the single region of concentration of biophysical stimuli separated into two locations proximal and distal to the site of the future bone collar. After the bone collar appeared (HH34), the concentrations peaked proximal and distal to the bone collar. This means that stress, strain and fluid velocity levels were highest at locations where the bone collar would form some time later. We propose that high cycles of stimulus occur in the

cartilaginous tissue as a promoter of ossification, where the cyclic nature of the stimulus is due to muscle contractions. A delay between patterns of high stimulus levels and bone collar formation indicates that mechanical stimuli could be influencing events prior to mineralization– they may stimulate chondrocyte hypertrophy. As the changes in biophysical stimuli patterns are most dramatic at the surface of the rudiment in the perichondrium, rather than at the core where chondrocytes first undergo hypertrophy, an intermediary signalling mechanism or pathway would be necessary to translate mechanical information from the surface to the core. Alternatively, a time-lag could exist between peak mechanical stimuli levels and the response of the inner cambial layer of the perichondrium, with stimuli levels prompting the formation of osteoblasts in conjunction with signalling from the hypertrophic core.

Some simplifications included in the analysis may have influenced the outcome of the model. Each muscle load was approximated as being distributed over an element face whereas, in reality, the tendon is inserted into the rudiment tissue. This simplification caused peak concentrations at the load application sites for stress and strain, as seen in Figure 3.6a-c. However, these additive peaks were at the proximal end of the rudiment, distant from the mid-diaphyseal region of interest. Furthermore, the material properties used were for murine embryonic cartilage and calcified cartilage rather than for avian tissues, as avian properties have not yet been measured. Constant material properties were used for the cartilage in the rudiment, and while it has been shown that the late-hypertrophic zone in rabbit growth plates has a higher Young's Modulus than the reserve zones (Radhakrishnan *et al.*, 2004), without similar testing of avian tissues, it cannot be assumed that avian growth plate material properties vary in a similar fashion. In addition, the cross-sectional areas of the muscle masses were calculated assuming that the muscle fibres were parallel. However, although different material properties or muscle force magnitudes may change the magnitudes of the stimuli, the resultant patterns will not be significantly altered.

It should be noted that the chick skeletal development differs from that of mammals. Avian long bones have no primary endochondral ossification centre and form bone tissue primarily via periosteal ossification (Fell, 1925).

Therefore, the analyses presented here do not address endochondral ossification per se, but are relevant to events that are shared by birds and mammals and precede mammalian endochondral ossification, such as chondrocyte hypertrophy and periosteal ossification.

The results of the analyses suggest that we revisit some of the hypotheses published previously. The epigenetic influences of mechanical forces have often been considered as having a direct relationship to cell differentiation; for example, Wong and Carter (1990b) suggested that high shear stress values lead to accelerated osteogenesis while Tanck et al. (2000) proposed that high strain values at the periphery of an embryonic rudiment increase the mineralization rate. Our results suggest a more complex relationship, where a cyclic pattern of stimulus levels is established which pre-disposes to bone formation at a later time. It is possible that the decreased cyclic stimulus levels at the mid-diaphysis due to expansion of the cartilaginous rudiment in this region could trigger the ossification progress; where these stimulus levels result from a bending moment induced by cyclic muscle forces.

In this study we set out to test the hypothesis that mechanical forces due to muscle contractions initiate and propagate periosteal ossification. We created a set of FE analyses at three different timepoints with a high level of accuracy for the geometry and loading conditions. A cycle of fluctuations of stress, strain, hydrostatic pressure and fluid flow concentrations were found on the perichondrium in regions of the rudiment that form bone sometime later, a number of hours before this ossification occurs. The results imply that, in order for a region to undergo ossification, levels of cyclic mechanical stimuli must be experienced in this region at a high level a number of hours in advance of mineralization. Our results are consistent with the view that a sustained period of cyclic stress promotes chondrocyte hypertrophy; therefore stimulating mineralization and subsequent bone collar formation.

Correlation of *in vivo* Mechanosensitive Gene Expression with Mechanical Stimulation

4.1.	**Introduction**	**52**
4.1.1.	In vivo identification of mechanosensitive genes	52
4.1.2.	Alteration of the embryonic mechanical environment	53
4.1.3.	Correlation of Patterns of Gene Expression and Biophysical Stimuli	54
4.1.4.	Candidate Mechanosensitive Genes	54
4.1.5.	Aims of this Chapter	56
4.2.	**Methods**	**57**
4.2.1.	Selection of Candidate Genes	57
4.2.2.	Probe Synthesis	59
4.2.3.	Sectioning	60
4.2.4.	*In situ* hybridisation	60
4.2.5.	Immobilisation	61
4.3.	**Results**	**63**
4.3.1.	Mechanosensitive gene expression patterns	63
4.3.2.	Viability and Efficacy of Immobilisation Treatment	67
4.3.3.	Effect of Immobilisation on Skeletal Morphology	68
4.3.4.	Effect of Immobilisation on Mechanosensitive Gene Expression	70
4.4.	**Discussion**	**77**
4.4.1.	Correlation gene expression patterns with mechanical stimulation	77
4.4.2.	Effect of Immobilisation on Mechanosensitive Genes	83
4.5.	**Conclusion**	**87**

4.1. Introduction

4.1.1. In vivo identification of mechanosensitive genes

Most mechanosensitive genes have been identified by *in vitro* studies where gene expression levels in mechanically stimulated cells in culture are compared with expression levels in non stimulated controls (e.g., Cillo *et al.*, 2000; Jackson *et al.*, 2006; Wong *et al.*, 2003). Although up- or down-regulation of genes *in vitro* due to mechanical stimulation is useful for identifying large numbers of candidate mechanosensitive genes, such studies examine the response in cells outside their normal tissue context. Therefore, further corroboration is needed to implicate these genes as mechano-transducers during specific events *in vivo.* A small number of studies have demonstrated a difference in quantitative gene expression levels following an alteration of the mechanical environment *in vivo* in adult animals. For example, MacLean *et al.* (2003) performed two types of *in vivo* analysis of the response of cells of the intervertebral disc, to dynamic compression and also to immobilisation using a rat tail model. The study examined mRNA levels in the annulus and found that the genes encoding collagen types I and II were downregulated by both dynamic compression and immobilisation while aggrecanase, collagenase and stromelysin mRNA levels were upregulated (MacLean *et al.*, 2003). Ng et al. (2006a; 2006b) applied repeated mechanical loading in the condylar cartilage of the rat using a stepwise mandibular advancement apparatus. When RNA was extracted from condylar cartilage, it was found that Ihh and PTHrP mRNA levels were upregulated by the loading regime (Ng *et al.*, 2006a; 2006b). RNA extraction from whole tissues was also used by Hardiman *et al.* (2005), who demonstrated changes in c-fos and osteocalcin mRNA levels in the periosteum after *in vivo* hindlimb suspension in a rat model, and by Raab-Cullen *et al.* (1994), who found that transforming growth factor-β (TGF-β) and insulin-like growth factor 1 (IGF-1) mRNA levels in the periosteum were elevated *in vivo* by four point bending of rat tibiae.

Observing an alteration in pattern of gene expression in the tissue rather than an increase or decrease in mRNA levels is perhaps more informative, as a change in location or pattern of gene expression within the context of specific

biological tissues and events can demonstrate not only the mechanosensitivity, but can also potentially identify the mechanoregulatory role of that gene. This is particularly important during development of the bone where events are hugely dynamic and localisation of events within the developing tissue can be very informative.

Kavanagh *et al.* (2006) examined the expression patterns of three signalling molecules; growth and differentiation factor 5 (GDF-5), FGF-4 and FGF-4, all of which are implicated in regulating joint formation, in the presumptive joint regions of control and immobilized chick embryonic hindlimbs. The authors found that joint line FGF-2 expression was diminished in immobilized limbs and concluded that FGF-2 has a direct mechano-dependant role in the cavitation process. The study of Kavanagh *et al.* (2006) is unique in that it is the only study to demonstrate a mechanoregulatory role for a gene in embryonic development by an alteration of the mechanical environment *in vivo*.

4.1.2. Alteration of the embryonic mechanical environment

Alteration of the mechanical environment of the mammalian embryo *in utero* provides a challenge due to the dependence of the embryo on its mother. The advantage of amniotes such as the chick is that the embryo grows independently *in ovo* and can be easily accessed and manipulated. For this very reason, many researchers have used the chick as a model system for examining aspects of skeletogenesis such as joint development (Kavanagh *et al.*, 2006; Lelkes, 1958; Mikic *et al.*, 2000) and formation of the skeletal elements (Hall and Herring, 1990; Hosseini and Hogg, 1991a, 1991b), as detailed in full in the Literature Review. As previously described, the most common method of immobilisation is through administration of the neuromuscular blocking drug decamethonium bromide, which prevents skeletal muscle contractions when dropped onto the chorioallantoic membrane above the embryo or injected into the air sac. When using the chick as a model system for skeletogenesis, however, it is important to keep in mind the differences between avian and mammalian long bone ossification, as detailed in the Literature Review.

4.1.3. Correlation of Patterns of Gene Expression and Biophysical Stimuli

It is also possible to identify potential mechanosensitive genes using computational modelling, where regions predicted to be under high mechanical stimulation are correlated with expression of certain genes by comparing gene expression patterns with patterns of biophysical stimuli such as the study performed by Lee *et al.* (1996). In this study, finite element analysis was used to determine the distribution of stress in a coronary lesion, which was compared with the expression pattern of matrix metalloproteinase 1 (MMP-1) in 12 unruptured human coronary lesions, and it was found that within a given lesion, the highest-stress region had twofold greater MMP-1 expression than the lowest-stress regions (Lee *et al.*, 1996), identifying MMP-1 as a candidate mechanosensitive gene.

Henderson *et al.* (2007) compared theoretically predicted patterns of growth-related stresses and strains generated during the growth of a skeletal condensation with *in vivo* expression patterns of chondrogenic and osteogenic genes, and proposed that predicted patterns of pressure correspond with expression patterns of chondrogenic genes and that predicted patterns of strain correspond with patterns of osteogenic genes (Henderson *et al.*, 2007). However, the biophysical stimuli were predicted using a simplified 2-D finite element model with two axes of symmetry and were compared with gene expression data from transverse sections, showing only limited information on the distribution of expression.

4.1.4. Candidate Mechanosensitive Genes

As reviewed in Section 1.1.2, a number of genes involved in embryonic bone formation have been identified as being mechanosensitive, such as those encoding Collagen X (ColX), Fibroblast Growth Factor receptor2 (FGFr2), Indian hedgehog (Ihh) and Parathyroid hormone-related protein (PTHrP, also known as Parathyroid hormone-like hormone, or Pthlh). The products of these genes influence progression of the growth plates by affecting proliferation or hypertrophy of the chondrocytes in the cartilage of the rudiment, steps preliminary to both endochondral and periosteal ossification.

Collagen X, which is synthesised by hypertrophic chondrocytes (Kielty *et al.*, 1985), has been identified as playing a role in matrix mineralization by Kwan *et al.* (1997), who generated ColX deficient mice which exhibited abnormal trabecular bone architecture, bone content and growth plate architecture (Kwan *et al.*, 1997). ColX was shown to be upregulated in *in vitro* cultures of bovine chondrocytes under cyclic tension and cyclic hydrostatic pressure (Wong *et al.*, 2003) and in *ex vivo* mechanical stimulation of neonatal rabbit distal femoral condyle explants (Sundaramurthy and Mao, 2006). Although a purely structural role is commonly assumed for ColX, it was chosen for examination in this study in order to examine a potential link between patterns of biophysical stimuli and hypertrophy events (ColX is used as a marker for hypertrophic chondrocytes).

FGFr2 was shown to mediate positive regulation of chondrocyte proliferation by Eswarakumar *et al.* (2002), who created a mouse line deficient in the mesenchymal splice variant of the gene (FGFr2IIIc), and found that the balance between proliferation and differentiation was shifted towards differentiation, leading to premature loss of growth and dwarfism in the long bones and axial skeleton (Eswarakumar *et al.*, 2002). FGFr2 was shown to be expressed in the perichondrium, periosteum and in proliferating chondrocytes in the mouse (Delezoide *et al.*, 1998), and has been shown to be downregulated following *in vitro* four point bending of MC3T3-E1 preosteoblasts (Jackson *et al.*, 2006) and upregulated in *in vitro* mechanical stimulation of bone marrow stromal cells (Li and Hughes-Fulford, 2006).

Ihh is also a positive regulator of proliferation (St-Jacques *et al.*, 1999), and controls the onset of chondrocyte hypertrophy primarily via PTHrP (Lanske *et al.*, 1996). Ihh null mice exhibited initially delayed, then reduced chondrocyte proliferation in the core of the element; and a complete absence of mature osteoblasts in the periosteum and in the core of the rudiment (St-Jacques *et al.*, 1999). This absence of mature osteoblasts meant that the Ihh null mice did not form a periosteal bone collar. Since Ihh is expressed in the prehypertrophic chondrocytes and not in the perichondrium/periosteum, Ihh signalling from the proliferative region is necessary to induce the differentiation of the perichondrium into an osteogenic tissue from which the first osteoblasts will

differentiate (St-Jacques *et al.*, 1999). So Ihh is required for formation of bone in the bone collar and also influences endochondral bone formation in the mouse. PTHrP signalling has also been shown to negatively regulate the switch from a proliferative immature chondrocyte to a post-proliferative mature hypertrophic chondrocyte (Weir *et al.*, 1996), as mice lacking PTHrP or its receptor exhibit dwarfism of the long bones due to premature chondrocyte maturation (Karaplis *et al.*, 1994; Lanske *et al.*, 1996). Ihh and PTHrP have been shown to be upregulated by mechanical stimulation; Ihh and PTHrP in *in vivo* mechanical stimulation of rat mandibular condyles (Ng *et al.*, 2006a; Ng *et al.*, 2006b), Ihh in *in vitro* cyclic mechanical stimulation of embryonic chick chondrocytes (Wu *et al.*, 2001) and PTHrP in *in vitro* cyclic mechanical stimulation of rat growth plate chondrocytes (Tanaka *et al.*, 2005).

4.1.5. Aims of this Chapter

In this chapter, I describe the expression patterns of the 4 genes listed above during bone collar formation in the tibiotarsus. Although previously classified as mechanosensitive in other situations, this study was designed to assess their involvement in transducing mechanical information provided by the developing limb musculature during ossification, by correlating their developmental expression patterns with the biophysical stimuli predicted to be acting in the developing rudiment. With the 3-D rudiment morphologies and the realistic muscle loading schemes of the finite element analyses described in Chapter 3, it was possible to compare the complex and time-dependant patterns of biophysical stimuli induced by embryonic muscle contractions with gene expression patterns at several timepoints. Genes which showed a correlation with patterns of mechanical stimuli were highlighted as potential 'mechano-transducers' of mechanical forces due to embryonic muscle contractions *in vivo*.

In order to further explore a direct link between mechanical stimulation due to muscle contractions and the expression of these candidate genes, an altered mechanical environment was created in the chick by preventing embryonic muscle contractions using a neuromuscular blocking agent, and the previously identified candidate mechanosensitive genes were characterised in control and

immobilised embryos in order to investigate their mechanoregulatory role *in vivo*.

4.2. Methods

Except where otherwise stated, all chemicals used were from Sigma, UK.

4.2.1. Selection of Candidate Genes

Selection of candidate genes for this study was based on three criteria: (1) evidence of mechanosensitivity *in vitro*; (2) evidence of a central role during initiation and/or progression of embryonic ossification during long bone development; (3) Evidence of detectable localised expression within developing mouse long bones. As mentioned in Section 1.2.2, there are limited published data on expression patterns of genes involved in ossification in the chick, and therefore published data for a range of candidate mechanosensitive genes were examined for distribution and timing of expression in the mouse limb (at analogous stages to our stages of interest in the chick) using the Mouse Genome Informatics (MGI) Database*. The four candidate genes selected based on these criteria were Collagen X (ColX), Fibroblast Growth Factor receptor2 (FGFr2), Indian hedgehog (Ihh) and Parathyroid hormone-related protein (PTHrP). The roles of these genes in bone formation and a summary of their expression profile in the mouse are given in Table 4.1, and a sample image of published gene expression patterns in the mouse for each gene is given in Figure 4.1. Although it could not be assumed that gene expression patterns would be the same for chick and mouse, these genes are highly conserved and early events of long bone ossification are the same for both species (see Section 2.2.1). Each gene was analysed at the same stages examined in the FE analysis, i.e., HH30, HH32 and HH34, with particular focus on the tibiotarsal rudiment.

---

* Mouse Genome Database (MGD), Mouse Genome Informatics Web Site, The Jackson Laboratory, Bar Harbor, Maine. World Wide Web (URL: http://www.informatics.jax.org). [April, 2007].

Table 4.1: Roles of candidate mechanosensitive genes selected for analysis, with role in bone formation and published expression profile in mouse. ColX: Collagen X, FGFr2: Fibroblast growth factor receptor 2, Ihh: Indian Hedgehog, PTHrP: Parathyroid hormone-related protein.

	Role in Bone Formation	**Expression Profile**
ColX	Role in matrix mineralization in growth plate (Kwan et al., 1997)	Hypertrophic chondrocytes: E14.5, E15.5, E16.5, forelimb & hindlimb (Dacquin et al., 2004; Maes et al., 2002; Yang et al., 2003)
FGFr2	Negative modulator of proliferation (positively affects terminal maturation) (Provot and Schipani, 2005)	Proliferating chondrocytes and perichondrium/periosteum: E14.5, proliferating chondrocytes (weak expression) and two stripes parallel to perichondrium, E16.5, forelimb (Minina et al., 2005)
Ihh	Inhibits hypertrophic chondrocyte differentiation (thereby delaying mineralization) (Vortkamp et al., 1996)	Pre-hypertrophic and hypertrophic chondrocytes: E14.5 & E16.5, tibia/forelimb (Inada et al., 1999; Long et al., 2001; Yang et al., 2003)
PTHrP	Negative regulator of switch from proliferative to hypertrophic chondrocyte (promotes longitudinal growth) (Provot and Schipani, 2005)	Periarticular region: E13.5 & E14.5, tibia/forelimb (Long et al., 2001; Yang et al., 2003), osteoblasts in bone marrow and bone collar, terminal hypertrophic chondrocytes: E16.5

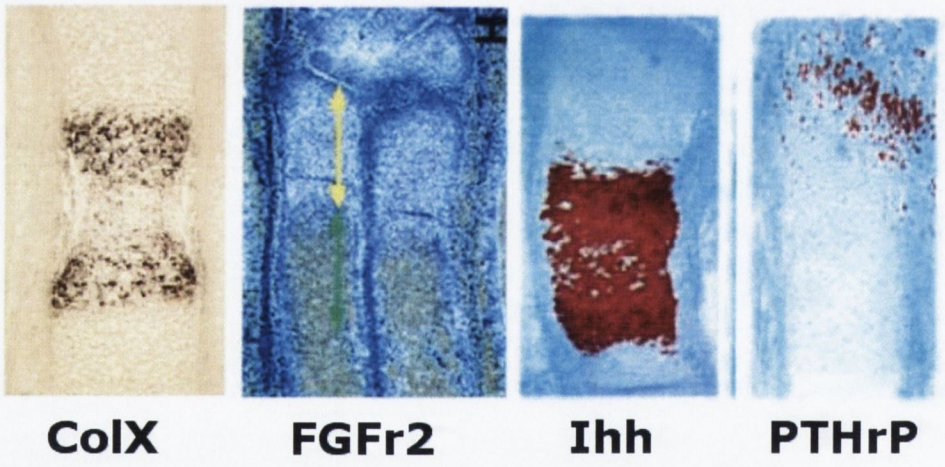


Figure 4.1: Sample expression patterns of candidate genes in the mouse at embryonic day (e) 14.5. ColX is expressed in the hypertrophic chondrocytes (Maes et al., 2002), FGFr2is expressed in the perichondrium and in the proliferative zone (Minina et al., 2005), Ihh is expressed in the pre-hypertrophic chondrocytes (Long et al., 2001) and PTHrP is expressed in the peri-articular cartilage (Long et al., 2001).

4.2.2. Probe Synthesis

The BBSRC (Biotechnology and Biological Sciences Research Council) ChickEST Database[1] and bank of Expressed Sequence Tags (ESTs) from the chick genome were used as a source of cDNA probes to study expression of the genes of interest. The database was searched for ESTs corresponding to each gene and two ESTs were selected for each based on confirmation of perfect alignment with the gene of interest following a Basic Local Alignment Search Tool (BLAST (Altschul *et al.*, 1997)) search through the National Center for Biotechnology Information (NCBI)[2], and on the length of the EST and its position within the cDNA of the gene of interest. ESTs of 0.5- 1.0 kb were preferred. The probe for ColX corresponds with chEST 62e2 and aligns with nucleotides 1605–2320 on Genbank sequence ref M13496.1. The probe for FGFr2 corresponds with chEST 699l24 and aligns with nucleotides 1967–2716 on Genbank ref NM_205319. The probe for PTHrP corresponds with chEST 533c1 and aligns with nucleotides 68–734 on Genbank ref AB175678. The Ihh cDNA clone was a gift from C. Tickle (Dundee) and corresponds to nucleotides 2–547 on Genbank ref NM_204957.

Bacteria were plated and single colonies expanded in liquid cultures; plasmid DNA extracted and purified (using a Maxiprep kit, Qiagen, UK). Each EST clone was sequenced to verify identity. Plasmid DNA was linearized with appropriate restriction enzymes (*Eco*R1 or *Not*1). Antisense and sense digoxigenin-labelled RNA probes were transcribed, according to insert orientation, from 1μg of linearized plasmid from T7 and T3 promoter sites in the pBluescript II KS+ vector (all components for *in vitro* transcription from Roche, Germany). DNA template was degraded by incubation of probes with RNase free DNase (Roche, Germany). The probes were then purified on G25 columns (Amersham Biosciences, USA) according to the manufacturer's instructions. Probe concentrations were determined by spectophotometry and probes were then stored at -20°C until needed.

---

[1] http://www.chick.manchester.ac.uk/, last accessed May 2007

[2] http://www.ncbi.nlm.nih.gov/BLAST/, last accessed May 2007

4.2.3. Sectioning

After dissection, limbs were fixed in 4% paraformaldehyde (PFA) in PBS over night, and dehydrated through a series of methanol/PBT (PBT= 0.1% Triton X-100 in PBS; 25, 50, 75%; 1×10 minute) washes, followed by 2×10 minutes 100% methanol washes and stored at –20°C in 30 or 50ml tubes until needed. On the morning of sectioning, limbs were re-hydrated through a series of methanol/PBT (75, 50, 25%; 1×10 minute) washes at 4°C. After 2×10 minutes washes in PBT, excess tissue surrounding the skeletal rudiments was removed in order to give optimal sectioning performance. For the HH30 and HH32 limbs, the femur was removed, and at older stages, the femur, metatarsals and surrounding tissue were removed from the tibiotarsus and fibula. The specimens were embedded in 4% Low Melting Agarose/PBS (Invitrogen, UK). 80 or 100 μm sections were cut in the longitudinal direction with a vibrating microtome (VT1000S, Leica) and stored in PBS in 12-well plates.

4.2.4. *In situ* hybridisation

After 2×10 minute washes in PBT, free-floating sections were treated with proteinase K (20μg/ml in PBT) for 5 minutes at room temperature. Sections were then washed twice in PBT and fixed for 20 minutes in 0.2% glutaraldehyde/4% paraformaldehyde (PFA). Fixation was followed by washes (3×5 minutes) in PBT at room temperature, and a further 30 minute PBT wash at 55°C. The sections were then prehybridised at 55°C overnight in a hybridization solution containing 2% blocking reagent (Roche, Germany), 50% formamide, 5 X SSC (Saline-sodium citrate buffer), 0.5% 3-[(3-Cholamidopropyl-[(3-Cholamidopropyl) dimethylammonio]-1-propanesulfonate (CHAPS), 500 μg/ml Heparin, 1 μg/ml Yeast RNA, 0.1% Tween 20 and 5 mM EDTA (ethylenediamine tetraacetic acid)). Antisense and sense probes were denatured at 80°C for 3 minutes and sections were then incubated at 55°C over 2-3 nights in hybridization solution containing either antisense or sense probe at minimum concentrations of 2 ng/μl.

Post-hybridization washes were carried out at 60°C as follows: 2 X 10 minutes in 2 X SSC; 3 X 20 minutes in 2 X SSC/0.1% CHAPS; 3 X 20 minutes in 0.2 X SSC/0.1% CHAPS. The sections were then washed for 2 X 10 minutes in TNT (100 mM Tris-HCl, pH 7.5, 150 mM NaCl, 1% Tween 20) at room

temperature and blocked in blocking buffer (0.1 M maleic acid, 0.15 M NaCl, 3% blocking reagent (Roche, Germany)) plus 10 % goat serum overnight at 4°C. Sections were incubated overnight in fresh blocking buffer (plus 10% serum) containing a 1:1000 dilution of anti-digoxigenin Fab fragments conjugated with alkaline phosphatase (Roche, Germany) at 4°C, with rocking. The sections were then washed (5 X 1 hour) at room temperature in TNT and left rocking in TNT over 2 nights at 4°C. On the day the signal was developed, sections were washed in 3 changes of NTMT (100 mM Tris-HCl, pH 9.5, 100 mM NaCl, 50 mM $MgCl_2$) for 15 minutes each. The chromogenic reaction was carried out in NTMT containing 17.5 µg/ml 4-nitro blue tetrazolium chloride (NBT; Roche, Germany) and 6.25 µg/ml 5-bromo-4-chloro-3-indolyl-phophate (BCIP; Roche, Germany). Sections were developed in the dark at room temperature with rocking for 6-8 hours and then fixed in 4% PFA/PBS for 1 hour before mounting on slides with Aquapolymount (Polysciences, Inc).

4.2.5. Immobilisation

Two sets of immobilisation experiments were performed at different timepoints; named Set A and Set B. At the start of the experiment, the eggs were divided into control and experimental groups, with slightly more eggs assigned to the experimental group as a higher mortality rate was anticipated in this group (Hosseini and Hogg, 1991a). The eggs were incubated for 3 days, after which 4ml of albumen was removed so that the embryo would sink down lower in the egg and a window could be cut into the egg without rupturing the chorioallantoic membrane. Administration of the neuromuscular blocking agent Decamethonium Bromide began at either day 5 or day 6 of incubation (two different sets of experiments were performed, referred to as Set A and Set B). A window was cut into the egg in order to administer the treatment and to observe movement of the embryo which was sealed after treatment using wide plastic tape. The eggs assigned to the experimental group were treated daily with 100µl of DMB in sterile HBSS (Hank's Buffered Saline Solution), while the control embryos were treated with 100µl of sterile HBSS. Before administration of the drug or saline solution, movement of the embryo was observed and recorded, and dead embryos were discarded. The treatment was repeated daily until the embryos were harvested, at days 8 and 11 for Set A,

and at days 8, 9 and 11 for Set B. The numbers of embryos, and timing of the treatments and dissections for Sets A and B are summarised in Table 4.2.

After dissection, the right limb was immediately removed for preparation for sectioning and subsequent *in situ* hybridisation. These were processed and sectioned as detailed in Section 4.2.3 and *in situ* hybridised as in Section 4.2.4, to analyse the expression of a subset of the candidate mechanosensitive genes. After staining, fixation and mounting, the sections were compared between control and immobilised groups to determine if the altered mechanical environment had an effect on gene expression. The rest of the embryo was stained for cartilage and bone using Alcian Blue (cartilage) and Alizarin Red (bone) as described in the Methods section of Chapter 3. After staining, the embryos were photographed, and the total length of the tibiotarsus and the length of the bone collar measured for each specimen. The proportion of the rudiment that had undergone calcification was then calculated, giving three parameters for each specimen (length, length bone, proportion bone). These parameters were analysed in the statistical package R (http://www.r-project.org/), and standard t-tests were performed in order to determine the effect of immobilisation on the three parameters.

Table 4.2: Summary of numbers and treatment timing for Sets A and B. Experimental embryos were treated with the neuromuscular blocking agent, control embryos were treated with saline solution only.

	# Eggs Incubated	**# Experimental**	**# Controls**	**Start Day of Treatments**	**Dissection Days**
Set A	200	120	80	5	8,11
Set B	180	100	80	6	8,9,11

4.3. Results

4.3.1. Mechanosensitive gene expression patterns

Collagen X

Collagen X (ColX) expression was found in the expected region of hypertrophic chondrocytes in the internal cartilage of the tibiotarsal rudiments (Figure 4.2), and also in the perichondrium/periosteum (Figure 4.2) at each stage. Expression in the hypertrophic region at stages HH30 and HH32 appeared as a band of increasing length at the mid-diaphysis. At stage HH34 two separate bands of expression proximal and distal to the mid-diaphysis appeared (only the distal band is seen in at HH34 due to a glancing section) as the hypertrophic zone expanded further.

On close examination of the expression in the hypertrophic zone at HH32 the staining throughout the zone appears not to be uniform with slightly more intense staining in the more lateral zone, close to the perichondrium. ColX expression in the perichondrium/periosteum was not previously reported and presents an interesting pattern: while at HH30 both the expression in the hypertrophic zone and in the perichondrium are localised at the mid-diaphysis, from HH32 the proximo-distal extent of the perichondrium staining extends significantly beyond the hypertrophic zone staining within. An interesting expression pattern was also seen in the metatarsals of the hindlimb at stage HH34, where two distinct bands of perichondrial expression were apparent proximal and distal to the bone collar, as shown in Figure 4.3, indicating that the dynamic pattern of ColX expression in the perichondrium proximal and distal to the bone collar is not unique to the tibiotarsus and also occurs in other limb long bones.

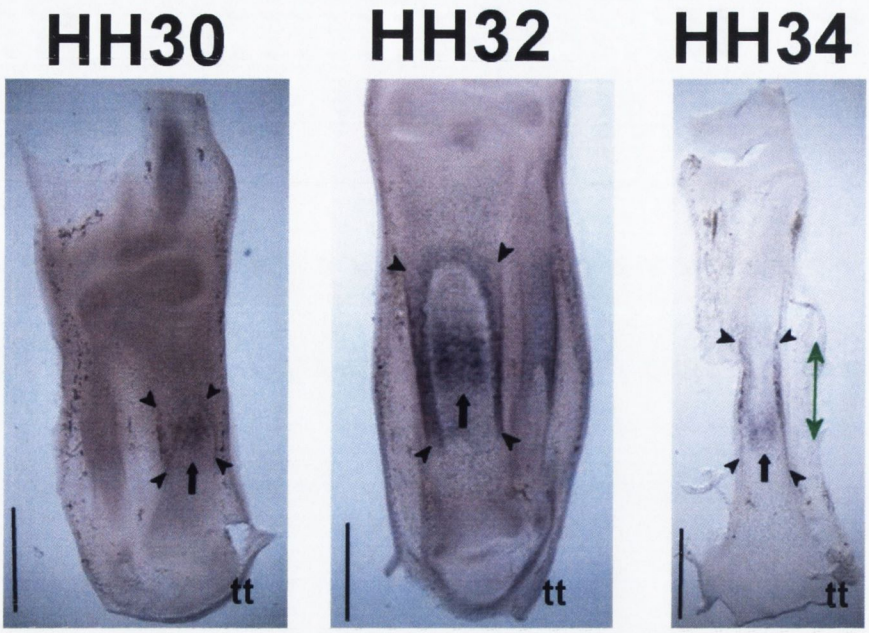


Figure 4.2: ColX expression patterns in sections of the avian hindlimb at stages HH30, HH32 and HH34. Up is distal, down is proximal. tt: tibiotarsis, The approximate location of the bone collar is indicated with a green line. ColX is expressed in the hypertrophic chondrocytes (arrows) and in the perichondrium/periosteum (arrow heads). Scale bars 1mm.



Figure 4.3: ColX expression in HH34 metatarsal rudiments showing bands of expression in the perichondrium (arrows). Scale bar 1mm.

FGFr2

FGFr2 was found to be expressed in the perichondrium and in the periarticular cartilage of the tibiotarsus at stages HH30 and HH32 and in the perichondrium and periosteum at HH34, as shown in Figure 4.4.

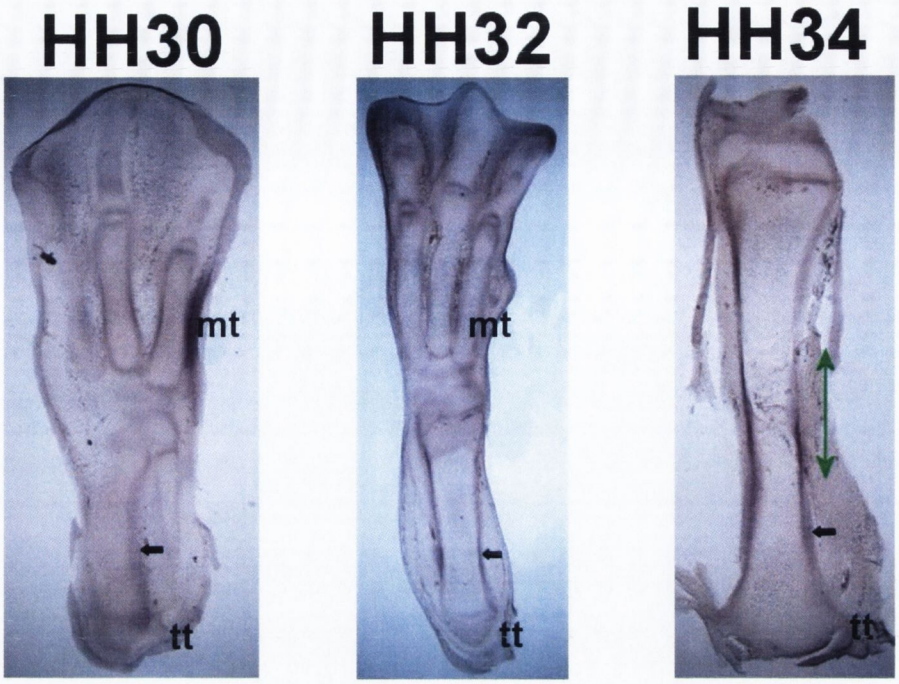


Figure 4.4: FGFr2 expression patterns in sections of the avian hindlimb at stages HH30, HH32 and HH34. Up is distal, down is proximal. tt: tibiotarsis, mt: metatarsals. The approximate location of the bone collar is indicated with a green line. FGFr2 is expressed in the perichondrium and periosteum (arrows).

Indian Hedgehog

Ihh was found to be expressed in bands within the cartilage core of the tibiotarsus for the three stages examined (Figure 4.5). At HH30, Ihh expression was found in a strong though diffuse band along much of the length of the diaphysis. At HH32, two bands of expression were clear proximal and distal to the mid-diaphysis, flanking the domain of ColX expression (highlighted with arrows in Figure 4.5), while at HH34, two distinct and separate bands of expression (arrows) proximal and distal to the approximate location of the newly-formed bone collar were evident. These proximal and distal domains are in the position of the pre-hypertrophic cartilage. Similar to ColX cartilage expression, at the later stage, staining was slightly more intense at the lateral edges of the domains (highlighted with red arrows in Figure 4.5, HH34). Comparing across the three stages, the overall intensity of the staining decreased significantly at later stages and particularly at HH34, which indicates a reduction in Ihh expression in more mature rudiments.

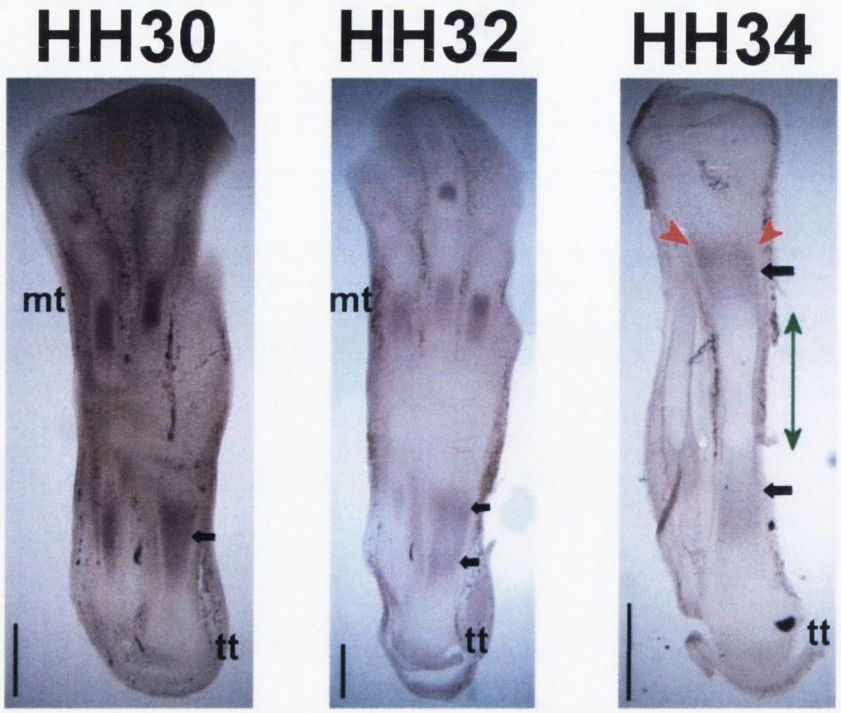


Figure 4.5: Ihh expression patterns in sections of the avian hindlimb at stages HH30, HH32 and HH34. Up is distal, down is proximal. tt: tibiotarsis, mt: metatarsals. The approximate location of the bone collar is indicated with a green line. Ihh is expressed in the hypertrophic (HH30) and pre-hypertrophic (HH30-32) zones (arrows), elevated lateral expression highlighted with red arrowheads. Scale bars 1mm.

PTHrP

PTHrP expression was evident in the periarticular regions of the rudiments of the hindlimb at stages HH30 and HH32, as highlighted with arrows in Figure 4.6. At stage HH34, although some PTHrP expression was present in the periarticular zone of the tibiotarsus (Figure 4.6), the expression was apparently downregulated from levels present at younger stages with the staining becoming more difficult to detect.

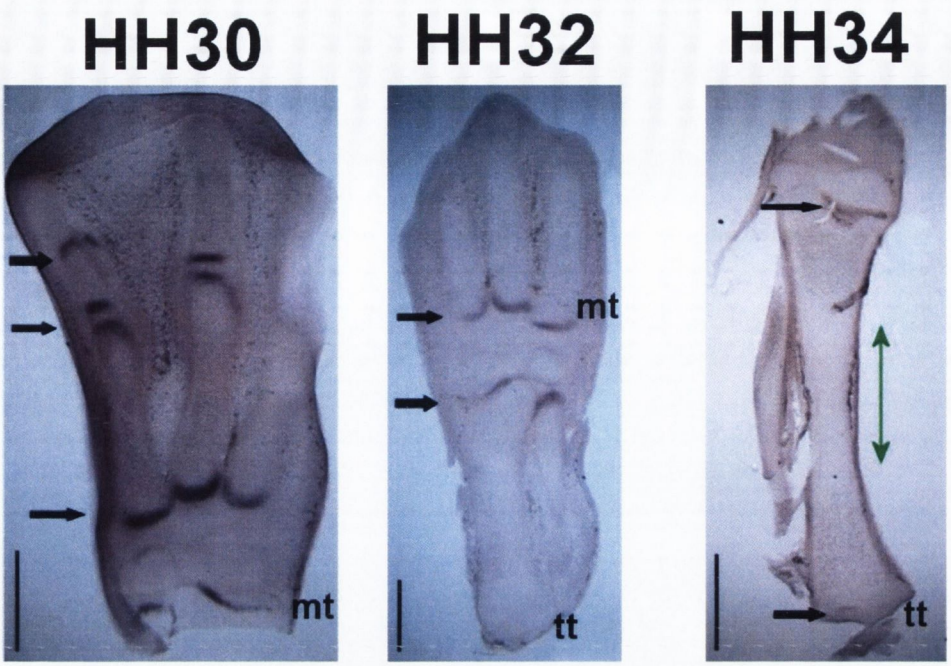


Figure 4.6: PTHrP expression patterns in sections of the avian hindlimb at stages HH30, HH32 and HH34. Up is distal, down is proximal. tt: tibiotarsis, mt: metatarsals. PTHrP is expressed in the peri-articular cartilage (arrows). Scale bars 1mm.

4.3.2. Viability and Efficacy of Immobilisation Treatment

As described in the Methods section of this chapter, two sets of immobilisation experiments were performed at separate times, namely Set A and Set B, where treatments for Set A started on day 5 of incubation as opposed to Day 6 for Set B (detailed records of the experiments are given in Appendix E). Overall survival rates were similar for both sets, with a 37.6% survival rate in Set A and 35.5% survival in Set B. During the experiments, when each egg was opened, the embryo was monitored for movement or lack thereof. Movement in the treated embryos was not eliminated in all specimens but was clearly reduced. In many of the immobilised specimens that were recorded as moving, the type of movement was different to that of controls, with a slow whole body 'swinging' movement often observed as opposed to jerky contractions of the limbs of control embryos. For each day, the percentage of immobilised embryos that were not moving was calculated as a measure of the efficacy of the treatment, as shown in Table 4.3. These efficacy rates were averaged over the course of the experiment to get the overall efficacy of the treatment. The

averaged efficacy rates were similar for Sets A and B, with 48% efficacy for Set A, and 53.1% efficacy for Set B (See Appendix E).

4.3.3. Effect of Immobilisation on Skeletal Morphology

A total of 48 control and 58 immobilised embryos were harvested over three timepoints; namely 8, 9 and 10 days of incubation, as detailed in Table 4.2. Control and immobilised embryos were grouped by incubation day at which they were harvested (i.e., day 8, 9 or 11), rather than by HH stage, in case the treatment had an effect on the development rate of the embryo. HH stage was also recorded for each specimen (Appendix E) and while no consistent effect on stage was seen with the drug, both the control and drug treatments yielded a greater range of stages at each day than for non experimental controls.

Immobilisation was found to have a dramatic effect on overall skeletal morphology. Immobilised embryos were smaller, with abnormal rib formation, joint contractures and spinal curvature, as shown for representative embryos in Figure 4.7. The tibiotarsi from the control and immobilised groups were measured and compared, grouped by day of harvest of the embryo. It was found that the tibiotarsal rudiments were significantly shorter in the immobilised group than in the control group for all days of the experiment, as shown in Figure 4.8. When the length of bone (Alizarin red staining) in the tibiotarsus was measured, a significant difference was found at day 11, but not at day 8 or 9 (Figure 4.8). At day 8, most of the rudiments had not yet started to ossify, and at day 9, although there is a trend indicating less bone content in the immobilised group (Figure 4.8), statistical significance was not achieved, most likely due to the low numbers harvested on this day, as detailed in Table 4.4. In order to demonstrate that the reduction in the length of the ossified region in the immobilised rudiments was not simply due to the reduction in overall length of the rudiment, the proportion of the rudiment that had undergone calcification was calculated and compared between the two groups. It was found that there was a significant difference between the control and immobilised groups at Day 11, as shown in Figure 4.9. Although no significant difference was found at day 9, a trend indicates a lower calcified proportion (Figure 4.9).

Table 4.3: Percentage of control and treated embryos moving on days 7-11 of experiment. The raw data are presented in Appendix E.

	Day 7	Day 8	Day 9	Day 10	Day 11
Control	81.9%	89.7%	95.5%	88.5%	100%
Treated	52.9%	59.3%	61.6%	33.43%	21.2%

Table 4.4: Number of specimens analysed per day of harvesting for control and immobilised groups.

	Control	Immobilised	Total
Day 8	13	23	36
Day 9	5	10	15
Day 11	30	25	55

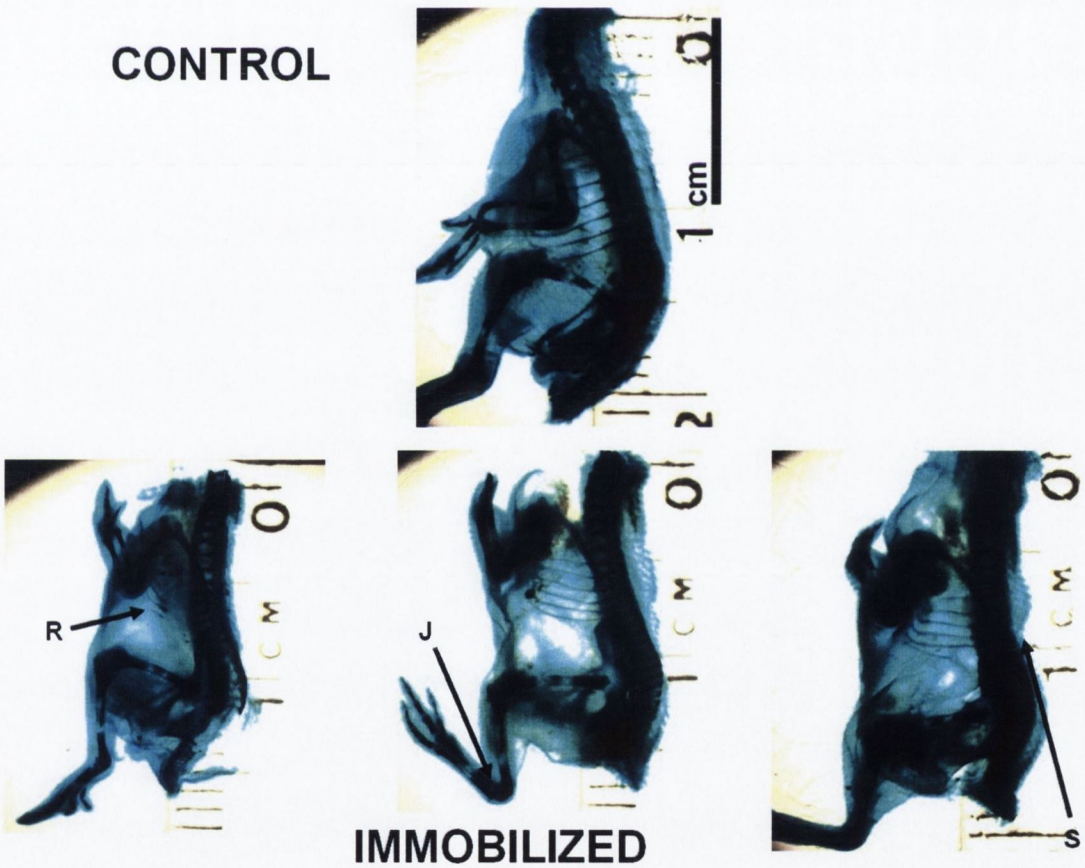


Figure 4.7: Representative control (top) and immobilised (bottom) embryos at stage HH36 (Scale bar on top picture shows 1cm, all photographs taken on same scale). Immobilised embryos exhibited abnormal rib formation (R), joint contractures (J) and spinal curvature (S).

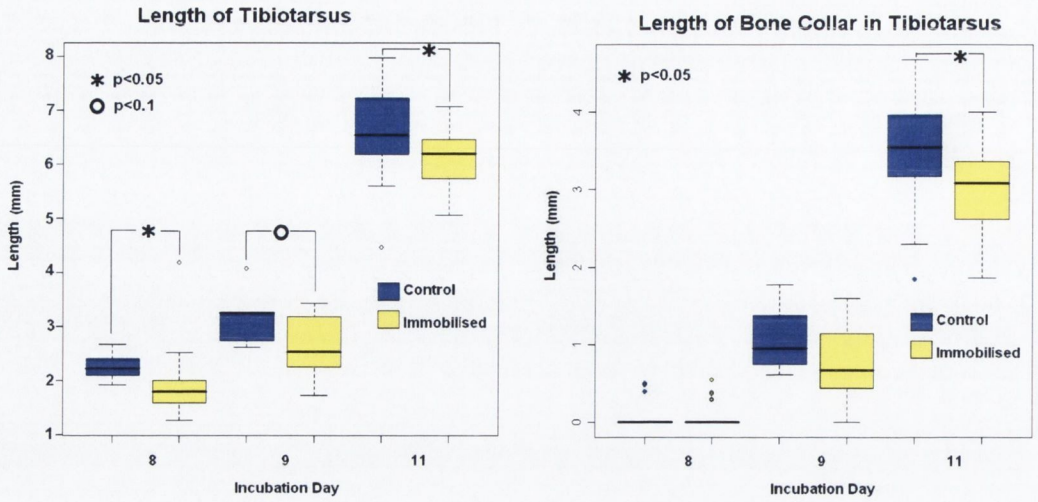


Figure 4.8: Overall length of tibiotarsus and length of bone in tibiotarsus for control (no drug treatment) and immobilised (neuromuscular blocking agent treatment) groups harvested at days 8, 9 and 11 of incubation.

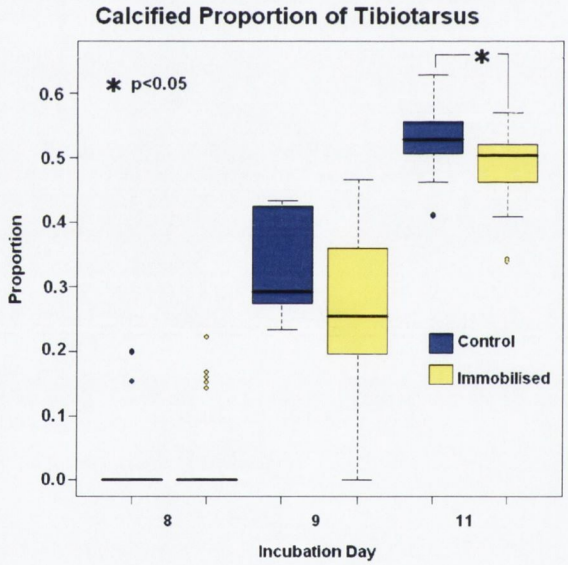


Figure 4.9: Calcified proportion of tibiotarsus for control and immobilised groups harvested at days 8, 9 and 11 of incubation.

4.3.4. Effect of Immobilisation on Mechanosensitive Gene Expression

Based on the expression patterns of the four candidate mechanosensitive genes, three genes were chosen for comparison between control and immobilized specimens. ColX and Ihh were prioritised due to the dynamic nature of their expression profiles over the three stages examined, and PTHrP was also selected due to its involvement in a feedback loop with Ihh. FGFr2 was not analysed in the experimental embryos as reported expression (in the mouse) in

the proliferating chondrocytes was not observed in the chick and because observed expression in the perichondrium (and periosteum, where present) remained constant throughout initiation and progression of the bone collar. A total of 42 control and 52 immobilized specimens from days 8, 9 and 11 of the experiment were sectioned for gene expression analysis. The sections were divided for staining between the three candidate genes; ColX, Ihh and PTHrP, often with sections from each limb divided between two or more genes. Due to problems with probes in some experiments or obtuse sections, only a subset of the sections exhibited staining after *in situ* hybridization, and the final numbers of specimens per gene and per timepoint are summarized in Table 4.5.

Table 4.5: Number of specimens successfully stained for ColX, Ihh and PTHrP expression at Days 8, 9 and 11.

	Day 8		**Day 9**		**Day 11**	
	Control	Immobilised	Control	Immobilised	Control	Immobilised
ColX	10	8	4	7	5	3
Ihh	12	15	2	7	7	10
PTHrP	9	12	n/a	n/a	n/a	n/a

Collagen X

As previously described, ColX expression is normally observed in the region of hypertrophic chondrocytes, in the periosteum (if present) and in the perichondrium extending proximal and distal to the hypertrophic zone. No obvious differences in this expression pattern were detected at day 8 or at day 11, as shown for sample sections in Figure 4.10A-B and Figure 4.10G-H. However, out of the eight immobilised specimens examined at day 9, differences were exhibited in three specimens in both the hypertrophic zone and the perichondrium, while the remaining five specimens yielded the same expression patterns as the controls. Firstly, in one immobilised specimen, ColX expression was observed with strikingly more intense expression close to the lateral surfaces of the hypertrophic zone (Figure 4.10D) as opposed to the more even expression across hypertrophic chondrocytes seen in the normal situation at this stage (Figure 4.10C). The expression in this treated embryo is more similar to the medio-lateral distribution of expression seen in the older day 11 control specimens (Figure 4.10G-H). The second alteration was seen in two (out of seven) immobilised specimens at day 9, where expression in the perichondrium did not extend proximally or distally beyond the hypertrophic

zone as seen in untreated specimens (compare Figure 4.10E and F with C and D).

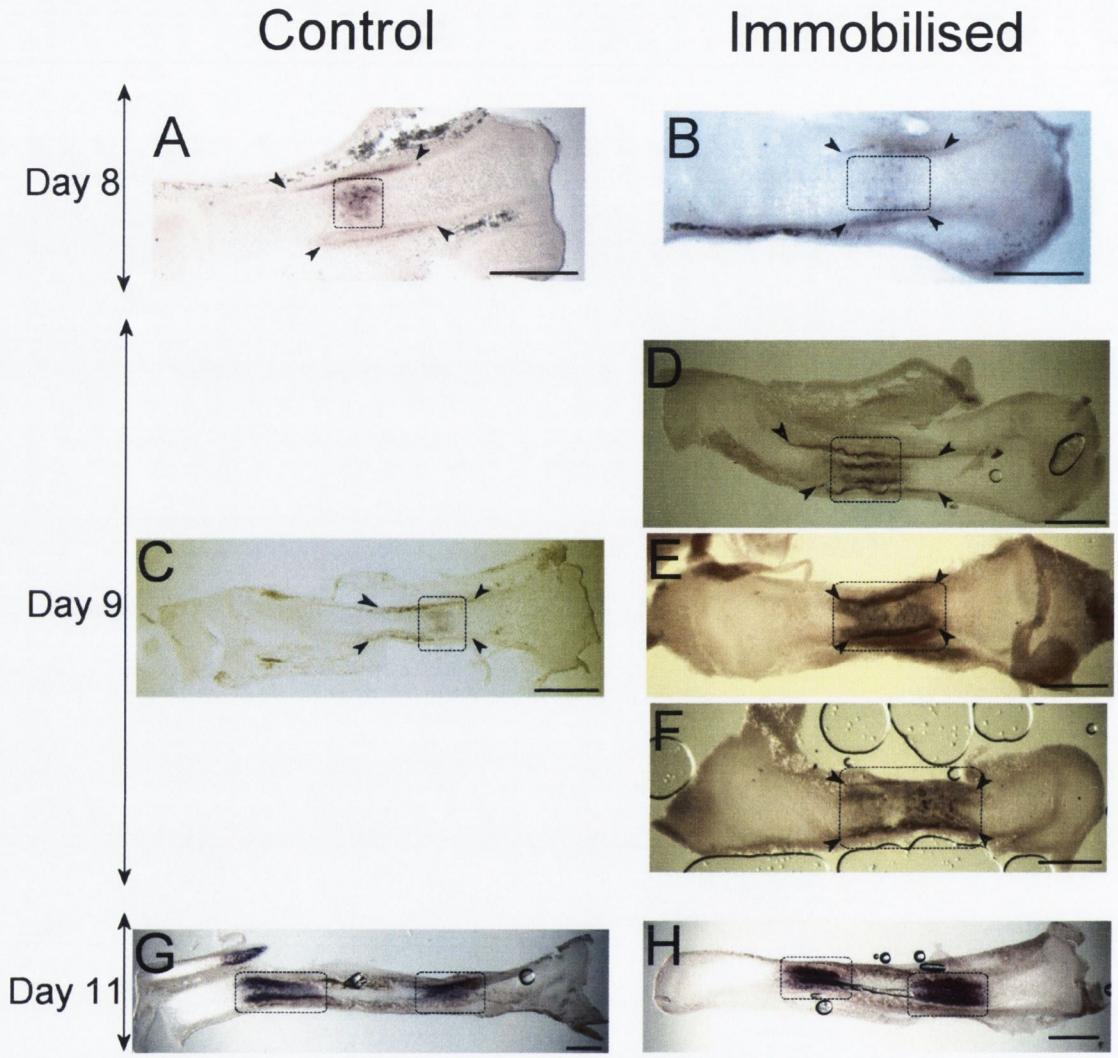


Figure 4.10: ColX expression at Days 8, 9 and 11 in the tibiotarsus in control and immobilised specimens. Scale bar 1mm. The expression in the hypertrophic region is demarcated by a dashed box; expression in the periosteum and perichondrium is highlighted by arrow heads. The section shown in C is a glancing section of non-experimental control specimen and only distal expression in the hypertrophic zone is visible. Note the non-uniform pattern of Col X expression at the mid-diaphysis in D. E-F: ColX staining in the perichondrium is more restricted proximo-distally and does not extend beyond the hypertrophic zone. G: ColX expression is concentrated at the periphery of the rudiment, H: expression across the width of the hypertrophic zones. G-H: Note that ColX expression is more intense at the periphery of the rudiment at this later stage of development.

Indian Hedgehog

A number of specimens from each of the three time points examined indicated that Ihh expression was affected by an altered mechanical environment due to immobilisation. As described previously, as development progresses in the limb, Ihh expression becomes slightly more intense at the lateral edges of the domain in the pre-hypertrophic chondrocytes. This is just visible on close examination in the normal specimens at HH32 (Figure 4.5). Immobilisation appears to have had the effect of accelerating this localised distribution with lateral concentrations of expression observed in one (of fifteen) specimens at day 8 (Figure 4.11), and in three (of seven) specimens at day 9 (Figure 4.12), with no similar patterns observed in controls at these time points. At day 11, concentrations of Ihh expression at the periphery were seen in both control and immobilised specimens (Figure 4.13), but the lateral expression tended to be more pronounced in the immobilised specimens, with a greater distance between the stripes of expression.

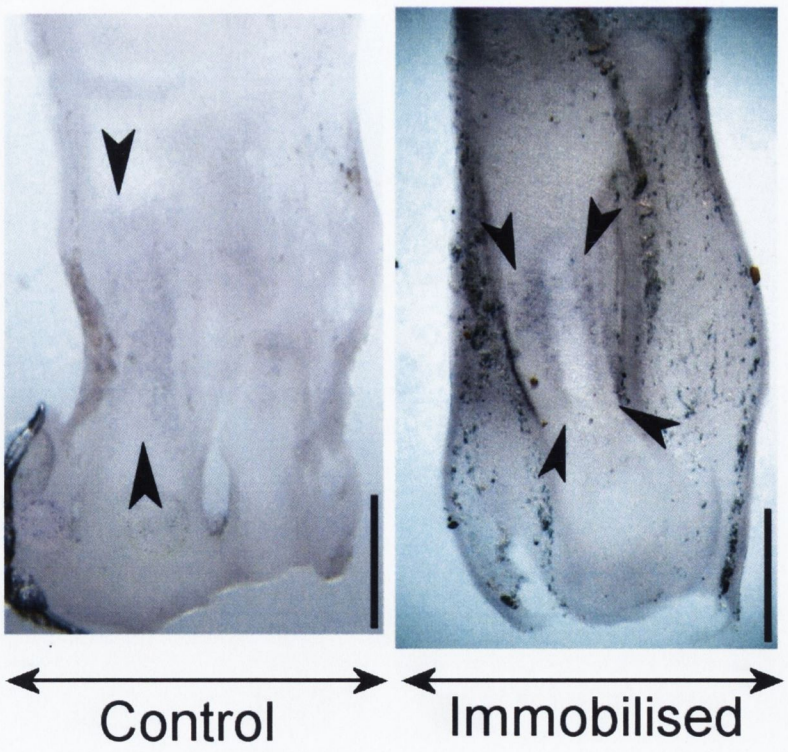


Figure 4.11: Ihh expression at Day 8 in the tibiotarsus in control and immobilised specimens. Scale bar 1mm. Expression in the pre-hypertrophic chondrocytes is highlighted by arrow heads.

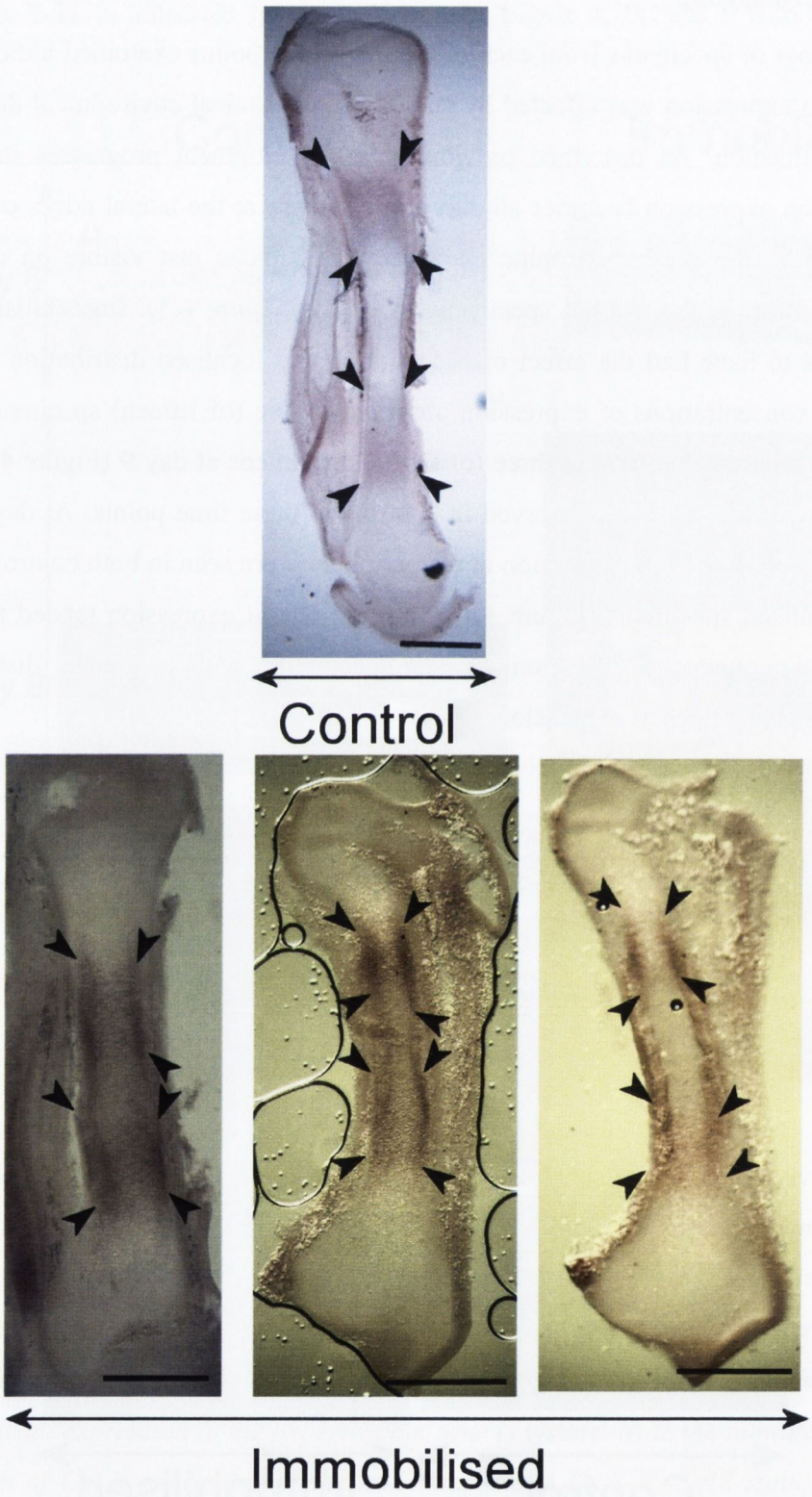


Figure 4.12: Ihh expression at Day 9 in the tibiotarsus in control (non-experimental control pictured) and immobilised specimens. Scale bar 1mm. Expression in pre-hypertrophic chondrocytes is demarcated by arrowheads.

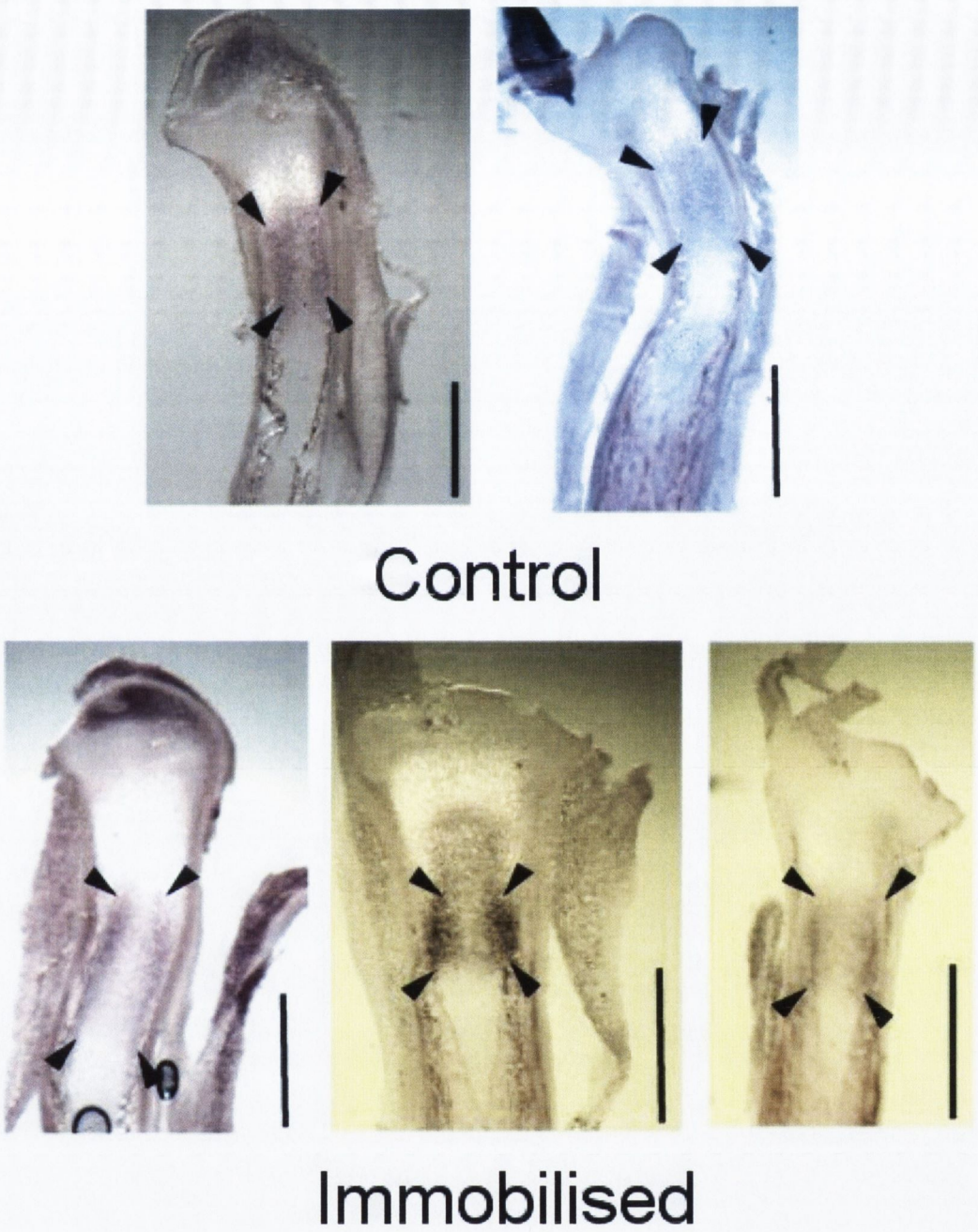


Figure 4.13: Ihh expression at Day 11 in representative tibiotarsi from the control and immobilised specimens. Extent of expression in pre-hypertrophic zone demarcated by arrowheads, note more pronounced lateral expression in immobilised specimens. Scale bars 1mm.

PTHrP

PTHrP was examined at day 8 only, and mostly in sections of the metatarsals where the staining is most prominent. Analysis of ColX and Ihh was prioritised at later stages. No differences in PTHrP expression were evident between the control and immobilised specimens, with expression as normal in the periarticular cartilage of the rudiments, as highlighted with arrows for a subset of the specimens in Figure 4.14.

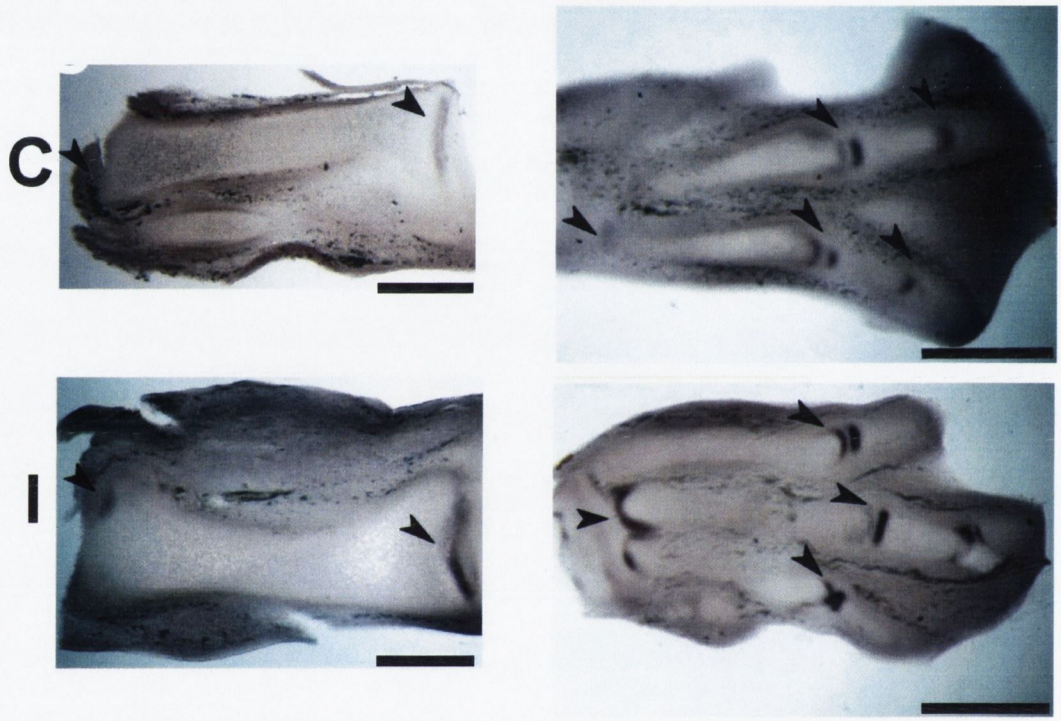


Figure 4.14: PTHrP expression at Day 8 in the tibiotarsus (left) and in the metacarpals (right) in control and immobilised specimens. Expression in the peri-articular cartilage is highlighted with arrow heads. Scale bars 1mm.

4.4. Discussion

4.4.1. Correlation gene expression patterns with mechanical stimulation

In this chapter, it was proposed that genes with a mechanoregulatory role in the bone formation process could be identified by comparison of patterns of biophysical stimuli and mechanosensitive gene expression patterns. As described in Chapter 3, the pattern of biophysical stimuli resulting from embryonic muscle contractions underwent distinctive changes over the three stages examined, where biophysical stimuli were predicted to be at high levels of concentration at imminent sites of periosteal bone formation at each stage. At HH30, stimuli levels peaked on the perichondrium at the mid-diaphysis of the rudiment. At HH32, two concentrations of stimuli were apparent proximal and distal to the mid-diaphysis, again on the surface of the rudiment, and by HH34, these concentrations moved further apart along the length of the rudiment, proximal and distal to the newly formed bone collar.

The expression patterns of four candidate mechanosensitive genes; ColX, FGFr2, Ihh and PTHrP, were characterised for stages HH30, HH32 and HH34 and were compared with patterns of biophysical stimuli. The expression patterns of these genes were illustrated schematically by stage from experimental data, as shown in Figure 4.15. The schematics were then compared with the predicted fluid velocity and maximum principal strain (averaged over flexion and extension contractions) from stage-matched finite element analyses (Figure 4.16, Figure 4.17). Two genes emerged as potential molecular targets of mechanical stimulation due to muscle contractions. FGFr2 was expressed in the perichondrium and periosteum, and PTHrP in the periarticular cartilage at all stages examined (Figure 4.15), therefore, neither of these genes showed a correlation with patterns of biophysical stimuli. However, aspects of the ColX and Ihh expression profiles at the three stages of interest followed patterns of events that reflect the stimuli patterns at the same stages.

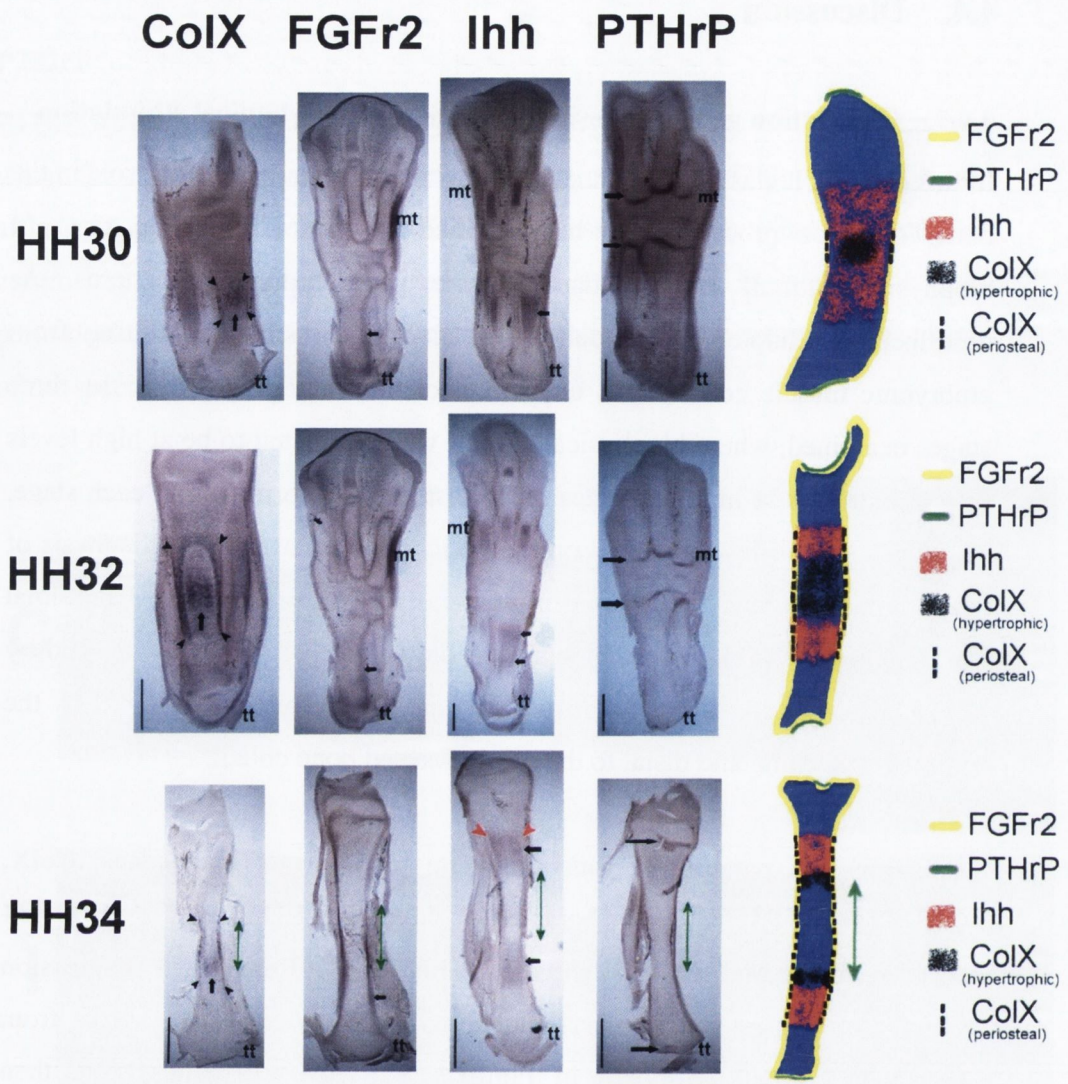


Figure 4.15: Schematics of ColX, FGFr2, Ihh & PTHrP expression patterns (right) from experimental data (left) in sections of the avian hindlimb at stages HH30, HH32 and HH34. tt: tibiotarsis, mt: metatarsals. The approximate location of the bone collar is indicated with a green line. ColX is expressed in the hypertrophic chondrocytes (arrows in photographs, diffuse black in schematic) and in the perichondrium/periosteum (arrow heads in photographs, dashed black line in schematic); FGFr2 is expressed in the perichondrium and periosteum (arrows in photographs, yellow line in schematic); Ihh is expressed in the hypertrophic (HH30) and pre-hypertrophic (HH30-32) zones (arrows in photographs, red regions in schematic), elevated lateral expression highlighted with red arrowheads in photographs; PTHrP is expressed in the peri-articular cartilage (arrows in photographs, green lines in schematic). Scale bars 1mm.

ColX was found to be expressed in the region of hypertrophic chondrocytes as previously reported, but also in the region of the perichondrium where bone would soon form (Figure 4.15), spreading proximally and distally beyond the hypertrophic zone domain at the core at HH30 and HH32 and ahead of the bone collar at HH34. Therefore its surface expression demonstrated a correlation with the patterns of biophysical stimuli at each of the three stages examined (Figure 4.16, Figure 4.17). When the expression pattern of ColX at HH36 was compared with the peak levels of principal strain predicted by the FE analyses at HH34, the patterns were strikingly similar (Figure 4.18), perhaps suggesting a delay in the relationship between the two patterns.

Ihh expression was observed in the region of pre-hypertrophic chondrocytes in the cartilage of the rudiment as expected. In the earlier stages examined, Ihh was expressed uniformly across the pre-hypertrophic zone, in one mid-diaphyseal region at HH30, and in two bands at increasing distances proximal and distal to the mid-diaphysis at later stages (Figure 4.15), the expression bands moving proximally and distally in synchrony with the biophysical stimuli at the surface. Although Ihh expression was not observed in the perichondrium where the highest concentrations of biophysical stimuli were predicted, expression of the gene was at the same longitudinal position in the rudiment as, and adjacent to, the peak levels of biophysical stimuli (Figure 4.16, Figure 4.17). It is possible that at these timepoints another gene could be involved in signalling from the perichondrial surface to the internal chondrocytes, or indeed, Ihh regulation could potentially be sensitive enough to respond to stimulation focused on adjacent perichondrial cells.

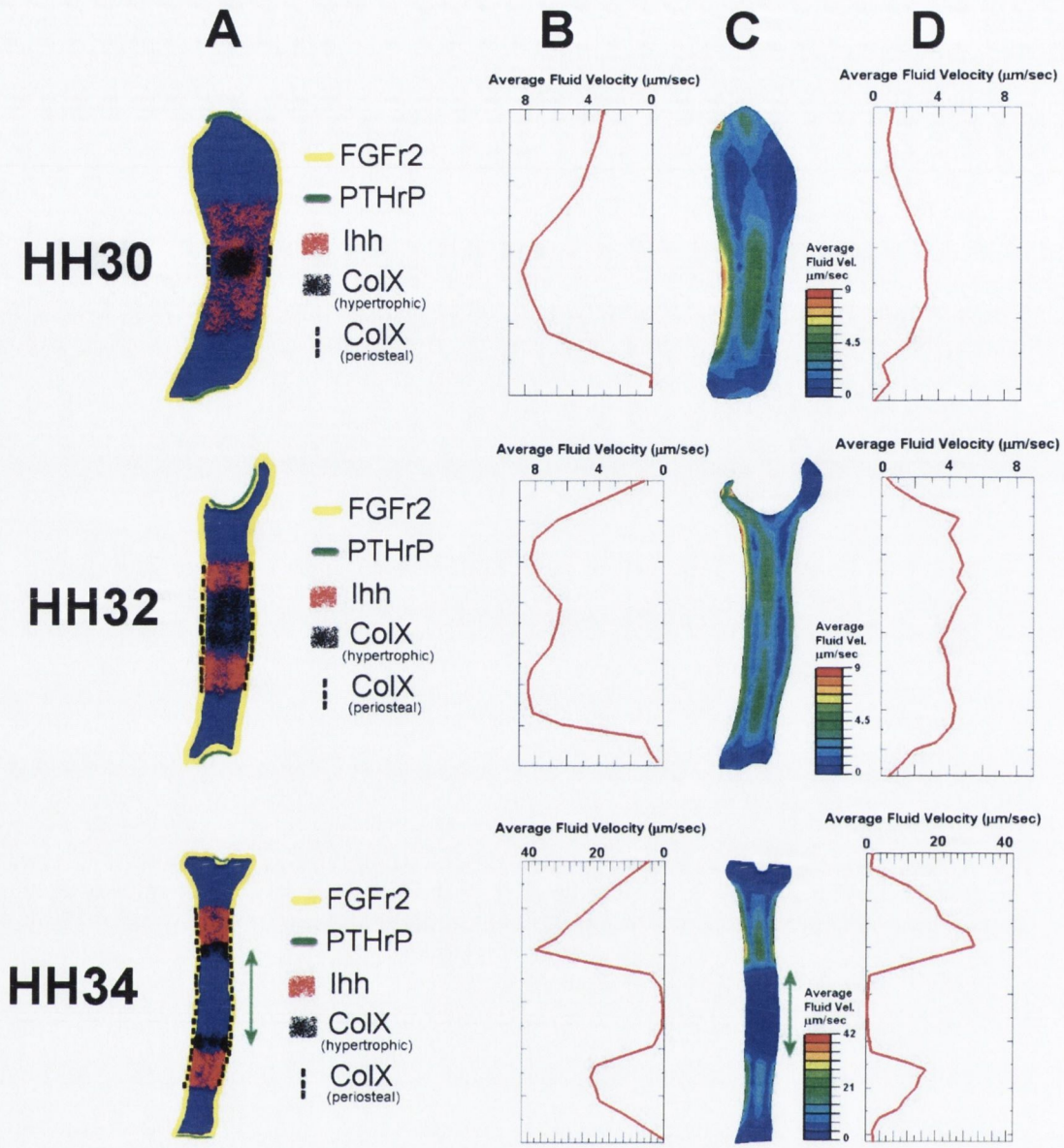


Figure 4.16: Comparison of candidate mechanosensitive genes (A) with fluid velocity averaged over flexion and extension contractions (B-D) in sections of chick tibiotarsus at stages HH30, HH32 and HH34. A: Fgfr2 (yellow) expression in perichondrium and periosteum (estimated length of periosteum illustrated with green arrows). PTHrP (green) expressed in peri-articular cartilage. Ihh (red) expressed in pre-hypertrophic chondrocytes. ColX (black) expressed in hypertrophic chondrocytes (diffuse colouring), and in perichondrium/periosteum (dashed line). B: average fluid velocity along a ventral path, C: average fluid velocity in mid-line cross-section, D: average fluid velocity along a dorsal path.

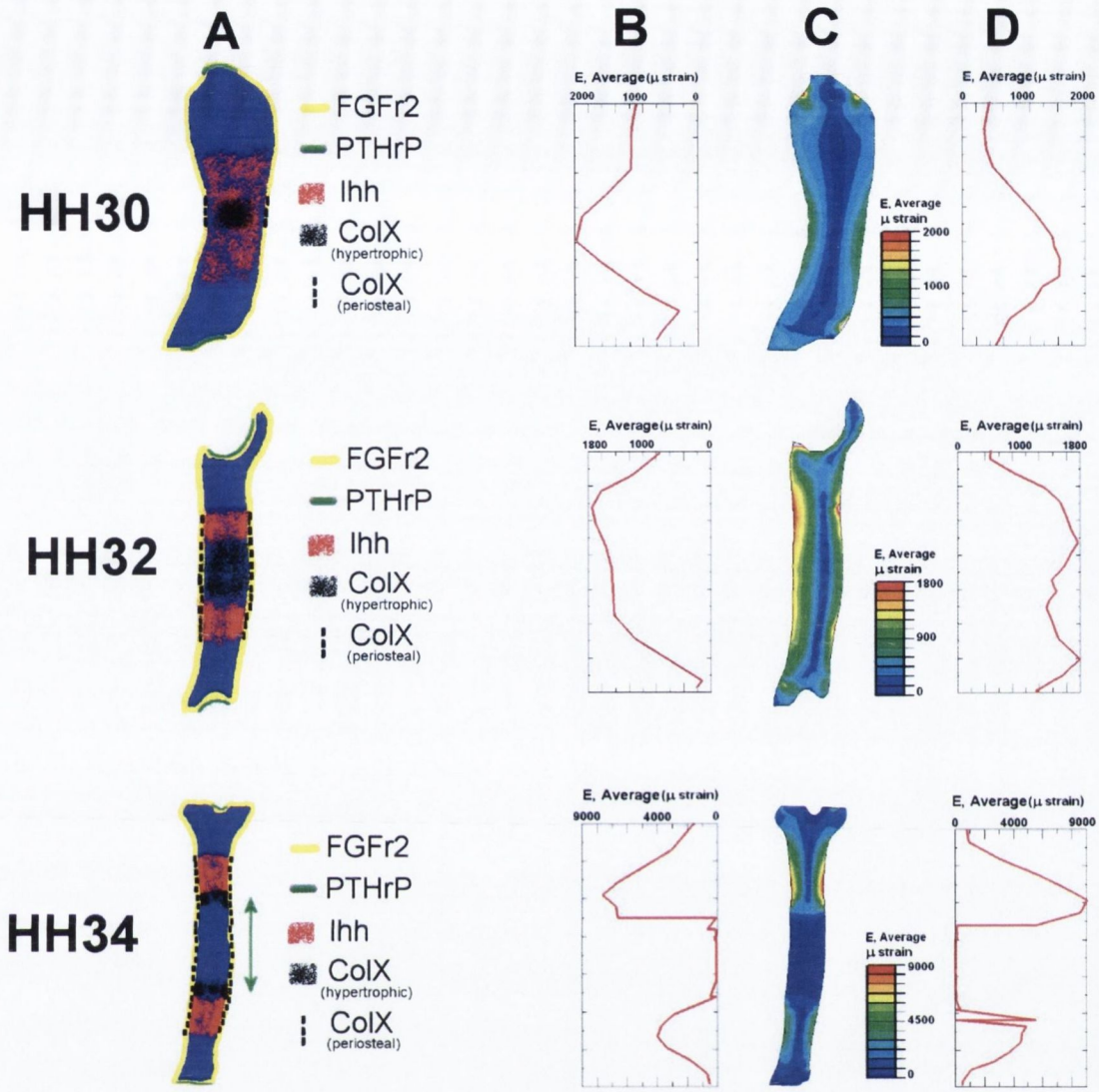


Figure 4.17: Comparison of candidate mechanosensitive genes (A) with maximum principal strain averaged over flexion and extension contractions (B-D) in sections of chick tibiotarsus at stages HH30, HH32 and HH34. A: Fgfr2 (yellow) expression in perichondrium and periosteum (estimated length of periosteum illustrated with green arrows). PTHrP (green) expressed in peri-articular cartilage. Ihh (red) expressed in pre-hypertrophic chondrocytes. ColX (black) expressed in hypertrophic chondrocytes (diffuse colouring), and in perichondrium/periosteum (dashed line). B: average maximum principal strain along a ventral path, C: average maximum principal strain mid-line cross-section, D: average maximum principal strain along a dorsal path.

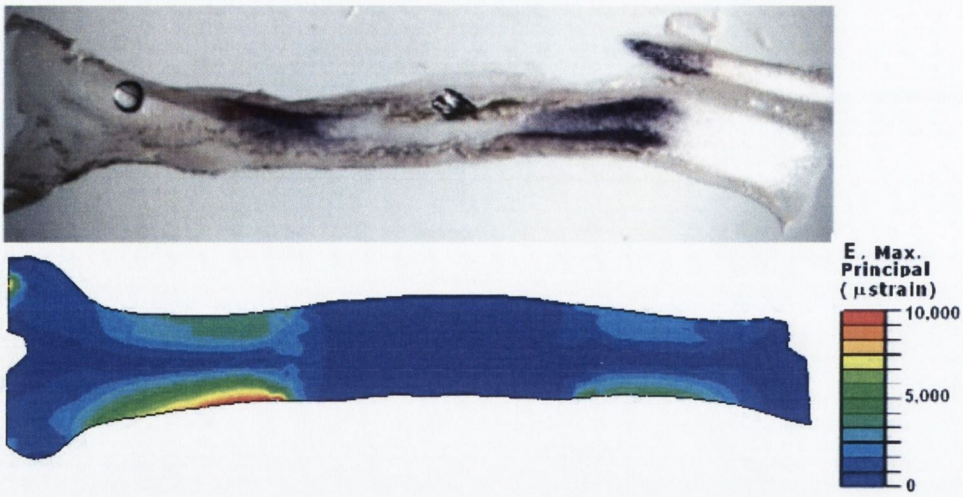


Figure 4.18: ColX expression in a longitudinal section of a HH36 tibiotarsus rudiment (top) correlates with the predicted pattern for maximum principal strain mid-flexion contraction at HH34 (bottom).

In addition, an extra detail of the Ihh expression pattern was discovered in this study: In the later stages examined, (HH34 and HH36), Ihh expression was no longer uniform across the width of the rudiment but was elevated close to the periphery (Figure 4.16; HH34). A similar peripheral elevation was also seen for ColX expression at HH36 (Figure 4.18) possibly reflecting a regulatory link between Ihh and ColX in the hypertrophy cycle, where ColX expression in hypertrophic chondrocytes follows Ihh expression in pre-hypertrophic chondrocytes (Provot and Schipani, 2005). The peripheral elevation of both Ihh and ColX expression at older stages could be related to the formation of cartilage cones in birds, structures which also occur in crocodiles and turtles (Haines, 1969). Cartilage cones are formed when erosion at the periphery of the cartilage progresses more quickly at the periphery of the cartilage in the developing long bone than at the centre of the shaft. This non-uniform pattern of erosion can lead to large fragments of cartilage becoming temporarily isolated in the marrow, but eventually erosion becomes general (Haines, 1969), as illustrated in Figure 4.19.

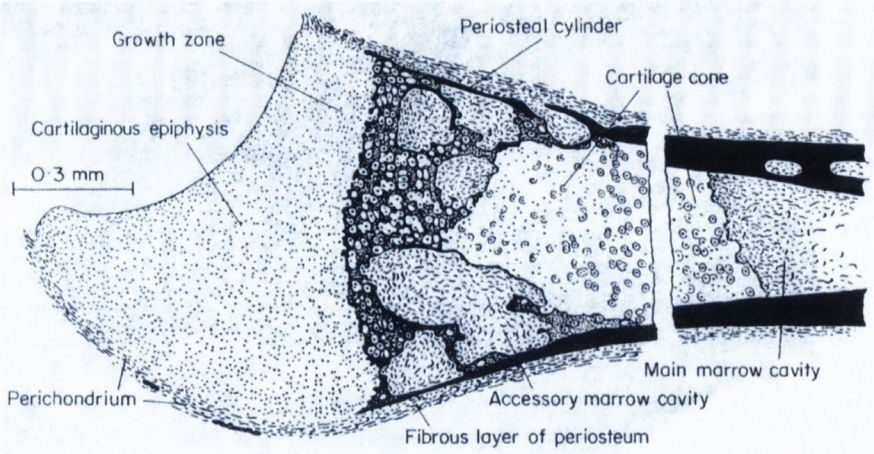


Figure 4.19: Proximal ulna of a young turtle, showing the cartilaginous epiphysis and multiple erosions of the hypertrophied cartilage of the shaft (from Haines, 1969).

Erosion of apoptotic chondrocytes to form bone marrow follows hypertrophy of chondrocytes (expressing ColX) which follows the progression of the chondrocyte into the pre-hypertrophic state (expressing Ihh), so the expression patterns documented here for ColX and Ihh are consistent with the hypertrophy and erosion patterns which lead to cartilage cone formation in the chick.

From this work it was proposed that ColX and Ihh are potential mechanoregulators of ossification in the chick, ColX directly influencing the formation of the periosteal bone collar in response to mechanical stimuli due to muscle contractions, and Ihh through an influence on pre-hypertrophic chondrocytes that are known to signal to the perichondrium and influence bone collar formation (St-Jacques *et al.*, 1999). Although it is not possible to test the validity of these proposed routes of direct mechanical influence on the genetic regulation of bone formation computationally, these results demonstrate how, by integrating computational and experimental approaches, predicted patterns of biophysical stimuli can be used to identify candidate mechanosensors in the embryonic skeleton, revealing prime candidates for experimental testing.

4.4.2. Effect of Immobilisation on Mechanosensitive Genes

In order to further test the hypothesis that ColX and Ihh may act as mechanoregulators of bone formation in the chick limb (Section 4.3.1), an

immobilisation assay was established. The morphological analysis of the immobilised embryos clearly demonstrated the effect of an altered mechanical environment on skeletal development, with immobilisation leading to shorter tibiotarsi and decreased bone collar formation at the stages examined. The slower rate of bone collar formation is of particular interest in the context of this study as it provided an effect potentially related to expression of ColX and Ihh. This study showed that aspects of the expression of both genes, which correlated with biophysical stimuli, indeed showed altered expression patterns following immobilisation in a proportion of specimens. This provides strong corroboration for the direct role of these genes in mechanoregulation of ossification in the chick long bone.

A very obvious feature of the immobilisation assay was the variability of the effect, with some embryos exhibiting movement despite treatment with a neuromuscular blocking agent. This variability was also reflected in the spectrum of morphological effects observed, documented for tibiotarsal and bone collar length (Section 4.3.3). It is therefore not surprising that the penetration of effect on gene expression was also incomplete with only a small proportion of immobilised specimens exhibiting altered expression patterns, (in the order of 20% of the successfully analysed immobilised embryos). The specimens that did exhibit an effect on the mechanosensitive gene expression patterns did not appear to move any less that the other experimental specimens (who did not exhibit an effect) which may indicate that the means of assessing the movement of the embryo was not precise enough, for it is to be expected that the less the specimen moves, the greater the effect on the mechanosensitive genes.

The identification of Ihh as a potential mechanoregulator of bone formation is of particular interest since this gene was previously shown to be a key regulator of bone formation in the mouse, and in particular formation of the bone collar, as reviewed in Section 1.2.1. The new aspect of Ihh expression revealed in the present chick study; the elevation of expression close to the periphery of the hypertrophic zone at later stages (described in Section 4.3.1), was precisely the aspect altered in a number of immobilised specimens with an earlier and greater increase in the relative level of expression at the periphery. At days 8

and 9, in a number of immobilised specimens the concentration at the periphery was very obvious in comparison to diffuse bands found in controls (Figure 4.11, Figure 4.12) and, while at day 11 peripheral elevation is seen in the normal situation, Ihh expression in the immobilised embryos tended to be located closer towards the periphery, and in more narrow regions than in controls (Figure 4.13). What has changed therefore is the timing and degree of peripheral elevation with an earlier and more obvious elevation when mechanical stimulation was reduced. An alteration in Ihh expression will affect the switch from a proliferative to a pre-hypertrophic chondrocyte. An increase in the rate of the differentiation of chondrocytes along the hypertrophic pathway will lead to a shorter rudiment, and as the treated limbs had shorter rudiments, it is possible that mechanical stimulation plays a role in maintaining the proliferation of immature chondrocytes through Ihh signalling.

Alteration to the expression of ColX was also observed in both sites of normal expression; the hypertrophic zone and in the perichondrium proximal and distal to this zone. While elevation of ColX expression at the periphery of the hypertrophic zone was only seen in control embryos at the latest stage examined (Day 11) (Figure 4.10G), in one immobilised specimen at day 9 of incubation a premature elevation of expression was also seen (Figure 4.10D). While this was only observed in a single specimen, it again emphasises a potential regulatory link between Ihh and ColX in the chondrocyte hypertrophy cycle and suggests that the effects seen here may be interlinked; the effect on ColX being downstream of the effect on Ihh.

An effect on ColX expression in the perichondrium was also seen at day 9 which could have occurred directly as a result of the altered mechanical environment. In two specimens it was observed that the expression in the perichondrium did not extend proximal and distal to the hypertrophic zone, to the regions predicted to have highest concentrations of biophysical stimuli (Figure 4.10E-F), as described for the normal developing limb. Therefore, these results indicate that ColX may have an influence on the progression of the perichondrium to the periosteum and/or the deposition of the calcified bone matrix which forms the bone collar, specifically in response to mechanical stimulation. This can be correlated with the delay in bone collar progression

seen in immobilised specimens (Section 4.3.3), implicating ColX in this process.

Although PTHrP has been identified as a mechanosensitive gene *in vitro* (Tanaka *et al.*, 2005) this study did not find any evidence of a change in the gene expression pattern during bone collar initiation in an altered mechanical environment, indicating that PTHrP is not a direct mechanoregulator of embryonic bone collar formation in the chick. However, only a limited number of specimens were analysed, and at a single time point.

Experimental Limitations

A number of factors in the experimental design limited the ability to cleanly assess the relationship between the candidate mechanosensitive genes and the mechanical environment. Firstly, as described in Section 4.3.2, immobilisation induced by decamethonium bromide treatment was not complete, and therefore not all specimens would be expected to show alterations to the same degree. Secondly, in order to maximise the chances of seeing an effect, expression of multiple candidate genes should ideally have been assessed in all treated specimens, but the number of informative sections from each specimen was limited so that only a subset of specimens was assayed for each candidate (Appendix E). Lastly, it was difficult to ensure uniform longitudinal sections with the vibratome sectioning procedure and some glancing and non-uniform thickness sections could not be used, leading to reduced numbers of specimens in the final analysis. In one of the few experimental specimens in which both ColX and Ihh were characterised, an effect was seen on both of the genes (Figure 4.20), illustrating that when immobilisation, sectioning and *in situ* hybridisation techniques were all successful, a clearer picture of the effect of an alteration in mechanical environment on molecular events was gained. It also gives strong support for the reliability of the results despite the small number of specimens revealing the effects.

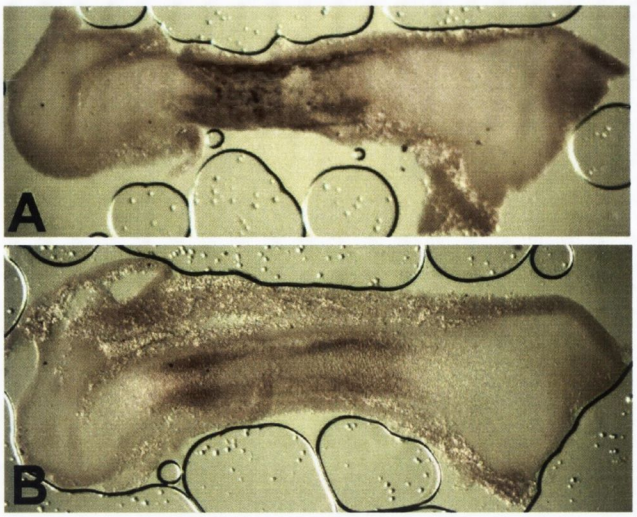


Figure 4.20: Two sections from same treated specimen (Day 9) showing alteration in gene expression patterns. (A) ColX expression in the perichondrium does not extend beyond the hypertrophic zone; (B) Ihh expression is concentrated at the peripheral edges of the rudiment.

The author believes it would be preferable to use a non-pharmacological technique to induce immobilisation, such as muscle ablation where the muscle is excised from the developing limb. This is a difficult technique to perform on young embryos, but when muscle ablation is successful, there is no variability in the efficacy of the treatment because no movement can take place in that limb. Such surgical techniques have the added advantage that one limb can be surgically altered with the other limb left as normal as an ideal stage-matched control, accounting for any individual variability in expression patterns. Therefore some means of cleanly removing the muscle in all experimental limbs would be greatly superior to a pharmacologic agent.

4.5. Conclusion

A number of candidate mechanosensitive genes were characterised in chick hindlimbs for stage-matched comparison with patterns of biophysical stimuli, and it was shown that aspects of ColX and Ihh expression correlated with mechanical stimuli induced by embryonic muscle contractions. It was hoped that these potential mechanoregulators of bone formation could be confirmed as mechanosensitive *in vivo* if their expression profile was altered due to an altered mechanical environment. An altered mechanical environment was

induced by immobilising chick embryos using a neuromuscular blocking agent, and it was found that the rate of bone collar formation was significantly impeded by immobilisation. The gene expression patterns were then compared between the control and immobilised groups, and a number of specimens exhibited differences in ColX and Ihh expression profiles. Although the numbers were low, the results offer an indication of how mechanical forces may influence the expression pattern of two mechanosensitive genes during bone formation; ColX and Ihh. The most convincing effect on ColX expression was seen in several specimens at day 9 of incubation, where expression in the perichondrium did not extend beyond the hypertrophic zone, or in other words, expression in the regions of predicted peak biophysical stimuli was absent. Ihh expression was also affected by immobilisation, where the normal elevated levels of expression at the periphery of the pre-hypertrophic zone were more exaggerated and observed earlier in development in the altered mechanical environment. These results indicate that ColX and Ihh are key mediators in translating information from the mechanical environment to the molecular regulation of bone formation in the embryo. These genes should now be the focus of further studies to confirm alteration following more complete and controlled immobilisation and to address the mechanism(s) through which the genes sense and transduce mechanical stimulation.

Evolution of mechanoregulation of bone growth will lead to non-optimal bone phenotypes*

5.1.	**Introduction**	**90**
5.2.	**Methods**	**92**
5.2.1.	Model genome and its relationship to the growth law	92
5.2.2.	Mutations	95
5.2.3.	Epigenetic variation	95
5.2.4.	Varying selection strength	95
5.2.5.	Implementation	96
5.3.	**Results**	**97**
5.3.1.	Behaviour of the bone growth model	97
5.3.2.	Behaviour of the evolution simulation	99
5.3.3.	Detailed test results	100
5.3.4.	Gene Frequency Data	103
5.4.	**Discussion**	**104**

* Published in: Nowlan, N.C. and Prendergast, P.J. "Evolution of mechanoregulation of bone growth will lead to non-optimal bone phenotypes", Journal of Theoretical Biology, 2005, Vol 235 (3), pp. 408-418.

5.1. Introduction

The development, growth, and remodelling of skeletal structures is a highly regulated process beginning with mesenchymal stem cell condensations in the early embryo and finishing with the homeostatic skeleton of the adult. It is widely accepted that both genetic and epigenetic factors determine the final shape and strength of the skeleton, and many authors have specifically proposed an epigenetic role for mechanical forces (Pauwels, 1960; Thompson, 1917; Wolff, 1986 (translated from Wolff, 1892)). Equations have been proposed to describe how mechanical forces modulate growth where a mechano-biological growth rate is superimposed on a baseline biological growth rate (Carter and Beaupré, 2001). Since the final skeletal structure is partly determined by mechanobiological growth, the mechanoregulatory responses that produce fitter skeletal structures should come to the fore in a population (Prendergast, 2002). Alexander (1981) investigated the most economical possible design for a bone of specified strength, and found that there exists an optimum ratio of inner to outer bone radii for strength with lightness. Currey and Alexander (1985) propose similar optimal ratios, assuming that the bones are designed to have a minimum mass to perform a particular function. At present, simulations of the growth and adaptation of skeletal structures are based on deterministic growth laws where the possible variation in the population is not included (van der Meulen and Huiskes, 2002).

Biomechanical modelling of bone growth and adaptation was presented by Cowin and Hegedus (1976) who proposed an open system in which the rate of change of bone mass was related to mechanical strain. Skalak et al. (1982) later formulated a continuum model of growth. Carter et al. (1987) proposed bone remodelling was targeted to produce a homeostatic level of an 'effective stimulus' and Huiskes et al. (1987) proposed that the process of bone remodelling was an adaptation that returned the strain energy density in the tissue to a homeostatic value. Bone growth models incorporating both biological and mechanobiological influences have been proposed by van der Meulen et al. (1993), for modelling the cross-sectional growth of long bones, and by Stevens et al. (1999), for modelling endochondral growth using a finite element model. An alternative approach is that remodelling of bone is in

response to microdamage (Martin, 2000), either to regulate microdamage to a homeostatic level (Prendergast and Taylor, 1994) or as the stimulus for the activation of the coupled responses of osteoclast and osteoblast cells (Huiskes *et al.*, 2000). Recently, the molecular genetics of bone growth and development has received much attention to identify, for example, the genes that influence bone mineral content (Karasik *et al.*, 2002), bone geometry (Klein *et al.*, 2002; Turner *et al.*, 2004), or lead to bone disorders such as osteoporosis (Peacock *et al.*, 2002), and osteopetrosis (de Vernejoul and Benichou, 2001). Experiments with embryos have established the importance of genes such as Indian hedgehog (Long *et al.*, 2004; Vortkamp *et al.*, 1996), parathyroid hormone-related protein (Lanske *et al.*, 1996) and fibroblast growth factors (Delezoide *et al.*, 1998; Deng *et al.*, 1996) for bone growth and development. While the size and mineral content of a bone are influenced by the processes of bone remodelling, it is probable that genes exist with the sole function of controlling bone response to mechanical loading, (i.e. mechanosensitive genes, (Carter *et al.*, 1998b)). Despite recent advances in the molecular biology of bone, the heritability and variance of the genes controlling bone growth and development remain as yet unknown (Boyce *et al.*, 1999).

We propose to create a model to simulate how mechanoregulation of bone growth is subject to selection pressures during evolution. To do this a genetic algorithm is used which relates the differential equation describing growth to a simplified representation of the genome. The simulation should give outputs describing the population genetics of bone growth and remodelling, i.e. the variance present in a population, and how or why this variation arose, or is maintained, through processes such as recombination through reproduction, changes in the external environment (de Jong and Gavrilets, 2000), genetic mutations (Waxman and Peck, 2003), and migration and random drift (Marroig and Cheverud, 2004; Tufto, 2000). The specific aim is to investigate whether or not changes in mechanoregulatory response can occur during evolution and, if so, how would this help us to better represent the adaptive behaviour in the individual skeleton. In particular, will all individuals in a modelled population reach a biomechanical optimum?

5.2. Methods

5.2.1. Model genome and its relationship to the growth law

Computational simulations are used to investigate the mechanoregulation of bone growth and development in a population over many generations. The bone growth model employed was proposed by van der Meulen et al. (1993). It simulates the growth of the cross section of a long bone from an embryonic bone collar to maturity, where the rate of bone apposition or deposition $\dot{r}_t$ is equal to the sum of the baseline biological rate $\dot{r}_b$ and the rate due to mechanobiological effects $\dot{r}_m$ as defined in equation 1.

$$\dot{r}_t = \dot{r}_b + \dot{r}_m \qquad (1)$$

The baseline biological rate is a decaying exponential function of time that decays to approximately zero by six years, as defined in Eqn. 2.

$$\dot{r}_b = \beta e^{-0.9t} \qquad (2)$$

where $\dot{r}_b$ is the baseline rate magnitude and β is the initial rate magnitude, taken as 10 μm/day in this model. The rate due to mechanobiological effects is dependant on the daily stress stimulus ψ, where the rate of change of radius due to mechanobiological effects is defined in Eqn. 3.

$$\dot{r}_m = c(\psi - \psi_{AS}) \qquad (3)$$

where $\dot{r}_m$ is the rate of bone apposition or resorption on either the inside (endosteal) or outside (periosteal) surfaces of the bone due to mechanobiological effects, ψ is the daily stress stimulus, ψ_{AS} is the attractor state (or desired level) stimulus on the bone, and c is a growth rate constant. The daily stress stimulus (ψ) denotes the mechanical stimulus to which the bone is exposed, and is calculated based on the number of cycles of a load, the tissue level effective stress and an empirical stress exponent (van der Meulen *et al.*, 1993). The constant c is in fact a time constant, which will affect how quickly the bone reacts (via apposition or resorption) to the stresses placed upon it. A higher value of c will lead to more expansion and thus a thinner bone. Through the rate constant c, the variation and convergence of the population is assessed.

We propose that the magnitude of c is determined as follows: a diploid gene set is defined for each individual, taking a finite number of loci, in this case five as shown in Figure 5.1. A simulation commences with the selection of 50 random numbers to form the gene pool; no new genes can be created except by mutation. The genes making up the gene set are numbers in the interval 0 to 1, although genes greater than 1.0 may result from mutations. Each locus is filled with a gene selected at random from the subsection of the gene pool allocated to that locus (i.e. the gene pool is divided into 5 sets of 10 genes, one set per locus). The c value is determined by the sum of the average of the genes at the 5 loci of gene sets a and b;

$$c = \sum_{i=1}^{n} \left(\frac{g_{ia} + g_{ib}}{2} \right) \quad (4)$$

where n is the number of genes, and g_{ia} and g_{ib} are genes from the a and b gene sets at locus i (as shown in Figure 5.1). The genes have no dominance, therefore the effect of having genes g1g2 is midway between the effects of having genes g1g1 and genes g2g2 (Hartl and Clark, 1997), i.e. co-dominance is assumed.

Using Eqn. (3) and Eqn. (4), a mechanobiological growth law is derived from the diploid gene set. Using this law, the bone of each member of the population is grown as described below. The fitness of each individual is assessed when they reach maturity, taken to be 20 years in this model. For the bone of a mammal, it is important to minimise mass, as heavy bones are more expensive to maintain. It is also important to minimise the maximum stress the bone is subjected to (in order to avoid breakage of the bone), which will be the periosteal stress, assuming the bone is in torsion.

a	g_{1a}	g_{2a}	g_{3a}	g_{4a}	g_{5a}
b	g_{1b}	g_{2b}	g_{3b}	g_{4b}	g_{5b}

Figure 5.1: Diploid gene set. Each number is assigned from the 50 numbers constituting the gene pool.

We use stress/mass as a measure of fitness, such that the bone with the minimum value of τ_{max}/mass will be at an optimum. The lower the maximum stress on the bone, the less likely it is to fail. Therefore, the lower the τ_{max}/mass, the fitter the bone. Individuals are selected for recombination according to their fitness relative to the rest of the population. For a population of p individuals, a number x is calculated such that $x = \sum_{i=1}^{p} i$,and the population is arranged in an ordered list such that the least fit individual is first and the most fit last. If *j* is the position in the list, each individual is assigned a probability of selection of *j/x*. The probabilities of selection for all individuals sum to one, and a number line is divided up in proportion to these probabilities, where the least fit individual will occupy a region of size *1/x* on the number line, and the most fit will occupy a region of size *p/x*. A random number between 0 and 1 is obtained, and the individual located at the space on the number line corresponding to this random number is selected for recombination. In this way, fitter individuals are favoured, while unfit individuals still have a chance of being chosen for recombination, and an element of randomness is still maintained in the selection process.

Once an individual has been selected for recombination, a 'germ' or haploid gene set is obtained from the genes of the 'parent'. The genes in the haploid germ are taken at random from the parent. Two parents are selected to form one child, as shown in Figure 5.2.

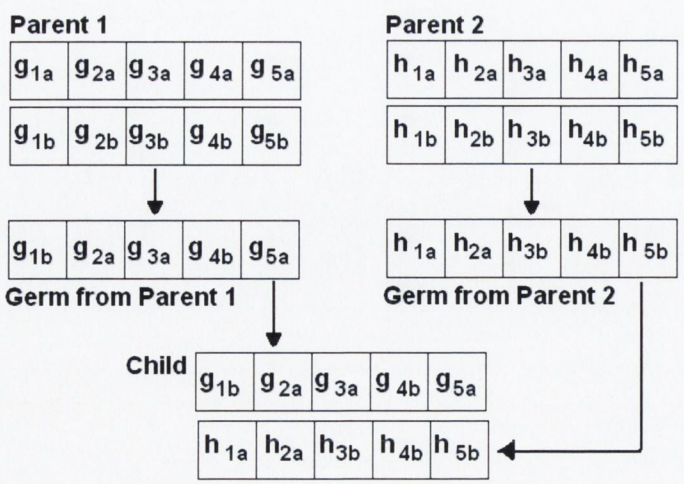


Figure 5.2: Recombination

5.2.2. Mutations

Mutations take the form of randomly halving or doubling the value of the gene to be mutated. Each gene has a 10^{-5} chance of being mutated (Roberts and Pembrey, 1985), and the mutations take place after the creation of a new gene set.

5.2.3. Epigenetic variation

The van der Meulen et al. (1993) model uses an age-dependant loading moment to simulate the loading history for an individual bone as shown in the mean curve in Figure 5.3. This moment was obtained from human body weight during growth (McCammon, 1970), and it was assumed that torsional moments and body weight would scale similarly with age (van der Meulen *et al.*, 1993), to give a plot of age versus applied torsional moment. Differences between individuals' nutrition, climate and exercise levels will result in a range of loading moments, and to account for this, an envelope of ±10% was plotted about the mean curve, as shown in Figure 5.3. Each individual is assigned a moment-age curve at random from within this envelope.

5.2.4. Varying selection strength

Changes in lifestyle (Ruff *et al.*, 1984) or changes in the environment (Raup, 1986) can cause the demands and/or fitness criteria on a bone to change. We include this in our model, where the effect of shifts in the environmental conditions can be investigated by varying the strength of selection cyclically. A high value for the strength of selection results in a competitive environment in which a high fitness conveys a significant reproductive advantage, whereas a low selection strength results in a more equal environment, where having an efficient bone conveys a less significant advantage (Table 5.1). In the simulations where a variable selection force is used, the strength of selection is varied cyclically between 1.0 and 0.5, where the value is changed by 0.1 every ten generations.

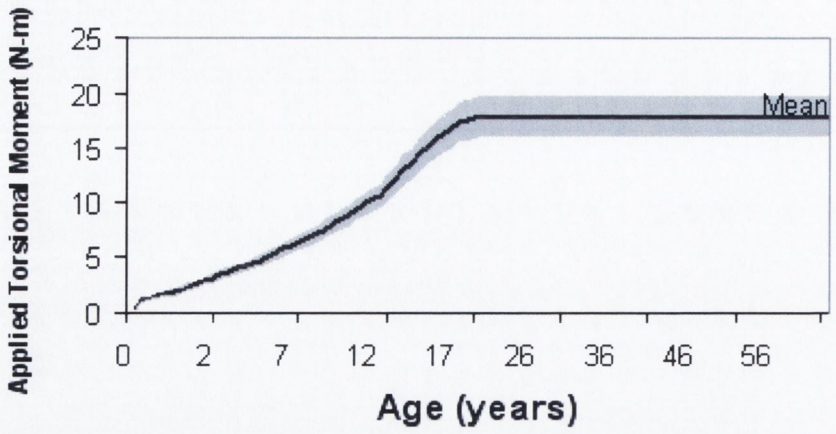


Figure 5.3: Torsional moment applied to simulation over lifetime of bone with 10% variation

5.2.5. Implementation

A gene pool is created and a population of $n = 1000$ individuals is initialised by assigning each individual a gene set. An environment is created, where the initial strength of the natural selection force is specified. In the next stage, mechanobiological laws are applied to grow each bone in the population to maturity. An individual's growth is determined by their gene-set and by the loading conditions applied. Parents are determined based on the relative fitness, or viability, of the individuals in the population, and the selection of parents is influenced by the current strength of the selection force, which can vary over time. Once a new generation has been created using the genes of the parent generation, the old generation is removed from the simulation. The passage of genes can be observed and analysed through generations. The simulation is run for 1,000 generations, equivalent to 20,000 years, as each generation is assessed and culled at 20 years of age. One iteration entails the growth, reproduction and death of one generation. The steps involved in one iteration are illustrated in Figure 5.4. The model is implemented in Java™, http://java.sun.com, using techniques adapted from genetic algorithms, as described by Holland (1975).

Table 5.1: Effect of varying strength of selection on probabilities of selection for a population of four individuals

Probability of Selection	Individual 1	Individual 2	Individual 3	Individual 4
Selection Strength = 1	0.1	0.2	0.3	0.4
Selection Strength = 0.5	0.175	0.225	0.275	0.325

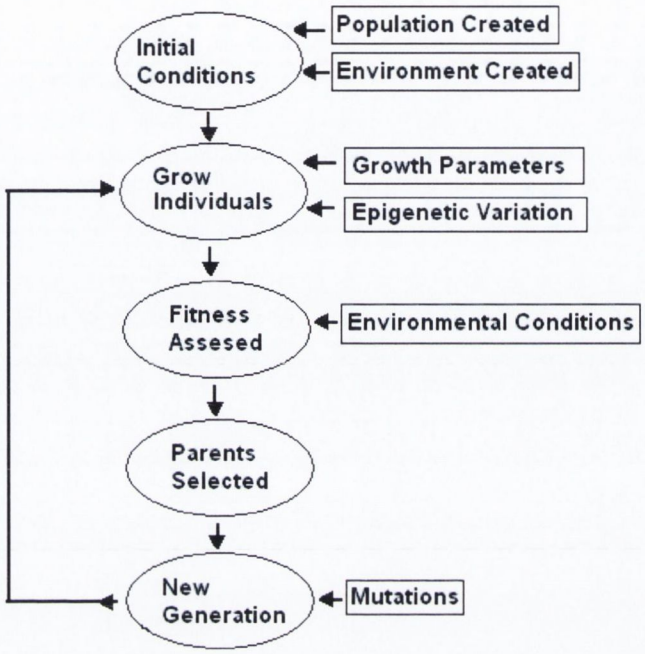


Figure 5.4: Schematic of Computational Implementation

5.3. Results

5.3.1. Behaviour of the bone growth model

The magnitude of the growth rate constant c, as given in Eqn. (4) affects the final shape of the bone at 20 years, where higher values of c result in a bone with greater periosteal and endosteal radii and correspondingly thinner cortical thickness, as shown in Figure 5.5. The constant c is a time constant, and the higher the c value, the quicker the bone will react to stresses by increasing its radii.

Assuming that every bone is grown with the same mean moment curve (Figure 5.3), an optimal bone, (i.e., the lowest τ_{max}/mass value at maturity) is created if c = 1.29, see Figure 5.6. Therefore, under average loading conditions a mechanoregulation rule with c = 1.29 will give the highest probability of

survival. However, the loading conditions applied to the growing bone will affect its growth and resultant shape. We found that applying a lower torsional moment results in increased fitness with increasing *c*, and applying a higher moment leads to a decreased fitness with increasing *c*, as shown in Figure 5.7.

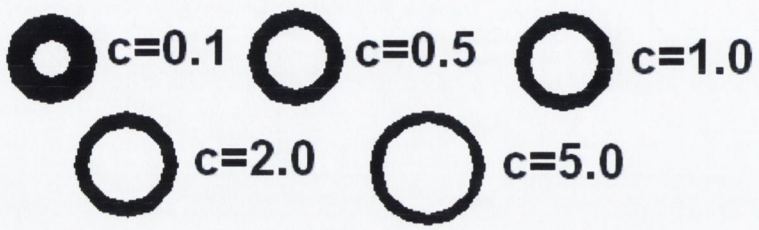


Figure 5.5: Effect of varying c on the growth of a bone. The bones shown were grown with the same mean loading curve.

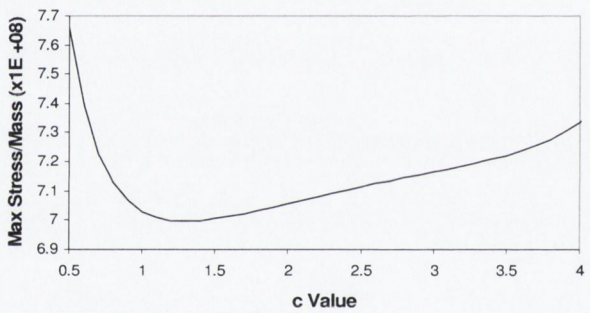


Figure 5.6: Stress/Mass, or fitness values, for bones grown with varying values of c when mean torsional moment is applied, as shown in Figure 5.3.

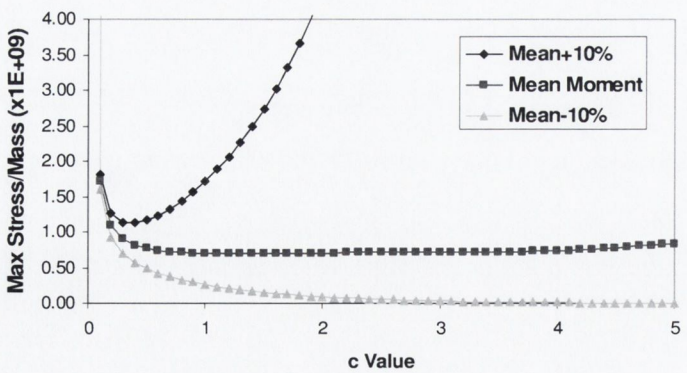


Figure 5.7: Stress/Mass, or fitness values, for bones grown with varying c, when the mean moment, the mean-10% and the mean+10% are applied. The middle curve is the same as the curve shown previously in Fig. 6.

5.3.2. Behaviour of the evolution simulation

Four kinds of simulation were performed:

Test 1) basic simulation,

Test 2) simulation including mutations,

Test 3) simulation including varying selection strength,

Test 4) simulation including both varying selection strength and mutations.

Each test was repeated twice (Run A and Run B) with the same initial gene pool and population configuration; the two runs could be expected to give different results because of the randomness of recombination. This duplication enabled us to analyse the effects of the processes occurring within the simulation, independently of the initial conditions. Therefore each series had eight simulations consisting of two runs (Runs A and B) of each of the four tests listed above, and the complete series was repeated four times for four different initial gene pools (Gene-pools 1-4). Therefore 32 simulations were performed altogether.

The evolution of the gene values and the corresponding c values were recorded for each individual throughout the simulation. These parameters can be used to compute variance (or lack thereof) in the population as evolution progresses. There are two possible final outcomes for each test: convergence to a single value of c, or non-convergence where c is multi-valued in the population and there are many genes. Therefore convergence implies that every individual in the population has the same gene set after 1000 generations whereas non-convergence implies that variance is present in the population. If the population converges, only 5 genes will be left in the gene pool, i.e. each of the 5 genes occupies the same locus for every gene set, where the gene is replicated twice. In the case of non-convergence, more than 5 genes will be present in the gene pool, and a range of c values will exist. It was found that some simulations converged whereas others did not; furthermore convergence did not occur to the same c value, nor did convergence occur to the optimal value of c=1.29, see Table 5.2.

Table 5.2: Test results of Gene-pools 1-4, including c value if population has converged. Within each Gene-pool, all of the four tests (Basic, + Mutations, + Varying Selection Strength, + Varying Selection Strength + Mutations) are performed with the same initial gene pool and initial population configuration.

Test	Run	Gene-pool 1	Gene-pool 2	Gene-pool 3	Gene-pool 4
Basic	A	Non-convergence	Convergence to c=1.415	Convergence to c=1.37	Convergence to c=1.195
	B	Non-convergence	Convergence to c=1.39	Convergence to c=1.365	Convergence to c=1.22
+ Mutations	A	Convergence to c=1.43	Convergence to c=1.285	Convergence to c=1.225	Convergence to c=1.365
	B	Convergence to c=1.37	Convergence to c=1.105	Non-convergence	Convergence to c=1.475`
+ Varying Selection Strength	A	Convergence to c=1.255	Convergence to c=1.405	Convergence to c=1.355	Non-convergence
	B	Non-convergence	Non-convergence	Convergence to c= 1.305	Non-convergence
+ Varying Selection Strength + Mutations	A	Non-convergence	Convergence to c=1.115	Convergence to c=1.47	Convergence to c=1.335
	B	Non-convergence	Non-convergence	Non-convergence	Convergence to c=1.275

5.3.3. Detailed test results

Test 1: Basic simulation

A basic simulation involves initialising a population and running the model without any genetic mutations or changes in the strength of the selection force. A basic simulation does however, like all of the simulations, include the epigenetic variation in applied loading. The initial population configuration has a large impact on determining the outcome of this particular simulation, because when two simulations were run with identical initial population configuration, the simulations could either both converge or both maintain variation, i.e. non-convergence occurs for both Run A and Run B in Gene-pool 1 whereas convergence occurs for both Runs A and B in Gene-pools 2, 3, and 4. In Run A of Gene-pool 1, a total of 13 genes still remain in the gene pool after 1000 generations, see Figure 5.8(a), giving rise to a range of c values from c = 1.105 to c = 1.585 (Figure 5.8(b)). It is important to note that in those cases where convergence occurs in both runs A and B, the populations do *not* converge to the same c value. For example, for the populations in Gene-pool 2, Run A converges to c = 1.415 whereas Run B converges to 1.39. Although the

populations have both converged, they have different final gene pool configurations, which give rise to different c values. Figure 5.9(a) shows the gene structure and Figure 5.9(b) shows the c value for one of these converged simulations, i.e. Gene-pool 2, Run A.

Test 2: Simulation including mutations

This test includes random mutations at the rate of 10^{-5} per gene per recombination. It was found that variation often remains in a population, but also that convergence can sometimes occur. When we ran two tests with the same initial population in Gene-pool 3, we saw that the population for Run A converged whereas the population in Run B maintained variance after 1000 generations. Therefore, unlike the situation with the basic simulation alone, the initial population configuration does *not* determine whether a population will converge or not. This means that the random processes contained within the simulation have a significant impact on the outcome. However, one feature remains the same as the basic simulation: if two tests within the same Gene-pool converge (e.g. Gene-pools 1, 2 and 4), then they converge to different c values (see Table 5.2).

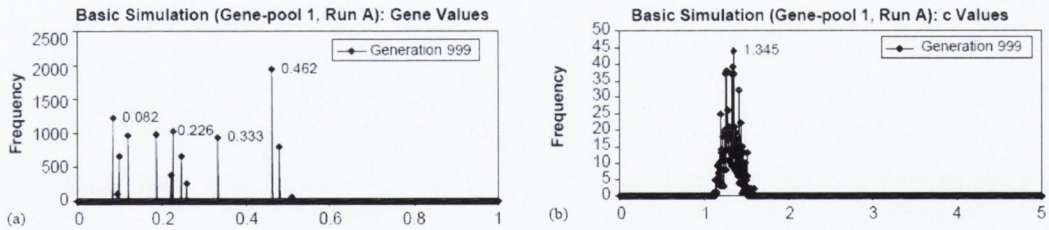


Figure 5.8: Results for basic simulation after 1000 generations, Gene-pool 1, Run A. (a) gene values, (b) c values.

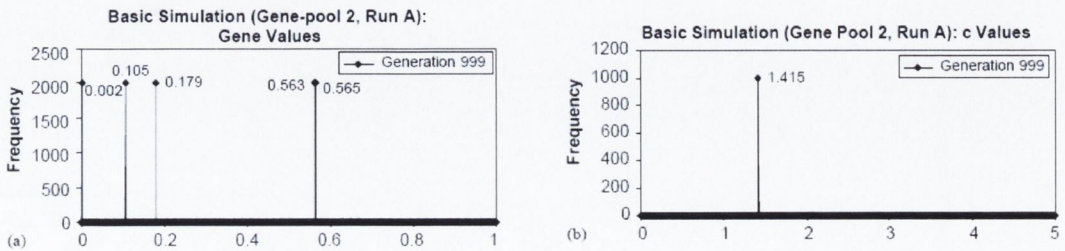


Figure 5.9: Results for basic simulation after 1000 generations, Gene-pool 2, Run A. (a) gene values, (b) c values

Test 3: Simulation including varying selection strength

In this test, the strength of the selection force is varied cyclically throughout the course of the simulation. Where two tests were performed with the same initial population configuration, one of the tests converged (Gene-pools 1 and 2), while the other maintained variation. Therefore, we found that the population can either converge or maintain variation after 1000 generations and, similar to the Mutations test, the outcome is not determined by the initial population configuration. In Gene-pool 3, the populations converged to different c values, while in Gene-pool 4, variation was found in both populations after 1000 generations. However, a different gene pool was maintained by the populations in Runs A and B in Gene-pool 4, and therefore a different spread in c values.

Test 4: Simulation including varying selection strength and mutations

The fourth and final type of test includes both varying selection strength and mutations. Once again, we found that if two tests are run with the same initial population configuration, the population can either converge or maintain variation in the gene pool; this occurred in Gene-pools 2 and 3 (Table 2). In Gene-pool 1, both populations maintained variation, while in Gene-pool 4, both populations converged, but to different values of c. Looking closer at the nature of this difference, Gene-pool 2, Run A converged to a gene pool of only 5 genes, which gave rise to a single c value of 1.115 (Figure 5.10(a) and Figure 5.10(b)). However, Gene-pool 2, Run B maintained many genes (Figure 5.11(a)) giving rise to a wide distribution of bone growth rate constants (Figure 5.11(b)).

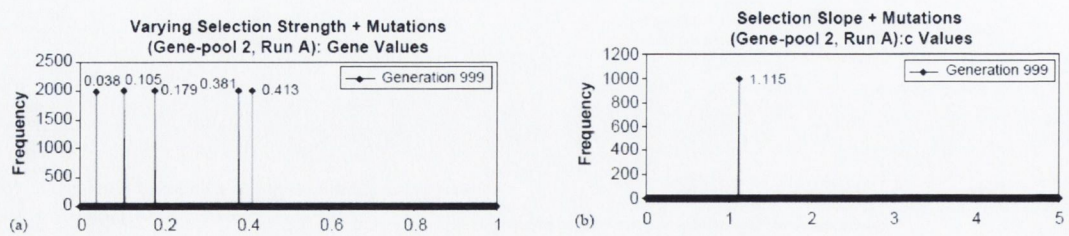


Figure 5.10: Results for simulation including varying selection strength + mutations after 1000 generations, Gene-pool 2, Run A. (a) gene values, (b) c values.

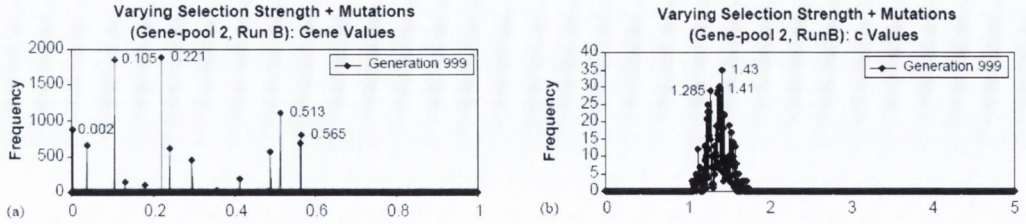


Figure 5.11 (a): Results for simulation including varying selection strength + mutations after 1000 generations, Gene-pool 2, Run B. (a) gene values, (b) c values.

5.3.4. Gene Frequency Data

The passage of each gene in the gene pool may be tracked throughout the simulation to obtain gene frequency graphs. Since there are 1000 individuals in the population, and each individual has 10 genes (5 diploid loci), each of the 5 genes will have a frequency of 2000 when dominant in the population. If a population converges, it is possible to see that most of the genes gradually decrease in frequency to zero, while 5 genes rise slowly to total dominance in the population. For Gene-pool 2, Run A, as previously described, convergence to a single *c* value occurs. This convergence is reflected in the gene frequency data, where 5 genes can be seen rising in frequency until they reach dominance at 850 generations (Figure 5.12). Gene-pool 2, Run B maintained variance in the population after 1000 generations and this can be seen in the gene frequency data, where a large number of genes are still present in the gene pool after 1000 generations and only 2 genes are approaching dominance (Figure 5.13).

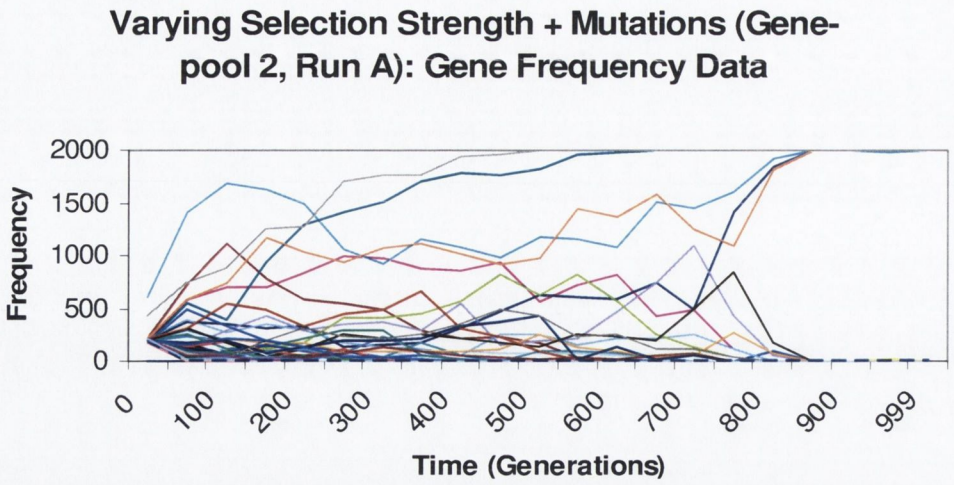


Figure 5.12: Gene frequency data (varying selection strength + mutations, Gene-pool 2, Run A)

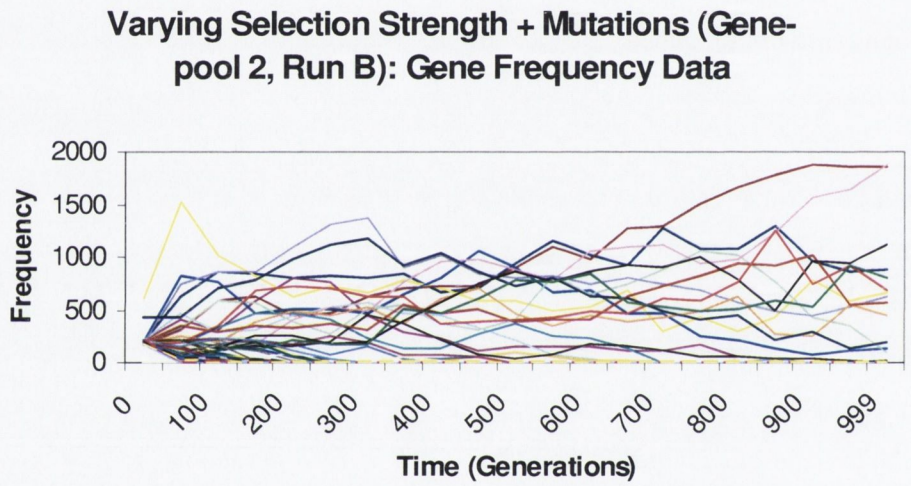


Figure 5.13: Gene frequency data (varying selection strength + mutations, Gene-pool 2, Run B)

5.4. Discussion

The results obtained suggest that the processes of natural selection will not optimize the mechanoregulation of growth within a population. Therefore a biomechanically optimal bone will not be grown. The bone growth rate constants listed in Table 5.2 show that many of the populations converged to a c value far from the optimum value of 1.29; therefore, this model would suggest that natural selection does not even guarantee that mechanoregulation will converge so that bones will grow to some near-optimal state. Another interesting aspect to the results is that the populations often do not converge to

one single value for c, but instead maintain a range of values after 1000 generations. Therefore, if the model is accepted, these results demonstrate that variance can exist among the parameters governing mechanoregulation during growth. In the four types of tests we carried out, there was no test that consistently either converged or maintained variation, and so it is impossible to predict the result until a test is run. For the basic simulation (no mutations and no shifts in external environment), we found that the initial population configuration has a significant impact on the final result, as simulations run with the same initial population gave the same result, i.e., either convergence or maintenance of variation. However, although they gave the same outcome in respect of convergence vs. non-convergence, they did not yield the same final gene pool, and therefore the resultant populations were still different. For the other three tests (mutations, varying selection strength, varying selection strength including mutations), we found that the random evolutionary processes determine the results because, even when two tests of the same type were run with the same initial population configuration, the tests often displayed different final results, with one test converging and the other maintaining variation. In addition, if two tests of the same type and initial configuration both converged, they would converge to different c values, giving, in effect, mechanoregulation algorithms for bone growth.

As with any model, a number of necessary simplifications have been included. Firstly, the bone growth model is rudimentary in that only cross-sectional growth of circular sections is considered. Secondly, the fitness of the bones is judged based on τ_{max}/mass, where the stress is calculated based on the maximum torsional moment applied. If other loads, such as axial or compressive loads were also included, it is likely that a different bone shape would be optimal, and therefore there would be a different optimal value of c. Currey and Alexander (1985) examined several different modes of failure for long bones (such as buckling, fracture etc.), and discovered that different theoretical optimal bone shapes exist for different failure modes. However, introducing a more complex loading would not change the effects of the processes contained within the model, nor the nature of the results obtained. Thirdly, with a computational model, it is impossible to replicate the complexity of the human genome, and our representation of the genes as

numbers having linear effect is obviously simplistic. Also, it is possible that a gene set of only five diploid genes is too limited, and that a larger gene set would allow more recombinations and mutations to occur and therefore individuals might have a better chance of reaching an optimum. However, our knowledge of the genes that impact on bone growth and remodelling, although much advanced, is still incomplete (Boyce *et al.*, 1999) and it is not known yet exactly how many genes impact on bone growth and remodelling (Gilbert, 2000). Finally, not every detail of population genetics has been included in the model; for example, epistemic interaction between the loci of the gene sets, or dominance of certain genes. Nonetheless, as it stands, the genetic part of the model includes many realistic features, such as a diploid recombination, co-dominance of alleles, frequencies of mutations, and interaction between the genotype and the environment. A varying environment is also representative of the real situation.

Although some aspects of the model are simplistic, it does represent the main features of molecular genetics relevant to the question posed in the introduction. For example,

- Genes for recombination are selected at random from the parent chromosomes. This occurs if the genes in question are not on the same chromosome, but located on several different chromosomes, which has been shown to be the case for the genes that influence bone mineral density (BMD) in humans (Karasik *et al.*, 2002), and bone geometry in mice (Klein *et al.*, 2002; Turner *et al.*, 2004). It is therefore acceptable to assume that the genes influencing bone growth are on different chromosomes, and this assumption is reflected in the model.
- We use a mutation rate of 10^{-5} per gene, which corresponds to the rates of between 10^{-5} and 10^{-6} new mutations per gene per recombination suggested by Roberts and Pembrey (1985).
- A ±10% variation in applied torsional moment is applied to the population. In the age vs. weight data of McCammon (1970), a standard deviation of roughly 10% is present for many of the early years, which shows that ±10% is a good approximation for loading variability, as the loading is assumed to scale to weight vs. age data (van der Meulen *et al.*, 1993). This variation represents the influence that environmental

variation can have on the growth of a bone, such as the studies effects of nutrition (Kriegl, 2004), climate (Kobyliansky *et al.*, 2000; Pearson, 2000), exercise levels (Bass *et al.*, 2002; Duncan *et al.*, 2002), and a host of other environmental influences.

Despite the importance of epigenetic factors, genetic factors are still considered to be the most important influence on bone formation. Slemenda et al (1996) investigated genetic effects on femoral neck geometry and bone mineral density using a twin study, where the heritability of bone mineral density, centre of mass and resistance to forces of the femoral neck were estimated as 0.72, 0.70, and 0.94 respectively. This quantity can be calculated by graphing the fitness of the offspring versus that of their parents, and measuring the slope of the line. A sample graph used to calculate the heritability is shown in Figure 5.14. The 10% loading moment variation included in our model gives rise to a heritability of approximately 0.68, which means that roughly 68% of the phenotypic characteristics will be attributable to genetic influences, while the other 32% of effects observable in the phenotype are attributable to the external environment. Therefore, the heritability of the genes in our model of 68% corresponds well to the experimentally calculated values for the heritability of the bone mass density and centre of mass of the femoral neck as detailed above and it provides a corroboration of our model.

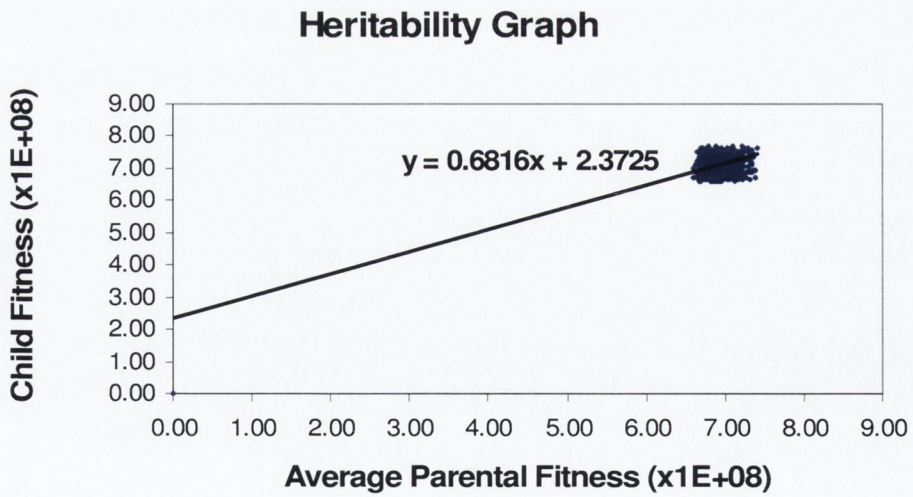


Figure 5.14: Sample heritability graph (for one recombination). Each point represents the fitness of the offspring versus the averaged fitness of the two parents for a sample generation. Heritability is calculated from the slope of the line through the points.

The simulation has elements in common with that of Siegal and Bergman (2002), who model an evolving developmental-genetic system. Their model suggests that canalization may occur as a result of developmental processes even without the influence of stabilizing selection. Canalization, as described by Waddington (1975) is the buffering of animal development such that, in the face of genetic and environmental perturbations, the optimum end result is still produced. In the results presented, none of the populations converge to the optimum mechanoregulatory response that would grow the fittest structure; that is to say they do not converge to c = 1.29. This outcome seems to contradict the well known optimality assumption, which is stated by Emlen (1987) as "the phenotype(s) characterizing the best adapted individuals possible in a population comes to dominate that population". Lewontin (1987) suggests that historical accidents of environmental fluctuation and genetic drift are responsible for shaping a species, rather than optimality. Our simulations would seem to support the view that optimization never takes control over the random elements and therefore that optimum structures are not evolved. Bagge (2000) (citing Roesler (1987)) states that, although bone has often been considered an optimal structure under the given loading conditions, bone cannot immediately attain an optimum structure under a varying load, because of the slow speed of adaptation. However, Bagge (2000) does assume that bone adaptation is an optimization process, and that the bone seeks to reach an optimal internal structure, but this is not what we have found with our model. Instead, we have found that, due to combinatorial aspect of the genetic processes acting during evolution, the algorithms governing bone growth and development would not optimise the skeleton – instead non-optimal structures are formed.

Although no population attained the optimal mechanoregulation constant of c=1.29, the populations that did converge did so to c values between 1.105 and 1.47, out of a range of possible c values between 0 and 5. It could perhaps be argued that the converged mechanoregulatory constants do not vary enough to produce dramatically different phenotypes between populations. However, even when two populations converge to a similar c value, the resultant gene pools are likely to be made up of completely different genes (compare Figure 5.9(a) and Figure 5.10(a)). To apply this to a real population, if the

mechanoregulatory gene set differs slightly between two individuals, both individuals may have a similar mechanoregulatory response to normal loading conditions. However, if some extreme loading condition is applied (a hip prosthesis for example), it is possible that slightly higher or lower rate of adaptation could lead to success or failure of the implant due to the mechanoregulatory response of the individual.

Archaeological data can give useful information on the adaptation of bones. Ruff and Hayes (1983) demonstrate that modern femoral cross-sections are more cylindrical in shape than samples from the Pecos Pueblo femora (dating from between 1300-1650 A.D.), and suggest that this difference could be due to changes in loads, although they do admit that this is a tentative hypothesis. Could the genes governing bone formation and remodelling have shifted, even in the last 500 years, to influence this change in shape? Examination of fossils has shown that there is a difference in the rates of bone remodelling between Pleistocene groups (1.8 million to 11,000 years ago) and the Pecos Pueblo population (Abbott *et al.*, 1996). The study showed that the later Pleistocene members of the genus Homo had greater bone mass, less bone turnover and smaller osteons than recent population, and this implies that bone remodelling laws have not remained constant over time, but are subject to selection pressures and consequently evolve in the same way as the skeletal structures themselves.

We conclude that the variation of mechanoregulation response within a population is dependant on the random evolutionary processes contained in the model, such as epigenetic variation and recombination. By exploring the mechanoregulation algorithms within a population, we would hope to better understand the remodelling response of the individual and its relationship to their genes, so as to better predict the effects of mechanical stimulation on bone growth and development, and in clinical procedures. Although limited by the simplicity of computational models relative to the complexity of skeletal growth, the model, we believe, does demonstrate that evolution with a finite number of genes can cause mechanoregulation to be trapped in non-optimal states (Weinans and Prendergast, 1996).

In conclusion, we have simulated the evolutionary change in ontogenetic mechanoregulation. We predict that changes in mechanoregulation response occur, which indicates that is it possible that variation can exist among the parameters governing the mechanoregulation of bone growth, remodelling, and adaptation in extant populations. This result would suggest that non-deterministic equations should be used when modelling bone growth or remodelling, such as in the patient-specific analysis of skeletal responses due to bone disease or surgery. However, perhaps the most significant result is that convergence to the optimum mechanoregulation equation was not found and this implies that sub-optimal bone phenotypes always occurred in the population.

Discussion

6.1. Introduction 112

6.2. Limitations of the present study 112

6.2.1. Evolution of mechanoregulation simulation 112

6.2.2. Material properties of embryonic tissues 113

6.2.3. Efficacy of the immobilisation agent 114

6.2.4. Mechanoregulation: of birds, mice and men 114

6.2.5. Mechanoregulatory control of tissue differentiation 115

6.3. Comparing Chick and Mouse Gene Expression Patterns 117

6.4. Mechanisms of mechanotransduction 121

6.5. Redefining mechanobiology 124

6.1. Introduction

A study of mechanoregulation of the avian embryonic skeleton has been presented, and a simulation of the evolution of mechanoregulation has also been described. The results presented in this thesis could have an impact on tissue engineering of skeletal tissues, but there are some limitations to the research, which are discussed in this chapter (Section 6.2). Mechanosensitive genes, characterised for the first time in the avian hindlimb, are compared with published gene expression patterns in the mouse, identifying potential molecular mechanisms leading to the divergent processes of embryonic ossification between the species (Section 6.3). The results arising from the work on mechanoregulation of skeletogenesis are discussed in the context of our current understanding of molecular mechanotransduction (Section 6.4). Finally, a framework for future research into embryonic mechanobiology is proposed (Section 6.5), where mechanical engineering, developmental biology and genetics approaches are integrated so as to advance the frontiers of knowledge and understanding of the mechanoregulation of skeletogenesis and potentially of other developmental systems.

6.2. Limitations of the present study

Some simplifications have been necessary in the course of this research; these simplifications and experimental limitations have been discussed in detail in the discussion section of each chapter, and the most significant limitations are addressed below.

6.2.1. Evolution of mechanoregulation simulation

The simulation of the evolution of a mechanoregulatory gene set included simplifications such as a 2-D cross-sectional representation of bone growth, use of torsional loading without axial or compressive loading, and a representative gene set of only five mechanosensitive genes. At present, only mechanoregulation of the post-natal skeleton is included in the model and, in light of the results presented in this thesis, the author proposes that mechanoregulation of the embryonic long bone should be included in the simulation. The author proposes that it would be possible to develop the bone growth model of van der Meulen *et al.* (1993) to include embryonic

mechanoregulation by using realistic geometries from OPT, and simulating the 'growth' of the rudiment based on mechanical forces due to muscle contractions. In the current bone growth model (van der Meulen *et al.*, 1993), a 2-D cross section is used to represent the growing bone, but with data from OPT, 3-D rudiment morphologies could be included in the simulation, allowing more complex loading schemes and fitness criteria. Rather than the representative genes used in the current model, genes which have been predicted to be mechanosensitive *in vivo*, such as Ihh and ColX, could be used in the gene set. Features of real genes such as interactions, and positive or negative regulation effects could also be included.

However, despite these simplifications, the evolution simulation offers a unique insight into mechanoregulation parameters at a population level, exploring questions that have not been previously examined using computational simulations. The results suggest that variation may exist in the parameters governing mechanoregulation in extant populations, meaning that non-deterministic equations should be used when modelling bone growth or bone-remodelling in population-based studies. The results also indicated that evolution pressures may lead to sub-optimal mechanoregulation rules, leading to sub-optimal bone phenotypes.

6.2.2. Material properties of embryonic tissues

There were limited data on material properties of embryonic skeletal tissue available for use in the finite element models. Therefore, muscle force values from embryonic rat tissue and material properties for murine embryonic cartilage and calcified tissue were used, and material properties in the hypertrophic or growth plate region were not adjusted. Viscoelasticity of the cartilage (Mak, 1986) was also not included. However, when sensitivity analyses were performed with varying material properties for cartilage and calcified tissue, and a range of values for the muscle, the patterns of stimuli were not significantly altered. It is presumed that if the material properties of the growth plate or hypertrophic regions were adjusted, the same pattern of stimuli would still be observed. Therefore, the hypothesis of a dynamic pattern of biophysical stimuli as a promoter of ossification in the avian long bone would still emerge if different tissue properties were used.

6.2.3. Efficacy of the immobilisation agent

When trying to corroborate the mechanosensitivity *in vivo* of the set of candidate genes, a limiting factor was the incomplete immobilisation by the neuromuscular blocking agent used *in ovo*. This meant an increase in the number of specimens that needed to be analysed to see an effect of the altered mechanical environment on gene expression patterns. It also led to variability in the observed effect on mechanosensitive genes. However, despite these difficulties, an effect on gene expression was seen for two of the genes; ColX and Ihh, in multiple specimens, identifying these genes as potential mechanoregulators of ossification in the chick limb. Future work on the avian model should use a more reliable and effective means of immobilisation, such as muscle ablation (Honjo and Eisen, 2005), surgical alteration of tendons (Kardon, 1998) or partial neural tube excision. If every specimen was affected to the same degree (for example, elimination of muscle in tibiotarsus of left limb), a more consistent and measurable effect on skeletal development, and on expression of mechanosensitive genes would be expected. In addition, some measure of the variability in mechanoregulation response could be extracted from such an experiment, potentially providing experimental data on the variability in skeletal mechanoregulatory response in a population of chicks, thereby either corroborating or refuting the results of the evolution simulation described in Chapter 5.

6.2.4. Mechanoregulation: of birds, mice and men

As experimental studies on human embryos are impracticable, we must turn to animal models in order to investigate embryonic osteogenesis. A limitation of the work presented in this thesis, in terms of biomedical relevance, is that the animal model used is the chick, an animal in which the long bones form primarily via periosteal ossification rather then by endochondral ossification. However, an advantage of studying the chick limb is that we can deepen our understanding of the bone collar. In the mouse, where the endochondral ossification at the core and the periosteal ossification of the collar progress simultaneously, it would be difficult to separate the effects of mechanical stimulation on the two distinct processes. Current understanding of bone development focuses on endochondral or intramembranous ossification, but it has been proposed that the process and control of periosteal ossification is

distinct from intramembranous ossification (St-Jacques *et al.*, 1999), and we know relatively little about its development. Studying the mammalian limb, and mechanoregulation of endochondral ossification, are the next natural steps in this research, but future work on the mouse will build upon and be significantly guided by the work completed to date on the chick.

The conclusions on ossification in the chick limb, proposed as part of this thesis, deepen our understanding of the molecular and mechanoregulatory controls of bone collar formation by identifying for the first time an *in vivo* mechanoregulatory role in ossification of two genes, ColX and Ihh, revealing prime candidates for further analysis, both in the chick and in other animal systems, and therefore represent a significant contribution to the current knowledge of skeletogenesis.

6.2.5. Mechanoregulatory control of tissue differentiation

Knowledge of the type, magnitude and frequency of mechanical stimuli regulating the formation of skeletal tissues is of utmost importance when trying to grow such tissues *in vitro*. The results from the finite element analyses presented in Chapter 3 suggest that biophysical stimuli may promote ossification in the chick long bone but, unfortunately, it was not possible from this study to conclude the precise nature of the mechanical stimulus, (such as stress, strain, fluid flow, pressure, or a combination of any of the above), causing mechanotransduction.

In computational simulations, a range of parameters have been hypothesised to promote ossification, such as low levels of hydrostatic stress and principal strain (Carter *et al.*, 1998a), local stress and strain magnitudes (Claes and Heigele, 1999) or low levels of octahedral shear strain and fluid velocity (Lacroix and Prendergast, 2002). Geris *et al.* (2004) demonstrated that a combination of octahedral shear strain and fluid velocity succeeded in predicting bone formation inside a bone chamber, placed in a rabbit tibia. Isaksson et al. (2006) performed a study in order to corroborate a range of mechanoregulatory algorithms with *in vivo* bone healing data from animal experiments, and concluded that an algorithm based on a combination of deviatoric (octahedral shear) strain and fluid velocity yielded results closest to

experimental data. Simulations including this combination of stimuli have been shown to predict tissue differentiation at implant interfaces (Prendergast and Huiskes, 1996; Prendergast *et al.*, 1997b), and bone formation during distraction osteogenesis (Isaksson *et al.*, 2006) and in osteochondral defects (Kelly and Prendergast, 2005). Quantitative thresholds relating values of deviatoric strain and fluid velocity to differentiation of precursor cells in undifferentiated tissue to fibrous tissue, cartilage or bone were proposed by Huiskes *et al.* (1997) as shown in Figure 6.1 from Lacroix *et al.* (2002).

As material properties for murine rather than avian embryonic tissue were used in the FE analyses of chick rudiments presented in this thesis, the predicted magnitudes of the octahedral shear strain and fluid velocity (as given in Table 6.1) and of other stimuli may not be physiological in the chick skeleton. However, if the stimuli magnitudes obtained were correct and the thresholds defined by Lacroix *et al.* (2002) were applied to the predicted stimulus values in imminent regions of bone formation, then cartilage or fibrous tissue rather than bone formation would be predicted.

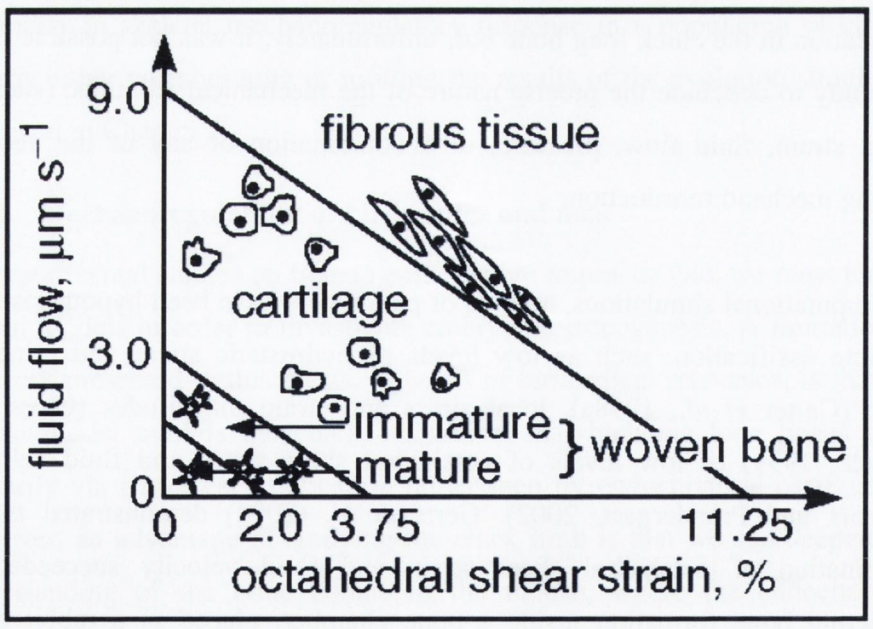


Figure 6.1: The mechanoregulation rule described by Lacroix et al. (2002), where relative levels of fluid flow and octahedral shear strain are predicted to direct cell differentiation towards different fates.

Table 6.1: Maximum values of octahedral shear strain and fluid velocity over flexion and extension contractions for HH30, HH32 and HH34 (from analyses presented in Chapter 3).

STAGE	Octahedral Shear Strain, %	Fluid Velocity, μm/sec
HH30	.55	9
HH32	.55	11
HH34	3.0	43

The model of Lacroix *et al.* (2002), was designed to predict adaptation of adult tissue, so it is possible that the combination of octahedral shear strain and fluid velocity could be the principal mechanoregulatory stimulus for embryonic bone formation, and that the threshold values need to be adjusted for embryonic tissue. If this were the case, that fetal and adult tissues respond differently to mechanical stimulation, there may be important ramifications if *in vitro* culturing of embryonic stem cells were to take place, as lessons learned from *in vitro* research on adult stem cells may have to be re-appraised.

However, as high stimulus values have commonly been assumed to inhibit, and low stimulus values to promote endochondral bone formation (Huiskes *et al.*, 1997; Lacroix *et al.*, 2002), it is possible that the high stimuli values obtained in this study indicate that that intramembranous ossification of the periosteal bone collar is directed by a different mechanoregulation rule. Alternatively, the high stimuli levels predicted at the core of the avian embryonic rudiment could play a role in preventing endochondral ossification. By performing FE analyses of the mammalian embryonic long bone and comparing the results with those from the chick, it would be possible to investigate if differences in predicted patterns of biophysical stimuli could explain differences in long bone ossification events between the species.

6.3. Comparing Chick and Mouse Gene Expression Patterns

As described in the Literature Review, late long bone ossification events are significantly different in mammals and birds, where the long bones of birds are formed primarily via periosteal ossification as opposed to a combination of periosteal and endochondral ossification in mammals. The results in Chapter 5 presented a systematic analysis of expression in the chick whereas published data largely describes developmental expression in the mouse. Given the

divergent molecular mechanisms directing vertebrate bone formation, it is useful to compare expression patterns of genes instrumental to bone formation between the chick and the mouse.

Expression of ColX in the hypertrophic zone in the avian hindlimb sections is similar to published expression data for the mouse (Dacquin *et al.*, 2004; Maes *et al.*, 2002; Yang *et al.*, 2003). However, in this study, ColX expression was also observed in the perichondrium, which has not been reported in the mouse (Figure 6.2). It is interesting to note that the clear perichondrial expression of ColX in the chick correlates with the predominant site of bone formation in this species, with no ossification at the core of the diaphysis. The ColX gene has been identified as playing a role in matrix mineralization in the growth plate (Kwan *et al.*, 1997). Therefore higher levels of ColX may be required in the periphery of the chick bone for progression of the periosteal bone collar.

In the chick, FGFr2 expression was found in the perichondrium and periosteum, a pattern that has also been reported in the mouse (Minina *et al.*, 2005). However, expression was also reported in proliferating chondrocytes in the mouse, and at e16.5, in two stripes of chondrocytes parallel to the perichondrium and distal to the Ihh expression domain, as shown in Figure 6.3 (Minina *et al.*, 2005). No equivalent expression in the proliferating chondrocytes was found in the present study in the chick, which may also relate to the absence of ossification in the core of the chick long bone.

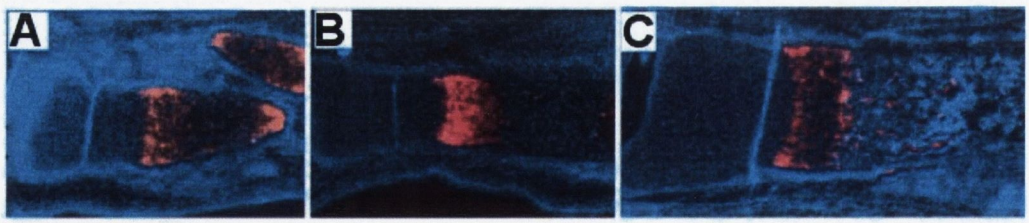


Figure 6.2: ColX expression (red) in the hypertrophic chondrocytes of the mouse long bone at (A): e14.5, (B): e16.5 and (C): newborn (adapted from Dacquin et al., 2004). Note the lack of detectable expression in perichondrium/periosteum.

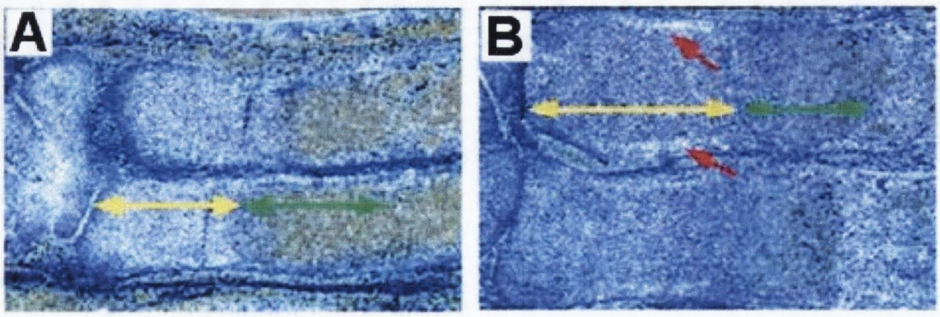


Figure 6.3: FGFr2 expression in the mouse forelimb, (A) e14.5 (equivalent to HH32/Day 8), FGFr2 expression in proliferating chondrocytes and the perichondrium. B: e16.5 (equivalent to HH36/Day 11), Elevated expression in two stripes of chondrocytes parallel to the perichondrium and distal to the Ihh expression domain (red arrows) and weak expression in proliferating chondrocytes (adapted from Minina et al., 2005). Yellow arrows demarcate the distance from the joint region to the Ihh expression domain. Green arrows demarcate the hypertrophic region.

While the expression profile of Ihh in the hypertrophic chondrocytes during the early stages of bone formation is similar in the chick and the mouse, the results obtained in this study indicate divergence in the Ihh expression profile some time after initiation of the bone collar. Firstly, in later stages in the chick, Ihh expression was commonly observed to be elevated at the periphery of the rudiment, rather than the continuous band across the width of the rudiment reported for the mouse at the equivalent stage, as shown in Figure 6.4 (Minina *et al.*, 2005). Secondly, it was found that Ihh expression in the chick at the latest stage examined (HH36) was downregulated (Figure 6.5), as was the expression of PTHrP by HH34, whereas no Ihh/PTHrP downregulation was reported during progression of the primary ossification centre in the mouse.

While no images of PTHrP expression at equivalent stages were found in the literature, Figure 6.4 compares Ihh expression in mouse limbs between e14.5 and e16.5, approximately equivalent to limb development at stages HH32 and HH36 in the chick; the study (Minina *et al.*, 2005) noted no change in intensity of expression between the two stages. This indicates that although the role of the Ihh-PTHrP feedback loop in early ossification events such as initiation of hypertrophy and stimulation of bone collar formation has been conserved between the chick and the mouse, progression of the periosteal bone collar in

the chick may not require the same levels of the Ihh/PTHrP gene products as progression of the primary endochondral ossification centre in the mouse.

It is possible that differences in gene expression profiles between the chick and the mouse could provide an insight into the different mechanisms that have evolved to govern ossification events between these animals. Molecular events implicated in early hypertrophy appear to be similar between the chick and mouse, but it appears that once initial bone formation has taken place, divergence occurs. However, as similar sections in stage matched specimens are not available for every gene in the mouse, it is difficult to form firm conclusions on the differences between the species. A detailed comparative study at corresponding stages is required.

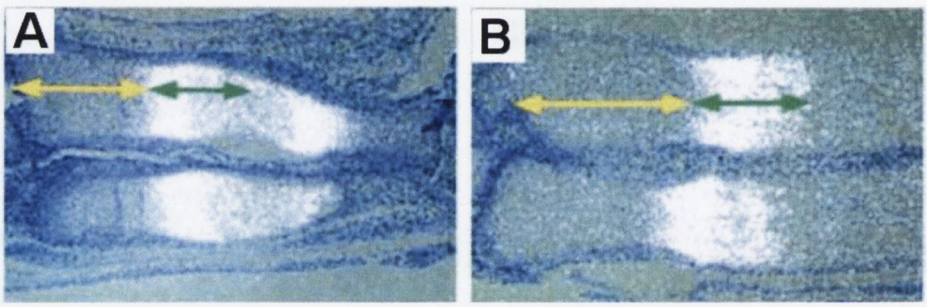


Figure 6.4: Ihh expression in the mouse forelimb showing no change in the intensity of detection between e14.5 (A) and e16.5 (B), equivalent to HH32 and HH36 (adapted from Minina et al., 2005). Yellow arrows demarcate the distance from the joint region to the Ihh expression domain. Green arrows demarcate the hypertrophic region.

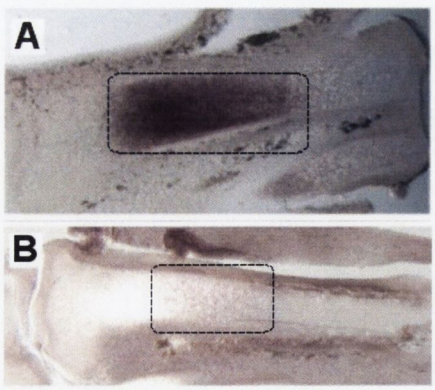


Figure 6.5: The intensity of staining following detection of Ihh mRNA in the pre-hypertrophic zone at HH36 (B) was consistently lower than at earlier stages (A: HH32).

6.4. Mechanisms of mechanotransduction

Cellular mechanotransduction is the translation by a cell of a mechanical stimulus to certain molecular events. According to Duncan and Turner (1995) there are four steps in mechanotransduction; (1) mechanocoupling, (2) biochemical coupling, (3) transmission of signal and (4) effector cell response, as illustrated in Figure 6.6. In mechanocoupling, an applied force is transmitted to the cell through the extracellular matrix (ECM) and the cell undergoes deformation, e.g. shearing or stretching. In the second step, biochemical coupling, the cell-level mechanical signals are translated into intracellular biochemical signals. In the transmission of signal, the cell communicates the transduced mechanical signal within itself and/or to other cells and may affect cellular events or processes such as proliferation or differentiation (the effector cell response). The effector cell response will most likely involve further modulation of gene expression and may initiate a cascade of events within the cell itself and in other neighbouring cells. Genes whose expression is modulated by the effector cell response can be detected as "mechanosensitive" genes.

In this study, which characterised the effect of an altered mechanical environment on embryonic bone formation, the transmission of signal was examined at the level of an effector cell response by characterising messenger RNA (mRNA) to reflect gene expression patterns (step 4), and the phenotypic consequence of effector cell responses was indirectly observed through reduced bone formation in the hindlimbs.

Although certain steps in mechanotransduction have been widely studied in recent years, large gaps remain in our understanding of the full pathway or pathways leading from mechanical stimuli to downstream responses. Many researchers have focused on either biochemical coupling, where a mechanical signal is transduced through the cell membrane (step 2), or on the effector cell response, where genes are activated or de-activated in the nucleus (step 4). The most widely studied cellular components involved in biochemical coupling are stretch-activated ion channels and integrins, but a range of other mechanosensitive cellular components such as primary cilia, cadherins and

cytoskeletal filaments have also been identified (Ingber, 2006). Stretch-activated ion channels allow the movement of Ca^{2+} and other ions in and out of cells, potentially activating transcription factors and signalling cascades (McMahon et al., (submitted); Wang and Thampatty, 2006). Integrins are transmembrane proteins which are thought to transfer mechanical signals from the ECM to the cytoskeleton, initiating cascades of signalling events leading to eventual gene transcription (Millward-Sadler and Salter, 2004).

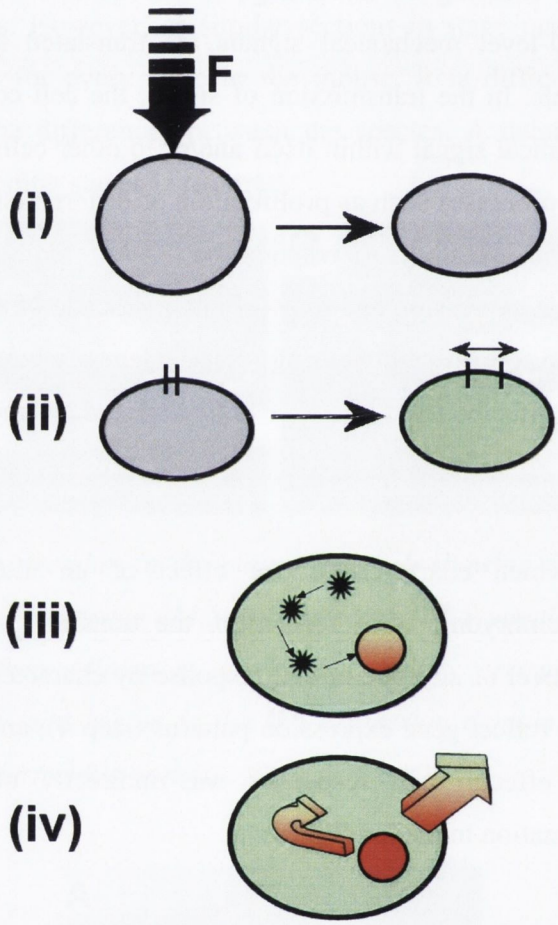


Figure 6.6: Cellular mechanotransduction can be considered as consisting of four steps (as defined by Duncan and Turner (1995)). (i) mechanocoupling: force (F) is transmitted to the cell from the extracellular matrix, (ii) biochemical coupling: cell-level mechanical signals such as stimulation of stretch activated channels are translated into intracellular biochemical signals, such as (for example) elevated calcium levels, (iii) transmission of signal: intracellular biochemical signals may activate transcription factors which bind to mechanosensitive genes, (iv) effector cell response: modulation of gene expression in nucleus.

In the effector cell response, genes are activated or de-activated in the nucleus of the cell; these are the genes that are described as mechanosensitive, such as those listed in brief in Table 1-1, and in more detail in Appendix D. Activation of a 'mechanosensitive gene' is a downstream effect of signalling cascades prompted by mechanical deformation of the ECM or the cell itself, but up- or down- regulation of the gene forms a key part of the puzzle that can be focussed on in developmental and genetic analyses.

The largest gap in our current understanding of mechanotransduction is the transmission of signal (step 3); the events between the output resulting from stimulation of the cell membrane, (e.g., elevated calcium levels due to activation of stretch activated ion channels, or via other methods), and regulation of so-called mechanosensitive genes. Presumably it involves the activation or stabilisation of specific transcription factors that bind to the regulatory elements of target "mechanosensitive" genes and influence their transcription. In the case of Ihh, which has been shown to be upregulated by mechanical stimulation in both *in vitro* (Wu et al., 2001) and *in vivo* (Ng *et al.*, 2006b, and this study), a number of levels of the pathway have been uncovered. Ihh has been shown to be necessary for normal chondrocyte proliferation (Karp *et al.*, 2000; St-Jacques *et al.*, 1999), and when chondrocytes were mechanically stimulated *in vitro,* both proliferation of chondrocytes and mRNA expression levels of Ihh were upregulated (Wu *et al.*, 2001; Wu and Chen, 2000). However, when gadolinium, an inhibitor of stretch activated channels, was applied, both proliferation (Wu and Chen, 2000) and Ihh expression levels (Wu *et al.*, 2001) were reduced to the levels of non-stimulated controls. Therefore, it has been suggested that Ihh regulates proliferation of chondrocytes through the activation of stretch activated channels by mechanical stimulation (Wu *et al.*, 2001). It remains to be discovered what transcription factors and other intracellular molecules form the link between stretch activated channels and upregulation of Ihh.

As ColX and Ihh have been demonstrated to be mechanosensitive in cartilage *in vivo* at specific developmental timepoints in this study, this opens the possibility of dissecting the upstream mechanisms involved in the response. A first step in such analysis would be to analyse genomic sequences of these

genes, and identify regulatory elements through which the genes are controlled. Regulatory elements bound by transcription factors that have been implicated in response to mechanical forces, e.g., Fos/c-fos (Raab-Cullen *et al.*, 1994), would be of particular interest. Using an *in vitro* culture system, the mechanosensitivity of each of these response elements could be measured, thereby identifying another step in the pathway to link activation of stretch activated channels or other mechanosensitive cellular components and upregulation of ColX and/or Ihh. This would be no simple task and would involve sophisticated genome analysis and iteration between cell culture assays and *in vivo* analysis to test the relevance of the findings, but it opens a possible route of investigation of the 'transmission of signal' step in the mechanotransduction events described by Duncan and Turner (1995).

6.5. Redefining mechanobiology

Despite the large body of evidence presented in the literature review that demonstrates the influence of mechanical forces on embryonic development, the concept of development mediated by such forces receives little attention by many molecular biologists. For example, in a special Insight feature of *Nature* in 2003 on 'Bone and Cartilage', articles reviewed the recent literature on 'The complexities of skeletal biology' (Karsenty); 'Developmental regulation of the growth plate' (Kronenberg) and 'Deciphering skeletal patterning: clues from the limb' (Mariani and Martin), and the influence of mechanical forces was mentioned in only one of these review articles, when Karsenty (2003) states that "we have no real clues of how bones sense and transduce mechanical forces and how this may affect gene expression". In molecular genetics textbooks, such as Lewin's Genes VIII (2004) for example, mention of mechanosensitive or mechanoresponsive genes and pathways is notably absent. It seems that a large gulf remains to be crossed between cell biologists, developmental biologists and bioengineers. Collaboration between these groups will be necessary to obtain a deeper understanding of the processes underlying embryonic mechanobiology.

A purely molecular biological approach to studying bone formation has led to an understanding of the molecular components involved, without considering the influence of mechanical forces, as represented in red in Figure 6.7A.

Following this purely biological path has yielded a wealth of knowledge on how molecular pathways and interactions promote embryonic bone formation, such as, for example, the discovery of the Indian Hedgehog (Ihh) and PTHrP negative feedback loop as a regulator of chondrocyte differentiation (Lanske *et al.*, 1996).

A mechanical approach to the same system could examine the effect of mechanical stimulation on bone formation, establishing an empirical relationship but without addressing the molecular or cellular mechanisms involved, as illustrated in blue in Figure 6.7B. Experiments in which the mechanical environment is altered using grafting or immobilisation experiments have corroborated the hypothesis of biophysical stimuli as an essential influence on bone formation, and have provided an insight into the extent and timing of these influences. Another body of work relevant to the mechanoregulatory system of bone has emerged in recent years with the discovery of a set of genes that can be up- or down-regulated by changes in mechanical stimulation, i.e. the mechanosensitive genes. Studies into such genes provide information on the output from the mechanoregulatory system of a tissue under mechanical stimulation, as shown in green in Figure 6.7C, but it is possible that genes that display mechanosensitivity in *in vitro* cultures may not necessarily have a mechano-regulatory role *in vivo* in all, or even in any, circumstance. Despite progress that has been made in identifying mechanosensitive genes and pathways, we still do not fully understand how mechanical stimulation is incorporated as input information to a cell leading to eventual cellular response such as proliferation or differentiation, as discussed in Section 6.4.

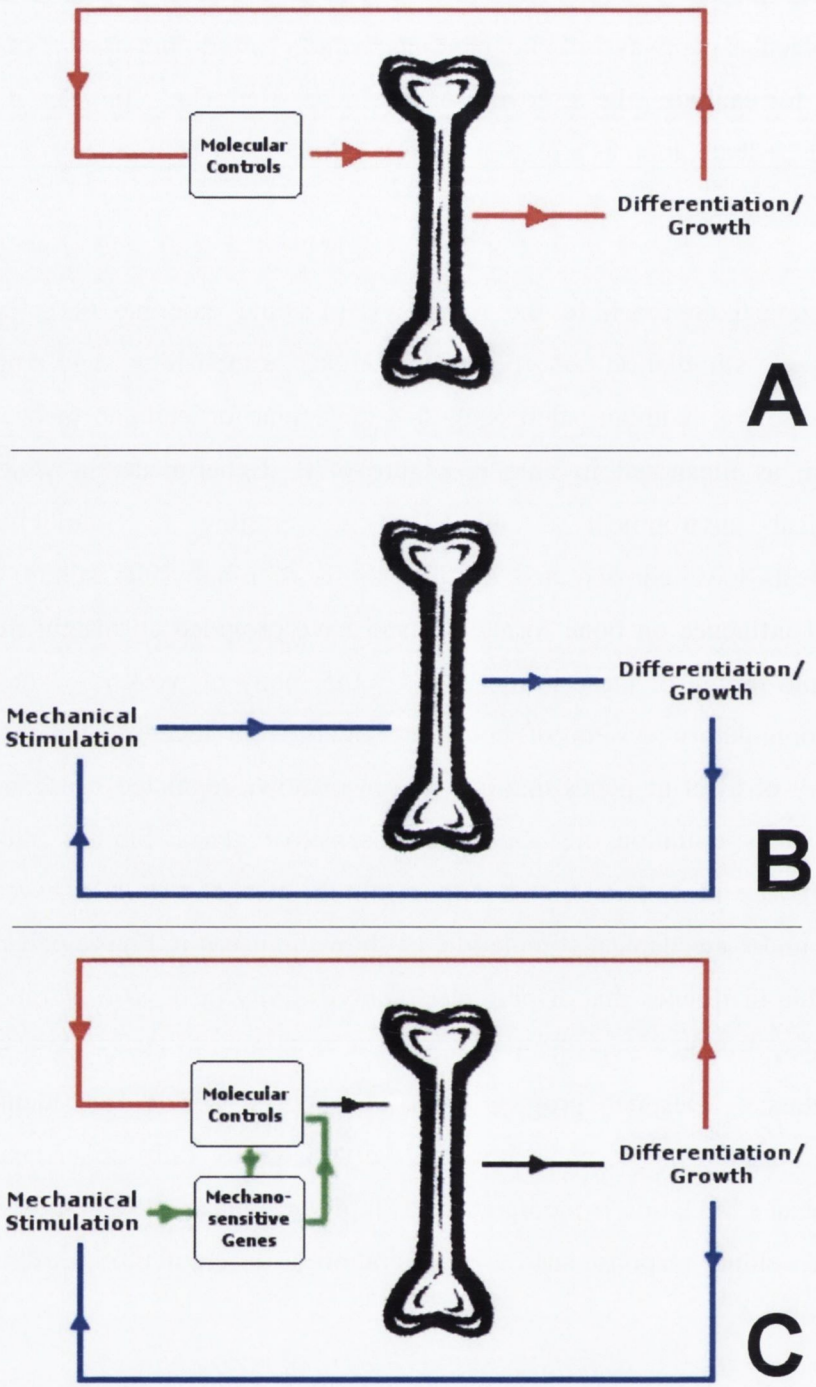


Figure 6.7: (A) Some biological methods examine effect of molecular controls of embryonic bone development; (B) a mechanical approach may study the effect of an alteration in mechanical environment without considering molecular components; (C) an integrated bioengineering approach to embryonic bone formation combines biological (in red), mechanical (in blue) and mechanosensitive gene analysis (in green) approaches.

Developmental biology, mechanical and mechanosensitive gene methods, when considered individually, provide important insights into bone development. However, by combining the techniques and results from these fields using an integrated approach, as shown in Figure 6.7C, there is the potential to significantly advance our understanding of bone development as a complete system. In the work presented in this thesis, the major conclusions are that stage-dependant patterns of biophysical stimuli induced by embryonic muscle contractions are necessary for normal bone formation in the chick, and that ColX and Ihh may play a mechanoregulatory role in the ossification process. This conclusion was reached by integrating developmental biology, genetics and engineering in an approach also known as a systems or systems biology approach. The term 'systems biology' has become widely used in recent years, but the approach is based on engineering methods, where mathematical models and experimental data are used to analyse and test potential solutions to a problem. The research methods used in this study involved more than an amalgamation of techniques or data from different fields, but encompassed an integrated way of approaching, assessing and understanding a complete system, where computational and experimental methods were used in tandem to propose and corroborate specific testable hypotheses relating to embryonic limb development.

In summary, the integrated approach used brought a greater depth of understanding and insight to the research than any of the component methods in isolation would have brought, and the author suggests that an integrated approach to skeletogenesis, and indeed to all aspects of development, has the potential to significantly advance the depth of knowledge and understanding in the field.

Conclusions

7.1.	**Main Results**	**130**
7.2.	**Perspectives**	**131**

7.1. Main Results

A model with which to predict patterns of biophysical stimuli as a result of embryonic muscle contractions in the skeletal rudiments was presented. Patterns of biophysical stimuli were correlated with gene expression patterns to identify candidate mechanosensitive genes, and the evolution of a mechanosensitive gene set was simulated using a computational model. The main results were as follows:

a) Biophysical stimuli were predicted to be at high levels in the regions of the perichondrium beneath which osteoid would soon be deposited, forming the periosteal bone collar. It was proposed that high cycles of stimulus at the surface promote bone collar formation, potentially by inducing chondrocyte hypertrophy at the core.

b) Collagen X (ColX) and Indian hedgehog (Ihh) expression patterns showed a correlation with stage-matched patterns of biophysical stimuli, while Fibroblast Growth Factor receptor2 (FGFr2) and Parathyroid hormone-related protein (PTHrP) did not, identifying ColX and Ihh as potential mechanoregulators of embryonic ossification.

c) The expression patterns of ColX, Ihh and FGFr2 in the chick were different to those reported for the mouse, correlating with the absence of ossification in the core of the chick long bone

d) When the mechanical environment was altered *in ovo* by the administration of a neuromuscular blocking agent, skeletal development in the chick was affected with a significant decrease in bone formation in the tibiotarsus.

e) Expression patterns of ColX and Ihh were altered in the presence of an altered mechanical environment in a small number of specimens, corroborating their mechanosensitivity *in vivo*. The likelihood of observing an altered expression patterns was reduced due to incomplete penetration of the neuromuscular blocking agent.

f) ColX expression in the perichondrium, the region correlating to the predicted peak values of biophysical stimuli, was downregulated in a number of immobilised embryos at one time point.

g) Ihh expression in the periphery of the rudiment, normally seen only in later stages of bone formation, was accelerated in early stages and

exacerbated in later stages by the altered mechanical environment due to immobilisation. This suggests that mechanical loading may have an inhibitory effect on maturation of the Ihh expression patterns, thereby promoting proliferation, and hence longitudinal growth of the rudiment.

h) The evolution of a mechanoregulatory gene set was simulated revealing that while in some populations variation was maintained, in other populations the individuals converged to one mechanoregulation rule; often a rule far from the biomechanical optimum.

The work presented here has provided a new insight into mechanoregulation of embryonic long bone ossification in the chick. This is the first study to use anatomically realistic rudiment and muscle morphologies in a finite element analysis of the embryonic limb. The complexity of these analyses enabled comparison of predicted biophysical stimuli patterns with gene expression patterns, therefore demonstrating a new means of identifying potential mechanosensitive genes. A means of corroborating candidate mechanosensitive genes as playing a mechanoregulatory role *in vivo* was proposed and tested. Additionally, this thesis has provided new knowledge on the evolution of the laws governing mechanoregulation of the skeleton.

7.2. Perspectives

Although the main objective of this thesis was achieved, i.e., to characterise the biophysical stimuli at a range of stages of chick limb development during spontaneous muscle contractions, and to relate changes in the distribution or magnitudes of these stimuli to the activity of a candidate set of mechanosensitive genes, a number of questions relating to the mechanoregulation of embryonic bone remain to be explored.

Although a potential relationship between patterns of biophysical stimuli and expression of ColX and Ihh has been identified, functional proof of the mechanoregulatory role played by these genes was not produced. Expression of ColX correlates with high levels of biophysical stimuli in the perichondrium prior to mineralization, indicating that ColX may play a role in the morphogenesis of the perichondrium into the periosteum. As described in the

Introduction, formation of the bone collar occurs when the perichondrial cells differentiate directly into osteoblasts, followed by the deposition of a calcified bone matrix, the "bone collar" around the cartilaginous core of the future long bone (Calplan and Pechak, 1987). The expression of ColX in the perichondrium could indicate its role in the direct differentiation of the perichondrial cells into osteoblasts, or alternatively that ColX regulates deposition and/or mineralization of the bone matrix which forms the new bone collar. The role of ColX in avian bone collar formation could potentially be investigated further by performing histological analyses of the structure of the newly formed periosteum and by examining other genes in the ColX pathway in an altered mechanical environment. Expression of Ihh in the internal cartilage of the rudiment also correlates with patterns of biophysical stimuli. At younger stages of bone development, Ihh expression is seen at the same longitudinal level of the rudiment as the surface concentrations of stimuli, while at later stages, Ihh expression, a marker of pre-hypertrophic chondrocytes, tends to be more concentrated at the lateral edges of the pre-hypertrophic zones, demonstrating a stronger correlation with patterns of biophysical stimuli. The gradual enhancement of Ihh expression at the periphery, which is accelerated by a reduction in mechanical forces, potentially indicates a complex pattern of hypertrophy during bone collar progression in the chick. Further research into other genes influencing chondrocyte proliferation and hypertrophy (such as those illustrated in Figure 1.3) may offer an insight into the role of Ihh in regulating bone formation.

The author believes that the key to further advancing our understanding of embryonic skeletal mechanobiology is to study a mammalian model, and compare it to the avian system. Mammalian long bone ossification involves a combination of endochondral ossification at the core and periosteal ossification in the collar, while avian long bone ossification proceeds via periosteal bone collar formation only. The work presented in Chapter 4 is the first to correlate differences in gene expression patterns between the chick and the mouse with the differences in ossification events, and the author believes that a detailed comparative study at corresponding stages would provide a unique insight into molecular events in embryonic ossification and into divergent evolution of skeletogenesis in these animal groups. By comparing patterns of biophysical

stimuli between the chick and the mouse, a deeper understanding of the influence of these stimuli on specific ossification events can be gained. For example, if the predicted patterns of biophysical stimuli were found to be similar between the species, and no concentrations of biophysical stimuli were found at the core of the rudiment in the mouse model, this would indicate that mechanical forces may be more important for periosteal bone collar ossification than for endochondral ossification. Lastly, altering the mechanical environment *in vivo* in the mouse provides more of a challenge than in the chick. However, a genetically modified mouse has been developed in which no skeletal muscle forms (Myf5 -/- MyoD-/- embryos, (Rudnicki *et al.*, 1993)), which provides a clean and consistent system with which to examine ossification in the absence of embryonic muscle contractions. In contrast to *in vitro* culture of limb explants, the external environment of the developing embryo is unaffected and phenotypically normal littermates of mouse embryos with 'muscleless limbs' could be used as controls. The author will study this mouse as part of her post-doctoral research, and the techniques used to investigate mechanoregulation of periosteal bone collar formation in the chick, as described in this thesis, will be developed and built upon to enhance our knowledge of mechanoregulation of mammalian ossification.

The work presented in this thesis has uncovered some interesting aspects in relation to the mechanoregulation of embryonic bone formation. Further work in this area has the potential to increase our understanding of mechanoregulation of mammalian ossification, which has implications for tissue engineering of skeletal tissues, and potentially for clinical applications such as minimising the effect of congenital neuromuscular diseases on foetal skeletal development.

Bibliography

Abbott, S., Trinkaus, E., Burr, D. B., 1996. Dynamic bone remodeling in later Pleistocene fossil hominids. Am J Phys Anthropol 99, 585-601.

Akiyama, H., Chaboissier, M. C., Martin, J. F., Schedl, A., de Crombrugghe, B., 2002. The transcription factor Sox9 has essential roles in successive steps of the chondrocyte differentiation pathway and is required for expression of Sox5 and Sox6. Genes Dev 16, 2813-28.

Alexander, R. M., 1981. Factors of safety in the structure of animals. Sci Prog 67, 109-30.

Altschul, S. F., Madden, T. L., Schaffer, A. A., Zhang, J., Zhang, Z., Miller, W., Lipman, D. J., 1997. Gapped BLAST and PSI-BLAST: a new generation of protein database search programs. Nucleic Acids Res 25, 3389-402.

Augat, P., Margevicius, K., Simon, J., Wolf, S., Suger, G., Claes, L., 1998. Local tissue properties in bone healing: influence of size and stability of the osteotomy gap. J Orthop Res 16, 475-81.

Bagge, M., 2000. A model of bone adaptation as an optimization process. J Biomech 33, 1349-57.

Bass, S. L., Saxon, L., Daly, R. M., Turner, C. H., Robling, A. G., Seeman, E., Stuckey, S., 2002. The effect of mechanical loading on the size and shape of bone in pre-, peri-, and postpubertal girls: a study in tennis players. J Bone Miner Res 17, 2274-80.

Bekoff, A., 1976. Ontogeny of leg motor output in the chick embryo: a neural analysis. Brain Res 106, 271-91.

Ben-Ami, Y., von der Mark, K., Franzen, A., de Bernard, B., Lunazzi, G. C., Silbermann, M., 1993. Transformation of fetal secondary cartilage into embryonic bone in organ cultures of human mandibular condyles. Cell Tissue Res 271, 317-22.

Blumer, M. J., Longato, S., Richter, E., Perez, M. T., Konakci, K. Z., Fritsch, H., 2005. The role of cartilage canals in endochondral and perichondral bone formation: are there similarities between these two processes? J Anat 206, 359-72.

Boyce, B. F., Hughes, D. E., Wright, K. R., Xing, L., Dai, A., 1999. Recent advances in bone biology provide insight into the pathogenesis of bone diseases. Lab Invest 79, 83-94.

Brothwell, D., 1975. Adaptive growth rate changes as a possible explanation for the distinctiveness of the Neanderthalers. Journal of Archaelogical Science 2, 161-163.

Brown, T. D., Singerman, R. J., 1986. Experimental determination of the linear biphasic constitutive coefficients of human fetal proximal femoral chondroepiphysis. J Biomech 19, 597-605.

Calplan, A. I., Pechak, D. G., 1987. The cellular and molecular embryology of bone formation. In: Peck, W. A. (Ed.) Bone and Mineral Research. Elsevier, New York.5, pp. 117-183.

Carter, D. R., Beaupré, G. S., 2001. Skeletal function and form: mechanobiology of skeletal development, aging and regeneration. Cambridge University Press, Cambridge.

Carter, D. R., Beaupre, G. S., Giori, N. J., Helms, J. A., 1998a. Mechanobiology of skeletal regeneration. Clin Orthop Relat Res, S41-55.

Carter, D. R., Mikic, B., Padian, K., 1998b. Epigenetic mechanical factors in the evolution of long bone epiphyses. Zoological Journal of the Linnean Society 123, 163-178.

Carter, D. R., Orr, T. E., Fyhrie, D. P., Schurman, D. J., 1987. Influences of mechanical stress on prenatal and postnatal skeletal development. Clin Orthop Relat Res 15, 237-50.

Carter, D. R., Wong, M., 1988. The role of mechanical loading histories in the development of diarthrodial joints. J Orthop Res 6, 804-16.

Cillo, J. E., Jr., Gassner, R., Koepsel, R. R., Buckley, M. J., 2000. Growth factor and cytokine gene expression in mechanically strained human osteoblast-like cells: implications for distraction osteogenesis. Oral Surg Oral Med Oral Pathol Oral Radiol Endod 90, 147-54.

Claes, L. E., Heigele, C. A., 1999. Magnitudes of local stress and strain along bony surfaces predict the course and type of fracture healing. J Biomech 32, 255-66.

Cowin, S. C., Hegedus, D. H., 1976. Bone Remodeling .1. Theory of Adaptive Elasticity. Journal of Elasticity 6, 313-326.

Crelin, E. S., Koch, W. E., 1967. An autoradiographic study of chondrocyte transformation into chondroclasts and osteocytes during bone formation in vitro. Anat Rec 158, 473-83.

Currey, J. D., Alexander, R. M., 1985. The Thickness of the Walls of Tubular Bones. Journal of Zoology 206, 453-468.

Dacquin, R., Mee, P. J., Kawaguchi, J., Olmsted-Davis, E. A., Gallagher, J. A., Nichols, J., Lee, K., Karsenty, G., Smith, A., 2004. Knock-in of nuclear localised beta-galactosidase reveals that the tyrosine phosphatase Ptprv is specifically expressed in cells of the bone collar. Dev Dyn 229, 826-34.

de Jong, G., Gavrilets, S., 2000. Maintenance of genetic variation in phenotypic plasticity: the role of environmental variation. Genet Res 76, 295-304.

de Vernejoul, M. C., Benichou, O., 2001. Human osteopetrosis and other sclerosing disorders: recent genetic developments. Calcif Tissue Int 69, 1-6.

Delezoide, A. L., Benoist-Lasselin, C., Legeai-Mallet, L., Le Merrer, M., Munnich, A., Vekemans, M., Bonaventure, J., 1998. Spatio-temporal expression of FGFR 1, 2 and 3 genes during human embryo-fetal ossification. Mech Dev 77, 19-30.

Deng, C., Wynshaw-Boris, A., Zhou, F., Kuo, A., Leder, P., 1996. Fibroblast growth factor receptor 3 is a negative regulator of bone growth. Cell 84, 911-21.

Doménech-Ratto, G., Fernández-Villacanas Marín, M., Ballester-Moreno, A., Doménech-Asensi, P., 1999. Development and segments of cartilage canals in the chick embryo. Eur J Anat 3, 121-126.

Duncan, C. S., Blimkie, C. J., Kemp, A., Higgs, W., Cowell, C. T., Woodhead, H., Briody, J. N., Howman-Giles, R., 2002. Mid-femur geometry and biomechanical properties in 15- to 18-yr-old female athletes. Med Sci Sports Exerc 34, 673-81.

Duncan, R. L., Turner, C. H., 1995. Mechanotransduction and the functional response of bone to mechanical strain. Calcif Tissue Int 57, 344-58.

Emlen, J. M., 1987. The Shape of Optimality. In: Dupré, J. (Ed.) The Latest on the Best. MIT Press, MA, pp. 163-177.

Eswarakumar, V. P., Monsonego-Ornan, E., Pines, M., Antonopoulou, I., Morriss-Kay, G. M., Lonai, P., 2002. The IIIc alternative of Fgfr2 is a positive regulator of bone formation. Development 129, 3783-93.

Fell, H. B., 1925. The histogenesis of cartilage and bone in the long bones of the embryonic fowl. Journal of Morphology and Physiology 40, 417-459.

Fell, H. B., 1931. The osteogenic capacity *in vitro* of periosteum and endosteum isolated from the limb skeleton of fowl embryos and young chicks. Anatomy 66, 157-180.

Fell, H. B., 1969. The effect of environment on skeletal tissue in culture. Embryologia (Nagoya) 10, 181-205.

Fell, H. B., Canti, R. G., 1934. Experiments on the development *in vitro* of the avian knee joint. Proc. Roy. Soc. B. 116, 316-351.

Fell, H. B., Robinson, R., 1929. The growth, development and phosphate activity of embryonic avian femora and limb-buds cultivated *in vitro*. in vitro Biochem. J. 23, 767-784.

Felts, W. J. L., 1959. Transplantation studies of factors in skeletal organogenesis: I. The subcutaneously implanted immature long-bone of the rat and mouse. American Journal of Physical Anthropology 17, 201-215.

Fuchs, H., 1908. Über das vorkommen selbständiger knöcherner epiphysen bei Sauropsiden. Anat. Anz. 32, 352.

Gardner, E., Gray, D. J., 1970. The prenatal development of the human femur. Am J Anat 129, 121-40.

Gegenbaur, C., 1898. Verleichende Anatomie der Wirbeltiere. Englemann.

Geris, L., Andreykiv, A., Van Oosterwyck, H., Sloten, J. V., van Keulen, F., Duyck, J., Naert, I., 2004. Numerical simulation of tissue differentiation around loaded titanium implants in a bone chamber. J Biomech 37, 763-9.

Germiller, J. A., Goldstein, S. A., 1997. Structure and function of embryonic growth plate in the absence of functioning skeletal muscle. J Orthop Res 15, 362-70.

Gilbert, S. F., 2000. Developmental Biology. Sinauer Associates, Inc., MA.

Glucksman, A., 1939. Studies on bone mechanics *in vitro* II. The role of tension and pressure in chondrogenesis. Anat Rec 73, 39-56.

Glucksman, A., 1941. The role of mechanical stresses in bone formation *in vitro*. Journal of Anatomy 76, 231-239.

Haines, R. W., 1942. The evolution of epiphyses and of endochondral bone. Biological Reviews 17, 267-292.

Haines, R. W., 1969. Epiphyses and Sesamoids. In: Gans, C. (Ed.) Biology of the Reptilia. New York Academy Press, New York, pp. 81-115.

Hall, B. K., 1987. Earliest evidence of cartilage and bone development in embryonic life. Clin Orthop Relat Res 225, 255-72.

Hall, B. K., 2005. Bones and Cartilage: Developmental and Evolutionary Skeletal Biology. Elsevier Academic Press, London.

Hall, B. K., Herring, S. W., 1990. Paralysis and growth of the musculoskeletal system in the embryonic chick. J Morphol 206, 45-56.

Ham, A. W., Cormack, D. H., 1979. Histophysiology of Cartilage, Bone and Joints. J.B. Lippincott, Philadelphia.

Hamburger, V., Hamilton, H. L., 1992. A series of normal stages in the development of the chick embryo. 1951. Dev Dyn 195, 231-72.

Hardiman, D. A., O'Brien, F. J., Prendergast, P. J., Croke, D. T., Staines, A., Lee, T. C., 2005. Tracking the changes in unloaded bone: Morphology and gene expression. Eur J Morphol 42, 208-16.

Hartl, D. L., Clark, A. G., 1997. Principles of Population Genetics. Sinauer Associates, Inc., MA.

Heegaard, J. H., Beaupré, G. S., Carter, D. R., 1999. Mechanically modulated cartilage growth may regulate joint surface morphogenesis. J Orthop Res 17, 509-17.

Henderson, J. H., Carter, D. R., 2002. Mechanical induction in limb morphogenesis: the role of growth-generated strains and pressures. Bone 31, 645-53.

Henderson, J. H., de la Fuente, L., Romero, D., Colnot, C. I., Huang, S., Carter, D. R., Helms, J. A., 2007. Rapid growth of cartilage rudiments may generate perichondrial structures by mechanical induction. Biomech Model Mechanobiol 6, 127-37.

Hogan, B., 1994. Manipulating the mouse embryo : a laboratory manual. Cold Spring Harbour Laboratory, Cold Spring Harbor (NY).

Hogg, D. A., 1980. A re-investigation of the centres of ossification in the avian skeleton at and after hatching. J Anat 130, 725-43.

Holland, J. H., 1975. Adaptation in Natural and Artificial Systems: An Introductory Analysis with Applications to Biology, Control and Artificial Intelligence. MIT Press, MA.

Honjo, Y., Eisen, J. S., 2005. Slow muscle regulates the pattern of trunk neural crest migration in zebrafish. Development 132, 4461-4470.

Hosseini, A., Hogg, D. A., 1991a. The effects of paralysis on skeletal development in the chick embryo. I. General effects. J Anat 177, 159-68.

Hosseini, A., Hogg, D. A., 1991b. The effects of paralysis on skeletal development in the chick embryo. II. Effects on histogenesis of the tibia. J Anat 177, 169-78.

Huiskes, R., Driel, W., Prendergast, P. J., SØBalle, K., 1997. A biomechanical regulatory model for periprosthetic fibrous-tissue differentiation. Journal of Materials Science: Materials in Medicine 8, 785-788.

Huiskes, R., Ruimerman, R., van Lenthe, G. H., Janssen, J. D., 2000. Effects of mechanical forces on maintenance and adaptation of form in trabecular bone. Nature 405, 704-6.

Huiskes, R., Weinans, H., Grootenboer, H. J., Dalstra, M., Fudala, B., Slooff, T. J., 1987. Adaptive bone-remodeling theory applied to prosthetic-design analysis. J Biomech 20, 1135-50.

Inada, M., Yasui, T., Nomura, S., Miyake, S., Deguchi, K., Himeno, M., Sato, M., Yamagiwa, H., Kimura, T., Yasui, N., Ochi, T., Endo, N., Kitamura, Y., Kishimoto, T., Komori, T., 1999. Maturational disturbance of chondrocytes in Cbfa1-deficient mice. Dev Dyn 214, 279-90.

Ingber, D. E., 2006. Cellular mechanotransduction: putting all the pieces together again. The FASEB Journal 20, 811-827.

Isaksson, H., van Donkelaar, C. C., Huiskes, R., Ito, K., 2006. Corroboration of Mechanoregulatory Algorithms for Tissue Differentiation during Fracture Healing: Comparison with In Vivo Results. Journal of Orthopaedic Research 25, 898-907.

Jackson, R. A., Kumarasuriyar, A., Nurcombe, V., Cool, S. M., 2006. Long-term loading inhibits ERK1/2 phosphorylation and increases FGFR3 expression in MC3T3-E1 osteoblast cells. J Cell Physiol 209, 894-904.

Jee, W. S. S., 1988. The skeletal tissues. In: Weiss, L., W. (Ed.) Cell and Tissue Biology. Urban & Schwarzenberg, Baltimore, Munich.

Karaplis, A. C., Luz, A., Glowacki, J., Bronson, R. T., Tybulewicz, V. L., Kronenberg, H. M., Mulligan, R. C., 1994. Lethal skeletal dysplasia from targeted disruption of the parathyroid hormone-related peptide gene. Genes Dev 8, 277-89.

Karasik, D., Myers, R. H., Cupples, L. A., Hannan, M. T., Gagnon, D. R., Herbert, A., Kiel, D. P., 2002. Genome screen for quantitative trait loci contributing to normal variation in bone mineral density: the Framingham Study. J Bone Miner Res 17, 1718-27.

Kardon, G., 1998. Muscle and tendon morphogenesis in the avian hind limb. Development 125, 4019-32.

Karp, S. J., Schipani, E., St-Jacques, B., Hunzelman, J., Kronenberg, H., McMahon, A. P., 2000. Indian Hedgehog coordinates endochondral bone growth and morphogenesis via Parathyroid Hormone related-Protein-dependent and-independent pathways. Development 127, 543-548.

Karsenty, G., 2003. The complexities of skeletal biology. Nature 423, 316-318.

Kavanagh, E., Church, V. L., Osborne, A. C., Lamb, K. J., Archer, C. W., Francis-West, P. H., Pitsillides, A. A., 2006. Differential regulation of GDF-5 and FGF-2/4 by immobilisation in ovo exposes distinct roles in joint formation. Dev Dyn 235, 826-34.

Kawakami, Y., Capdevila, J., Buscher, D., Itoh, T., Rodriguez Esteban, C., Izpisua Belmonte, J. C., 2001. WNT signals control FGF-dependent limb initiation and AER induction in the chick embryo. Cell 104, 891-900.

Kelly, D. J., Prendergast, P. J., 2005. Mechano-regulation of stem cell differentiation and tissue regeneration in osteochondral defects. J Biomech 38, 1413-22.

Kielty, C. M., Kwan, A. P., Holmes, D. F., Schor, S. L., Grant, M. E., 1985. Type X collagen, a product of hypertrophic chondrocytes. Biochem. J 227, 545-554.

Klein-Nulend, J., Veldhuijzen, J. P., Burger, E. H., 1986. Increased calcification of growth plate cartilage as a result of compressive force in vitro. Arthritis Rheum 29, 1002-9.

Klein, R. F., Turner, R. J., Skinner, L. D., Vartanian, K. A., Serang, M., Carlos, A. S., Shea, M., Belknap, J. K., Orwoll, E. S., 2002. Mapping quantitative trait loci that influence femoral cross-sectional area in mice. J Bone Miner Res 17, 1752-60.

Kobyliansky, E., Karasik, D., Belkin, V., Livshits, G., 2000. Bone ageing: genetics versus environment. Ann Hum Biol 27, 433-51.

Kriegl, J. M., Oyserman, S., Roller, S.A., Blumenfeld, J., Volkman, S.K., Nashi, S., Hall, J.M., McCreadie, B.R., Goldstein, S.A., 2004. Influences of nutrition and physical forces on bone structure/function properties. In Proceedings of the Orthopaedic Research Society.

Kronenberg, H. M., 2003. Developmental regulation of the growth plate. Nature 423, 332-336.

Kwan, K. M., Pang, M. K. M., Zhou, S., Cowan, S. K., Kong, R. Y. C., Pfordte, T., Olsen, B. R., Sillence, D. O., Tam, P. P. L., Cheah, K. S. E., 1997. Abnormal compartmentalization of cartilage matrix components in mice lacking collagen X: Implications for function. Journal of Cell Biology 136, 459-471.

Lacroix, D., Prendergast, P. J., 2002. A mechano-regulation model for tissue differentiation during fracture healing: analysis of gap size and loading. J Biomech 35, 1163-71.

Lacroix, D., Prendergast, P. J., Li, G., Marsh, D., 2002. Biomechanical model to simulate tissue differentiation and bone regeneration: application to fracture healing. Med Biol Eng Comput 40, 14-21.

Landmesser, L., Morris, D. G., 1975. The development of functional innervation in the hind limb of the chick embryo. J Physiol 249, 301-26.

Lanske, B., Karaplis, A. C., Lee, K., Luz, A., Vortkamp, A., Pirro, A., Karperien, M., Defize, L. H., Ho, C., Mulligan, R. C., Abou-Samra, A. B., Juppner, H., Segre, G. V., Kronenberg, H. M., 1996. PTH/PTHrP receptor in early development and Indian hedgehog-regulated bone growth. Science 273, 663-6.

Lau, K. H., Kapur, S., Kesavan, C., Baylink, D. J., 2006. Up-regulation of the Wnt, estrogen receptor, insulin-like growth factor-I, and bone morphogenetic protein pathways in C57BL/6J osteoblasts as opposed to

C3H/HeJ osteoblasts in part contributes to the differential anabolic response to fluid shear. J Biol Chem 281, 9576-88.

Lee, R. T., Schoen, F. J., Loree, H. M., Lark, M. W., Libby, P., 1996. Circumferential stress and matrix metalloproteinase 1 in human coronary atherosclerosis. Implications for plaque rupture. Arterioscler Thromb Vasc Biol 16, 1070-3.

Lee, T. C., Taylor, D., 1999. Bone remodelling: Should we cry Wolff? Irish Journal of Medical Science 168, 102-105.

Lelkes, G., 1958. Experiments in vitro on the role of movement in the development of joints. J Embryol Exp Morphol 6, 183-6.

Lewin, B., 2004. Genes VIII. Pearson/Prentice Hall.

Lewontin, R. C., 1987. The Shape of Optimality. In: Dupré, J. (Ed.) The Latest on the Best. MIT Press, MA, pp. 151-159.

Li, C. F., Hughes-Fulford, M., 2006. Fibroblast growth factor-2 is an immediate-early gene induced by mechanical stress in osteogenic cells. J Bone Miner Res 21, 946-55.

Long, F., Chung, U. I., Ohba, S., McMahon, J., Kronenberg, H. M., McMahon, A. P., 2004. Ihh signaling is directly required for the osteoblast lineage in the endochondral skeleton. Development 131, 1309-18.

Long, F., Linsenmayer, T. F., 1998. Regulation of growth region cartilage proliferation and differentiation by perichondrium. Development 125, 1067-73.

Long, F., Zhang, X. M., Karp, S., Yang, Y., McMahon, A. P., 2001. Genetic manipulation of hedgehog signaling in the endochondral skeleton reveals a direct role in the regulation of chondrocyte proliferation. Development 128, 5099-108.

MacLean, J. J., Lee, C. R., Grad, S., Ito, K., Alini, M., Iatridis, J. C., 2003. Effects of immobilization and dynamic compression on intervertebral disc cell gene expression in vivo. Spine 28, 973-81.

Maes, C., Carmeliet, P., Moermans, K., Stockmans, I., Smets, N., Collen, D., Bouillon, R., Carmeliet, G., 2002. Impaired angiogenesis and endochondral bone formation in mice lacking the vascular endothelial growth factor isoforms VEGF164 and VEGF188. Mech Dev 111, 61-73.

Mak, A. F., 1986. The apparent viscoelastic behavior of articular cartilage--the contributions from the intrinsic matrix viscoelasticity and interstitial fluid flows. J Biomech Eng 108, 123-30.

Mariani, F. V., Martin, G. R., 2003. Deciphering skeletal patterning: clues from the limb. Nature 423, 319-325.

Marroig, G., Cheverud, J. M., 2004. Did natural selection or genetic drift produce the cranial diversification of neotropical monkeys? Am Nat 163, 417-28.

Martin, R. B., 2000. Toward a unifying theory of bone remodeling. Bone 26, 1-6.

McCammon, R. W., 1970. Human growth and development Thomas, Springfield, Ill., U.S.A.

Mikic, B., Isenstein, A. L., Chhabra, A., 2004. Mechanical modulation of cartilage structure and function during embryogenesis in the chick. Ann Biomed Eng 32, 18-25.

Mikic, B., Johnson, T. L., Chhabra, A. B., Schalet, B. J., Wong, M., Hunziker, E. B., 2000. Differential effects of embryonic immobilization on the development of fibrocartilaginous skeletal elements. J Rehabil Res Dev 37, 127-33.

Millward-Sadler, S. J., Salter, D. M., 2004. Integrin-dependent signal cascades in chondrocyte mechanotransduction. Ann Biomed Eng 32, 435-46.

Minina, E., Kreschel, C., Naski, M. C., Ornitz, D. M., Vortkamp, A., 2002. Interaction of FGF, Ihh/Pthlh, and BMP signaling integrates chondrocyte proliferation and hypertrophic differentiation. Dev Cell 3, 439-449.

Minina, E., Schneider, S., Rosowski, M., Lauster, R., Vortkamp, A., 2005. Expression of Fgf and Tgfbeta signaling related genes during embryonic endochondral ossification. Gene Expr Patterns 6, 102-9.

Minina, E., Wenzel, H. M., Kreschel, C., Karp, S., Gaffield, W., McMahon, A. P., Vortkamp, A., 2001. BMP and Ihh/PTHrP signaling interact to coordinate chondrocyte proliferation and differentiation. Development 128, 4523-4534.

Morey, E. R., Baylink, D. J., 1978. Inhibition of bone formation during space flight. Science 201, 1138-41.

Murray, P. D., Drachman, D. B., 1969. The role of movement in the development of joints and related structures: the head and neck in the chick embryo. J Embryol Exp Morphol 22, 349-71.

Murray, P. D. F., 1926. An experimental study of the development of the limbs of the chick. Proc. Linn. Soc. N.S.W. 51, 187-263.

Murray, P. D. F., Selby, D., 1930. Intrinsic and extrinsic factors in the primary development of the skeleton. Wilheim Roux' Arch. Entwicklungmech. Org. 122, 629-662.

Ng, A. F., Yang, Y. O., Wong, R. W., Hagg, E. U., Rabie, A. B., 2006a. Factors regulating condylar cartilage growth under repeated load application. Front Biosci 11, 949-54.

Ng, L. J., Wheatley, S., Muscat, G. E. O., Conway-Campbell, J., Bowles, J., Wright, E., Bell, D. M., Tam, P. P. L., Cheah, K. S. E., Koopman, P., 1997. SOX9 Binds DNA, Activates Transcription, and Coexpresses with Type II Collagen during Chondrogenesis in the Mouse. Developmental Biology 183, 108-121.

Ng, T. C., Chiu, K. W., Rabie, A. B., Hagg, U., 2006b. Repeated mechanical loading enhances the expression of Indian hedgehog in condylar cartilage. Front Biosci 11, 943-8.

Nowlan, N. C., Murphy, P., Prendergast, P. J., 2006. The influence of mechanical forces in the growing embryonic limb. In Transactions of the 52nd Annual Meeting of the Orthopaedic Research Society. Chicago, Illinois.

Nowlan, N. C., Murphy, P., Prendergast, P. J., 2007. Mechanobiology of embryonic limb development. Ann N Y Acad Sci 1101, 389-411.

Ornitz, D. M., Marie, P. J., 2002. FGF signaling pathways in endochondral and intramembranous bone development and human genetic disease. Genes Dev 16, 1446-65.

Osborne, A. C., Lamb, K. J., Lewthwaite, J. C., Dowthwaite, G. P., Pitsillides, A. A., 2002. Short-term rigid and flaccid paralyses diminish growth of embryonic chick limbs and abrogate joint cavity formation but differentially preserve pre-cavitated joints. J Musculoskelet Neuronal Interact 2, 448-56.

Otto, F., Thornell, A. P., Crompton, T., Denzel, A., Gilmour, K. C., Rosewell, I. R., Stamp, G. W. H., Beddington, R. S. P., Mundlos, S., Olsen, B. R.,

2004. Cbfa1, a Candidate Gene for Cleidocranial Dysplasia Syndrome, Is Essential for Osteoblast Differentiation and Bone Development. Developmental Cell 6, 317-318.

Palacios, J., Rodriguez, J. I., Ruiz, A., Sanchez, M., Alvarez, I., DeMiguel, E., 1992. Long bone development in extrinsic fetal akinesia: an experimental study in rat fetuses subjected to oligohydramnios. Teratology 46, 79-84.

Pauwels, F., 1960. Eine neue Theorie über den einfluss mechanischer Reize auf die Differnzierung der Stützgewebe. Z. Anat. Entwickl. 121, 478, (Translated by Maquet, P., Furlong R., as A new theory concerning the influence of mechanical stimuli in the differentiation of supporting tissues, in Biomechanics of the Locomotor Apparatus, Springer, Berlin, 1980, 375-407).

Peacock, M., Turner, C. H., Econs, M. J., Foroud, T., 2002. Genetics of osteoporosis. Endocr Rev 23, 303-26.

Pearson, O. M., 2000. Activity, climate, and postcranial robusticity: implications for modern human origins and scenarios of adaptive change. Curr Anthropol 41, 569-607.

Prendergast, P. J., 1997. Finite element models in tissue mechanics and orthopaedic implant design. Clin Biomech 12, 343-366.

Prendergast, P. J., 2002. Mechanics applied to skeletal ontogeny and phylogeny. Meccanica 37, 317-334.

Prendergast, P. J., 2004. Computational Mechanobiology. In: Cerralaza, M., Doblaré, M., Martínez, G., Calvo, B. (Eds.), Computational Bioengineering: Current Trends and Applications. Imperial College Press, London, pp. 117-133.

Prendergast, P. J., Huiskes, R., 1996. Finite element analysis of fibrous tissue morphogenesis—A study of the osteogenic index with a biphasic approach. Mechanics of Composite Materials 32, 144-150.

Prendergast, P. J., Huiskes, R., Soballe, K., 1997a. Biophysical stimuli on cells during tissue differentiation at implant interfaces. J Biomech 30, 539-548.

Prendergast, P. J., Huiskes, R., Soballe, K., 1997b. ESB Research Award 1996. Biophysical stimuli on cells during tissue differentiation at implant interfaces. J Biomech 30, 539-48.

Prendergast, P. J., Taylor, D., 1994. Prediction of bone adaptation using damage accumulation. J Biomech 27, 1067-76.

Provot, S., Schipani, E., 2005. Molecular mechanisms of endochondral bone development. Biochem Biophys Res Commun 328, 658-65.

Raab-Cullen, D. M., Thiede, M. A., Petersen, D. N., Kimmel, D. B., Recker, R. R., 1994. Mechanical loading stimulates rapid changes in periosteal gene expression. Calcif Tissue Int 55, 473-8.

Radhakrishnan, P., Lewis, N. T., Mao, J. J., 2004. Zone-specific micromechanical properties of the extracellular matrices of growth plate cartilage. Ann Biomed Eng 32, 284-91.

Raup, D. M., 1986. Biological extinction in earth history. Science 231, 1528-33.

Reiser, P. J., Stokes, B. T., 1982. Development of contractile properties in avian embryonic skeletal muscle. Am J Physiol 242, C52-8.

Roberts, J. A. F., Pembrey, M. E., 1985. An Introduction to Medical Genetics. Oxford University Press.

Rodriguez, J. I., Garcia-Alix, A., Palacios, J., Paniagua, R., 1988a. Changes in the long bones due to fetal immobility caused by neuromuscular disease. A radiographic and histological study. J Bone Joint Surg Am 70, 1052-60.

Rodriguez, J. I., Palacios, J., Garcia-Alix, A., Pastor, I., Paniagua, R., 1988b. Effects of immobilization on fetal bone development. A morphometric study in newborns with congenital neuromuscular diseases with intrauterine onset. Calcif Tissue Int 43, 335-9.

Rodriguez, J. I., Palacios, J., Ruiz, A., Sanchez, M., Alvarez, I., Demiguel, E., 1992. Morphological changes in long bone development in fetal akinesia deformation sequence: an experimental study in curarized rat fetuses. Teratology 45, 213-21.

Roesler, H., 1987. The history of some fundamental concepts in bone biomechanics. J Biomech 20, 1025-34.

Rubin, E., Farber, J. L., 1988. Pathology. Lippincott, Philadelphia.

Rudnicki, M. A., Schnegelsberg, P. N., Stead, R. H., Braun, T., Arnold, H. H., Jaenisch, R., 1993. MyoD or Myf-5 is required for the formation of skeletal muscle. Cell 75, 1351-9.

Ruff, C. B., Hayes, W. C., 1983. Cross-sectional geometry of Pecos Pueblo femora and tibiae--a biomechanical investigation: I. Method and general patterns of variation. Am J Phys Anthropol 60, 359-81.

Ruff, C. B., Larsen, C. S., Hayes, W. C., 1984. Structural changes in the femur with the transition to agriculture on the Georgia coast. Am J Phys Anthropol 64, 125-36.

Sarin, V. K., Carter, D. R., 2000. Mechanobiology and joint conformity regulate endochondral ossification of sesamoids. J Orthop Res 18, 706-12.

Sato, M., Ochi, T., Nakase, T., Hirota, S., Kitamura, Y., Nomura, S., Yasui, N., 1999. Mechanical tension-stress induces expression of bone morphogenetic protein (BMP)-2 and BMP-4, but not BMP-6, BMP-7, and GDF-5 mRNA, during distraction osteogenesis. J Bone Miner Res 14, 1084-95.

Schweitzer, R., Chyung, J. H., Murtaugh, L. C., Brent, A. E., Rosen, V., Olson, E. N., Lassar, A., Tabin, C. J., 2001. Analysis of the tendon cell fate using Scleraxis, a specific marker for tendons and ligaments. Development 128, 3855-66.

Scott, C. C., Athanasiou, K. A., 2006. Mechanical impact and articular cartilage. Crit Rev Biomed Eng 34, 347-78.

Sharpe, J., Ahlgren, U., Perry, P., Hill, B., Ross, A., Hecksher-Sorensen, J., Baldock, R., Davidson, D., 2002. Optical projection tomography as a tool for 3D microscopy and gene expression studies. Science 296, 541-5.

Shefelbine, S. J., Carter, D. R., 2004. Mechanobiological predictions of growth front morphology in developmental hip dysplasia. J Orthop Res 22, 346-52.

Shiang, R., Thompson, L. M., Zhu, Y. Z., Church, D. M., Fielder, T. J., Bocian, M., Winokur, S. T., Wasmuth, J. J., 1994. Mutations in the transmembrane domain of FGFR3 cause the most common genetic form of dwarfism, achondroplasia. Cell 78, 335-342.

Sironen, R. K., Karjalainen, H. M., Elo, M. A., Kaarniranta, K., Torronen, K., Takigawa, M., Helminen, H. J., Lammi, M. J., 2002. cDNA array reveals mechanosensitive genes in chondrocytic cells under hydrostatic pressure. Biochim Biophys Acta 1591, 45-54.

Skalak, R., Dasgupta, G., Moss, M., Otten, E., Dullumeijer, P., Vilmann, H., 1982. Analytical description of growth. J Theor Biol 94, 555-77.

Slemenda, C. W., Turner, C. H., Peacock, M., Christian, J. C., Sorbel, J., Hui, S. L., Johnston, C. C., 1996. The genetics of proximal femur geometry, distribution of bone mass and bone mineral density. Osteoporos Int 6, 178-82.

St-Jacques, B., Hammerschmidt, M., McMahon, A. P., 1999. Indian hedgehog signaling regulates proliferation and differentiation of chondrocytes and is essential for bone formation. Genes Dev 13, 2072-86.

Stensiö, E. A., 1932. The Cephalispids of Great Britian. British Museum (Nat. Hist.), London.

Stevens, S. S., Beaupré, G. S., Carter, D. R., 1999. Computer model of endochondral growth and ossification in long bones: biological and mechanobiological influences. J Orthop Res 17, 646-53.

Sundaramurthy, S., Mao, J. J., 2006. Modulation of endochondral development of the distal femoral condyle by mechanical loading. J Orthop Res 24, 229-41.

Taber, L. A., Humphrey, J. D., 2001. Stress-modulated growth, residual stress, and vascular heterogeneity. J Biomech Eng 123, 528-35.

Tanaka, N., Ohno, S., Honda, K., Tanimoto, K., Doi, T., Ohno-Nakahara, M., Tafolla, E., Kapila, S., Tanne, K., 2005. Cyclic mechanical strain regulates the PTHrP expression in cultured chondrocytes via activation of the Ca2+ channel. J Dent Res 84, 64-8.

Tanck, E., Blankevoort, L., Haaijman, A., Burger, E. H., Huiskes, R., 2000. Influence of muscular activity on local mineralization patterns in metatarsals of the embryonic mouse. J Orthop Res 18, 613-9.

Tanck, E., Van Donkelaar, C. C., Jepsen, K. J., Goldstein, S. A., Weinans, H., Burger, E. H., Huiskes, R., 2004. The mechanical consequences of mineralization in embryonic bone. Bone 35, 186-90.

Tanck, E., van Driel, W. D., Hagen, J. W., Burger, E. H., Blankevoort, L., Huiskes, R., 1999. Why does intermittent hydrostatic pressure enhance the mineralization process in fetal cartilage? J Biomech 32, 153-61.

Thompson, D. W., 1917. On Growth and Form. Cambridge University Press, Cambridge.

Thorogood, P., 1983. Morphogenesis of Cartilage. In: Hall, B. K. (Ed.) Cartilage Vol.2; Development, Differentiation and Growth. Academic Press, New York, London.

Trepczik, B., Lienau, J., Schell, H., Epari, D. R., Thompson, M. S., Hoffmann, J. E., Kadow-Romacker, A., Mundlos, S., Duda, G. N., 2007. Endochondral ossification in vitro is influenced by mechanical bending. Bone 40, 597-603.

Tufto, J., 2000. Quantitative genetic models for the balance between migration and stabilizing selection. Genet Res 76, 285-93.

Turner, C. H., Schriefer, J. L., Horton, L. G., Shultz, K. L., Beamer, W. G., 2004. Fine mapping of genetic trait loci linked to skeletal structure in mice. In Proceedings of the Orthopaedic Research Society.

Turner, R. T., 1999. Mechanical signaling in the development of postmenopausal osteoporosis. Lupus 8, 388-92.

van der Meulen, M. C., Beaupré, G. S., Carter, D. R., 1993. Mechanobiologic influences in long bone cross-sectional growth. Bone 14, 635-42.

van der Meulen, M. C., Huiskes, R., 2002. Why mechanobiology? A survey article. J Biomech 35, 401-14.

Van Donkelaar, C. C., Witvoet-Braam, S. W., Huiskes, R., 2006. Geometry of perichondrium determines location of early bone formation in long bones. In Transactions of the 52nd Annual Meeting of the Orthopaedic Research Society. Chicago, Illinois.

Vortkamp, A., Lee, K., Lanske, B., Segre, G. V., Kronenberg, H. M., Tabin, C. J., 1996. Regulation of rate of cartilage differentiation by Indian hedgehog and PTH-related protein. Science 273, 613-22.

Waddington, C. H., 1975. The Evolution of an Evolutionist. Edinburgh University Press.

Wang, J. H. C., Thampatty, B. P., 2006. An Introductory Review of Cell Mechanobiology. Biomechanics and Modeling in Mechanobiology 5, 1-16.

Watson, D. M. S., Gill, E. L., 1925. The structure of certain Palaenisoids and the relationships of that group with other bony fish. Proc. Zool. Soc. Lond., 815.

Waxman, D., Peck, J. R., 2003. The anomalous effects of biased mutation. Genetics 164, 1615-26.

Weinans, H., Prendergast, P. J., 1996. Tissue adaptation as a dynamical process far from equilibrium. Bone 19, 143-9.

Weir, E. C., Philbrick, W. M., Amling, M., Neff, L. A., Baron, R., Broadus, A. E., 1996. Targeted overexpression of parathyroid hormone-related peptide in chondrocytes causes chondrodysplasia and delayed endochondral bone formation. 93, 10240-10245.

Wilkinson, D. G., 1992. Whole mount in situ hybridization of vertebrate embryos. In: Wilkinson, D. G. (Ed.) In situ hybridization: A Practical Approach IRL Press, Oxford, pp. 75-83.

Williamson, A. K., Chen, A. C., Sah, R. L., 2001. Compressive properties and function-composition relationships of developing bovine articular cartilage. J Orthop Res 19, 1113-21.

Wolff, J., 1986. The Law of Bone Remodelling. (Das Gesetz der Transformation der Knochen, Kirschwald, 1892). . Springer, Berlin.

Wong, M., Carter, D. R., 1990a. A theoretical model of endochondral ossification and bone architectural construction in long bone ontogeny. Anat Embryol (Berl) 181, 523-32.

Wong, M., Carter, D. R., 1990b. Theoretical stress analysis of organ culture osteogenesis. Bone 11, 127-31.

Wong, M., Germiller, J., Bonadio, J., Goldstein, S. A., 1993. Neuromuscular atrophy alters collagen gene expression, pattern formation, and mechanical integrity of the chick embryo long bone. Prog Clin Biol Res 383B, 587-97.

Wong, M., Siegrist, M., Goodwin, K., 2003. Cyclic tensile strain and cyclic hydrostatic pressure differentially regulate expression of hypertrophic markers in primary chondrocytes. Bone 33, 685-93.

Wu, Q., Zhang, Y., Chen, Q., 2001. Indian hedgehog is an essential component of mechanotransduction complex to stimulate chondrocyte proliferation. J Biol Chem 276, 35290-6.

Wu, Q. Q., Chen, Q., 2000. Mechanoregulation of chondrocyte proliferation, maturation, and hypertrophy: ion-channel dependent transduction of matrix deformation signals. Exp Cell Res 256, 383-91.

Yang, Y., Topol, L., Lee, H., Wu, J., 2003. Wnt5a and Wnt5b exhibit distinct activities in coordinating chondrocyte proliferation and differentiation. Development 130, 1003-15.

Yoshida, C. A., Yamamoto, H., Fujita, T., Furuichi, T., Ito, K., Inoue, K., Yamana, K., Zanma, A., Takada, K., Ito, Y., 2004. Runx2 and Runx3 are essential for chondrocyte maturation, and Runx2 regulates limb growth through induction of Indian hedgehog. Genes & Development 18, 952-963.

Young, N. M., 2003. A reassessment of living hominoid postcranial variability: implications for ape evolution. J Hum Evol 45, 441-64.

Zhao, Q., Eberspaecher, H., Lefebvre, V., De Crombrugghe, B., 1997. Parallel expression of Sox9 and Col2a1 in cells undergoing chondrogenesis. Dev Dyn 209, 377-86.

Appendix A

Staining Protocols

Alcian Blue/Alizarin Red Staining

(Adapted from Hogan *et al.*, 1994)

1. Dissect embryos into ice-cold PBS removing hind limbs.
2. Fix in 95% ethanol for 3-5 days at -4°C.
3. Stain cartilage by placing embryo in enough Alcian Blue stain (0.1% in 95% ethanol) to cover the body. Leave embryos in stain for 8 hours at room temperature.
4. Rinse embryo twice in 95% ethanol. Wash overnight in 95% ethanol for 24 hours, replace 95% ethanol and let sit for another 24 hours.
5. Clear specimens in 1% Potassium hydroxide (KOH) for 3 hours (or until embryo is sufficiently clear).
6. If staining with Alizarin Red: Stain in Alizarin Red (0.005% in 2% KOH) for 2-4 hours (room temperature, not rocking). Clear in 2% KOH until sufficiently cleared, up to 12 hours (room temperature, not rocking).
7. Fix in 4% PFA overnight.
8. Store in PBS + 1/100 of Sodium Azide.

Anti-Myosin Antibody Staining

1. Wash in 50% methanol, fix in Dents (1:4 DMSO: MeOH) for 2 hours (DMSO= Dimethyl Sulfoxide)
2. Wash in 50% 1x Tris-Buffered Saline Tween-20 (TBST) for ½ hour
3. Fix in 100% 1xTBST overnight (embryos should not be sitting on top of each other)
4. Block in 10% serum in 1xTBST plus 0.01% Na Azide at 4°C with rocking over 1 or more nights
5. Change to new block + primary antibody (MF20), 1 in 20 dilution: 2ml block + 100µl antibody (in each tube)
6. Dilute in primary antibody for 5-6 days, rocking and at a slant at 4°C (Save antibody for reuse)
7. Wash at least 4 times in 1xTBST and overnight
8. Wash a further 2 times in 1xTBST and twice in block

9. Add secondary antibody (Alexa Fluor goat anti-mouse IgG 528) to fresh block, 1 in 200 dilution (5ml = 5ml block + 25 µl antibody). Expose antibody to light as little as possible. (Note: IGG 528 (TXR fluorescence) works better for chick, 488(GFP fluorescence better for mouse)
10. Cover tubes with tinfoil, leave overnight rocking and at a slant at 4°C
11. Wash in 1xTBST twice for ten min

10xTBST

To make 100ml:

8.0g NaCl

0.2g KCl

12.5ml 2M Tris:HCl pH 7.5 (neuro lab)

10ml 10% Tween-20 (1ml in 10ml H20)

Bring to 100ml with sterile dH20

Appendix B

Muscle Force Values

*Table B.1: Muscle force values for stages 30, 32 and 34. Ventral muscles active in flexion, dorsal in extension. 2 specimens per stage measured, average value used in simulation. ** force halved to account for short length of muscle*

VENTRAL MUSCLES				
Stage	**Muscle#**	**Area (mm^2)**	**Flexion Force (N)**	**Total Force (N)**
HH30_A	2	1.58E-01	1.76E-04	
	3	1.58E-01	1.76E-04	3.51E-04
HH30_B	2	1.68E-01	1.87E-04	
	3	1.68E-01	1.87E-04	3.73E-04
HH30: Average	**2**	**1.63E-01**	**1.81E-04**	
	3	**1.63E-01**	**1.81E-04**	**3.62E-04**
HH32_A	1	1.84E-01	2.04E-04**	
	2_3	2.16E-01	2.40E-04	
	3_4	2.16E-01	2.40E-04	4.81E-04
HH32_B	1	1.33E-01	1.47E-04**	
	2_3	1.94E-01	2.15E-04	
	3_4	1.94E-01	2.15E-04	4.30E-04
HH32: Average	**1**		**8.78E-05**	
	2_3		**2.28E-04**	
	3_4		**2.28E-04**	**5.43E-04**
HH34_A	1_v_a	2.98E-01	3.30E-04	
	2_v_p	5.69E-01	6.32E-04	9.62E-04
HH34_B	1_v_a	3.43E-01	3.81E-04	
	2_v_p	4.65E-01	5.16E-04	8.97E-04
HH34: Average	**1_v_a**		**3.56E-04**	
	2_v_p		**5.74E-04**	**9.29E-04**
DORSAL MUSCLES				
HH30_A	1	5.01E-02	5.56E-05	
	2	1.06E-01	1.18E-04	
	3	3.47E-02	3.85E-05	2.12E-04
HH30_B	1	4.56E-02	5.07E-05	
	2	1.06E-01	1.18E-04	
	3	3.27E-02	3.63E-05	2.05E-04
HH30: Average	**1**		**5.31E-05**	
	2		**1.18E-04**	
	3		**3.74E-05**	**2.09E-04**
HH32_A	1	7.25E-02	8.04E-05	
	2	5.54E-02	6.14E-05	
	3	1.15E-01	1.27E-04	
	4	6.59E-02	7.32E-05	3.42E-04
HH32_B	1	6.93E-02	7.69E-05	
	2	3.76E-02	4.17E-05	
	3	1.15E-01	1.28E-04	
	4	4.03E-02	4.47E-05	2.91E-04
HH32: Average	**1**		**7.87E-05**	
	2		**5.16E-05**	
	3		**1.28E-04**	
	4		**5.89E-05**	**3.17E-04**
HH34_A	1	2.73E-01	3.03E-04	
	2	2.73E-01	3.03E-04	6.07E-04
HH34_B	1	2.86E-01	3.18E-04	
	2	2.86E-01	3.18E-04	6.36E-04
HH34: Average	**1**		**6.21E-04**	
	2		**3.11E-04**	**9.32E-04**

Appendix C

Detailed Finite Element Analysis Results

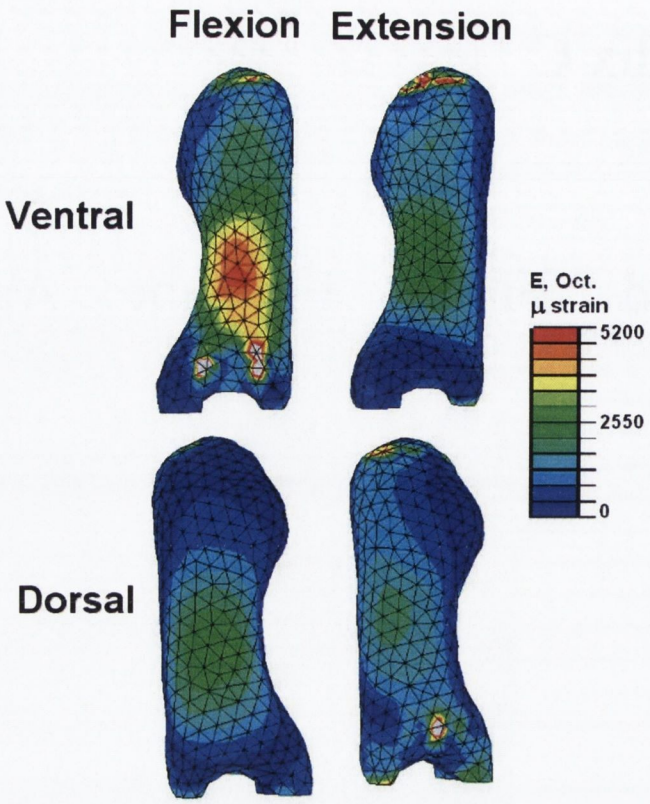


Figure C.1: Octahedral shear strain, μstrain, HH30_A.

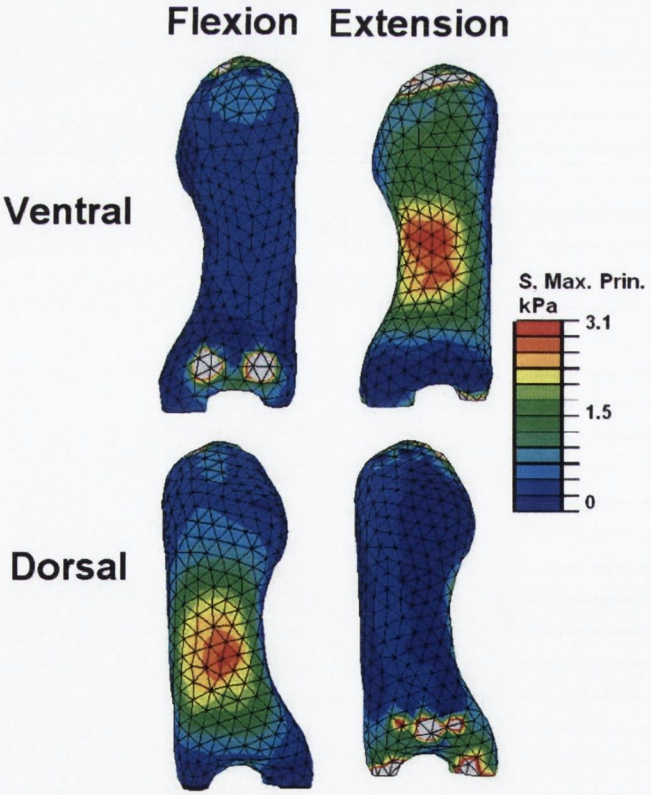


Figure C.2: Maximum principal stress, kPa, HH30_A

HH30_A

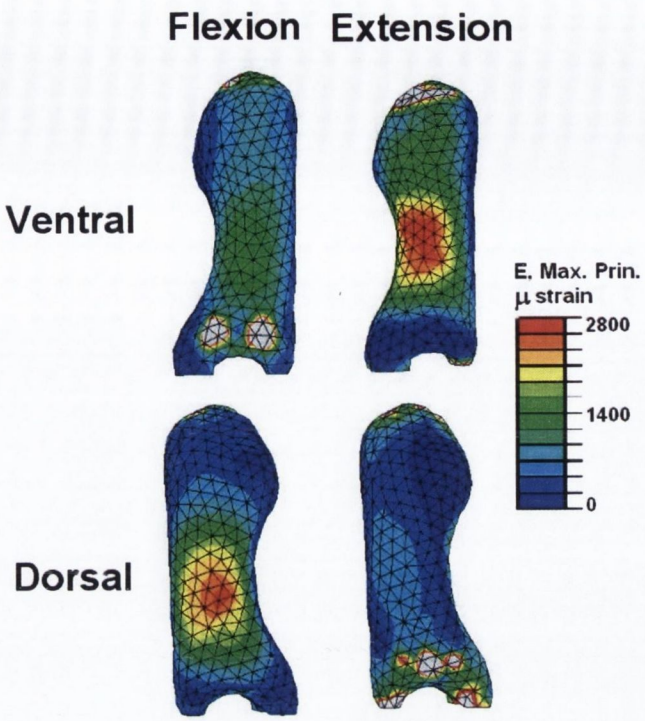


Figure C.3: Maximum principal strain, μstrain, HH30_A

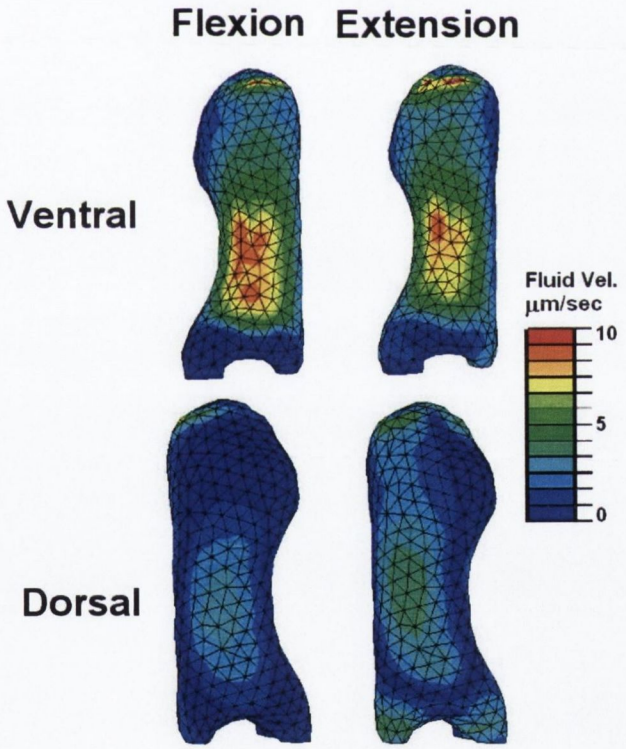


Figure C.4: Fluid Velocity, μm/sec, HH30_A.

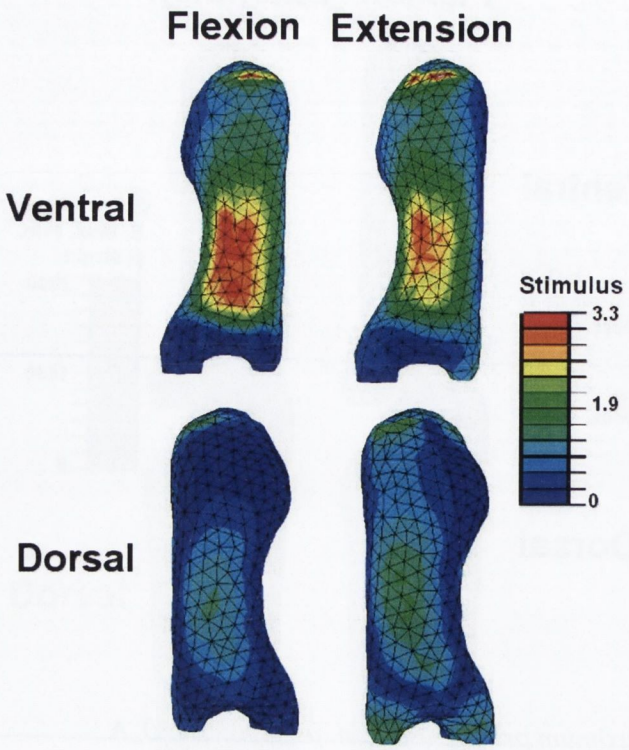


Figure C.5: Stimulus, HH30_A.

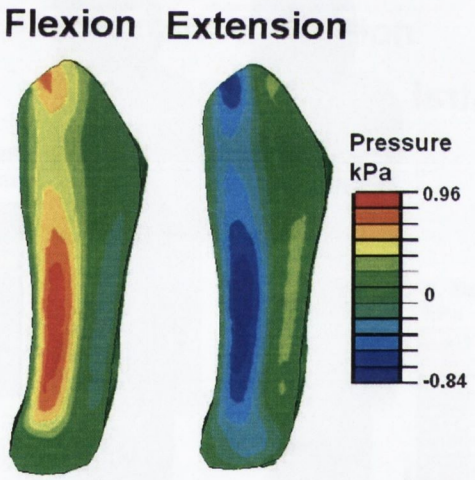


Figure C.6: Pore fluid pressure, kPa, HH30_A.

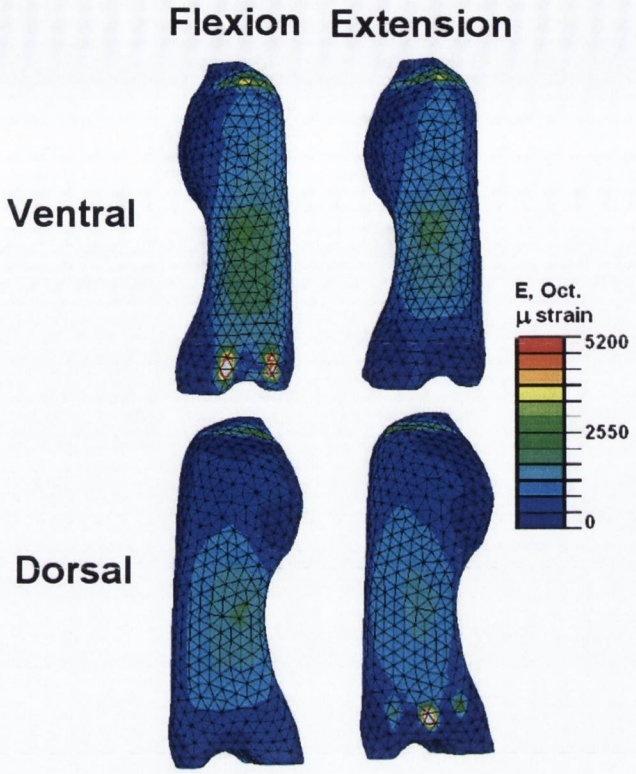


Figure C.7: Octahedral shear strain, μstrain, HH30_B.

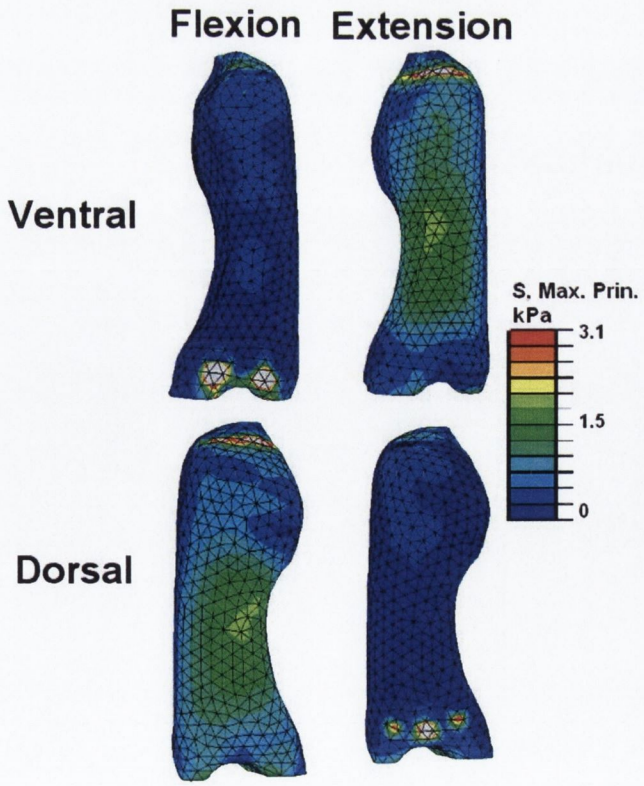


Figure C.8: Maximum principal stress, kPa, HH30_B.

HH30_B

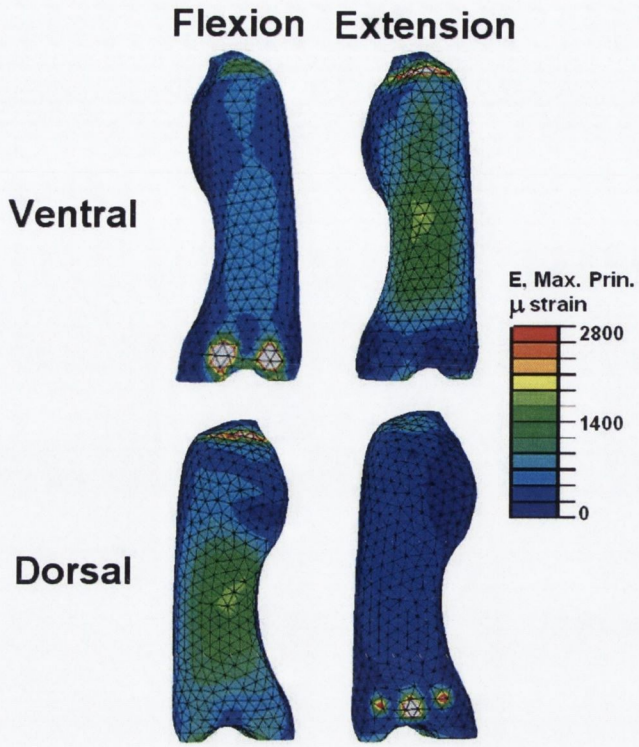


Figure C.9: Maximum principal strain, μstrain, HH30_B.

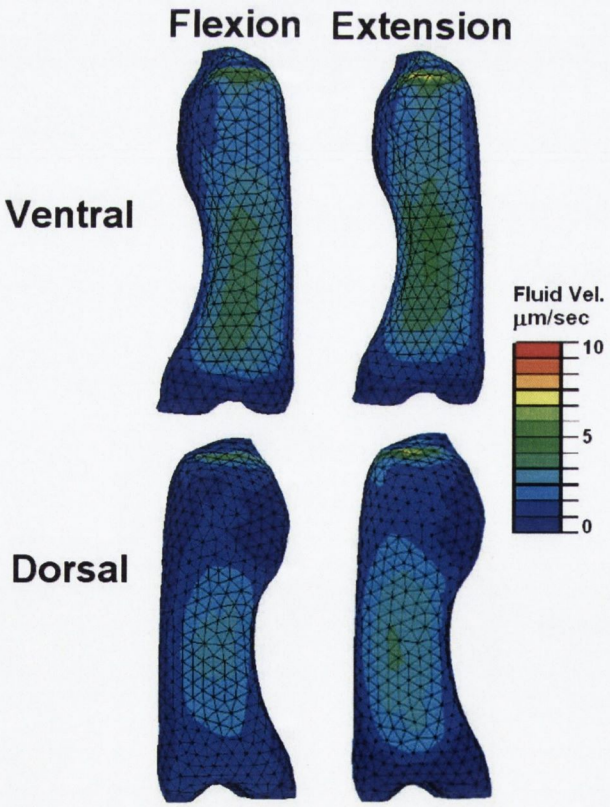


Figure C.10: Fluid velocity, μm/sec, HH30_B.

HH30_B

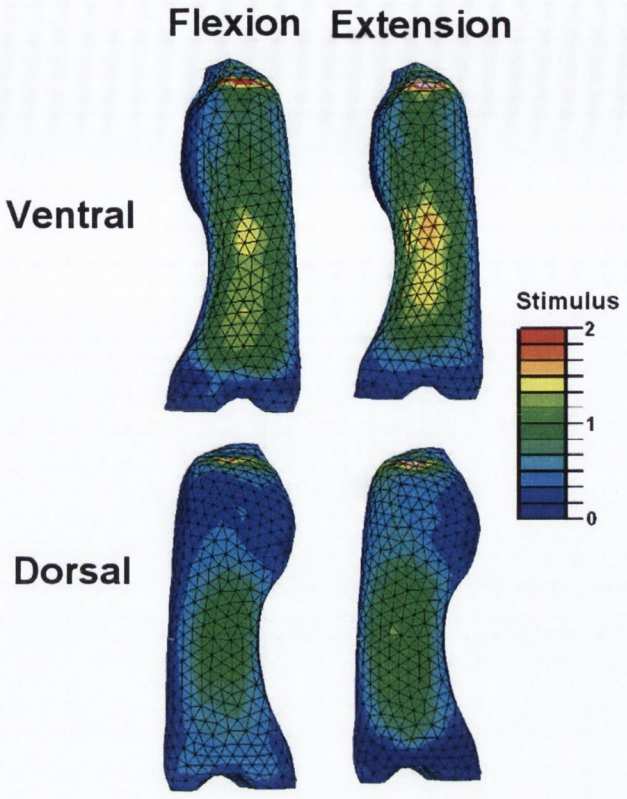


Figure C.11: Stimulus, HH30_B.

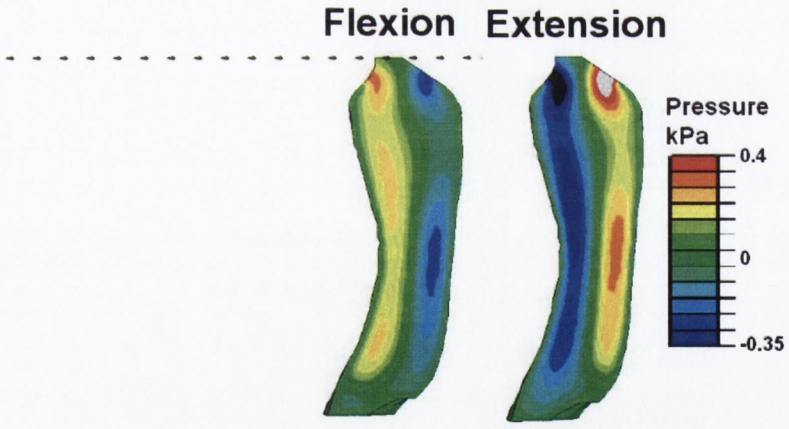


Figure C.12: Pore fluid pressure, kPa, HH30_B.

HH32_A

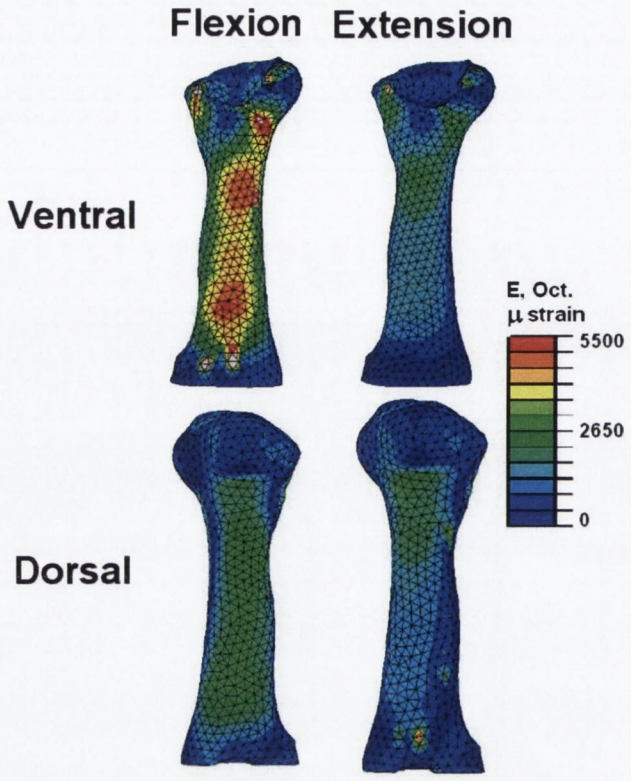


Figure C.13: Octahedral shear strain, μstrain, HH32_A.

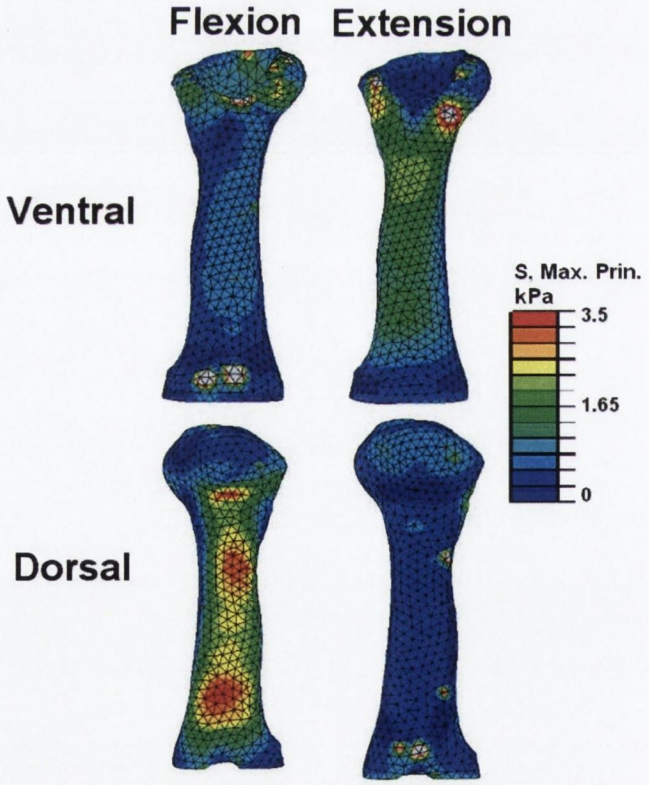


Figure C.14: Maximum principal stress, kPa, HH32_A.

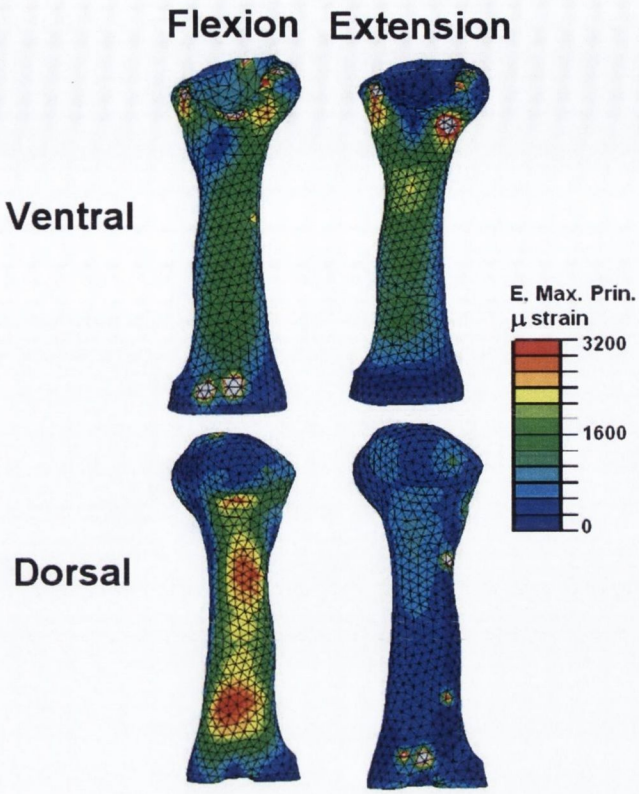


Figure C.15: Maximum principal strain, μstrain, HH32_A.

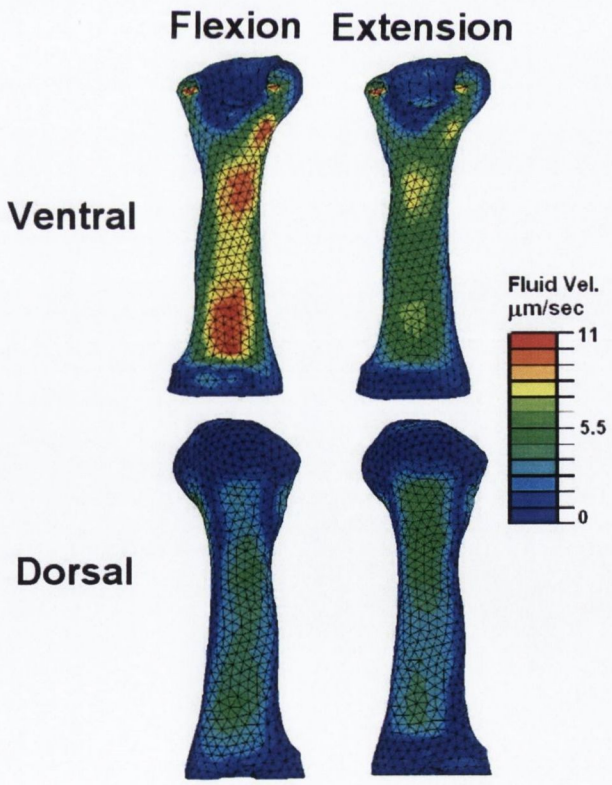


Figure C.16: Fluid velocity, μm/sec, HH32_A.

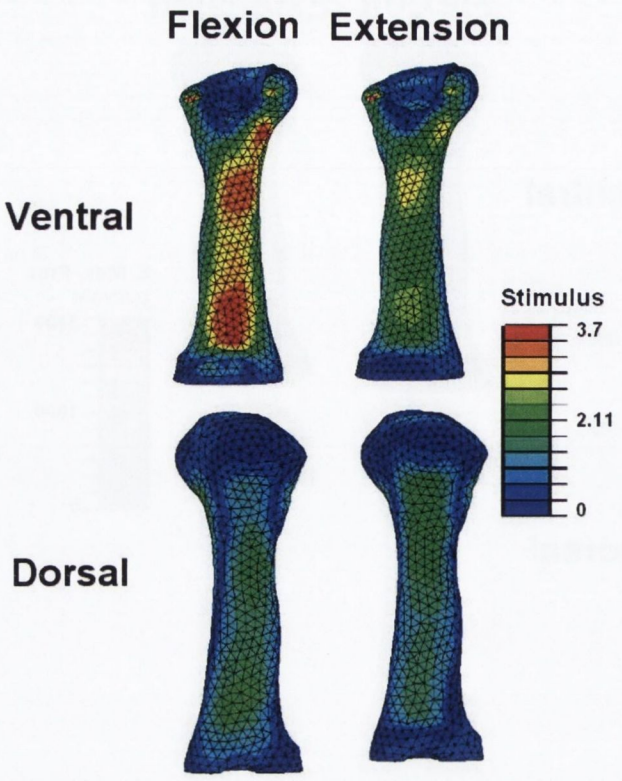


Figure C.17: Stimulus, HH32_A.

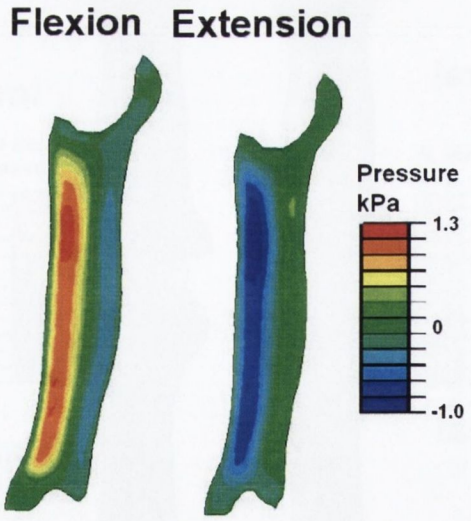


Figure C.18: Pore fluid pressure, kPa, HH32_A.

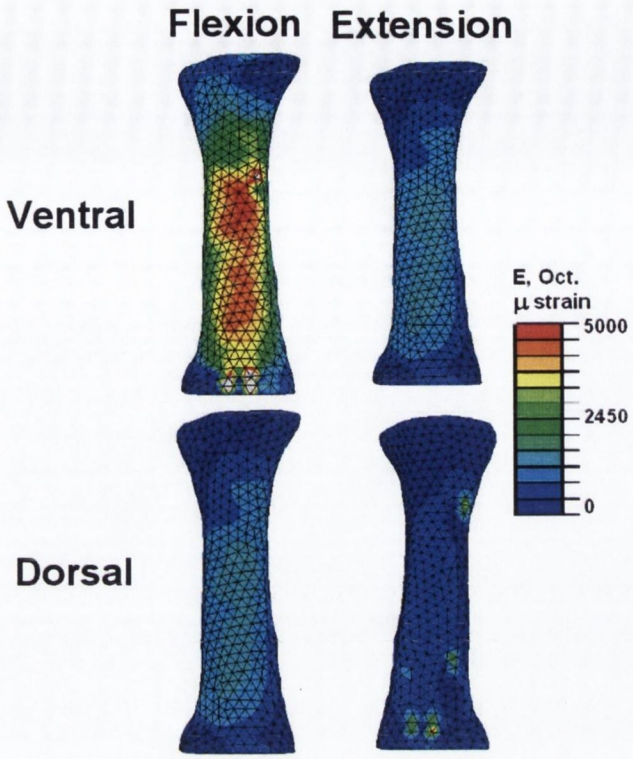


Figure C.19: Octahedral shear strain, μstrain, HH32_B.

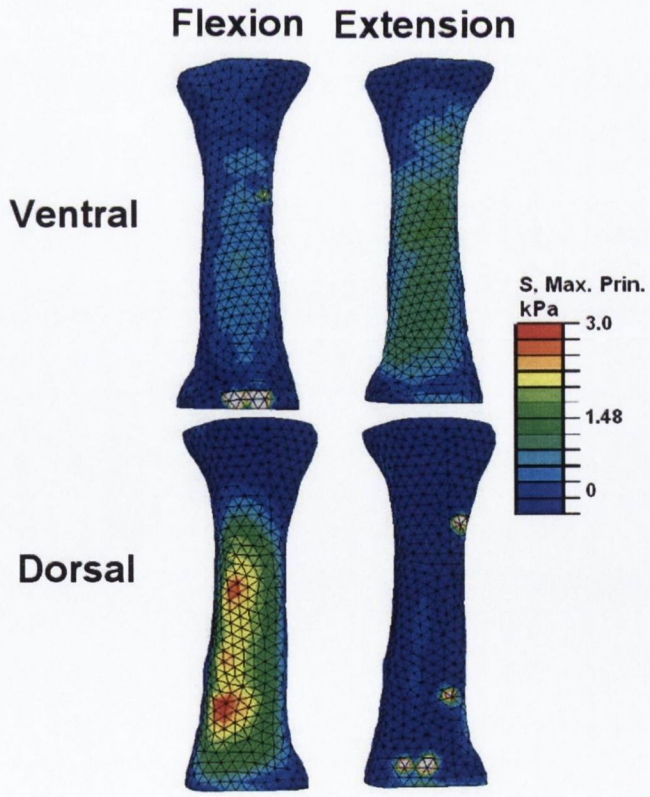


Figure C.20: Maximum principal stress, kPa, HH32_B.

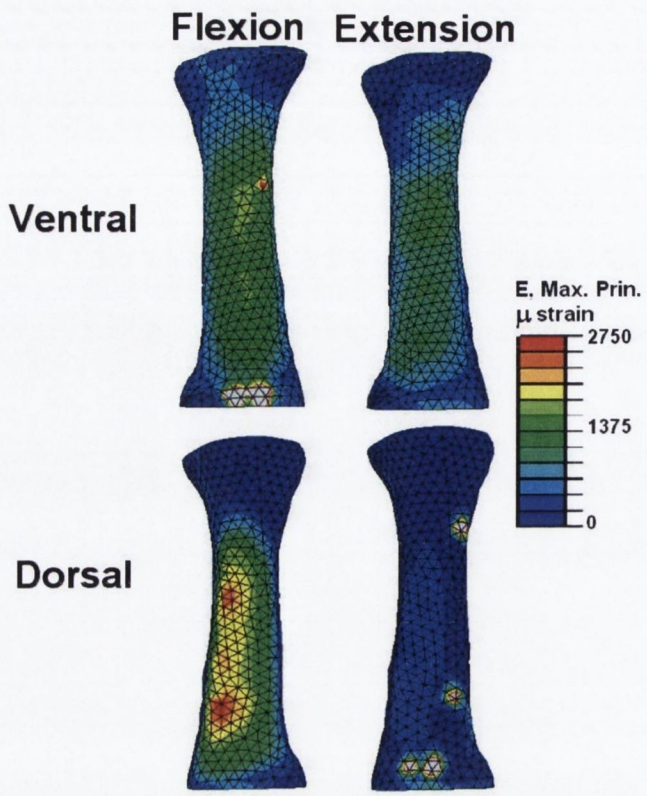


Figure C.21: Maximum principal strain, μstrain, HH32_B.

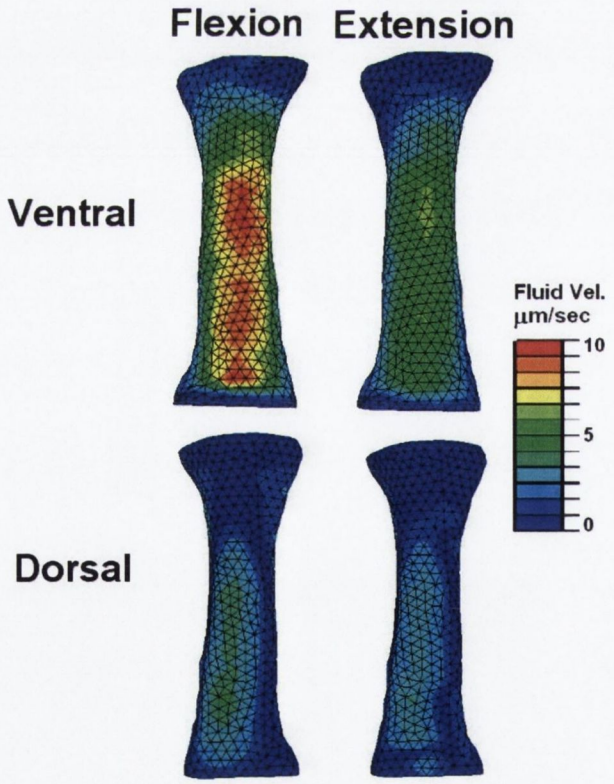


Figure C.22: Fluid velocity, μm/sec, HH32_B.

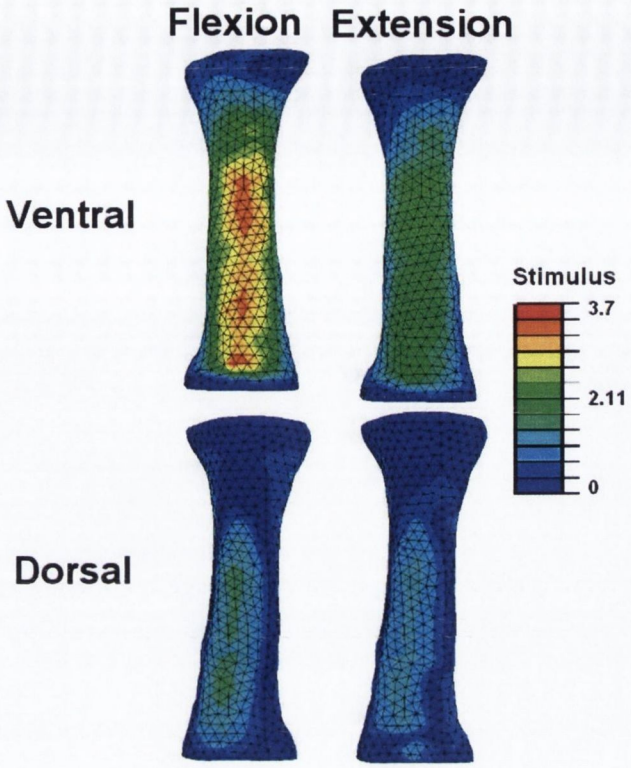


Figure C.23: Stimulus, HH32_B.

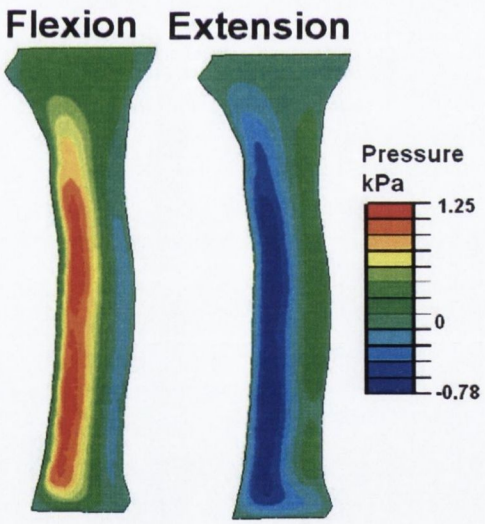


Figure C.24: Pore fluid pressure, kPa, HH32_B.

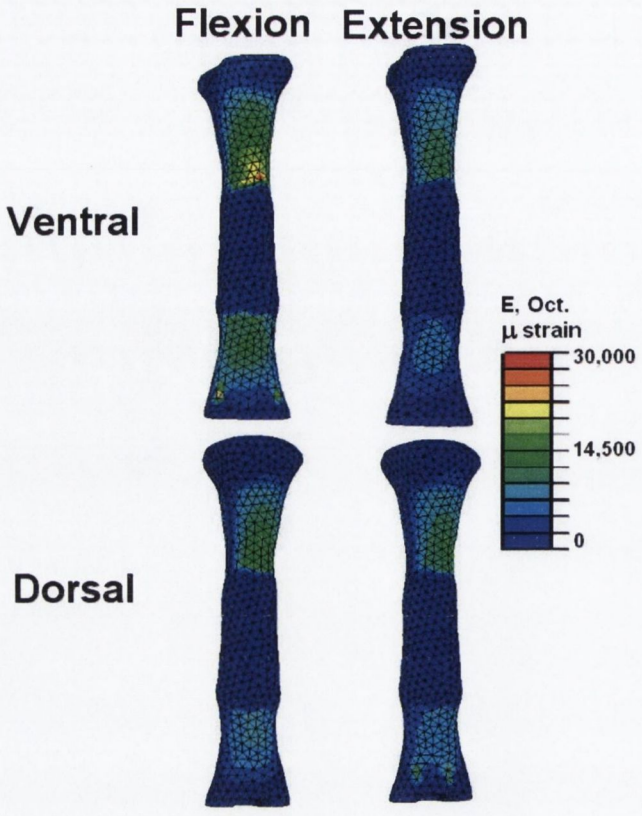


Figure C.25: Octahedral shear strain, μstrain, HH34_A.

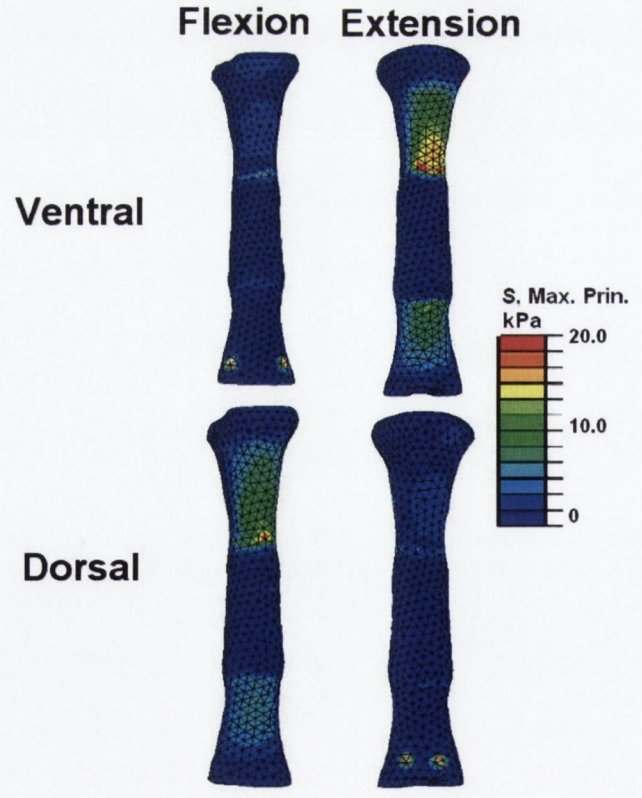


Figure C.26: Maximum principal stress, kPa, HH34_A.

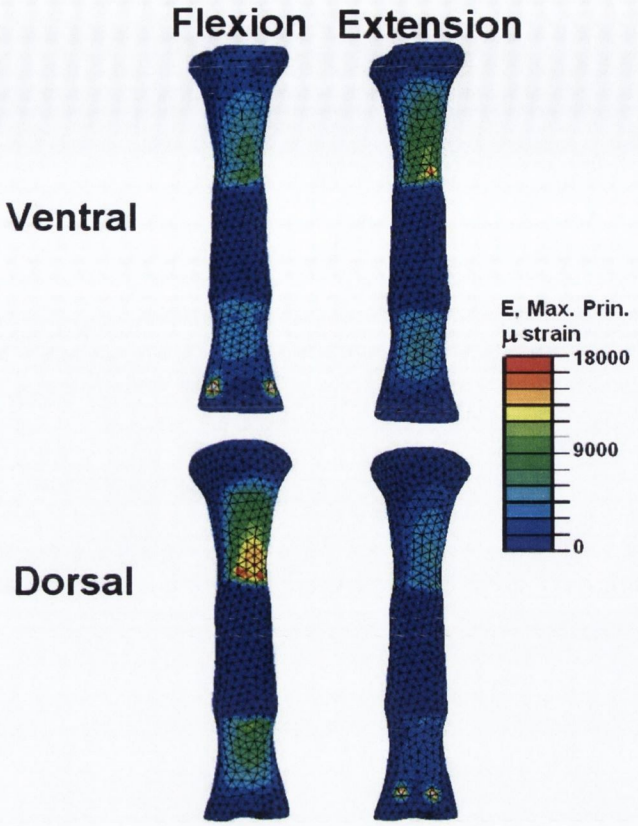


Figure C.27: Maximum principal strain, μstrain, HH34_A.

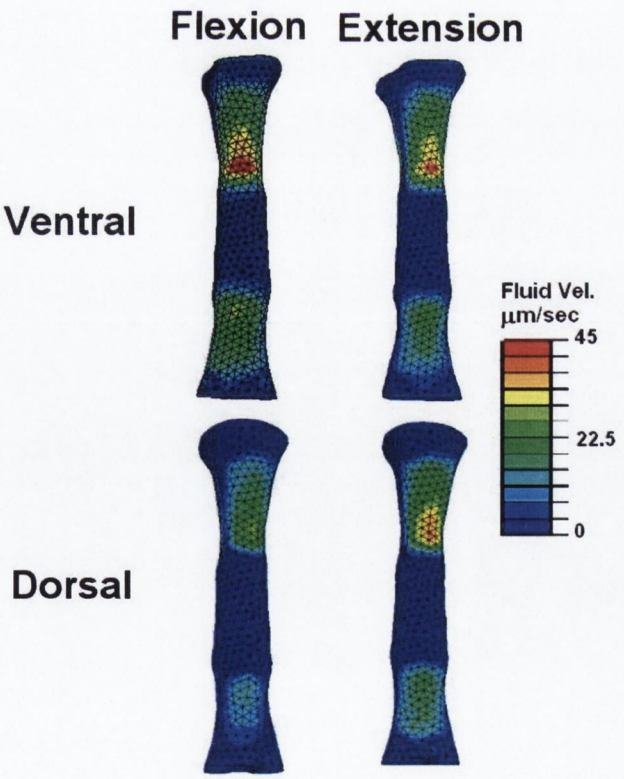


Figure C.28: Fluid velocity, μm/sec, HH34_A.

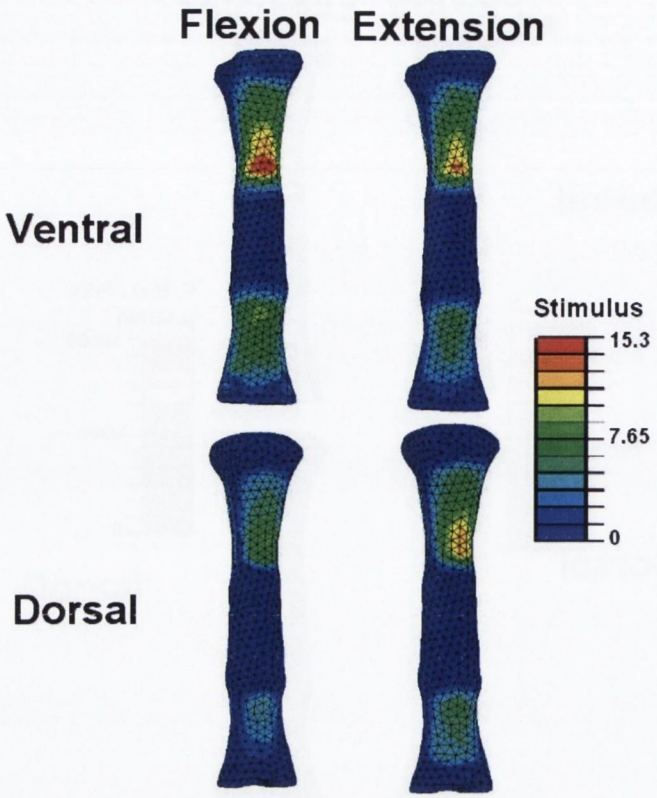


Figure C.29: Stimulus, HH34_A.

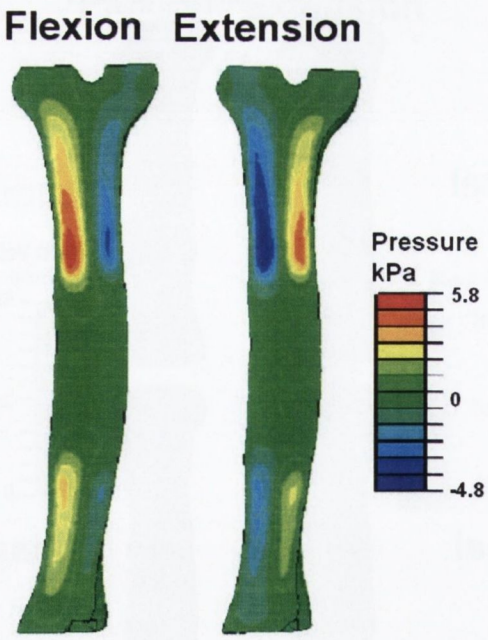


Figure C.30: Pore fluid pressure, kPa, HH34_A.

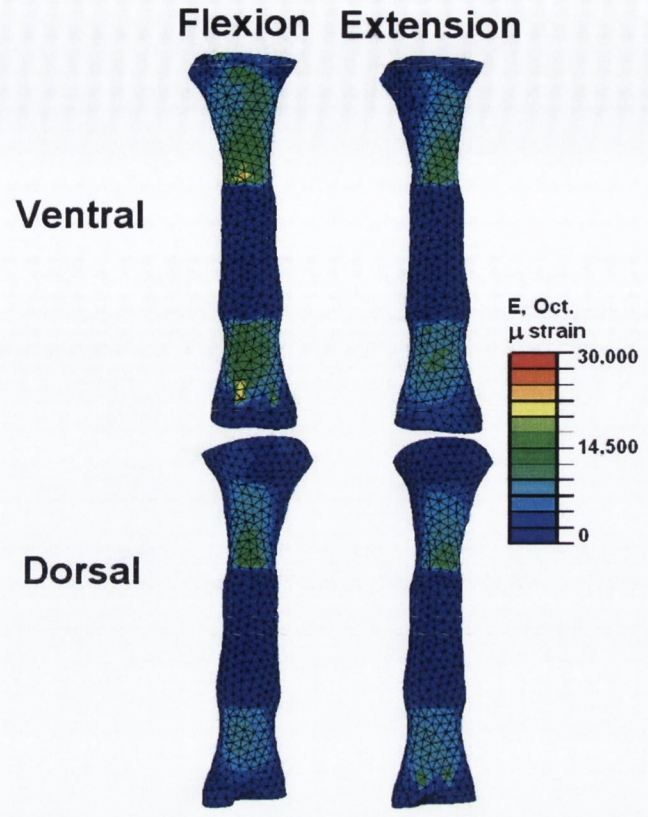


Figure C.31: Octahedral shear strain, μstrain, HH34_B.

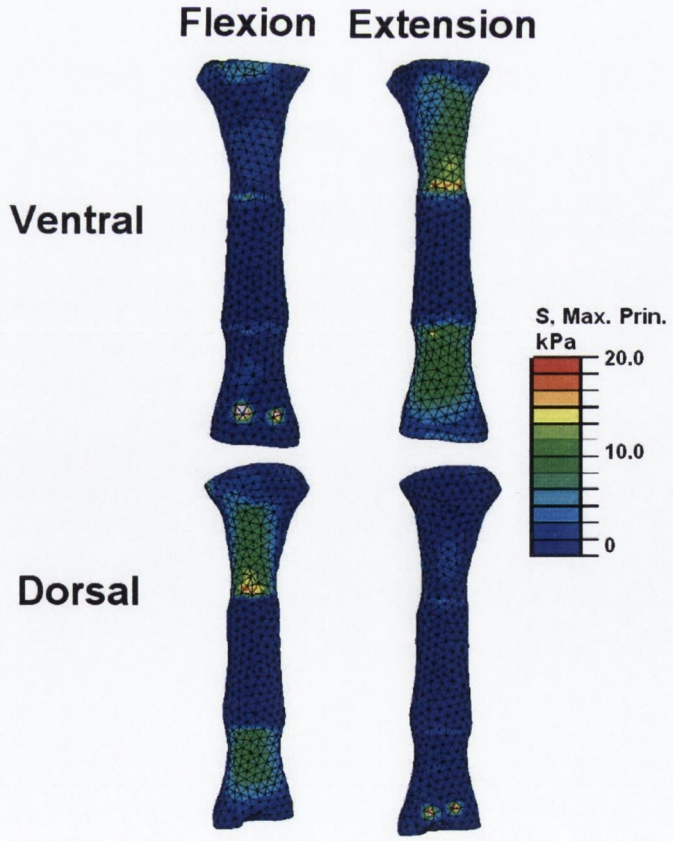


Figure C.32: Maximum principal stress, kPa, HH34_B.

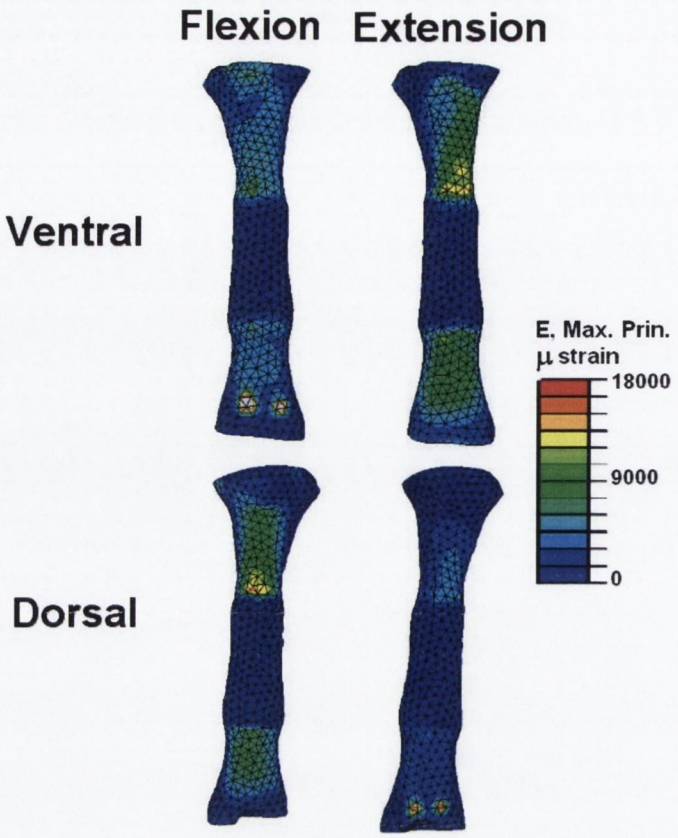


Figure C.33: Maximum principal strain, μstrain, HH34_B.

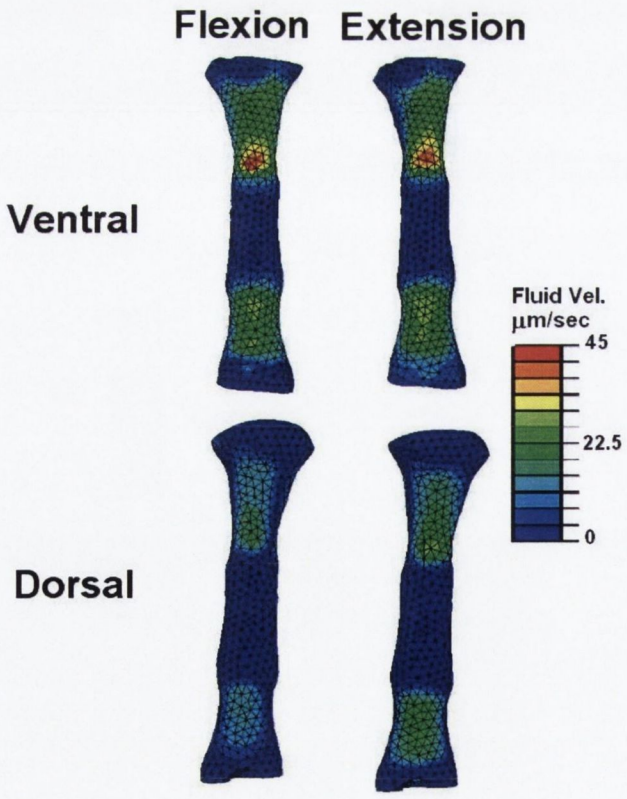


Figure C.34: Fluid velocity, μm/sec, HH34_B.

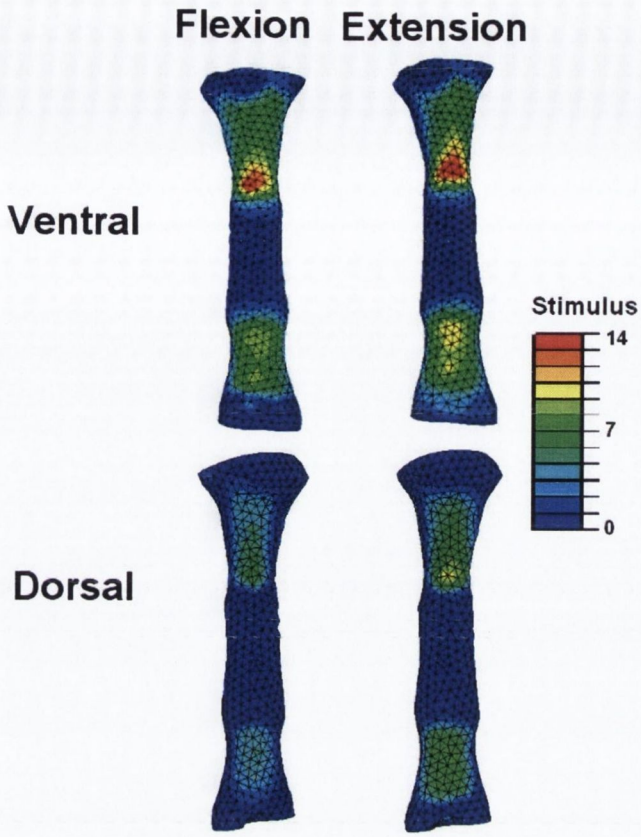


Figure C.35: Stimulus, HH34_B.

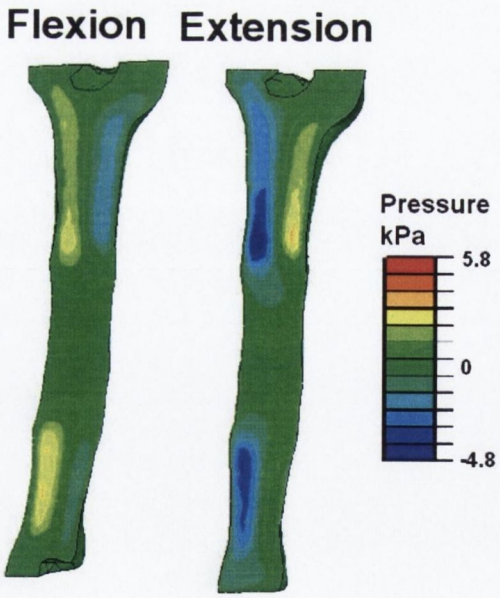


Figure C.36: Pore fluid pressure, kPa, HH34_B.

Appendix D

Mechanosensitive Gene Data

Table D.1: Mechanosensitive gene data from literature; gene name (and alternative gene name(s) if applicable), evidence of mechanosensitivity, and data on up- or down-regulation by mechanical stimulation.

Gene	Role	Evidence of Mechano-sensitivity	Reaction to mechanical stimulation
Bglap1/2 (Osteocalcin)	Inhibitor of osteoblast (and bone) formation (Ducy *et al.*, 1996), recruitment and differentiation of osteoclasts (Glowacki *et al.*, 1991)	In vivo four point bending of rat tibiae (Raab-Cullen *et al.*, 1994), In vitro four point bending of MC3T3-E1 preosteoblasts (Jackson *et al.*, 2006)	Downregulated (Raab-Cullen *et al.*, 1994)Upregulated (Jackson *et al.*, 2006)
BMP-2	Positive regulation of osteoblast differentiation(Hong *et al.*, 2005)	In vivo femoral distraction osteogenesis (rat) (Sato *et al.*, 1999)	Upregulated (Sato *et al.*, 1999)
BMP-4	Positive regulation of osteoblast differentiation (Yamaguchi *et al.*, 2000)	In vitro shear stressed human umbilical vein endothelial cells (McCormick *et al.*, 2001), In vitro fluid shear stimulation of C3H and B6 murine osteoblasts (Lau *et al.*, 2006), In vivo femoral distraction osteogenesis (rat) (Sato *et al.*, 1999), *in vitro* oscillatory shear stress stimulation of enodthelial cells (Sorescu *et al.*, 2003)	Upregulated (Lau *et al.*, 2006; Sato *et al.*, 1999; Sorescu *et al.*, 2003); Downregulated (McCormick *et al.*, 2001)
ColX (Col10a1)	Potential regulator of matrix mineralization in growth plate matrix (Kwan *et al.*, 1997)	In vitro bovine chondrocytes under cyclic tension and cyclic hydrostatic pressure, (Wong *et al.*, 2003), Ex vivo mechanical stimulation of neonatal rabbit distal femoral condyle explants (Sundaramurthy and Mao, 2006)	Upregulated (Sundaramurthy and Mao, 2006; Wong *et al.*, 2003)
ERK1/2	Positive reulator of osteoblast differentiation (Jackson *et al.*, 2006)	In vitro four point bending of MC3T3-E1 preosteoblasts (Jackson *et al.*, 2006)	Downregulated (phosphrylation) (Jackson *et al.*, 2006)
FGF-2 (Basic fibroblast growth factor (bFGF))	Stimulates proliferation of osteoblasts, also involved in bone resorption (Montero *et al.*, 2000) Stimulates chondrocyte hypertrophy (Minina *et al.*, 2002)	In vitro tensile stretch stimulation of human osteoblast-like cells (Cillo *et al.*, 2000), In vitro mechanical stimulation of bone marrow stromal cells from Fgf2-/- and Fgf2+/+ mice (Li and Hughes-Fulford, 2006), In vitro four point bending of MC3T3-E1 preosteoblasts (Jackson *et al.*, 2006)	Upregulated (Cillo *et al.*, 2000; Jackson *et al.*, 2006; Li and Hughes-Fulford, 2006)
FGFr-1	Osteoblast differentiation ((Iseki *et al.*, 1999) Potential regulator of differentiation of hypertrophic chondrocytes (Ornitz and Marie, 2002)	In vitro four point bending of MC3T3-E1 preosteoblasts (Jackson *et al.*, 2006)	Downregulated (Jackson *et al.*, 2006)
FGFr-2	Negative modulator of proliferation (positively affects terminal maturation) (Provot and Schipani, 2005)	In vitro mechanical stimulation of bone marrow stromal cells from Fgf2-/- and Fgf2+/+ mice (Li and Hughes-Fulford, 2006), In vitro four point bending of MC3T3-E1 preosteoblasts (Jackson *et al.*, 2006)	Downregulated (Jackson *et al.*, 2006) Upregulated (Li and Hughes-Fulford, 2006)
FGFr-3	Negatively regulates chondrocyte proliferation and differentiation (Wang *et al.*, 1994)	In vitro four point bending of MC3T3-E1 preosteoblasts (Jackson *et al.*, 2006)	Upregulated (Jackson *et al.*, 2006)
FGFr-4	Potential regulator of preosteoblast proliferation and differentiation in intramembranous ossification (Cool *et al.*, 2002)	In vitro four point bending of MC3T3-E1 preosteoblasts (Jackson *et al.*, 2006)	Downregulated (Jackson *et al.*, 2006)
Fos (c-fos)	Essential for osteoclast differentiation and bone remodellling ((Grigoriadis *et al.*, 1994)	In vivo four point bending of rat tibiae (Raab-Cullen *et al.*, 1994), In vitro stimulation of Mc3T3-E1 cells (Li and Hughes-Fulford, 2006)	Upregulated (Li and Hughes-Fulford, 2006; Raab-Cullen *et al.*, 1994)

Gene	Role	Evidence of Mechano-sensitivity	Reaction to mechanical stimulation
IGF-1	Positive regulator of chondrocyte proliferation (Yakar *et al.*, 2002)	In vitro fluid shear stimulation of C3H and B6 murine osteoblasts (Lau *et al.*, 2006), In vitro tensile stretch stimulation of human osteoblast-like cells (Cillo *et al.*, 2000), In vivo four point bending of rat tibiae (Raab-Cullen *et al.*, 1994),	Upregulated (Cillo *et al.*, 2000; Raab-Cullen *et al.*, 1994), Receptor Upregulated, (Lau *et al.*, 2006)
Ihh	Inhibits hypertrophic chondrocyte differentiation (thereby delaying mineralization) (Vortkamp *et al.*, 1996)	In vivo mechanical stimulation of mandibular condyle (rat) (Ng *et al.*, 2006a; Ng *et al.*, 2006b), In vitro cyclic mechanical stimulation of embryonic chick chondrocytes (Wu *et al.*, 2001)	Upregulated (Ng *et al.*, 2006b; Wu *et al.*, 2001)
IL-1 beta	Stimulates bone resorption and inhibits bone formation (Nguyen *et al.*, 1991)	In vitro stimulation of mouse embryonic day 10 limb bud cells (Takahashi *et al.*, 1998)	Downregulated (Takahashi *et al.*, 1998)
Il-6	Promotes (early) osteoclast formation and bone resorption (Roodman *et al.*, 1992)	In vitro tensile stretch stimulation of human osteoblast-like cells (Cillo *et al.*, 2000)	Upregulated (Cillo *et al.*, 2000)
MMP-13 (Collegenase-13)	Degradation of cartilage collagen and aggrecan, regulation of terminal hypertrophic condrocyte apoptosis (Stickens *et al.*, 2004)	In vitro bovine chondrocytes under cyclic tension and cyclic hydrostatic pressure, (Wong *et al.*, 2003)	Upregulated (cyclic tension), downregulated (cyclic hydrostatic pressure), (Wong *et al.*, 2003)
PTHrP (Pthlh)	Negative regulator of switch from proliferative to hypertrophic chondrocyte (promotes longitudinal growth) (Weir *et al.*, 1996)	In vivo mechanical stimulation of mandibular condyle (rat) (Ng *et al.*, 2006a; Ng *et al.*, 2006b), In vitro cyclic mechanical stimulation of rat growth plate chondrocytes (Tanaka *et al.*, 2005)	Upregulated (Ng *et al.*, 2006b; Tanaka *et al.*, 2005)
Runx2 (Cbfa1)	Regulator of osteoblast differentiation (Yamaguchi *et al.*, 2000)	In vitro bovine chondrocytes under cyclic tension and cyclic hydrostatic pressure (Wong *et al.*, 2003), Ex vivo mechanical stimulation of neonatal rabbit distal femoral condyle explants (Sundaramurthy and Mao, 2006)	Upregulated (Sundaramurthy and Mao, 2006, Wong et al., 2003, Jackson et al., 2006) (Jackson *et al.*, 2006; Sundaramurthy and Mao, 2006; Wong *et al.*, 2003)
Spp1 (Osteopontin)	Osteoblast differentiation (Iseki *et al.*, 1999)	Ex vivo mechanical stimulation of neonatal rabbit distal femoral condyle explants (Sundaramurthy and Mao, 2006), In vivo four point bending of rat tibiae (Raab-Cullen *et al.*, 1994), In vitro four point bending of MC3T3-E1 preosteoblasts (Jackson *et al.*, 2006)	Downregulated (Raab-Cullen *et al.*, 1994), Upregulated (Jackson *et al.*, 2006) (Sundaramurthy and Mao, 2006)
TGFbeta	Involved in bone formation and resorption: stimulates osteoblast proliferation, blocks later stages of differentiation & mineralization (Bonewald and Mundy, 1990)	In vitro fluid shear stimulation of C3H and B6 murine osteoblasts (Lau *et al.*, 2006), In vitro tensile stretch stimulation of human osteoblast-like cells (Cillo *et al.*, 2000), In vivo four point bending of rat tibiae (Raab-Cullen *et al.*, 1994)	Upregulated (Cillo *et al.*, 2000; Lau *et al.*, 2006; Raab-Cullen *et al.*, 1994)

Gene	Role	Evidence of Mechano-sensitivity	Reaction to mechanical stimulation
VEGF	Regulator of angiogenesis in the growth plate, embryonic growth plate morphogenesis: hypertrophic chondrocyte apoptosis; positive regulator of differentiation of hypertrophic chondrocytes, osteoblasts, enodthelial cells and osteoclasts (Gerber *et al.*, 1999)	In vitro chondrocyte cell line under continuous hydrostatic pressure (Sironen *et al.*, 2002), In vitro bovine chondrocytes under cyclic tension and cyclic hydrostatic pressure, (Wong *et al.*, 2003)	Upregulated (Sironen *et al.*, 2002; Wong *et al.*, 2003)

Appendix E

Immobilisation Specimen Data

Table E.1: Summary data for immobilisation experiments; numbers of control and experimental specimens, survival rates and rates of movement.

IMMOBILIZATION 1: February 2006								
Day	**#Experimental**	**#Harvested**	**Survival Rate**	**Moving**	**Not Moving**	**Unknown**	**%Moving**	**%Not Moving**
5	101	0	n/a	n/a	n/a	n/a	n/a	n/a
6	85	0	84.16%	27	57	3	31.76%	67.06%
7	71	0	83.53%	52	16	3	73.24%	22.54%
8	65	15	91.55%	36	38	1	55.38%	58.46%
9	40	0	80.00%	31	7	2	77.50%	17.50%
10	28	0	70.00%	12	15	1	42.86%	53.57%
11	16	16	57.14%	5	11	0	31.25%	68.75%
Average			30.69%				52.00%	47.98%

Day	**#Controls**	**#Harvested**	**Survival Rate**	**Moving**	**Not Moving**	**Unknown**	**%Moving**	**%Not Moving**
5	56	0	n/a	n/a	n/a	n/a	n/a	n/a
6	42	0	75.00%	24	18	0	57.14%	42.86%
7	36	0	85.71%	35	0	1	97.22%	0.00%
8	34	7	94.44%	32	0	0	94.12%	0.00%
9	26	0	96.30%	26	0	0	100.00%	0.00%
10	23	0	88.46%	23	0	0	100.00%	0.00%
11	21	21	91.30%	21	0	0	100.00%	0.00%
Average			50.00%				91.41%	7.14%

IMMOBILIZATION 2: December 2006								
Day	**#Experimental**	**#Harvested**	**Survival Rate**	**Moving**	**Not Moving**	**Unknown**	**%Moving**	**%Not Moving**
6	78	0	n/a	39	18	21	50.00%	23.08%
7	61	0	78.21%	20	16	8	32.79%	26.23%
8	49	8	80.33%	31	16	2	63.27%	32.65%
9	35	10	85.37%	16	16	3	45.71%	45.71%
10	25	0	100.00%	6	18	1	24.00%	72.00%
11	9	9	36.00%	1	8	0	11.11%	88.89%
Average			34.62%				35.38%	53.10%

	#Controls	**#Harvested**	**Survival Rate**	**Moving**	**Not Moving**	**Unknown**	**%Moving**	**%Not Moving**
6	63	0	n/a	31	10	22	49.21%	15.87%
7	48	0	76.19%	32	6	10	66.67%	12.50%
8	34	6	70.83%	29	3	2	85.29%	8.82%
9	22	5	78.57%	20	1	1	90.91%	4.55%
10	13	0	76.47%	10	1	2	76.92%	7.69%
11	12	12	92.31%	12	0	0	100.00%	0.00%
Average			36.51%				78.17%	8.24%

*Table E.2: Data for experimental specimens from immobilisation experiments. Lengths refer to length of tibiotarsus and length of bone in tibiotarsus. Proportion of bone is equal to length of bone in tibiotarsus/length of tibiotarsus. "Proportion Days Moving" refers to proportion of days movement was observed in specimen from Day 6 onwards (e.g., Specimen E7 was moving 2 days out of 3, therefore proportion of days moving was 2/3, or 0.67. "Effect" column indicates specimens that gene expression patterns showed an effect of treatment. * Effect on Day 11 Ihh specimens not listed due to similarity of expression patterns between control and immobilised specimens. (See Section 4.3.4)*

Name		Stage	Days	Experiment	Length (mm)	Length of bone (mm)	Proportion Bone	Proportion Days Moving	Gene Analysed	Effect
E	7	32	8	2	1.80	0.29	0.16	0.67	ColX, Ihh, PTHrP	
E	28	32	8	2	1.79	0.00	0.00	1.00	ColX, Ihh, PTHrP	
E	72	31.5	8	2	1.69	0.00	0.00	1.00	ColX, Ihh, PTHrP	
E	81	31	8	2	1.26	0.00	0.00	0.33		
E	83	31.5	8	2	1.46	0.00	0.00	0.33		
E	92	32	8	2	1.74	0.00	0.00	0.67	Ihh, PTHrP	
E	96	32	8	2	1.55	0.00	0.00	0.67	Ihh	
E	99	32	8	2	1.96	0.30	0.15	0.67	Ihh, PTHrP	
E	109	32	8	1	2.52	0.36	0.14	0.00	ColX, Ihh, PTHrP	
E	120	31	8	1	2.28	0.38	0.17	1.00	Ihh, PTHrP	Ihh
E	155	32	8	1	2.46	0.54	0.22	0.67	ColX, Ihh, PTHrP	
E	165	30	8	1	1.56	0.00	0.00	0.33		
E	166	31	8	1	1.99	0.00	0.00	1.00	ColX, Ihh, PTHrP	
E	168	30	8	1	1.79	0.00	0.00	0.33		
E	169	31	8	1	1.67	0.00	0.00	0.00	Ihh, PTHrP	
E	173	30	8	1	1.48	0.00	0.00	0.33		
E	176	31	8	1	2.01	0.00	0.00	1.00		

Name		Stage	Days	Experiment	Length (mm)	Length of bone (mm)	Proportion Bone	Proportion Days Moving	Gene Analysed	Effect
E	178	30.5	8	1	1.75	0.00	0.00	0.67	Ihh	
E	179	30.5	8	1	1.81	0.00	0.00	0.67		
E	182	31	8	1	2.50	0.00	0.00	0.67	Ihh	
E	183	32	8	1	1.96	0.00	0.00	1.00	ColX, Ihh, PTHrP	
E	188	31	8	1	1.52	0.00	0.00	0.67	Ihh	
E	190	30	8	1	1.62	0.00	0.00	0.33		
E	13	34	9	2	2.75	0.65	0.24	0.75		
E	16	33	9	2	1.72	0.00	0.00	0.25	ColX, Ihh	
E	30	33	9	2	2.25	0.44	0.20	0.25	ColX, Ihh	ColX
E	31	34	9	2	2.38	0.78	0.33	0.75	ColX, Ihh	
E	57	33	9	2	2.68	0.68	0.25	0.25	ColX, Ihh	ColX, Ihh
E	59	32.5	9	2	1.91	0.00	0.00	0.00		
E	63	33.5	9	2	3.22	1.22	0.38	1.00	ColX, Ihh	ColX
E	64	33.5	9	2	3.19	1.14	0.36	0.75	ColX	
E	65	33	9	2	3.44	1.60	0.47	0.50	Ihh	Ihh
E	84	33	9	2	2.32	0.59	0.25	0.75	ColX, Ihh	Ihh
E	4	35	11	2	5.44	2.22	0.41	0.67	Ihh	**
E	10	35	11	2	5.78	2.58	0.45	0.17		
E	24	35.5	11	2	6.44	3.02	0.47	0.83		
E	47	35	11	2	7.07	4.00	0.57	0.17	Ihh	**
E	60	36	11	1	6.58	3.19	0.48	0.50	Ihh	**
E	67	35	11	2	6.45	3.64	0.56	0.67		
E	80	35	11	2	6.23	3.08	0.49	0.17	Ihh	**
E	85	35	11	2	5.06	2.45	0.48	0.50		
E	86	35	11	2	5.42	1.86	0.34	0.33		

Name		Stage	Days	Experiment	Length (mm)	Length of bone (mm)	Proportion Bone	Proportion Days Moving	Gene Analysed	Effect
E	87	35	11	2	5.47	2.81	0.51	0.17	Ihh	**
E	89	35.5	11	1	5.91	2.89	0.49	0.33		
E	96	36	11	1	6.30	2.71	0.43	0.67	Ihh	**
E	100	36	11	1	6.19	3.15	0.51	0.33		
E	123	36	11	1	6.84	3.90	0.57	0.83		
E	124	36	11	1	7.01	3.54	0.50	0.33		
E	126	36	11	1	6.19	3.43	0.55	1.00	ColX	
E	128	36	11	1	6.69	3.50	0.52	0.33	ColX, Ihh	**
E	138	36	11	1	6.45	3.36	0.52	0.67	ColX, Ihh	**
E	141	36	11	1	5.74	2.55	0.44	0.33		
E	142	36	11	1	6.02	3.25	0.54	0.50		
E	147	35.5	11	1	6.15	3.13	0.51	0.17		
E	148	36	11	1	6.57	3.36	0.51	0.50	Ihh	**
E	192	36	11	1	5.74	2.91	0.51	0.50	Ihh	**
E	195	35.5	11	1	6.40	2.17	0.34	0.50		
E	197	36	11	1	5.66	2.62	0.46	0.33		

Table E.3: Data for control specimens from immobilisation experiments. Lengths refer to length of tibiotarsus and length of bone in tibiotarsus. Proportion of bone is equal to length of bone in tibiotarsus/length of tibiotarsus. "Proportion Days Moving" refers to proportion of days movement was observed in specimen from Day 6 onwards (e.g., Specimen C10 was moving 5 days out of 6, therefore proportion of days moving was 5/6, or 0.83.

Name		Stage	Day	Experiment	Length (mm)	Length of bone (mm)	Proportion Bone	Proportion Days Moving	Genes Analysed
C	9	36	11	1	7.89	4.39	0.56	1.00	ColX, Ihh
C	10	36	11	1	7.98	4.08	0.51	0.83	ColX, Ihh
C	11	36	11	1	7.88	4.11	0.52	0.83	
C	15	36	11	1	7.72	4.47	0.58	1.00	
C	16	36	11	1	7.11	3.77	0.53	1.00	Ihh
C	18	36	11	1	7.39	4.29	0.58	1.00	ColX
C	19	35.5	11	1	6.42	3.29	0.51	1.00	Ihh
C	23	36	11	1	6.52	3.77	0.58	1.00	
C	24	36	11	1	6.27	3.43	0.55	1.00	Ihh
C	27	36	11	1	6.37	3.32	0.52	0.83	
C	28	35	11	1	6.24	3.16	0.51	0.83	Ihh
C	29	36	11	1	6.18	3.01	0.49	1.00	
C	30	36	11	1	5.93	3.27	0.55	0.83	
C	32	36	11	1	6.19	3.24	0.52	1.00	
C	34	36	11	1	7.10	3.75	0.53	1.00	
C	38	31	8	1	2.25	0.00	0.00	1.00	ColX, Ihh, PTHrP
C	39	35.5	11	1	5.61	2.30	0.41	0.83	ColX
C	42	36	11	1	7.53	4.41	0.59	0.83	
C	46	36	11	1	6.72	3.88	0.58	1.00	
C	49	32	8	1	2.66	0.00	0.00	1.00	ColX, Ihh, PTHrP
C	51	36	11	1	7.23	3.91	0.54	1.00	

Name		Stage	Day	Experiment	Length (mm)	Length of bone (mm)	Proportion Bone	Proportion Days Moving	Genes Analysed
C	54	30.5	8	1	2.41	0.47	0.20	0.67	
C	57	31.5	8	1	2.28	0.00	0.00	1.00	ColX, Ihh, PTHrP
C	63	31.5	8	1	1.99	0.00	0.00	0.67	ColX, Ihh, PTHrP
C	69	31	8	1	2.22	0.00	0.00	1.00	ColX, Ihh, PTHrP
C	98	31	8	1	2.16	0.00	0.00	0.67	ColX, Ihh, PTHrP
C	2	32	8	2	1.92	0.00	0.00	0.33	ColX, Ihh
C	4	32	8	2	2.50	0.50	0.20	1.00	ColX, Ihh, PTHrP
C	6	33.5	9	2	3.25	0.95	0.29	0.50	
C	7	32	8	2	2.14	0.00	0.00	1.00	Ihh, PTHrP
C	13	34	9	2	3.25	1.38	0.42	1.00	ColX, Ihh
C	14	34	9	2	4.08	1.77	0.43	0.75	ColX, Ihh
C	18	33	9	2	2.74	0.75	0.27	1.00	ColX
C	21	31.5	8	2	2.09	0.00	0.00	0.67	Ihh
C	24	33	9	2	2.61	0.61	0.23	1.00	ColX
C	27	35	11	2	5.77	2.70	0.47	1.00	
C	34	36	11	2	6.56	3.59	0.55	1.00	
C	35	35	11	2	5.96	2.99	0.50	0.83	Ihh
C	36	35.5	11	2	5.91	2.73	0.46	1.00	
C	46	35	11	2	4.46	1.84	0.41	0.83	
C	47	36	11	2	6.69	3.49	0.52	0.50	
C	51	35	11	2	5.60	2.80	0.50	0.83	
C	61	35	11	2	6.33	3.40	0.54	1.00	
C	67	36	11	2	6.79	3.78	0.56	0.83	
C	68	32	8	2	2.04	0.00	0.00	1.00	ColX, Ihh
C	73	36	11	2	6.98	3.96	0.57	0.83	
C	75	32	8	2	2.57	0.39	0.15	0.67	ColX, Ihh, PTHrP